AD-A062 506 NAVAL ACADEMY ANNAPOLIS MD F/G 5/11

PROCEEDINGS OF THE GENERAL MEETING (18TH) OF THE AMERICAN TOWIN--ETC(U)

1977 B JOHNSON, B NEHRLING

UNCLASSIFIED NL

1 OF 4

AD
A062506

LEVEL III

PROCEEDINGS OF

THE EIGHTEENTH GENERAL MEETING OF THE

AMERICAN TOWING TANK CONFERENCE

AD A062506

AD 62 507

DDC FILE COPY

VOLUME ONE

GENERAL REPORT

RESISTANCE AND FLOW SESSION

PROPULSION SESSION

23—25 AUGUST 1977

ANNAPOLIS, MARYLAND

SPONSORED BY:

ONR
NAVSEA
USNA
NAMB

BRUCE JOHNSON

BRUCE NEHRLING

EDITORS

C

(6) PROCEEDINGS OF

THE ~~EIGHTEENTH~~ (18th) GENERAL MEETING OF THE

AMERICAN TOWING TANK CONFERENCE, 23-25 August 1977, Annapolis, Maryland.

Volume I.

GENERAL REPORT,

RESISTANCE AND FLOW SESSION

and

PROPULSION SESSION,

23 - 25 August 1977

(11) 1977

Annapolis, Maryland

(12) 305 p.

(10) Bruce Johnson

Bruce Nehrling

Editors

Sponsored by

U. S. Naval Academy

Office of Naval Research

Naval Sea Systems Command

ABSTRACT

PREFACE

The Eighteenth General Meeting of the American Towing Tank Conference was held in Annapolis, Maryland from the 23rd to the 25th of August 1977. The conference sessions were held in Rickover Hall, the Engineering Studies Complex at the United States Naval Academy. The 18th ATTC was attended by 226 delegates and observers from North and South America and a number of foreign guests who were at the Naval Academy to attend a meeting of the Presentation and Information Committee of the International Towing Tank Conference (ITTC). As part of the Conference, a dedication ceremony for the new 380 foot Naval Academy Model Basin was held on Wednesday afternoon, the 24th of August. During this dedication, water samples from the towing tanks represented at the conference were poured into the model basin in a "mixing of the waters" ceremony.

ABSTRACT

The business meeting of the 17th ATTC recommended that a new technical committee be established to prepare a state-of-the-art report on those subjects covered by the Propeller and Performance committees of the ITTC. The addition of a Propulsion Committee to the 18th ATTC raised the number of technical sessions to six. This expansion required two sessions to be held on the morning of the second day and resulted in some of the sessions exceeding their time allocation. As a result, the time available for discussions of committee reports and contributed papers was less than at previous conferences. What was gained, however, was an excellent collection of State-of-the-Art reports and contributed papers on all topics covered by the ITTC. Coming one year prior to the meeting of the ITTC, the Proceedings of the ATTC now constitute a significant summary of the activities of its member organizations in North and South America. As such, it complements the efforts of the ITTC to disseminate that knowledge which has been acquired during the years between its conferences.

The chairman of each technical committee was responsible for the contents and presentation of his committee's State-of-the-Art report during the technical sessions. He also selected the written contributions which were presented and discussed during his session. The editors would like to compliment these chairmen and all members of the technical committees for their outstanding efforts during the conference and for the excellent material contained in these proceedings. Their dedicated work is greatly appreciated by all who attended the conference and who read these proceedings. Specifically we would like to thank the Resistance and Flow Committee (Prof. Louis Landweber, Chairman); the Propulsion Committee (Mr. Raymond Wermter, Chairman); the Cavitation Committee (Prof. Blaine Parkin, Chairman); the Systems and Techniques Committee (Mr. Peter Ward Brown, Chairman); the Maneuvering Committee (Mr. William Smith, Chairman); and the Seakeeping Committee (Prof. J. Randolph Paulling, Chairman).

We would like to join the conference participants in thanking the Naval Academy's Division of Engineering and Weapons, Captain John R. Wales, Director, for hosting the conference. We would also like to express our gratitude to the Naval Sea Systems Command for supporting the salaries of several members of the organizing committee while working on the conference. In addition, we are especially indebted to Mr. Stanley Doroff and the Fluid Dynamics Branch of the Office of Naval Research for their financial assistance in the publication of these Proceedings. Their support allows us to provide a permanent contribution to the literature of the towing tank community.

Finally, we wish to take this opportunity to acknowledge the contributions made by the other members of the organizing committee: NAVSEA Research Professor Jack Hoyt, who acted as co-chairman in coordinating the housing, the Dedication Ceremony and many other details; Mr. Max Altmann, who acted as secretary and coordinated the tours of the Hydromechanics Laboratory; Professor Roger Compton who arranged the social events; LCDR William Harris, coordinator for the Rickover Hall tours and bus transportation; Mr. John Hill who organized the coffee breaks; Mr. Robert Keane, of NAVSEC, who provided personnel for the registration desk; CDR Henry Schmidt and LCDR Sam Lowrie, CF, who handled parking and public relations; and LCDR Ronald Ruys, who acted as treasurer and assisted in coordinating many other aspects of the conference. We are also indebted

to Ms. Inez Johnson (and to the many other secretaries who prepared the State-of-the-Art reports and written contributions) for the excellent preparation of this manuscript.

BRUCE JOHNSON

BRUCE NEHRLING

CONTENTS

VOLUME I

	Page
PREFACE	i
TABLE OF CONTENTS	iii
PROGRAM	ix
COMMITTEES	xi
GENERAL BUSINESS SESSION	xiii
BANQUET REMARKS BY REAR ADMIRAL LISANBY	xv
PARTICIPANTS	xix
AIMS AND ORGANIZATION OF THE AMERICAN TOWING TANK CONFERENCE	xxxiii
PAST MEETINGS OF THE AMERICAN TOWING TANK CONFERENCE	xxxv
A. RESISTANCE AND FLOW SESSION	
Report of the Resistance and Flow Committee	1
Written Contributions	
1. Ship Boundary Layer Research Since about 1974: A Progress Report by J. H. McCarthy, David W. Taylor Naval Ship Research and Development Center	5
2. Wave Resistance by J. V. Wehausen, University of California, Berkeley	21
3. Still Water Resistance of Single - Step Planing Hull by C. T. Wang, Institute of Naval Architecture, NTU	33
4. A Prediction Method for the Viscous Drag of Ships and Underwater Bodies with Surface Roughness and/or Drag-Reducing Polymer Solutions by P. S. Granville, David W. Taylor Naval Ship Research and Development Center	41
5. The Effect of Initial Acceleration on Ship Wave Pattern and Wave Survey Methods by S. M. Calisal, United States Naval Academy	57
6. Effect of Wake on Wave Resistance by L. Landweber, Iowa Institute of Hydraulic Research	67
Discussion of Committee Report and Written Contributions	69
B. PROPULSION SESSION	
Report of the Propulsion Committee	71
Written Contributions	

1. Activities of ITTC Performance Committee by R. Wermter, David W. Taylor Naval Ship Research and Development Center 75

2. A Review of the 15th ITTC Propeller Committee by R. A. Cumming, David W. Taylor Naval Ship Research and Development Center 81

3. Scale Effect and Propeller Induction on the Wake by T. T. Huang, David W. Taylor Naval Ship Research and Development Center 101

4. Recent Developments in the Analytical Prediction of Thrust Deduction by B. D. Cox, David W. Taylor Naval Ship Research and Development Center 113

5. Experimental and Prediction Techniques for Estimating Added Power Requirements in a Seaway by W. G. Day, Jr., A. M. Reed and W. C. Lin, David W. Taylor Naval Ship Research and Development Center 121

6. Performance of Ducted Propellers Fitted to Surface Craft by W. S. Gearhart and R. E. Henderson, Applied Research Laboratory, The Pennsylvania State University 143

7. Partially Submerged and Supercavitating Propeller Systems by J. O. Scherer, HYDRONAUTICS, Incorporated 161

8. Waterjet Propulsion System Performance Analysis by E. R. Miller, Jr., HYDRONAUTICS, Incorporated 167

9. A Survey of Propulsion - Vehicle Interactions on High - Performance Marine Craft by M. B. Wilson, David W. Taylor Naval Ship Research and Development Center 201

10. Waterjet Propulsor Thrust Measurement Using a Reaction Elbow by R. E. Eilers and L. S. Shrout, Boeing Marine Systems 251

11. Experimental Determination of Periodic Propeller Blade Loads in a Towing Tank by R. J. Boswell and S. D. Jessup, David W. Taylor Naval Ship Research and Development Center 263

12. Experimental Determination of the Wake af a High Block Ship by C. A. Scragg 271

Discussion of Committee Report and Written Contributions 279

VOLUME II

C. CAVITATION SESSION

Report of the Cavitation Committee 285

Written Contributions

1. Cavitation Inception - A Review - Progress since 17th ATTC by W. B. Morgan and F. B. Peterson, David W. Taylor Naval Ship Research and Development Center 291

2. Review of Wall Effects on Fully Developed Cavity Flows by E. S. Baker, David W. Taylor Naval Research and Development Center 309

3. Scale Effects in Models with Forced or Natural Ventilation Near the Free Water Surface by R. S. Rothblum, David W. Taylor Naval Ship Research and Development Center 349

4. A Review of Cavitation Erosion Scaling Research by G. D. Mehta and A. F. Conn, HYDRONAUTICS, Incorporated 361

5. An Experimental Investigation of Wall Effects on Supercavitating Hydrofoils of Finite Span by M. R. Maixner, United States Navy 383

6. Leading Edge Cavitation on Lifting Surfaces with Thickness by M. P. Tulin and C. C. Hsu, HYDRONAUTICS, Incorporated 401

7. Application of a CAVIJET™ System for Removing Marine Fouling and Rust by A. F. Conn, HYDRONAUTICS, Incorporated 415

Discussion of Committee Report and Written Contributions 429

D. SEAKEEPING SESSION

Report of the Seakeeping Committee 435

Written Contributions

1. Review of Status for Prediction of Unstabilized and Stabilized Ship Roll Motion by G. G. Cox, David W. Taylor Naval Ship Research and Development Center 441

2. Experiment - Theory Correlation: Linear Ship Motion and Loading Theory by J. F. Dalzell, Davidson Laboratory, Stevens Institute of Technology 449

3. Performance Predictions (Slamming and Wetness) by D. C. Murdey, Marine Dynamics and Ship Laboratory, Ottawa 463

4. Facilities for Seakeeping Tests, Including Means of Generating Waves, Currents, Wind and Other Environmental Conditions by M. A. Abkowitz, Massachusetts Institute of Technology 465

5. Environmental Conditions by D. Hoffman, Webb Institute 471

6. Testing of Unconventional Ocean Platforms by F. N. Biewer, Offshore Technology Corporation 479

7. Dynamic Stability and Capsizing by R. A. Barr, HYDRONAUTICS, Incorporated 485

8. Seakeeping Design Base for Air Cushion Vehicles by D. D. Moran, David W. Taylor Naval Ship Research and Development Center 497

9. Digital Synthesis of Modelled Irregular Seaway Time Histories by J. B. Peters, David W. Taylor Naval Ship Research and Development Center 513

10. A Note on the Application of Modern Control Theory to Ship Roll Stabilization by P. H. Whyte, Defense Research Establishment Atlantic, Canada 517

11. Comparisons of Theory with Experiment for Ship Rolling in Oblique Seas by R. T. Schmitke, Defense Research Establishment Atlantic, Canada 533

12. Criteria for Ship Speed in Rough Weather by A. R. J. M. Lloyd and R. N. Andrew, Admiralty Experiment Works, England 541

13. Simulation of Buoy Motion in Breaking Waves by G. L. Petrie, Hoffman Maritime Consultants Incorporated 567

Discussion of Committee Report and Written Contributions 569

VOLUME III

E. MANEUVERING SESSION

Report of the Steering and Maneuvering Committee 571

Written Contributions

1. Ship Maneuvering Characteristics in Deep and Shallow Water (Applications of Captive Model Test Results) by H. Eda, Davidson Laboratory, Stevens Institute of Technology 587

2. The Application of Rotating Arm Data to the Prediction of Advanced Ship Maneuvering Characteristics by J. A. Fein, David W. Taylor Naval Ship Research and Development Center 601

F. SYSTEMS AND TECHNIQUES SESSION

Report of the Systems and Techniques Committee 615

Written Contributions

1. An Optical Data Transmission System for Telemetry and Control by B. Grabois, ITT Gilfillan 617

2. The U. S. Naval Academy Hydromechanical Laboratory Data Acquisition, Control, and Analysis System by J. C. Gebhardt, CADCOM, Incorporated, S. Williams III, Computer Sciences Corporation, and R. H. Compton, United States Naval Academy 625

3. Dual Flap Wavemaker Phasing and Motion Apportionment by Linear Regression by A. Clark and M. Menken, MTS Systems Corporation 705

4. An Algorithm for Predicting Breaking Waves in a Towing Tank by C. H. Anderson, MTS Systems Corporation and B. Johnson, United States Naval Academy 719

5. A Computer Controlled Wave Generation System for the U. S. Naval Academy by C. H. Anderson, MTS Systems Corporation and B. Johnson, United States Naval Academy 737

6. Digital Control of D. C. Tow Tank Drives with Phase-Locked Loop Techniques by R. H. Osman, Robicon Corporation 755

Program of the Eighteenth General Meeting of the

American Towing Tank Conference

23-25 August 1977

Rickover Hall
United States Naval Academy

Tuesday - 23 August

8:00 a.m.	Registration	
9:00 a.m.	Welcome RADM Kinnaird R. McKee, Superintendent, USNA CAPT John R. Wales, Director, Division of Engineering & Weapons	
9:30 a.m.	Technical Session I: Chairman:	RESISTANCE AND FLOW Louis Landweber
2:00 p.m.	Technical Session II: Chairman:	PROPULSION Raymond Wermter
4:30 p.m.	Open House, Rickover Hall	
6:30 p.m.	Cocktail Hour, Officers Club	

Wednesday - 24 August

8:15 a.m.	Technical Session III: Chairman:	MANEUVERABILITY William Smith
10:30 a.m.	Technical Session IV: Chairman:	CAVITATION Blaine Parkin
2:00 p.m.	Technical Session V: Chairman:	SYSTEMS AND TECHNIQUES Peter Ward Brown
4:30 p.m.	Dedication Ceremony - Naval Academy Model Basin	
6:30 p.m.	Reception and Banquet - Officers Club	

Thursday - 25 August

9:00 a.m.	Technical Session VI: Chairman:	SEAKEEPING Randolph Paulling
2:00 p.m.	Business Session Chairman:	 Bruce Johnson
2:30 p.m.	Open House, Rickover Hall	

COMMITTEES OF THE 18th ATTC

EXECUTIVE COMMITTEE

The Executive Committee of the ATTC consists of the Chairman of the current conference, the chairmen of the three previous conferences, and the ATTC delegate to the executive committee of the ITTC.

Prof. Bruce Johnson, Chairman
Dr. Jack W. Hoyt
Dr. Paulo C. Leone
Mr. Sydney T. Mathews
Prof. Theodore Y. Wu

TECHNICAL COMMITTEES

<u>Resistance and Flow Committee</u>

Prof. Louis Landweber, Chairman
Dr. Wen-Chin Lin
Mr. Justin H. McCarthy
Prof. John V. Wehausen
Prof. Theodore Y. Wu

<u>Propulsion Committee</u>

Mr. Raymond Wermter, Chairman
Mr. Richard A. Cumming
Mr. William G. Day, Reporter
Mr. Walter S. Gearhart
Dr. Robert E. Henderson
Mr. Michael Michailidis
Mr. Eugene R. Miller
Mr. J. Otto Scherer

<u>Maneuvering Committee</u>

Mr. William E. Smith, Chairman
Dr. Haruzo Eda
Dr. Paulo C. Leone
Prof. Michael G. Parsons
Prof. William Webster

<u>Cavitation Committee</u>

Dr. Blaine R. Parkin, Chairman
Mr. Elwyn S. Baker
Dr. Andrew F. Conn
Mr. Gabor F. Dobay, Vice Chairman
Dr. Gurmukh D. Mehta
Dr. William B. Morgan
Dr. Frank B. Peterson
Mr. Richard S. Rothblum

<u>Systems and Techniques Committee</u>

Mr. Peter Ward Brown, Chairman
Mr. William Barkley
Mr. Gabor F. Dobay
Dr. Drasco Gospodnetic
Prof. Bruce Johnson

<u>Seakeeping Committee</u>

Prof. J. Randolph Paulling, Chairman
Prof. Martin A. Abkowitz
Mr. Frank N. Biewer
Dr. Roderick A. Barr
Mr. Geoffrey G. Cox
Mr. John F. Dalzell
Prof Dan Hoffman
Mr. David C. Murdey

LOCAL ORGANIZING COMMITTEE

Mr. Max Altmann, Secretary
Prof. Roger Compton
Mr. Stanley Doroff
LCDR William Harris
Mr. John Hill
Prof. Jack W. Hoyt, Co-Chairman
Prof. Bruce Johnson, Chairman
Mr. Robert Keane
LCDR Sam Lowrie, CN
Prof. Bruce Nehrling
LCDR Ronald Ruys
CDR Henry Schmidt
CAPT John R. Wales

ATTC BUSINESS SESSION

The meeting was brought to order at 1430, 25 August 1977, by the Chairman, Prof. Johnson.

Mr. Mathews, ATTC representative to the ITTC, reported on the final budget for the ITTC held in Ottawa in 1975. He indicated that partial costs of the conference were borne by US Companies and the Office of Naval Research, Canadian Companies, and the North American attendees. The major funding sponsor was the National Research Council of Canada. Since government support seems to be more difficult to arrange each year, this may be the last "hosted" ITTC.

Mr. Mathews indicated that the next ITTC would be held in the Netherlands Sep 3-9, 1978. Several conference of interest to attendees are also being planned in Europe around these dates.

Mr. Mathews reported on the results of a survey to determine his successor as ATTC representative to the ITTC. Two organizations with candidates were prepared to support the substantial travel costs involved. In a second poll of ITTC delegates and ATTC executive committee members, Dr. Breslin of Davidson Laboratory was favored by a large majority for this position. After being recommended by Mr. Mathews, the Conference approved this nomination, and Dr. Breslin will take office following the next ITTC. Dr. Breslin gave a short acceptance speech following his election.

Dr. Cummins noted the superb job done by Mr. Mathews and the Conference endorsed this view by applause.

Prof. Johnson introduced the topic of the location of the next conference, and after some discussion, the invitation received from Dr. Couch for the University of Michigan was accepted for the 19th ATTC. Further, the 20th ATTC has been invited to Davidson Laboratory, the site of the first ATTC meeting in 1938, as being a most fitting anniversary location. Placed in reserve for future consideration is an invitation from Dr. Parkin of ARL, Penn State.

The final topic of the meeting was the general meeting arrangement of the ATTC. No recommendations for a change in committee structure were received. It was suggested, however, in selecting Chairman for the Technical Committees, that the selectee pledge to do his utmost to have his state-of-the-act report available two months before the conference to permit printing, mailing, and full study by the Conference attendees. Dr. Cummins noted the strong technical tone of the conference. Prof. Lewis suggested a closer time limit on oral presentations in order to ensure more complete discussions of the papers. Simultaneous sessions were discussed but rejected. Mr. Mathews suggested that each technical committee be alert to problems of operation in ice, as there will be 5 major ice tank facilities in North America before the next ATTC, and the topic will be of increasing technical and commercial concern.

After announcements concerning the deadline for submission of final changes and discussion on the 18th ATTC papers, the meeting was adjourned at 1600.

J. W. HOYT
Recorder

Rear Admiral Lisanby's Remarks at the

Banquet of the

18th American Towing Tank Conference

U. S. Naval Academy

24 August 1977

In deference to the flavor of our international gathering, let me say Buenas Noches, Boas Tardes, Dobry Vecher, Hao Bu Hao, and good evening ladies and gentlemen. It is reassuring to see such a fine turnout for the 18th American Towing Tank Conference. I am always pleased to return to this site of many important memories of my midshipman days, and I am especially honored to join such an august scientific gathering.

The dedication of the towing tank this afternoon in Rickover Hall brings the naval scientific community another outstanding, educational and research tool. At the dedication ceremony we heard from both Rear Admirals Kauffman and King who, among others on the Academy staff, were the force behind having this tank built. I echo their awards tonight.

We have truly come a long way since the turn of the century when Rear Admiral David Taylor advocated and supervised the construction of the country's first experimental model basin at the Washington Navy Yard. That basin was one of the world's finest until DTMB -- The David Taylor Model Basin -- was dedicated in 1939 at the Naval Ship Research and Development Center, Carderock, Md. and now, the Academy's magnificent new towing tank will further expand our ability to develop more naval officers in the tradition of Admiral Taylor. They, with the civilian scientists and engineers, will solve the hydrodynamic problems inherent in ship design.

And it is this ability to delve into the unknown and glean understanding that I wish to consider for a few moments. The unglamorous word for this scientific inquiry is research. We engineers understand all too well that serendipity alone accounts for very few scientific advances. Most development results from prolonged, often exhaustive, investigation. And in today's world, that means money -- lots of it!

Throughout my 27-year career I have become increasingly impressed with the necessity for a more equitably organized approach to research. And, for tonight's consideration, let's limit ourselves to research. I don't wish to be overly dramatic, but the future viability of our Naval Fleet is at stake. That viability, however, may be in question today with the apparent funding disparity afforded naval surface ship development in light of the burgeoning technology in all other area.

Let's consider these disparities of the R&D process more closely and then suggest possible improvements.

In Fiscal Year 1976 vehicle exploratory development (less machinery and propulsion systems) for Air Force, Army and Navy aircraft received a total of $75 million. The Navy, on the other hand, received only $20 million for all ship exploratory development and that includes surface ships, submarines, advanced ships and amphibious ships. In other words, military aircraft received nearly four times as many exploratory R&D dollars as naval ships. If we broaden our view of these exploratory development funds and also include industry, NASA, Maritime Administration and the Coast Guard, in 1976 approximately 10 times as much money was spent on aircraft as on ship R&D of an exploratory nature.

The climate for surface ship R&D is not improving. In Fiscal Year 1976 only slightly more than 2.2% (or $75 million) of the total Navy R&D budget of $3.3 billion

was designated for surface ship platforms, excluding ship design. This trend continued through the three-month transition. However, in Fiscal Year '77 there has been a noticeable decrease in surface ship R&D to the extent that it is now only slightly more than one and one-half percent (or $61 million) of the total Navy R&D budget of $3.7 billion.

Since tonight we are concerned especially with hydrodynamics research, I was appalled to learn that in Fiscal Year 1977 there was only $354 thousand -- out of those several billions -- specifically devoted to seakeeping R&D efforts in support of surface ship design. And I understand that R&D funding for this important work will be reduced in Fiscal Year 1978. Does this mean that we know everything we need to know about seakeeping in naval ship design? Of course, it does not. It reflects rather poorly on our own short sightedness. Because what could be more central to our Navy than the ability to sail and fight independent of sea state?

In discussing these dollar comparisons, it is important to keep in mind that ships and submarines do not have a strong industrial technology base as aircraft have because warships bear little or no resemblance to their commercial cousins, and the technological transfer is slight. It is for this reason that it is incumbent on the Navy to maintain a strong in-house technology base for ships and, as I stated earlier, that takes money!

Loosening the pursestrings of surface ship R&D, however, will not help us much if we do not improve our basic approaches to R&D. So, within the short amount of time remaining, let's consider now at least five suggestions for improving surface ship R&D with particular emphasis on ship hydrodynamics.

The first suggestion for improved surface ship R&D is, Better Coordination, cooperation and communication among Navy policy makers, researchers, designers, and ship forces in establishing R&D priorities. In this regard, these individuals should give equal consideration to solving the many technical problems in designing surface ships as to developing aircraft, submarines, and the more exciting advanced or high performance ships such as hydrofoils, air cushion vehicles, surface-effect-ships, and swath ships.

If each program does not receive appropriate priority, long-term consequences may occur. This may be happening today with surface ship R&D, unlike that for advanced ship and submarine R&D. For example, the Navy is undertaking a major product improvement program for the fin stabilizer system for the guided missile frigate, (FFG-7 Class), but it will be funded with ship construction dollars, not R&D money, and it will be tailored necessarily to the FFG-7 Class. As a result, extensive model testing to investigate the cavitation characteristics of various fin shapes could not be accomplished under the FFG-7 program, even though this information would be extremely valuable to our overall technical data base. This approach of trying to accomplish such developmental efforts on a piece-meal fashion as part of a ship acquisition program should not be continued because scheduling and, at times, funding constraints of ship construction programs preclude adequate scope and depth of the required developmental work.

Until adequate R&D funding is obtained, the operational effectiveness of the U. S. Navy's surface ships will continue to be compromised by many design deficiencies related to the hydrodynamic aspects of ship performance.

With all the advantages of our modern day computer technology, uncompensated ship motion represents the single largest error factor remaining in the surface ship gunfire problem today. These and other deficiencies, in many cases, have resulted in ships which either fail to meet performance requirements, or which are unnecessarily larger are more costly, both to acquire and to operate. For example despite considerable progress in theoretical treatments of ship resistance problems, the naval ship designer still uses Taylor standard series data in the early stages prior to model tests. What

the designer needs are analytical methods to predict accurately the effects of various hull form parameters on hull resistance, particularly for the higher beam-to-draft ratios of today's naval ship designs. These analytical methods must be validated with extensive models and full scale testing. A specific challenge for the experimental researcher will be to develop new experimental techniques for predicting appendage drag.

Another hydrodynamic design problem is that methods for predicting hull-propulsor interactions, that is, thrust deduction and wake fraction, are based largely on historical, empirical data. However, the ship designer again needs more analytical methods to determine the effects of changes to the underwater hull form and appendages so that he can investigate refinements to alternative designs and ascertain their impact on hydrodynamic performance.

A third unresolved deficiency in hydrodynamic-related design is the lack of adequate analytical methods to predict the loads associated with slamming and wave-slap. This lack of knowledge in sea loading could adversely affect the ability of the local structure to withstand high sea states, a critical situation which already has, in the past, resulted in serious structural damage to flight deck sponsons. Deck-edge elevators, and other structures exposed to the sea.

For instance, during recent feasibility studies of a V/stol cruiser, it was impossible to ensure that the flight deck sponsons would not be subject to unacceptable slamming loads. This uncertainty resulted in a three-month delay in the development of the concept, and in the time-frame of today's navy ship construction program, such a delay may force an option to be discarded because the technical uncertainities cannot be resolved before a decision must be made.

In addition to the three deficiencies already discussed, I briefly would like to mention four more research areas where the hydrodynamicscts can contribute to improving ship design. These are: (1) developing analytical and experimental techniques to predict speed and power in waves; (2) developing analytical and experimental techniques to assist in investigating dynamic station keeping, including modeling of ship control in waves; (3) performing additional ship-model correlation tests, including the effects of fouling on ship performance, and (4) developing analytical and experimental techniques to assess alternative design arrangements of the hull, propeller, rudder, and other appendages -- with special emphasis placed on propeller tip clearance and location of the rudder with respect to the propeller.

Let us now return to my five basic suggestions for improving ship R&D. In addition to better coordination in establishing priorities, there should be more pooling together of resources among the engineering community as we are doing this week. By doing so, researchers, designers, operating forces, government agencies, industry and engineering societies will profit by each other's findings.

Already, we ship designers have applied newly-developed computer programs for defining hull lines to reduce significantly the time required to fabricate fiberglass ship models. In addition we have extended this transfer of knowledge a bit further by using new computer-aided design methods to construct wooden models. Also, we are using computer and data acquisition technology to improve the timeliness in processing test data. By continuing to adopt such improvements, the ship designer and the experimental researcher will be able to obtain results from model tests to map out research strategies and coordinate challenging R&D efforts. This is happening with the reorganization of the Naval Sea Systems Command Hydromechanics Committee, and the Seakeeping Workshop, held at the Naval Academy in 1975. The objective of that workshop was to develop a seakeeping R&D program and, as a result, significant contributions have been made to our ship design capabilities despite meager funding for this program.

The fourth suggestion for improving surface ship R&D is sharpening the long-range vision of the ship designer so that he or she can look ahead and predict 15 years hence what our ships will require. This ability is required because it now takes that long

for a ship or weapon system to evolve from conceptual design to operational readiness.

As the navy's ship design activity, the Naval Ship Engineering Center must ensure that its engineers exhibit that sense of vision so that they, more than anyone else, know the long-range needs of naval ships. By exhibiting this sense of vision, NAVSEC will retain its ship design expertise and avoid the pitfalls of inadequate or inaccurate design work, the most serious consequence of which may be the significant costs associated with changes to operational equipment after the ship has been designed.

Post-construction fixes recently associated with our inability to predict cavitation performance reliably during the design of propellers for recent ship designs are examples of how significant costs may be associated with equipment changes after the ship has been designed.

This shortfall in design technology must be addressed not only for propeller design, but also for the design of high speed surface combatants which can more effectively use their sonar at higher speeds.

Having a continuing educational program available to sharpen further the engineer's design vision is the fifth and my last suggestion for improving surface ship R&D. Such a curriculum is being implemented now in the Naval Sea Systems Command and in the Naval Ship Engineering Center to supplement an existing training program. Already, the existing program has enabled NAVSEC to send several of its engineers to graduate school to specialize or obtain a broader background in ship hydrodynamics.

This intensification of professional education, geared to the special needs of the command, will improve the transfer of research technology into the ship design process and ensure that NAVSEC retains its ship design expertise.

This evening I have attempted to touch on the importance of surface ship R&D, the funding disparity in ship R&D compared to other Navy R&D programs, the adverse effects on surface ship design capability because of that disparity, and how the present R&D processes might be improved. Although my comments by no means address the subject entirely, let alone the specific area of ship hydrodynamics R&D, perhaps they will form a basis on which later discussion might follow so that remedies will be forthcoming. These remedies must include not only additional funding but the technical contributions of the scientific community gathered here tonight.

In the meantime, let us continue to push forward, keeping in mind that our ability to make our naval ships effective is the basis on which our fleet and our nation will judge us.

I appreciate having the opportunity to address you this evening.

Participants

The 18th American Towing Tank Conference

23-25 August 1977, Annapolis, Maryland

Prof. Martin A. Abkowitz
Mass. Institute of Technology
Room 5-319
Dept. of Ocean Engineering
Cambridge, Massachusetts 02139

Mr. Joseph C. Alonge
Computer Science Corporation
6565 Arlington Blvd.
Falls Church, Virginia 22046

Mr. Max Altmann
Hydromechanics Laboratory
U. S. Naval Academy
Annapolis, Maryland 21402

Mr. Charles H. Anderson
MTS Systems Corporation
Box 24012
Minneapolis, Minnesota 55424

Mr. R. N. Andrew
Admiralty Experiment Works
Haslar, Gosport, Hants
ENGLAND

Prof. Roger Arndt
Penn State University
233 State University
University Park, PA 16802

Admiral Augusto Brito
Instituto Universitario Politecnico
De Las Fuerzas
Armadas Nacionales (IUPFAN)
La Carlota, Caracas, Venezuela

Mr. Eugene M. Avallone
1343 Kinloch Circle
Arnold, Maryland 21012

Mr. Elwyn S. Baker
DTNSRDC Code 1532
Bethesda, Maryland 20084

Dr. John L. Baldwin
Naval Surface Weapons Center
Silver Spring, Maryland 20910

Mr. N. K. Bales
DTNSRDC Code 1568
Bethesda, Maryland 20084

Mrs. Susan M. Lee Bales
DTNSRDC Code 1568
Bethesda, Maryland 20084

Mr. E. Band
BLA Inc.
1910 Forest Drive
Annapolis, Maryland 21401

Dr. Roderick A. Barr
HYDRONAUTICS, Inc.
7210 Pindell School Road
Laurel, Maryland 20810

Mr. D. F. Bastian
Waterway Experimental Station
Chesapeake Bay Office
P.O. Box 148
Stevensville, Maryland 21666

Mr. William Beduhn
MTS Systems Corporation
Box 24012
Minneapolis, Minnesota 55424

Prof. R. Bhattacharyya
Naval Systems Engineering Dept.
U. S. Naval Academy
Annapolis, Maryland 21402

Mr. Frank N. Biewer
Offshore Technology Corp.
578 Enterprise Street
Escondido, California 92025

Mr. Bruce J. Black
ABA-EMS, Incorporation
P.O. Box 500
Pinellas Park, Florida 33565

Midshipman Donald Boland, 1/C
Bancroft Hall
U. S. Naval Academy
Annapolis, Maryland 21402

Mr. John W. Bosque
HYDRONAUTICS, Inc.
7210 Pindell School Road
Laurel, Maryland 20810

Mr. Robert J. Boswell
DTNSRDC
Code 154
Bethesda, Maryland 20084

Mr. Ebb Bosworth
Hydromechanics Laboratory
U. S. Naval Academy
Annapolis, Maryland 21402

Mr. John W. Brandau
RPM Company
P.O. Box 277
Slidell, LA 70459

Dr. John P. Breslin
Director, Davidson Laboratory
711 Hudson Street
Hoboken, New Jersey 07030

Captain A. L. Bress
Naval Sea Systems Command
Code 03
Washington, D. C. 20362

Ensign Michael F. Brock
DTNSRDC Code 1524
Bethesda, Maryland 20084

Mr. Peter Ward Brown
Davidson Laboratory
711 Hudson Street
Hoboken, New Jersey 07030

Mr. Fred Brownell
DTNSRDC Code 1524
Bethesda, Maryland 20084

LCDR Robert Burns
Naval Systems Engineering Dept.
U. S. Naval Academy
Annapolis, Maryland 21402

Mr. George Butzow, President
MTS Systems Corporation
Box 24012
Minneapolis, Minnesota 55424

Mr. David W. Byers
NAVSEC
Department of the Navy
Washington, D. C. 20362

Prof. S. M. Calisal
Naval Systems Engineering Dept.
U. S. Naval Academy
Annapolis, Maryland 21402

Mr. Harold E. Cartright
HYDRONAUTICS, Inc.
7210 Pindell School Road
Laurel, Maryland 20810

Mr. Ken Casperson
MTS Systems Corporation
411 N. Washington Street
Alexandria, Virginia 22314

Mr. Michael A. Chaszeyka
Office of Naval Research
536 South Clark Street
Chicago, Illinois 60605

Mr. Allen Clark
MTS Systems Corporation
Box 24012
Minneapolis, Minnesota 55424

Mr. Richard W. Clark, Vice-President
MTS Systems Corporation
Box 24012
Minneapolis, Minnesota 55424

Mr. Stuart B. Cohen
Naval Architecture Research Office
U. of Michigan
Ann Arbor, Michigan 48109

Prof. Roger H. Compton
Naval Systems Engineering Dept.
U. S. Naval Academy
Annapolis, Maryland 21402

Mr. Edward Comstock
NAVSEC Code 6136
Department of the Navy
Washington, D. C. 20362

Dr. Andrew F. Conn
HYDRONAUTICS, Inc.
7210 Pindell School Road
Laurel, Maryland 20810

Prof. Richard B. Couch
University of Michigan
126 W. Eng. Bldg.
Ann Arbor, Michigan 48109

Mr. Bruce Cox
DTNSRDC Code 1544
Bethesda, Maryland 20084

Mr. Geoffrey G. Cox
DTNSRDC Code 1568
Bethesda, Maryland 20084

Mr. William A. Crago
Experimental & Electronic Lab
British Hovercraft Corp.
E. Cowes, Isle of Wight, ENGLAND

Mr. Leroy Crosby
Waterways Experiment Station
Chesapeake Bay Office
P.O. Box 148
Stevensville, Maryland 21666

Mr. R. A. Cumming
DTNSRDC Code 1544
Bethesda, Maryland

Dr. William E. Cummins
DTNSRDC Code 1500
Bethesda, Maryland 20084

Mr. Douglas Dahmer
DTNSRDC Code 1544
Bethesda, Maryland 20084

Mr. J. F. Dalzell
Davidson Laboratory
Stevens Inst. of Technology
711 Hudson Street
Hoboken, New Jersey 07030

Mr. Robert S. Dart
DTNSRDC Code 1503
Bethesda, Maryland 20084

Mr. William G. Day, Jr.
DTNSRDC Code 1524
Bethesda, Maryland 20084

Mr. Moray P. Dewhurst
NORDCO, LTD
P.O. Box 8833
St. Johns, Newfoundland
A1B 3T2, Canada

Mr. Thomas P. Dixon
ITT Gilfillan
7821 Orion Avenue
Van Nuys, California 91324

Mr. Gabor Dobay
DTNSRDC Code 1532
Bethesda, Maryland 20084

CDR Brian E. Dodridge, RN
British Navy Staff
P.O. Box 4855
Washington, D. C. 20008

Mr. S. Doroff
Office of Naval Research
Code 438
800 N. Quincy Street
Arlington, Virginia 22217

Mr. Leon Droppert
Delft Hydraulics Lab
P.O. Box 177
Delft, The NETHERLANDS

Dr. Haruzo Eda
Stevens Institute of Technology
Davidson Laboratory
Hoboken, New Jersey 07030

Mr. Robert E. Eilers
Mail Stop 73-07
The Boeing Company
P.O. Box 3707
Seattle, Washington 98124

Mr. Phillip Eisenberg
HYDRONAUTICS, Inc.
Suite 701, 1101 15th St., N.W.
Washington, D. C. 20005

Mr. Steve Enzinger
Hydromechanics Lab
U. S. Naval Academy
Annapolis, Maryland 21402

Mr. Robert Falls
Maritime Administration
Code M940
14th Street, S.E.
Washington, D. C. 20005

Mr. James A. Fein
DTNSRDC Code 1572
Bethesda, Maryland 20084

Mr. David Ferris
Westinghouse Ocean Research & Engr.
Annapolis, Maryland 21402

Mr. Nathan R. Fuller
Code 6136 NAVSEC
Department of the Navy
Washington, D. C. 20362

LCDR Kenneth Fusch
Naval Systems Engineering Dept.
U. S. Naval Academy
Annapolis, Maryland 21402

Mr. Thomas P. Garraway
CAA Scientific
P.O. Box 1234
Darien, Conn. 06820

Mr. Larry Gear
ABA Electromechanical Systems, Inc.
P.O. Box 500
Pinellas Park, Florida 33565

Mr. Walt Gearhart
Applied Research Lab
P.O. Box 30
State College, PA 16801

Dr. John Gebhardt
CADCOM, Inc.
Annapolis, Maryland 21403

Mr. Morton Gertler
HYDRONAUTICS, Inc.
7210 Pindell School Road
Laurel, Maryland 20810

Dr. Julio G. Gianotti
Gianotti & Buck Assoc. Inc.
5711 Sarvis Ave., Suite 402
Riverdale, Maryland 20840

Mr. John Dallas Gill
Harbor Branch Foundation
2824 Solomons Island Road
Edgewater, Maryland 21037

Prof. T. C. Gillmer
1 Shipwright Harbor
Annapolis, Maryland 21401

Mr. Bill Glaser
AKROEX, Inc.
Annapolis, Maryland

Ms. Ruth S. Goldberg
DTNSRDC Code 1524
Bethesda, Maryland 20084

Mr. Daniel J. Goldstein
NAVSEC Code 6136
Department of the Navy
Washington, D. C. 20362

Mr. Alex Goodman
HYDRONAUTICS, Inc.
7210 Pindell School Road
Laurel, Maryland 20810

Dr. D. Gospodonetic
National Research Council
2140 Dutton Cresc
Ottawa, Ontario KIJ 6K4, Canada

Mr. Bernard Grabois
ITT Gilfillan
P.O. Box 7713
Van Nuys, California 91409

Mr. Paul S. Granville
DTNSRDC
Code 1541
Bethesda, Maryland 20034

Mr. Tom Harrington
NAVSEC
Departmemt of the Navy
Washington, D. C. 20362

LCDR Bill Harris
Naval Systems Engineering Dept.
U. S. Naval Academy
Annapolis, Maryland 21402

Midshipman Chris Hartman, 1/C
Bancroft Hall
U. S. Naval Academy
Annapolis, Maryland 21402

Mr. Bruce W. Harting, President
ABA Electromechanical Systems, Inc.
P.O. Box 500
Pinellas Park, Florida 33565

Mr. Richard Hecker
DTNSRDC Code 1524
Bethesda, Maryland 20084

Dr. Robert Henderson
Applied Research Lab
P.O. Box 30
State College, PA 16801

Mr. Henk Heslinga
Delft Hydraulics Lab
P.O. Box 177
Delft, The NETHERLANDS

Mr. John Hill
Hydromechanics Lab
U. S. Naval Academy
Annapolis, Maryland 21402

Prof. Dan Hoffman
Webb Institute of Naval Arch.
Glen Cove, New York 11542

Mr. Carvel Holton
Hydromechanics Lab
U. S. Naval Academy
Annapolis, Maryland 21402

Prof Jack Hoyt
Naval Systems Engineering Dept.
U. S. Naval Academy
Annapolis, Maryland 21402

Mr. John Hoyt
Hydromechanics Lab
U. S. Naval Academy
Annapolis, Maryland 21402

Dr. C. Hsu
HYDRONAUTICS, Inc.
7210 Pindell School Road
Laurel, Maryland 20210

Dr. Thomas T. Huang
DTNSRDC Code 1552
Bethesda, Maryland 20084

Mr. John F. Ince
U. S. Dept. of Commerce
Maritime Administration
Washington, D. C. 20230

19

Mr. Douglas S. Jenkins
DTNSRDC Code 1524
Bethesda, Maryland 20084

Mr. Stuart Jessup
DTNSRDC Code 1544
Bethesda, Maryland 20084

Prof. Bruce Johnson
Naval Systems Engineeering Dept.
U. S. Naval Academy
Annapolis, Maryland 21402

Mr. Robert A. Johnson
NAVSEC Code 6136
Department of the Navy
Washington, D. C. 20362

Dr. Robert S. Johnson
NAVSEC Code 6114
Department of the Navy
Washington, D. C. 20362

Mr. William E. Jones
Experimental Engineering, LTD
Niagra Falls, Canada

Mr. Marvin J. Kahn, President
AAI Corporation
P.O. Box 6767
Baltimore, Maryland 21204

Mr. Gabor Karafiath
DTNSRDC Code 1532
Bethesda, Maryland 20084

Dr. Paul Kaplan
Oceanics Inc.
Plainfield, N. J.

RADM Draper L. Kauffman, USN (Ret)
P.O. Box 1088
Ponte Verdra Beach, Florida 20362

Mr. Robert G. Keane
NAVSEC Code 6136
Department of the Navy
Washington, D. C. 20362

LCDR Bill Kelly, RN
Naval Systems Engineering Dept.
U. S. Naval Academy
Annapolis, Maryland 21402

RADM Randolph W. King, USN (Ret)
Executive Director
Maritime Transportation Research Bd.
2101 Constitution Avenue
Washington, D. C. 20418

Ensign Kevin Kinports
U. S. Naval Academy
Annapolis, Maryland 21402

Mr. Karl Kirkman
HYDRONAUTICS, Inc.
7210 Pindell School Road
Laurel, Maryland 20810

Dr. T. Kowalski
Dept. of Ocean Engineering
University of Rhode Island
Kingston, Rhode Island 02881

Midshipman Jon Kutler, 1/C
Bancroft Hall
U. S. Naval Academy
Annapolis, Maryland 21403

Dr. H. Lackenby
White Cottage
Orchard Dell
West Chillington, Pulborough
West Sussex RH20 2LB
ENGLAND

Dr. Pierre LaFrance
DTNSRDC Code 1532
Bethesda, Maryland 20084

Mr. Alexander C. Landsburg
U. S. Dept. of Commerce
Maritime Administration
Washington, D. C. 20230

Mr. Fred Lange
MTS Systems Corp.
Box 24012
Minneapolis, Minnesota 55424

Mr. Aden C. Langford
DTNSRDC Code 1576
Bethesda, Maryland 20084

Prof. Louis Landweber
The University of Iowa
Institute of Hydraulic Research
Iowa City, Iowa 52242

Mr. Marc P. Lasky
U. S. Dept. of Commerce
Maritime Administration
Washington, D. C. 20230

Mr. David R. Lavis
BLA Inc.
1910 Forest Drive
Annapolis, Maryland 21401

Mr. E. J. Lecourt
ARCTEC, Inc.
9104 Red Branch Road
Columbia, Maryland 21045

Dr. Choung M. Lee
DTNSRDC Code 1561
Bethesda, Maryland 20084

Dr. L. J. Leggat
Defense REsearch Establishment Atl.
Grove Street
Dartmouth, Nova Scotia
Canada B2Y 3Z7

Dr. Paulo C. Leone
Inst. De Pesquisas Tecnologicas
Cidade Universitaria, CP 7141
Sao Paulo, Brazil

Mr. George Levine
U. S. Dept. of Commerce
Maritime Administration
Washington, D. C. 20230

Prof Edward V. Lewis
Webb Institute of Naval Arch.
Crescent Beach Road
Glen Cove, New York 11542

Mr. Alan C. Lin
DTNSRDC Code 1524
Bethesda, Maryland 20084

Dr. Wen-Chin Lin
DTNSRDC Code 1524
Bethesda, Maryland 20084

RADM James Lisanby
NAVSEC
Department of the Navy
Washington, D. C. 20362

Mr. Walter H. Livingston
DTNSRDC Code 1572
Bethesda, Maryland 20084

LCDR Sam Lowrie (CAF)
Naval Systems Engineering Dept.
U. S. Naval Academy
Annapolis, Maryland 21402

LT Michael R. Maixner, USN
203A Lyra Drive
So. Weymouth, MA 02190

Mr. Robert A. Major
ARCTEC, Incorporation
9104 Red Branch Road
Columbia, Maryland 21045

Mr. S. T. Mathews
National Research Council of Canada
Marine Dynamics & Ship Lab
Ottawa, Ontario K1A OR6, Canada

Ensign Richard L. Mauren
DTNSRDC Code 1720.6
Bethesda, Maryland 20084

Prof. Dr. L. Mazarredo
Escuela T. S. De Ing. Navales
Ciudad-Universitaria
Madrid 3 Spain

Mr. Ronald J. Mcalear
Avondale Shipyards, Inc.
P.O. Box 50280
New Orelans, LA 70150

Mr. J. McCarthy
DTNSRDC Code 1552
Bethesda, Maryland 20084

Prof Michael E. McCormick
Naval Systems Engineering Dept.
U. S. Naval Academy
Annapolis, Maryland 21402

Mr. Marvin Menkin
MTS Systems Corporation
Box 24012
Minneapolis, Minnesota 55424

Mr. Michael Michailidis
Marine Dynamics & Ship Laboratory
National Research Council
Ottawa, Ontario K1A OR6, Canada

Mr. M. D. Miles
Marine Dynamics & Ship Laboratory
National Research Council
Ottawa, Ontario K1A OR6, Canada

Mr. Gene Miller
HYDRONAUTICS, Inc
7210 Pindell School Road
Laurel, Maryland 20810

Ensign Ronald L. Miller
DTNSRDC Code 1552
Bethesda, Maryland 20084

Mr. Vincent J. Monacella
DTNSRDC Code 1504
Bethesda, Maryland 20084

Dr. Robert F. Mons
Westinghouse Electric Corp.
P.O. Box 1488
Annapolis, Maryland 21404

Dr. David D. Moran
DTNSRDC Code 1552
Bethesda, Maryland 20084

CDR Juan Moreno
Instituto Universitario Politecnico
De Las Fuerzas
Armadas Nacionales (IUPFAN)
La Carlota, Caracas, Venezuela

Dr. William B. Morgan
DTNSRDC Code 154
Bethesda, Maryland 20084

Mr. David C. Murdey
Marine Dynamics & Ship Laboratory
National Research Council
Ottawa, Ontario KIA OR6, Canada

Prof. Bruce Nehrling
Naval Systems Engineering Dept.
U. S. Naval Academy
Annapolis, Maryland 21402

Dr. Evgeny Nikolaev
Head of the Ship Dynamics Lab
Krylov Ship Research Institute
M158 Leningrad USSR

Mrs. Margaret D. Ochi
DTNSRDC Code 1572
Bethesda, Maryland 20084

Dr. John F. O'Dea
DTNSRDC Code 1524
Bethesda, Maryland 20084

Mr. Richard H. Osman
Robicon Corporation
100 Sagamore Hill Road
Pittsburgh, PA 15239

Mr. Frank Ostronic
Program Development
Computer Sciences Corporation
6565 Arlington Blvd.
Fall Church, Virginia 22046

Mr. Anthony Paladino
NAVSEA 037
Department of the Navy
Washington, D. C. 20362

Dr. Blaine R. Parkin
Applied Research Lab
P.O. Box 30
State College, PA 16801

Prof. Michael G. Parsons
Dept. of Naval Arch. & Marine Engr.
U. of Michigan
Ann Arbor, Michigan 48109

Prof. J. R. Paulling
University of California
Dept. of Naval Architecture
College of Engineering
Berkeley, California 94720

Dr. T. Peirce
Naval Sea Systems Command
Code 03512
Department of the Navy
Washington, D. C. 20362

Dr. G. Ross Peters
Engineering & Applied Science
Memorial University
St. Johns, Newfoundland, Canada

Mr. J. Brooks Peters
DTNSRDC Code 1572
Bethesda, Maryland 20084

Dr. Frank B. Peterson
DTNSRDC Code 1552
Bethesda, Maryland 20084

Mr. Robert S. Peterson
DTNSRDC Code 1630
Bethesda, Maryland 20084

Mr. Paul Peterson, Consultant
MTS Systems Corporation
Box 24012
Minneapolis, Minnesota 55424

Dr. P. C. Pien
DTNSRDC Code 1521
Bethesda, Maryland 20084

Mr. John Piraino
MTS Systems Corporation
Box 24012
Minneapolis, Minnesota 55424

Dr. M. A. Plint
Plint & Partners LTD
Fishponds Road
Wokingham, Berkshire RG11 2QG

Prof. Allen Plotkin
Dept. of Aerospace Engineering
University of Maryland
College Park, Maryland 20742

Midshipman Anthony Quatroche, 1/C
U. S. Naval Academy
Annapolis, Maryland 21402

Mr. John Reason
American Bureau of Shipping
45 Broad Street
New York, New York 10004

Mr. Earl I. Reinhardt
MTS Systems Corporation
Box 24012
Minneapolis, Minnesota 55424

Mr. Kenneth D. Remmers
DTNSRDC Code 1524
Bethesda, Maryland 20084

Dr. Wolfgang Reuter
Naval Ship Engineering Center
Crystal City
Arlington, Virginia 20362

Mr. Edward Richard
DTNSRDC
Bethesda, Maryland 20084

Midshipman David Rigdon, 1/C
U. S. Naval Academy
Annapolis, Maryland 21402

Mr. Robert F. Roddy
DTNSRDC Code 1524
Bethesda, Maryland 20084

Mr. L. C. Ruth
ADTECH
9750 Duffer Way
Gaithersburg, Maryland 20760

LCDR Ron Ruys, USN
Naval Systems Engineering Dept.
U. S. Naval Academy
Annapolis, Maryland 21402

Dr. Nils Salvesen
DTNSRDC Code 1552
Bethesda, Maryland 20084

Mr. Gabriel L. Santore
DTNSRDC Code 1556
Bethesda, Maryland 20084

Dr. Daniel Savitsky
Davidson Laboratory
Stevens Inst. of Technology
Hoboken, New Jersey 07030

Mr. Norman Scheffner
Waterways Experiment Station
Chesapeake Bay Office
P.O. Box 148
Stevensville, Maryland 21666

Mr. J. Otto Scherer
HYDRONAUTICS, Inc.
7210 Pindell School Road
Laurel, Maryland 20081

Dr. Ing. M. Schmiechen
Versuchasanstalt Fur Wasserbau
Und Schiffbau
1 Berlin 12 Schleuseninsel
Federal Republic of Germany

Mr. R. T. Schmitke
Defense Research Est. Atlantic
P.O. Box 1012
Dartmouth, N.S. Canada

Dr. K. E. Schoenherr
7053 Western Avenue, N.W.
Washington, D. C. 20015

Dr. Carl A. Scragg
DTNSRDC Code 1524
Bethesda, Maryland 20084

Mr. Alfred C. Seebode
409 Kings Highway South
Cherry Hill, New Jersey 08034

Mr. Frederick Seibold
Manager, Marine Sciences Prog.
Office of Maritime Technology
U. S. Dept. of Commerce
Maritime Administration
Washington, D. C. 20230

Mr. Larry S. Shrout
Mail Stop 73-07
The Boeing Company
P.O. Box 3707
Seattle, Washington 98124

Mr. Bill Smith
DTNSRDC Code 1576
Bethesda, Maryland 20084

Mr. David M. Smith
Computer Sciences Corp.
6565 Arlington Blvd.
Falls Church, Virginia 22046

Dr. Manley St. Denis
Naval Systems Engineering Dept.
U. S. Naval Academy
Annapolis, Maryland 21402

Ensign Christopher L. Stathos
DTNSRDC Code 1524
Bethesda, Maryland 20084

Mr. Eric S. Strasel
DTNSRDC Code 1524
Bethesda, Maryland 20084

Mr. John Stricker
DTNSRDC Code 2721
Bethesda, Maryland 20084

Mr. William Tam
Marine Research Center
Chicago Bridge and Iron
Plainfield, Ill, 60544

Mr. Marshall P. Tulin
HYDRONAUTICS, Inc.
1101 15th St., N.W. Suite 701
Washington, D. C. 20005

Dr. Paul R. Van Mater
Gianotti & Buck Assoc, Inc.
5711 Sarvis Ave., Suite 402
Riverdale, Maryland 20840

CDR George P. Vance
Engineering Department
U. S. Coast Guard Academy
New London, Conn.

Mr. Richard L. Van Iderstine
U. S. Navy Oceanographic Office
Suitland, Maryland

Mr. Lyssimachos Vassilopoulos
Marine Vibration Associates
375 Conord Avenue
Belmont, Mass. 02178

Dr. Richard B. Wade
TETRA TECH
630 N. Rosemead
Pasadena, California 91107

Captain John R. Wales, USN
Director, Division of Engr & Weapons
U. S. Naval Academy
Annapolis, Maryland 21402

Prof Chun-Tsung Wang
Director, Inst. of Naval Arch.
National Taiwan University
Taipei, Taiwan, REPUBLIC OF CHINA

Prof. Lawrence W. Ward
Webb Inst. of Naval Arch.
Glen Cove, New York 11542

Mr. Randy Watkins
Hydromechanics Laboratory
U. S. Naval Academy
Annapolis, Maryland 21402

Dr. John V. Wehausen
University of California
Dept. of Naval Architecture
Berkeley, California 94720

Mr. Herman Wente
Sandia Laboratories, Div 1335
Albuquerque, N. M. 87115

Mr. Raymond Wermter
DTNSRDC Code 1520
Bethesda, Maryland 20084

Mr. Eugene E. West
DTNSRDC Code 1524
Bethesda, Maryland 20084

Mr. Joseph M. Wetzel
St. Anthony Falls Hydraulic Lab
Mississippi River at 3rd Ave., S.E.
Minneapolis, Minnesota 55414

Mr. Patrick Whyte
56 Hampton Green
Colby Village
Darmouth, Nova Scotia
Canada B2V

25

Midshipman Paul A. Wiedorn, 1/C
U. S. Naval Academy
Annapolis, Maryland 21402

Dr. Peter F. Wiggins
Chairman, Naval Systems Engr Dept.
U. S. Naval Academy
Annapolis, Maryland 21402

Mr. Daniel L. Wilkins
Marine & Aero Designs
2824 Solomons Island Road
Edgewater, Maryland 21037

Dr. Michael B. Wilson
DTNSRDC Code 1532
Bethesda, Maryland 20084

Dr. Theodore Y. Wu
Prof. of Engineering Science
California Inst. of Technology
Pasadena, California 91125

Mr. Hugh Y. Yeh
DTNSRDC Code 1524
Bethesda, Maryland 20084

Dr. Bohyum Yim
DTNSRDC Code 1542
Bethesda, Maryland 20084

Dr. Konstantin Zagustin
Instituto De Mecanica De Fluidos
Facultad De Ingenieria
Universidad Central De Venezuela
Caracas, Venezuela

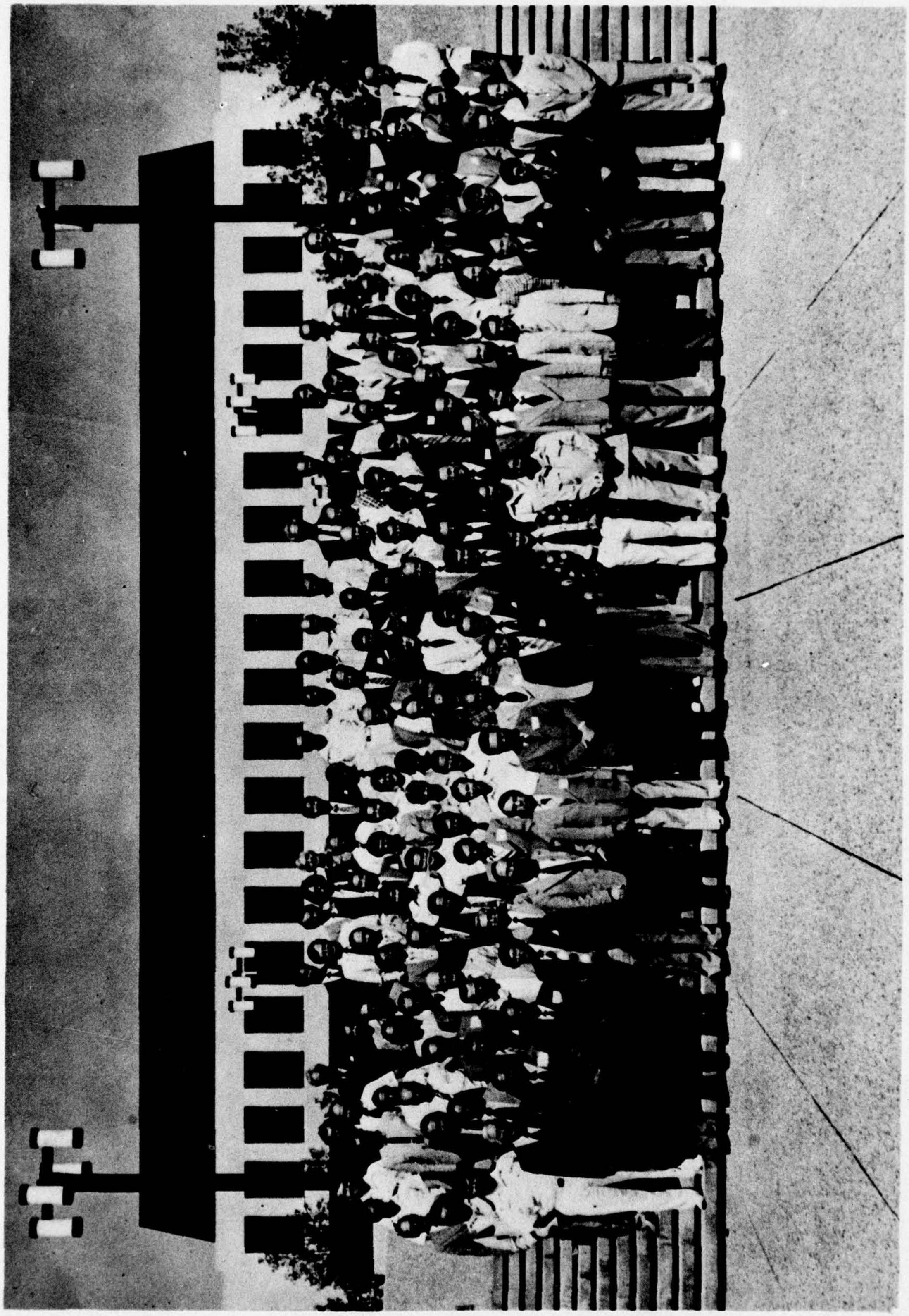

NOTES FOR GUIDANCE

AIMS AND ORGANIZATION OF THE AMERICAN TOWING TANK CONFERENCE

The American Towing Tank Conference is a voluntary association of establishments having a responsibility in the prediction of hydromechanic performance of ships and other waterborne craft and their appendages from tests on scaled models.

The objective of the Conference is to promote exchange of knowledge between tank staffs for the purpose of improving methods and techniques. This includes an exchange of knowledge on the design of facilities, equipment and instrumentation, on experimental and construction techniques, and on scaling laws. As a means to this end, the Conference seeks to correlate testing among the various member establishments in order to facilitate the interpretation of experience, and to issue standards.

The Conference seeks to attain its objective by holding formal meetings triennially and through the encouragement of informal working relationship among the member establishments.

Membership in the Conference is by establishment and is open, upon invitation, to all establishments in the western hemisphere. All the member establishments agree to the free and full exchange of all information on the foregoing subjects which is neither proprietary nor of a classified military nature. (To that end mutual agreements on exchange of publications and data of interest will be entered into.)

The members or delegates will be persons holding positions of primary responsibility in Towing Tanks or Water Tunnels, Shipbuilding Research Associations or Departments of Naval Architecure of a University in which prominence is given to the subjects pertaining to the objects of the Conference. A few delegates can be invited who were not qualified as above but who have rendered services to the aim of Conference, as well as observers.

The Conferences assembles from time to time in different countries of the American Continent. Since 1938 it has assembled at three-year intervals.

The details of organization of any particular Conference is the responsibility of the host country.

The Conference is a purely communicative body; it has no authority of financial sponsorship; its membership is voluntary and self-supporting.

Each establishment may be represented by one or more members at triennial formal meetings of the Conference.

Although representation is not limited, it is the intent that it be kept reasonably small so that fruitful discussions can be obtained at the working level. The Conference intends to meet formally at each of the member establishments in rotation, the sequence being decided by the membership.

The scope of the Conference is set by the Executive Committee, based on the recommendations of the previous general meetings.

The Executive Committee shall comprise the nominated representatives of the Institutions at which the last three conferences were held plus Chairman of the S.N.A.M.E. Hydrodynamics Committee, plus the representative of the Institution at which the next Conference is to be held.

In the event that the Chairman of the Hydrodynamics of S.N.A.M.E. does not serve as a member of the Executive Committee of the A.T.T.C., the Executive Committee may invite

28

another official to serve on the Executive Committee.

If a member of the Executive Committee resigns, a replacement shall be selected by his institution.

Also the American representative on the I.T.T.C. Standing Committee shall, ex-officio, be a member of the A.T.T.C. Executive Committee.

The A.T.T.C. membership of the Standing Committee of the I.T.T.C. will be rotated. The representative will normally serve through two I.T.T.C. Conferences.

The A.T.T.C. representative on the I.T.T.C. Standing Committee shall:

a. hold a senior position in a model basin;

b. be acquainted with the operation of the I.T.T.C.;

c. have means for financing attendance at an annual meeting of the I.T.T.C. Executive Committee.

A newly appointed A.T.T.C. representative on the I.T.T.C. Standing Committee shall take office after the I.T.T.C. Conference subsequent to the A.T.T.C. Conference at which he is appointed.

The Chairman of the Executive Committee shall be the nominated representative of the Institution at which the next Conference is to be, viz, he is the Chairman of the next Conference.

The Secretary of the A.T.T.C. shall be any person so nominated by the Conference Chairman.

The Executive Committee shall appoint Chairman of such Technical Committees as are felt necessary for the effective conduct of the Conference.

The Chairman of such Technical Committees will appoint such persons as they consider necessary for the effective conduct of such Committees, and further will be responsible for the production of the State-of-the-Art reports and the soliciting of papers to be presented to the Conference.

The accepted reports by the staff of the Conference are discussed in the Technical Sessions during the meetings, first formally and then informally. To this end, those reports are previously forwarded, well in advance of the dates of the Conference, to the Chairman of the Conference Organizing Committee, who arranges for copies to be transmitted to each member. The same applies to the formal contributions which any member may make to the Conference. If the Chairman of the Technical Committee considers that any contribution is unacceptable to be concerned, as the object of the Conference, he should reject it.

The Chairman of each Technical Session, in association with the Chairman of the Technical Committee concerned, formulate decisions and recommendations arising from the Session. The decisions and recommendations will then be considered and agreed upon at the concluding Session of the Conference.

The Chairman of the Conference Organizing Committee will arrange for the publication of the Proceedings of the Conference.

The venue of the next Conference is subject to the invitation of an Institution, and such invitation shall be accepted by the Executive Committee after a vote of the delegates present at the Business Meeting.

MEETINGS OF THE AMERICAN TOWING TANK CONFERENCE

1st	14 - 15 April 1938	Experimental Towing Tank Hoboken, New Jersey
2nd	19 - 20 September 1939	1st day - Receiving Ship Building Navy Yard, Washington 2nd day - David Taylor Model Basin
3rd	14th November 1940	Waldorf Astoria, New York, N. Y.
4th	14th November 1941	Waldrof Astoria, New York, N. Y.
5th	29 - 30 September 1943	David Taylor Model Basin
6th	12 - 13 November 1946	Experimental Towing Tank Hoboken, New Jersey
7th	7 - 8 October 1947	Newport News Shipbuilding & Dry Dock Co., Newport News, Va.
8th	11 - 13 October 1948	University of Michigan, Ann Arbor, Michigan
9th	11 - 14 September 1950	National Research Council of Canada Ottawa, Canada
10th	4 - 6 May 1953	Massachusetts Institute of Technology, Cambridge, Mass.
11th	12 - 14 September 1956	David Taylor Model Basin Washington, D. C.
12th	31 Aug - 2 Sep 1959	University of California, Berkeley, California
13th	5 - 7 September 1962	University of Michigan, Ann Arbor, Michigan
14th	9 - 11 September 1965	Webb Institute of Naval Architecture, Glen Cove, N. Y.
15th	25 - 28 June 1968	National Research Council of Canada, Ottawa, Canada
16th	9 - 13 August 1971	Instituto de Pesquisas Tecnólogicas São Paulo, Brazil
17th	18 - 20 June 1974	California Institute of Technology Naval Undersea Center Pasadena, California
18th	23 - 25 August 1977	U. S. Naval Academy Annapolis, Maryland

30

18th

AMERICAN TOWING TANK CONFERENCE
Annapolis, Maryland USA

REPORT OF RESISTANCE AND FLOW COMMITTEE

August 1977

United States Naval Academy

REPORT OF RESISTANCE AND FLOW COMMITTEE

The report of the Resistance and Flow Committee is dedicated to the memory of Roger Brard, who, for many years, was Chairman of the Resistance Committee of the International Towing Tank Conference. Under his leadership, the Committee actively monitored and reported on progress in the various aspects of the determination and prediction of ship resistance, a field to which he applied his unusual mathematical talents to make major personal contributions. As a former towing-tank director, he was interested in all aspects of ship hydrodynamics, and especially contributed to the theory of ship maneuverability. He will be missed by the ship hydrodynamic fraternity, which has lost one of its brightest stars.

Because the Committee has not met prior to the present conference, and state-of-the-art reports and other contributions were not submitted in advance, it has not been possible to prepare a Committee report. As a basis for discussion, the Chairman proposes the following recommendations:

1. Towing tanks should acquire equipment and adopt techniques for determining viscous resistance by means of wake surveys and wave resistance by means of wave-pattern measurements. The effect of tank seiche on the wake-survey and wave-pattern measurements should be considered.

2. The effects of the boundary layer and wake on the wave resistance determined from wave-pattern measurements should be investigated.

3. Measurements of the pressure distribution and the three-dimensional boundary layer on a ship model and on full scale at various Froude numbers should be undertaken. Several sets of such model measurements at "zero" Froude number are already available. The results should be compared with predictions from three-dimensional boundary-layer theory.

4. Separation of flow is a much more complex phenomenon in a three-dimensional boundary layer than on a two-dimensional or axisymmetric one. An experimental investigation is needed to identify regions of separation along a hull, and the effects of Reynolds number.

5. There has recently been considerable progress in the development of higher-

order ship wave theory. This theory should be applied to compute the wave resistance of a ship form at various Froude numbers.

6. Various phenomena that occur at the bow of a ship model, such as the extent of laminar flow, wave breaking, and the formation of bilge vortices, require experimental and theoretical investigation.

SHIP BOUNDARY-LAYER RESEARCH SINCE ABOUT 1974:
A PROGRESS REPORT

by

Justin H. McCarthy

David W. Taylor Naval Ship Research & Development Center

INTRODUCTION

This survey briefly reviews progress in ship boundary-layer research, both theoretical/computational and experimental, since about 1974. The review covers the following topic areas: laminar boundary-layer instability and transition; axisymmetric boundary layers; equivalent bodies of revolution; three-dimensional ship boundary layers; and one paper on flat-plate boundary layers. Except for the brief section on stability and transition, only turbulent boundary layers, on smooth surfaces, are discussed. The very complex problem of turbulent flow separation* on ship sterns, bilge and shoulder vortices, and the interaction between surface-ship wave making and boundary-layer development are only mentioned in passing. Drag reduction by polymer additives or compliant coatings is not discussed.

While major efforts have been expended on boundary-layer research over the past several years, and significant progress has been made, totally reliable methods are not yet available for computing the thick boundary layers which exist on the afterbodies of either axisymmetric or three-dimensional hulls. Thus, solutions of the crucial problems of predicting ship form drag and propeller inflow velocities, at both model and full-scale Reynolds numbers, remain to be completed. Successful solution of the stern flow problem will require more experimental data, to provide the empirical information needed to evaluate boundary-layer theory, and development of more advanced computational methods to treat the complex interaction of the stern boundary layer with the outer potential flow.

LAMINAR BOUNDARY-LAYER INSTABILITY AND TRANSITION

Methods for computing the stability of general three-dimensional laminar boundary layers are not available. However, since 1973, largely-unpublished major effects, mostly in the United States, have been undertaken to develop and experimentally evaluate methods for the prediction of laminar-flow boundary-layer

*Flow separation on two- and three-dimensional bodies is treated at length in numerous papers published in AGARD Conference Proceedings No. 168, the proceedings of a Fluid Dynamics Panel Symposium held in Gottingen during May 1975.

instability and transition to turbulent flow on axisymmetric bodies. This work has been motivated mainly by a desire to develop techniques for the design of low-drag underwater bodies which maximize the extent of laminar flow by slowing the growth rate of boundary-layer instabilities through careful choice of body shape and/or use of surface heating. Reshotko (1976) and Berger and Aroesty (1977) give general reviews of the current state-of-knowledge on boundary-layer stability and transition. The basic problem of quantitatively and fundamentally coupling the growth of boundary-layer instabilities with the transition process remains unsolved and must be treated empirically. In the absence of significant external disturbances, e.g., ambient turbulence and surface roughness, the most reliable predictions of the initial growth of laminar boundary-layer instabilities, on two-dimensional or axisymmetric bodies, have been obtained from numerical solutions of the Orr-Sommerfeld equations for linear stability, following the computational prescriptions laid down by Smith and Gamberoni (1956) and Wazzan, Okamura and Smith (1968). Within this framework, Kosekoff, Ko and Merkle (1976) have proposed accounting for the global effects of distributed surface roughness through an enhanced viscosity in the laminar boundary-layer momentum equations; the added viscosity prodcues distorted mean velocity profiles which tend to destabilize the boundary layer. The coupling between ambient free-stream turbulence and boundary-layer instabilities is poorly understood.

Fluctuating surface shear stresses and/or pressures in regions of flow transition on axisymmetric bodies have been experimentally investigated by Arakeri (1975), McCarthy, Power, and Huang (1976) and Huang and Hannan (1976). For relatively fine, convex bodies undergoing natural flow transition, in the absence of laminar separation or turbulence stimulators, hot-film and microphone data indicate that the frequency bands of the most unstable Tollmein-Schlichting waves are satisfactorily predicted by linear stability theory. McCarthy, et al (1976) found that measured locations of natural flow transition on relatively fine forebodies correlated well with computed disturbance amplification ratios, A/A_o, of e^{11}, where A_o is the initial disturbance amplitude at the location of neutral stability. Subsequent experiments by Power (1977) on models having relatively blunt bows revealed that natural transition occurred at significantly lower values of A/A_o, down to about e^6. Thus, transition is not uniquely correlated with a single value of amplification ratio computed from linear stability theory, but depends on body shape as well as other factors. In the case of axisymmetric bodies which experience laminar separation, its occurrence and location were accurately predicted by the Curle-Skan modified-Thwaites pressure-gradient criterion. The experimental data showed that the extent of the separation bubble over which transition to turbulent flow occurred was very short at body-diameter Reynolds numbers of about 10^6.

From a "tankery" standpoint the most important findings of the investigations of McCarthy, Power, and Huang (1976) and Power (1977) were the quite far aft locations of transition on untripped axisymmetric bodies, in some cases about 10-percent of model length, even at model length Reynolds numbers as high as 4×10^7. In some data-analysis methods, it is assumed that the parasitic drag of a turbulence trip, normally located at 5-percent of model length, can be closely estimated as the difference between the measured values of model resistance with and without the trip installed, at the highest model speeds investigated. In cases where natural transition on the smooth body occurs further aft than the trip location, stimulator drag will be overestimated and the residual (or form) drag of the hull can be seriously underpredicted. For competing forebody shapes the relative drags can also be mispredicted because of different extents of laminar flow. A data analysis method to avoid this problem on axisymmetric bodies is proposed in the paper by McCarthy, et al.

AXISYMMETRIC BOUNDARY LAYERS

Considerable progress has been made since 1974 towards developing improved analytical methods for predicting turbulent boundary layers on bodies of revolution. Significant gains, both theoretical/computational and experimental, have taken place in the understanding and modeling of the thick boundary layers which occur on axisymmetric sterns. For cases in which flow separation does not occur, a number of promising new methods are now available for computing stern flows and body drag at both model and full-scale Reynolds numbers. However, further verification of the methods is required and the problem of separated stern flow still remains to be solved. The most recent attempt to analyze axisymmetric afterbody separation appears to be due to Presz and Pitkin (1974, 1976).

On the experimental side, extensive new model stern pressure, shear stress and velocity data have been obtained by Patel, Nakayama and Damian (1974) for a prolate spheroid having a conical tail; by Huang, Wang, Santelli and Groves (1976) for three sterns of increasing fullness, two convex and one inflected, the latter having separation at the shoulder; and by Patel, Lee and Guven (1977) for a laminar-flow body having a cusped tail. Related experimental data for the thick boundary layer on a long circular cylinder are given by Afzal and Singh (1976). All of these new data have proven extremely valuable for motivating and evaluating new boundary-layer prediction methods. The experimental investigations have shown that the tail pressure distribution is the result of a complex interaction of the thick boundary layer with the outer potential flow. The experimental data of Patel and his coworkers show that transverse pressure gradients across the boundary layer, and longitudinal and transverse curvature effects, are important factors when computing stern boundary-layer development. Thus, conventional thin-

boundary-layer theory is not adequate for treating the tail flow on bodies of revolution.

The initial experimental data described above led Patel (1974) and Granville (1975b) to develop simple integral-entrainment methods for calculation of the velocity-profile shape parameter of thick boundary layers. Both works neglected normal stress effects and employed an axisymmetric form of Head's entrainment equation; Patel used a simple power-law family of velocity profiles and Granville used the velocity similarity laws to cover a range of Reynolds numbers. Patel recommended that experimental values of tail pressure distribution be used to account for the transverse pressure change across the boundary layer. Subsequently, Nakayama, Patel and Landweber (1976) devised an iterative method for computing the interaction between the exterior potential flow and the interior boundary-layer/wake flow subject to the condition that the velocity remains continuous across the outer edge of the boundary layer and wake. The additional pressure and curvature terms that appear in the momentum-integral equation for the thick boundary layer and near wake were retained and the pressures on the body surface and the edge of the boundary layer and wake were iteratively computed. Agreement between computed and measured body surface pressures was shown to be good for the two bodies considered; the pressure coefficients along the outer edge of the boundary layer and wake were over-predicted in the tail region. Body drags were over-predicted by 5- to 10-percent.

A second theoretical/numerical method to cope with thick boundary layers has recently been proposed by Dyne (1977). In this "streamline curvature" method, thin-boundary-layer theory is used to compute boundary-layer velocity profiles forward of some point on the stern; by extrapolation, tail streamlines which satisfy continuity are then constructed. The momentum equations are subsequently iteratively satisfied both along and across streamlines, beginning with the assumptions that the transverse pressure gradient is simply related to the longitudinal velocity and curvature along a streamline, and that total head is preserved along streamlines. In principal the method appears to embody the generality of the method developed by Nakayama, Patel and Landweber (1976), although the iterative approach is different. In each case agreement between theoretical and measured pressure distributions is about the same. Computed boundary-layer velocity profiles by Dyne's method are in good agreement with experimental data for the one case considered. More stringent tests of the methods proposed by both Nakayama, et al and Dyne are required for non-separating sterns having low length/diameter ratios.

Still another method, developed by Huang, et al (1976, 1977), short-circuits the complex thick-boundary-layer, transverse-pressure-gradient problem by iteratively computing pressures on the boundary-layer displacement - thickness surface, and its extension into the wake, in a manner similar to that proposed by Myring (1972,

1976). Huang's work includes treatment of propeller - induction effects on stern boundary-layer development and provides a rational method for theoretically computing the change from the nominal wake distribution to the effective wake distribution experienced by a propeller at both model and full-scale Reynolds numbers. The basic boundary-layer computations employ a simple modification of the differential/eddy-viscosity approach of Cebeci and Smith (1974). In the modification, the thin-boundary-layer calculations are assumed accurate only up to about 95-percent of body length; far-field wake characteristics, which depend on total drag, are marched upstream to about 5-percent of body length downstream of the body. A quintic polynomial with adjustable coefficients is then used to represent the displacement thickness in the stern/near-wake region, and the final stern pressure distribution is iteratively computed starting with the body potential-flow pressure distribution and an estimated body drag. Agreement between computed and measured pressure, shear stress, and velocity distributions is shown to be good for a relatively fine stern, similar to the sterns studied by Patel and Dyne. For two fuller sterns, the fullest having shoulder separation, agreement between theory and experiment was not good. However, the location of flow separation (zero shear stress) on the fullest stern was accurately predicted.

Several comparisons of theoretical thin-boundary-layer predictions of axisymmetric body drag with model experimental data have appeared since 1973. Nakayama and Patel (1973) used Granville's form of the Squire-Young formula to compute values of drag on the hull up to successively further aft stations on the stern. The predicted drag was simply taken to be the maximum of the values computed along the stern, thereby crudely accounting for the thick-boundary-layer pressure defect on the stern. Drag predictions were in good agreement with most of Gertler's (1950) experimental drag data for Series 58 models. Hess (1976) concluded that a version of the simple integral drag formula of Granville (1953, 1974), evaluated in the same "maximum-drag" manner as above, gave as good or better drag predictions for selected Series 58 models than the elaborate thin-boundary-layer differential method of Cebeci and Smith (1974). White (1977) subsequently concluded, from a comparison with experimental drag data for about 50 models, including Series 58, that the simple drag formula tended to over-predict drag and was not generally reliable for predicting the order of merit of competing hull shapes. Kerney and White (1975), using an updated version of Granville's (1953) thin-boundary-layer momentum-integral approach, also found that drags tended to be over-predicted. It is worth noting that care must be exercised when making comparisons between theory and experiment because some drag data, such as drag data for the Series 58 models, may suffer from the effects of significant (and variable) lengths of laminar flow on the bow (see McCarthy, Power, and Huang (1976)). In some cases theoretical methods may only appear to over-predict drag.

EQUIVALENT BODIES OF REVOLUTION

Because of the difficulties associated with computation of fully three-dimensional boundary-layer flows, it has been suggested that an "equivalent body-of-revolution" representation of a ship might yield satisfactory predictions of ship friction and form drags when evaluating competing hull forms. Granville (1973, 1975a), and more recently Garcia and Zarzurco (1976), have further proposed that partial form factors for ship models be deduced from boundary-layer theory using an "equivalent body-of-revolution" approach to analyze the drag data rather than the traditional "constant form-drag" approach of Froude. Granville argues, from physical reasoning, that the equivalent body-of-revolution to be used to compute pressure distribution should have the same longitudinal distribution of cross-sectional area as a reflex model of the ship; boundary-layer development is then to be calculated for an equivalent body-of-revolution having the reflex model's longitudinal distribution of wetted area. Nakayama, Patel, and Landweber (1974) found that either definition of the equivalent body of revolution, in the case of LUCY ASHTON, results in nearly the same drag predictions. Limited support of the notion that form drag depends only on the gross characteristics of a ship may be derived from the experiments of Grim and Blume (1975) on two hulls having different beams and bilge radii but the same distributions of sectional area. Evaluation of their drag data using the Hughes-Prohaska extrapolation method showed both hulls to have nearly the same values of form factor. Matheson and Joubert (1974) and Joubert, Sinclair and Hoffman (1977) have shown experimentally that equivalent bodies of revolution having the same surface area distributions as reflex models of LUCY ASHTON and a block coefficient 0.80 tanker do not provide good representations of the longitudinal distributions of average hull shear stress or pressure. In cases where three-dimensional bilge or shoulder vortices and stern flow separation occur, the equivalent body-of-revolution approach is unlikely to be very useful. Because of its intrinsic simplicity, however, additional work should be conducted to further evaluate the equivalent-body-of-revolution approach for predicting ship drag. A much larger family of hull types than heretofore considered should be evaluated, with emphasis on hulls not having significant flow separation. Perhaps an equivalent body of revolution defined to have the reflex model's longitudinal distribution of girthwise-mean potential-flow pressure would produce better results. Adoption of thick-boundary-layer methods to calculate the stern boundary-layer might also be helpful in some cases, yielding better predictions of drag and perhaps reasonable estimates of the circumferential-mean nominal wake profiles at the propeller plane.

THREE-DIMENSIONAL SHIP BOUNDARY LAYERS

In a 1975 review of three-dimensional boundary-layer theory, Eichelbrenner concluded that the only available computational methods were integral methods which

relied on too many simplifying assumptions to be reliable, and that extensive new experimental research was essential for further progress. Since 1975 there has been a great increase in the amount of research on external three-dimensional turbulent boundary layers, both theoretical/computational and experimental. Several additional ship model boundary-layer experiments have been conducted thereby providing an expanded data base for evaluation of theoretical computations. Unfortunately, despite improvements in theoretical/computational methods, by both integral and differential approaches, the pressure, shear stress and velocity distributions on ship sterns can not be accurately and reliably computed; only the relatively-thin boundary-layer flow forward of the stern can be satisfactorily predicted. Problems can also arise in the bow region if strong crossflows or bilge vortices occur. As in the case of axisymmetric bodies, the stern difficulties result from inadequate treatment of the complex interaction between the thick stern boundary layer and the outer potential flow; this is true even in cases where bilge or shoulder vortices are not present and significant stern flow separation does not occur. Another difficulty when performing calculations arises from the problem of how and where to specify the initial and boundary conditions, either theoretically or experimentally, when commencing the turbulent boundary-layer computations. The further problem of specifying a ship's potential-flow pressure distribution in the presence of a free surface is also not yet solved and will not be addressed here, except to mention that Vollheim (1975a), Himeno (1976), and Adee (1976) have recently proposed approaches to the problem of boundary-layer/wave interaction.

Among numerous recently-published review articles and books dealing, at least in part, with external three-dimensional boundary layers, the following should be mentioned: the survey of integral calculation methods for ships by Kux (1974), the summary of ship boundary-layer research in Japan by Kitagawa (1975), the review of alternative theoretical closure models for boundary-layer equations by Reynolds (1976), the summary of recent computational advances by Nash and Patel (1977); and two books dealing with various aspects of turbulent boundary layers by Cebeci and Smith (1974) and Bradshaw, et al (1976). Tani (1977) gives an interesting history of boundary-layer theory. Fannelop and Krogstad (1975) provide a valuable summary of 23 papers presented at the Euromech 60 Colloquium held in Trondheim on external three-dimensional turbulent boundary layers. Most of the new computational methods presented were based on finite-difference numerical approaches and designed to exploit the capabilities of high-speed digital computers. The majority of the contributions focused on the crossflow problem of swept wings, although some ship-model boundary-layer data were presented. Competitive calculations (the "Trondheim Trials") were made by three integral and six differential methods for a set of seven test problems. In some cases displacement thickness effects were theoretically estimated or experimental pressure distributions employed. The

results showed some large discrepancies between predictions given by the different methods, the location of turbulent flow separation being particularly difficult to predict.

Larsson (1976) summarizes most of the experimental data on ship/model boundary layers obtained prior to 1974. Since then important additional data have been obtained on double models of ship hulls in wind tunnels at length Reynolds numbers on the order of $3\text{-}7 \times 10^6$. Measurements of surface pressures and velocity profiles on double-hull models are given by Hauke (1975) and Vollheim (1975b) for a block coefficient 0.80 hull, and by Larsson (1976) for a block coefficient 0.675 cargo liner. Shear stress, in addition to pressure and velocity, distributions were measured by Sachdeva and Preston (1976) for a full-form tanker model mounted on a ground-board, and by Hoffman (1976) for a double-model of a block coefficient 0.85 bulk carrier. In these experiments pressures were obtained from surface pressure taps, velocities from either 3- or 5-hole pitot tubes or hot wires, and shear stresses from Preston tubes. The quality of the data appears to be excellent and, as well be seen below, the data has served as a basis for evaluation of boundary-layer prediction methods. As could be expected, in all cases cited for which computations were performed, measured stern pressures were lower than pressures computed on the hull surface by potential-flow theory over roughly the last 5-percent of ship length.

Of special interest are the series of boundary-layer velocity measurements of Namimatsu and Muraoka (1974) in the stern region forward of the propeller of RYUKO MARU, a block coefficient 0.83 ship, and two scale models. The full-scale ship is 300m long and the models are 30 m and 7 m long. The principal conclusions of this work were that the stern boundary layer was significantly thinner at full scale than at model scale, and bilge vortices originating in the vicinity of station 2 were present at all scales. Wind-tunnel velocity surveys and pressure and shear stress measurements, with and without a propeller operating, have recently been conducted on a 3 m model of RYUKO MARU by Scragg (1977). Additional stern boundary-layer velocity distributions have been reported by Tanaka, Suzuki and Himeno (1977) for 2 m, 4 m, 7 m, and 10 m geosims of a high-speed container ship. For this range of model sizes the measured change in boundary-layer velocity profiles was significant.

A number of momentum-integral computational methods have been proposed since 1974. Larsson (1975) has developed a method which uses a streamline coordinate system, the Hess-Smith method to compute potential-flow pressures, Head's entrainment equation, Michel's crossflow profile and, initially, a small crossflow approximation which decouples the streamwise and transverse momentum equations. This approach to the boundary-layer calculations is similar to that proposed by von Kerczek (1973), except that Larsson did consider second-order corrections by iteratively introducing the displacement surface for stern pressure calculations and relaxing

the small-crossflow approximation. In the stern region theoretically-computed distributions of shear stress, momentum thickness and crossflow angle, with or without corrections, did not agree well with Larsson's (1976) experimental data for a block coefficient 0.675 cargo liner model. Comparisons with Larsson's data are about the same for predictions made using a small-crossflow integral method developed by Tanaka and Himeno (1975). Tanaka, Suzuki and Himeno (1977) have reported similar poor agreement between stern flows measured on models of a block coefficient 0.80 tanker and a 0.57 container ship and predicted by both the integral methods of Himeno and Tanaka (1975) and Okuno (1976). The latter method employs the small crossflow approximation and Mager profiles, as used by von Kerczek (1973). Sachdeva and Preston (1975, 1976) have developed an integral method which uses a non-orthogonal curvilinear coordinate system, Gadd's potential-flow computation method, and Mager/Johnston crossflow profiles. Predicted girthwise distributions of shear stress, momentum thickness and shape factor were not in good agreement with experimental model data for two ships. Finally, it should be mentioned that Hatano, Mori, Fukashima and Yamazaki (1975) have proposed a method which appears to compute boundary-layer velocity profiles and separation from a surface-vorticity representation of the hull boundary layer.

Finite-difference methods of solution of the three-dimensional boundary-layer equations have been proposed by Cebeci, Kaups and Ramsey (1975) and Chang and Patel (1975). Both methods employ orthogonal curvilinear coordinate systems, the former choosing streamlines as a coordinate and the latter choosing the intersection of the hull by transverse vertical planes as a coordinate. In each method Reynolds stresses are related to the mean-velocity field through an eddy-viscosity model. Neither method attempts to compute viscous corrections to potential-flow pressure distributions, and Cebeci's method adopts the small crossflow approximation. Chang and Patel compute boundary layers on an ellipsoid and a double elliptic hull for which experimental data are not available. Cebeci obtains good agreement between computations and experiment in the case of infinite swept wings. In the case of Larsson's (1976) reflex ship-model data, agreement between predictions of the Cebeci theory and experiment is no better in the stern region than was the case for integral methods; forward of the stern agreement was good, as was the case for integral methods. It is apparent that more complex computational methods must be developed to predict stern boundary-layer flows.

FLAT PLATE BOUNDARY LAYER

Granville (1975c) has derived a new frictional drag-coefficient formula for turbulent flow on flat plates at low values of Reynolds number. The derivation proceeds form the traditionally-assumed overlap of the inner and outer velocity-similarity laws except that at low Reynolds numbers the velocity defect in the

outer portion of the boundary layer is assumed to depend on viscosity as well as the usual variables. The law of the wall remains unchanged, whereas the outer law becomes

$$\frac{U-u}{u_\tau} = A \ln y/\delta + B_2(\sigma),$$

where B_2 is a velocity-defect factor which varies with $\sigma = U/u_\tau$ at low Reynolds numbers; at high Reynolds numbers B_2 is a constant. Integration of the momentum equation and an empirical fit of $B_2(\sigma)$ led to the frictional drag coefficient formula,

$$C_F = \frac{a}{(\log R_n - b)^2} + \frac{c}{R_n}$$

where a=0.0776, b=1.88, and c=60. This formula is a generalization of the form of the ITTC - 1957 correlation line which has a=0.075, b=2, and c=0. Granville's proposed formula is in good agreement with the ITTC - 1957 correlation line at low values of R_x. At high values of R_n the Granville, ITTC, and Schoenherr lines are all in good agreement. Thus, it appears that the ITTC - 1957 model/ship friction correlation line can also be considered a flat-plate line resulting from a low-Reynolds number modification of the same velocity similarity laws which can be used to derive the Schoenherr line for flat plates.

REFERENCES

Adee, B.H. (1976), "Wave-Making and Frictional Resistance for Practical Ship Forms," Proceedings of the International Seminar on Wave Resistance, Tokyo.

Arakeri, V.H. (1975), "A Note of the Transition Observations on an Axisymmetric Body and Some Related Fluctuating Wall Pressure Measurements," American Society of Mechanical Engineers, Journal of Fluids Engineering, Vol. 97, Series 1, No. 1.

Berger, S.A. and Aroesty, J. (1977), "e^9: Stability Theory and Boundary-Layer Transition," Rand Corporation Report R-1998-ARPA, Santa Monica, California.

Bradshaw, P. (editor) (1976), Turbulence, Springer-Verlag, Berlin, Germany.

Cebeci, T. and Smith, A.M.O. (1974), "Analysis of Turbulent Boundary Layers," Academic Press, New York.

Cebeci, T., Kaups, K., and Ramsey, J., (1975), "Calculation of Three-Dimensional Boundary Layers on Ship Hulls," Proceedings of the 1st International Conference on Numerical Ship Hydrodynaimcs, Gaithersburg, Maryland, U.S.A., (see also Douglas Aircraft Company Report MDC J6867, 1975).

Chang, K.C. and Patel, V.C. (1975), "Calculation of Three-Dimensional Boundary Layers on Ship Forms," Iowa Institute of Hydraulic Research Report 178, University of Iowa.

Dyne, G. (1977), "A Theoretical Scale Effect Study on the Propulsion Coefficients of a Body of Revolution," Symposium on Hydrodynamics of Ships and Off-Shore Propulsion Systems, Høvik outside Oslo, Norway.

Eichelbrenner, E.A. (1973), "Three-Dimensional Boundary Layers," Annual Reviews of Fluid Mechanics, Vol. 5, Annual Reviews, Inc., Palo Alto, California, U.S.A.

Fannelop, T.K. and Krogstad, P.A. (1975), "Three-Dimensional Turbulent Boundary Layers in External Flows: A Report on Euromech 60," Journal of Fluid Mechanics, Vol. 71, Part 4.

Garcia, J.M. and Zazurca, J.A.A., (1976), "Calculo de la Resistencia Viscosa de un Buque a Partir de la de Cuerpos de Revolution Equivalentes," Inginieria Naval, Vol. 44.

Gertler, M. (1950), "Resistance Experiments on a Systematic Series of Streamlined Bodies of Revolution for Application to the Design of High-Speed Submarines," David Taylor Model Basin Report C-297.

Granville, P.S. (1953), "The Calculation of the Viscous Drag of Bodies of Revolution," David Taylor Model Basin Report 849.

Granville, P.S. (1973), "A Modified Froude Method for Determining Full-Scale Resistance of Surface Ships From Towed Models," David Taylor Naval Ship Research and Development Center Report 4201 (also Journal of Ship Research, Vol. 18, 1974).

Granville, P.S. (1975a), "Partial Form Factors from Equivalent Bodies of Revolution for the Froude Method of Predicting Resistance," Proceedings of the First Ship Technology and Research (STAR) Symposium, Society of Naval Architect and Marine Engineers, Washington, D.C.

Granville, P.S. (1975b), "Similarity-Law Entrainment Method for Thick Axisymmetric Turbulent Boundary Layers in Pressure Gradients," David Taylor Naval Ship Research and Development Center Report 4525.

Granville, P.S. (1975c), "Drag and Turbulent Boundary Layer of Flat Plates at Low Reynolds Numbers," David Taylor Naval Ship Research and Development Center Report 4682 (also Journal of Ship Research, Vol. 21, No. 1, 1977).

Grim, O. and Blume, P. (1975), "Resistance Tests of Two Models with the Same Area Curve," Proceedings of the 14th International Towing Tank Conference, Vol. 3, Ottawa, Canada.

Hatano, S., Mori, K., Fukashima, M., and Yamazaki, R. (1975), "Calculation of Velocity Distributions in Ship Wake," Journal of the Society of Naval Architects of Japan, Vol. 138.

Hauke, W. (1975), "Grenzshichtmessungen an Modellschiffen im Wind-kanal," Schiffbauforschung, Sonderheft.

Hess, J.L. (1976), "On the Problem of Shaping an Axisymmetric Body to Obtain Low Drag at Large Reynolds Numbers," Journal of Ship Research, Vol. 20, No. 1.

Himeno, Y. (1976), "Displacement Effect of Three-Dimensional Turbulent Boundary Layer and Wake of Ship," Proceedings of the International Seminar on Wave Resistance, Tokyo, Japan.

Hoffman, H.P. (1976), "Untersuchung der 3-Dimensionalen, Turbulenten Grenzschicht an einem Schiffsdoppelmodell in Windkanal," Institut fur Schiffbau der Universitat Hamburg Report 343.

Huang, T.T. and Hannan, D.C. (1976), "Pressure Fluctuations in the Region of Flow Transition," David Taylor Naval Ship Research and Development Center Report 4723.

Huang, T.T., Wang, H.T., Santelli, N., and Groves, N.C. (1976), "Propeller/Stern/Boundary-Layer Interaction on Axisymmetric Bodies: Theory and Experiment," David Taylor Naval Ship Research and Development Center Report 76-0113.

Huang, T.T. and Cox, B.D. (1977), "Interaction of Afterbody Boundary Layer and Propeller," Symposium on Hydrodynamics of Ship and Off-Shore Propulsion Systems," Høvik outside Oslo, Norway.

Joubert, P.N., Sinclair, T.J., and Hoffmann, P.H., (1977), "A Further Study of Bodies of Revolution," Submitted to Journal of Ship Research.

Kerney, K.P. and White, N.M. (1975), "Description and Evaluation of a Digital-Computer Program for Calculating the Viscous Drag of Bodies of Revolution," David Taylor Naval Ship Research and Development Center Report 4641.

Kitagawa, H. (1975), "Brief Review of the Experimental Study on Viscous Flow Problems of Ships in Japan," Bulgarian Scientific Methodological Seminar on Experimental Ship Hydrodynamics, Varna, Bulgaria.

Kosecoff, M.A., Ko, D.R.S., and Merkle, C.L. (1976), "An Analytical Study of the Effect of Surface Roughness on the Stability of a Heated Water Boundary Layer," Physical Dynamics, Inc. Report PDT-76-131.

Kux, J. (1974), "Three-Dimensional Turbulent Boundary Layers," Proceedings of the 10th ONR Symposium on Naval Hydrodynamics, Cambridge, Massachusetts, U.S.A.

Larsson, L. (1975), "A Calculation Method for Three-Dimensional Turbulent Boundary Layers on Shiplike Bodies," Proceedings of the 1st International Conference on Numerical Ship Hydrodynamics, Gaithersburg, Maryland, U.S.A. (also Statens Skeppsprovningsanstalt Report 77, Goteborg, Sweden, 1976).

Larsson, L. (1976), "An Experimental Investigation of the Three-Dimensional Turbulent Boundary Layer on a Ship Model," Proceedings of the 11th Symposium on Naval Hydrodynamics, London, England (also Statens Skeppsprovningsanstalt Report 76, Goteborg, Sweden, 1976).

Matheson, N. and Joubert, P.N. (1974), "A Note on the Resistance of Bodies of Revolution and Ship Forms," Journal of Ship Research, Vol. 18, No. 3.

McCarthy, J.H., Power, J.L., and Huang. T.T. (1976), "The Roles of Transition, Laminar Separation, and Turbulence Stimulation in the Analysis of Axisymmetric Body Drag," Proceedings of the 11th ONR Symposium on Naval Hydrodynamics, London, England.

Myring, D.F. (1972), "The Profile Drag of Bodies of Revolution in Subsonic Axisymmetric Flow," Royal Aircraft Extablishment TR 72234.

Myring, D.F. (1976), "A Theoretical Study of Body Drag in Subcritical Axisymmetric Flow," The Aero Quarterly, Vol. 27, Part 3.

Nakayama, A. and Patel, V.C. (1973), "Calculation of the Viscous Resistance of Bodies of Revolution," Iowa Instute of Hydraulic Research Report 151, University of Iowa.

Nakayama, A., Patel, V.C., and Landweber, L. (1976), "Flow Interaction Near the Tail of a Body of Revolution; Part I: Flow Exterior to Boundary Layer and Wake; Part 2: Iterative Solution for Flow Within and Exterior to Boundary Layer and Wake," American Society of Mechanical Engineers, Journal of Fluids Engineering, Vol.98, Series 1, No. 3.

Namimatsu, M. and Muraoka, K. (1974), "Wake Distribution of Full Form Ship," Ishikawajima-Harima Heavy Industries Engineering Review, Vol. 7, No. 3, Tokyo, Japan, (also Proceedings of the 14th International Towing Tank Conference, Ottawa, Canada, 1975).

Nash, J.F. and Patel, V.C. (1977), "Advances in Turbulent Boundary-Layer Calculation Methodology," Symposium on Turbulent Shear Flows, Pennsylvania State University, Vol. 1.

Patel, V.C. (1973), "A Simple Integral Method for the Calculation of Thick Axisymmetric Turbulent Boundary Layers," Iowa Institute of Hydraulic Research Report 150, University of Iowa (also Aero Quarterly, Vol. 25, Part 1, 1974).

Patel, V.C., Nakayama, A., and Damian, R. (1974), "Measurements in the Thick Axisymmetric Turbulent Boundary Layer," Journal of Fluid Mechanics, Vol. 63, Part 2.

Patel, V.C., Lee, Y.T., and Guven, O. (1977), "Measurements in the Thick Axisymmetric Turbulent Boundary Layer and the Near Wake of a Low-Drag Body of Revolution," Symposium on Turbulent Shear Flows, Pennsylvania State University, Vol. 1.

Power, J.L. (1977), "Drag, Flow Transition and Laminar Separation on Nine Bodies of Revolution Having Different Forebody Shapes," David Taylor Naval Ship Research and Development Center Report 77-0065.

Presz, W.M. and Pitkin, E.T. (1974), "Flow Separation Over Axisymmetric Afterbody Models," Journal of Aircraft, Vol. 11.

Presz, W.J. and Pitkin, E.T. (1976), "Analytical Model of Axisymmetric Afterbody Flow Separation," Journal of Aircraft, Vol. 13, No. 7.

Reshotko, E. (1976), "Boundary-Layer Stability and Transition," Annual Reviews in Fluid Mechanics, Vol. 9, Annual Reviews, Inc., Palo Alto, California, U.S.A.

Reynolds, W.C. (1976), "Computation of Turbulent Flows," Annual Reviews in Fluid Mechanics, Vol. 8, Annual Reviews, Inc., Palo Alto, California, U.S.A.

Sachdeva, R.C. and Preston, J.H. (1975), "Theoretical Calculations of Boundary Layers on Ship Hulls," Transactions of Northeast Coast Institution of Engineers and Shipbuilders, Vol. 92, No. 1.

Sachdeva, R.C. and Preston, J.H. (1976), "Investigation of Turbulent Boundary Layers on a Ship Model," Schiffstechnik, Vol. 111.

Scragg, C.A. (1977), "Experimental Determination of the Wake of a High Block Ship," Proceedings of the 18th American Towing Tank Conference, Annapolis, Maryland, U.S.A.

Smith, A.M.O. and Gamberoni, N. (1956), "Transition, Pressure Gradient and Stability Theory," Douglas Aircraft Company Report ES 26388.

Tanaka, I., Himeno, Y., and Matsumoto, N. (1975), "Calculation of Three-Dimensional Boundary Layer and Wake of Ships," Proceedings of the 14th International Towing Tank Conference, Ottawa, Canada.

Tanaka, I. and Himeno, Y. (1975), "First-Order Approximation to Three-Dimensional Turbulent Boundary Layer and Its Application to Model-Ship Correlation," Journal of the Society of Naval Architects of Japan, Vol. 138.

Tanaka, I., Suzuki, T., and Himeno, Y. (1977), "Examples of Calculation of Stern Flow Field Using Boundary Layer Theory Approach," Proceedings of the Symposium on Hydrodynamics of Ships and Offshore Propulsion Systems, Høvik outside Oslo, Norway.

Tani, I. (1977), "History of Boundary-Layer Theory," Annual Reviews in Fluid Mechanics, Vol. 9, Annual Reviews, Inc., Palo Alto, California, U.S.A.

Vollheim, R. (1975a), "Wellenbildung und Reibungswirkung als Ursachen des Schiffswiderstundes," Schiffbauforschung, Sonderheft.

Vollheim, R. (1975b), "Measurement and Calculation of the Boundary Layer of Full Double-Hulled Models," Bulgarian Scientific Methodological Seminar on Experimental Ship Hydrodynamics, Varna, Bulgaria.

von Kerczek, C.H. (1973), "Calculation of Turbulent Boundary Layer on a Ship Hull at Zero Froude Number," Journal of Ship Research, Vol. 17.

Wazzan, A.R., Okamura, T.T., and Smith, A.M.O. (1968), "Spatial and Temporal Stability Charts for the Falkner-Skan Boundary-Layer Profiles," Douglas Aircraft Company Report DAC-67086.

White, N.M. (1977), "A Comparison Between A Simple Drag Formula and Experimental Drag Data for Bodies of Revolution," David Taylor Naval Ship Research and Development Center Report 77-0028.

WAVE RESISTANCE

by

John V. Wehausen
University of California, Berkeley

There has been a remarkable amount of activity in the field of wave resistance during the last two or three years. Much of this activity was concentrated in the International Seminar on Wave Resistance held in Tokyo and Osaka during February 3-9, 1976. Another smaller concentration of activity was in the First International Conference on Numerical Ship Hydrodynamics, held in Gaithersburg, Md., during October 20-22, 1975. The Proceedings of both meetings have already been published. The existence of these Proceedings makes my task easier in some respects but perhaps more difficult in others, as will be explained below.

The preparation of a bibliography for wave resistance is made much easier by the existence of the Proceedings of the Tokyo-Osaka Seminar. As an Appendix (pp. 15-18) to his Introductory Remarks, T. Inui has provided a list of all papers on wave resistance published in Japan from January 1963 to June 1975. As a complement to Inui's list I prepared for approximately the same period a list of papers on wave resistance published elsewhere (pp. 18-29). Consequently, it seems necessary only to supplement these two lists by papers that were overlooked or have appeared since that time. The bibliography following this report attempts to do this.

The same Proceedings have lightened my task in still another way. Part I consists primarily of expository accounts of the present status of various aspects of wave resistance, each written by an expert, each accompanied by an ample list of references pertaining to the subject under discussion. These are the papers in the attached Bibliography by Newman, Bessho, Ogilvie, Baba, Eggers, Yokoo and Tanaka, Jinnaka, Tsutsumi and

and Ogiwara, Gadd, Inui and Kajitani, Pien, Nakamura, and Maruo. It would be superfluous to add further expositions to these already available ones.

The wealth of ideas and results in these Proceedings as well as in the many papers inspired by the meetings themselves makes it very difficult to provide a succinct account of developments in the last three years. Instead I shall content myself with a discussion of two directions of development of the theory that seem to me to be particularly promising.

The first of these is the low-Froude-number expansion of the wave resistance. For those who haven't thought much about this, a warning is in order. A first reaction is to ask why one should bother with such an approximation, for everyone knows that wave resistance is of no significance at low Froude numbers. However, such a reaction tacitly defines the word "low" as a value for which the wave resistance is insignificant, say Fn < 0.1 for normal ship forms. The situation is analogous to the use of the word "thin" in the thin-ship approximation. There too, there have been frequent objections that this approximation could not possibly be useful because it required a ship shaped like a knife edge. In both cases the useful range of values has to be determined by comparison with values obtained by experiment, mathematical estimates being apparently beyond our powers. In the case of the thin ship, nature has not been kind; ships to which the approximation may be usefully applied really are thinner than normal ones. The situation with the low-Froude-number approximation appears to be different. The comparisons available up to now appear to be very promising, even for ships with relatively large block coefficients and at Froude numbers appropriate to the block coefficient.

The first serious attempt to develop a low-Froude-number expansion appeared in a report by Ogilvie [Wave resistance: the low speed limit, Univ. of Mich., Dept. of Naval Arch. Mar. Engrg., No. 002 (Aug. 1968), iii + 29pp.]. The treatment was two-dimensional and the body was

supposed to be submerged. The work was overlooked for some years as a practical prescription until Baba and Takekuma (1975) extended the treatment to three dimensions and surface vessels. In addition, they performed experiments in which the velocity field near a ship's hull was measured. The results of these experiments appeared to support the fundamental ideas behind the Ogilvie development. A coherent exposition of this work together with some calculations is given in a report by Baba (1976).

A somewhat different approach to Baba's approximation is given by Newman (1976a, pp. 37-40) and a quite different approach has been developed by Maruo (1976c). In addition, Keller (1974) has propcsed a low-Froude-number approximation based upon his earlier work in geometrical optics. This procedure has now been elaborated in a manuscript that presumably will be published in the near future. Independently of Keller, and perhaps not quite as systematically, Inui and Kajitani (1977) have proposed a modification of Baba's work that is based upon a paper of Ursell's [Steady wave patterns on a non-uniform steady fluid flow, J. Fluid Mech. 9 (1960), 333-345]. The approximations used in Ursell's paper are shown to be essentially the geometric-optics approximation.

There have been other investigations of low-Froude-number expansions by Dagan (1975) and others, but these have had a somewhat different purpose, namely, to examine the nature of such series rather than to develop new formulas for calculating wave resistance (although the latter is probably their ultimate goal). Roughly in this category is a recent investigation by J. M. Vanden Broeck, L. W. Schwartz and E. O. Tuck, in process of publication. Some part of it will also be presented at the Second International Conference on Numerical Ship Hydrodynamics. In addition to providing insights into the properties of low-Froude-number expansions, this study also provides information about the nature of the flow near the bow and stern of barge-like vessels.

Why do the investigations of Baba and of Inui and Kajitani seem especially promising? The reason is primarily pragmatic. Baba has compared calculated values with results of model tests. Particularly impressive are some comparisons to be shown at the Second International Conference on Numerical Ship Hydrodynamics in which calculations and tests have been made for conventional hull forms with block coefficients C_B = 0.56, 0.74, 0.78 and 0.86. Inui and Kajitani have made calculations for three Inuids of B/L = 0.765, 0.1275 and 0.1545, C_B = 0.455, 0.430, 0.451. For all three they compare measured values with those predicted by Baba's approximation; for the last they show a further comparison with values calculated according to their modification of Baba's procedure. This figure is reproduced here. The agreement seems remarkably good up to Fn = 0.30. I don't wish to leave the impression that the problem of calculating wave resistance for practical Froude numbers can be considered nearly solved. Indeed, sinkage has not been taken into account, but yet plays an important role for full ships. And Baba's own calculations show a much better agreement with measured values, even for a hull with C_B = 0.444, than is indicated by the displayed figure. Such discrepancies are still to be explained. However, the results seem so much better than can be obtained from Michell's integral, especially for full forms, that some optimism seems justified. Other papers on the low-Froude-number approximation will be found in the Bibliography.

The other promising direction is the development of mapping methods. Interest in such methods was apparently aroused by papers by Emerson [Trans. Roy. Inst. Naval Arch. 109 (1967), 241-281] and Gadd [ibid. 115 (1973), 377-392] that showed that a mapping proposed by Guilloton [Bull. Ass. Tech. Mar. Aéron. 64 (1969), 538-574] resulted in calculated values for the wave resistance that appeared to be in much better accord with measured values than those given by Michell's integral. Guilloton's procedure uses Michell's integral but maps the originally given hull into

a new one determined by the Michell potential. The Michell resistance is then applied to this new hull.

Because Guilloton's ideas were based upon physical intuition rather than a systematic approximation scheme, this success was an immediate challenge to try to provide a foundation. This was done independently by Noblesse [J. Ship Res. 19 (1975), 140-148] and G. Dagan [ibid., 149-154]. An independent mapping approach by the author [ibid., 13 (1969), 12-22] led to a mapping based upon first-order streamlines rather than isobars as in Guilloton. Calculations based upon this method have been made by Hong (1977) and compared with Guilloton's method and experiment. On balance, Guilloton's method seems to give a better approximation. The most recent systematic development of the mapping method is in a paper by Noblesse and Dagan (1976). In spite of the promise of such methods, there are as yet no calculated values for the improvements upon Guilloton's mapping suggested in these papers. Presumably these will come.

BIBLIOGRAHPY

Adachi, H. On the interference between bow-generated waves and parallel middle-body at low Froude numbers. Proc. 14th Internat. Towing Tank Conf., Ottawa, 1975, vol. 3, pp. 137-144.

Adachi, H. Some consideration on the sheltering effect of a ship with long parallel middle body. Internat. Sem. Wave Resist., Tokyo-Osaka. 1976, pp. 277-285, disc. 449-450.

Adee, Bruce H. Fluid flow around a ship's hull. Proc. 1st Internat. Conf. Numer. Ship Hydrodyn., Oct. 1975, pp. 435-454.

Adee, B. H. Wave-making and frictional resistance for practical ship forms. Internat. Sem. Wave Resist., Tokyo-Osaka, 1976, pp. 333-340, disc. 454-455.

Aleksandrov, K. V. Jet flow about a wedge-shaped post intersecting a free surface. (Russian) Izv. Akad. Nauk SSSR. Mekh. Zhidk. Gaza 1976, no. 4, 140-143.

Andersson, B. J. On ship waves in shallow water. Internat. Sem. Wave Resist., Tokyo-Osaka, 1976, pp. 341-348.

Andersson, B. J. On the mathematical model of a ship. Internat. Sem. Wave Resist., Tokyo-Osaka, 1976. p. 391, disc. 458.

Baba, Eiichi. Ship form improvement by use of wave pattern analysis. Japan Shipbldg. Mar. Engrg. 8, no. 1, 35-43 (1974).

Baba, E. Analysis of surface flow near the bow of flat ships. Japan Shipbldg. Mar. Engrg. 9, no. 2, 5-18 (1975).

Baba, E. Wave-breaking resistance of ships. Internat. Sem. Wave Resist., Tokyo-Osaka, 1976, pp. 75-92, disc. 412-418.

Baba, E. Wave resistance of ships in low speed. Mitsubishi Tech. Bull. no. 109 (1976), 20 pp.

Baba, E.; Takekuma, Katsuyoshi. A study in free-surface flow around bow of slowly moving full forms. J. Soc. Naval Arch. Japan 137 (1975) 1-10.

Baba, E.; Takekuma, K. A study on flow characteristics around bow of full forms. Proc. 14th Internat. Towing Tank Conf., Ottawa, 1975, vol. 3, pp. 183-192.

Bai, Kwang June. A localized finite-element method for steady, two-dimensional free-surface flow problems. Proc. 1st Internat. Conf. Numer. Ship Hydrodyn., Oct. 1975, pp. 209-229.

Bessho, M. Line integral, uniqueness and diffraction of wave in the linearized theory. Internat. Sem. Wave Resist., Tokyo-Osaka, 1976. pp. 45-55, disc. 401-405.

Bessho, M. On the wave-making resistance of a vertical plate partly immersed in water (two-dimensional problem). (Japanese) Trans. West-Japan Soc. Naval Arch. No. 51 (1976), 253-267.

Brard, Roger. Le problème de Neumann-Kelvin. C. R. Acad. Sci. Paris, Ser. A 278 (1974), 163-167.

Brard, R. Comments on the methods of determining separately the viscous and wave components of the resistance of a surface ship model. Proc. 14th Internat. Towing Tank Conf., Ottawa, 1975, vol. 3, pp. 43-56.

Brard, R. Compléments sur le problème de Neumann-Kelvin. C. R. Acad. Sci. Paris. Ser. A 278 (1974), 379-384.

Brard, R. Introductory lecture. Internat. Sem. Wave Resist., Tokyo-Osaka, 1976, pp. 1-6.

Brard, R. Some comments on ship wave theory. Schiffstechnik 23 (1976), 153-159.

Bruzzone, Dario; D'Agostino, Leopoldo. Il metode del taglio longitudinale per la determinazione sperimentale della resistenza d'onda. Mar. Ital. 74 (1976), no. 4, 65-69.

Chang, M.S.; Pien, P.C. Hydrodynamic forces on a body moving beneath a free surface. Proc. 1st Internat. Conf. Numer. Ship Hydrodyn., Oct. 1975, pp. 539-559.

Chapman, R. B. Hydrodynamic drag measurements on SWATH ship components. Naval Undersea Center, San Diego, Calif., Rep. NUC TP 406 (1974), 32 pp.

Chapman, R. B. Free-surface effects for yawed surface-piercing plates. J. Ship Res. 20 (1976), 125-136.

Chen, H. S.; Mei, C. C. Calculations of two-dimensional ship waves by a hybrid element method based on variational principles. Proc. 1st Internat. Conf. Numer. Ship Hydrodyn., Oct. 1975, pp. 95-111.

Chumak, A. E. On the theory of the ship of least wave resistance. Trudy Nikolaev. Korablestroit. Inst. vyp. 102 (1975), 92-96.

Dagan, G. Waves and wave resistance of thin bodies moving at low speed: the free-surface nonlinear effect. J. Fluid Mech. 69 (1975), 405-416.

Dagan, G. Non-linear wave resistance and coordinate straining. Internat. Sem. Wave Resist., Tokyo-Osaka, 1976, pp. 267-270, disc. 449.

D'Agostino, Leopoldo. I metodi di misura per la determinazione della resistenza d'onda. Mar. Ital. 73 (1975), no. 9, 213-217.

Dern, Jean-Claude. Un problème de Neumann-Kelvin bien posé. C. R. Acad. Sci. Paris. Ser. A 284 (1977), 1163-1165.

Doctors, Lawrence J. The experimental wave resistance of an accelerating two-dimensional pressure distribution. J. Fluid Mech. 72 (1975), 513-527.

Eggers, K. On the role of line integral terms for the improvement of wave resistance calculations. Proc. 14th Internat. Towing Tank Conf., Ottawa, 1975, vol. 3, pp. 259-265.

Eggers, K. W. H. Wave analysis, state of the art 1975. Internat. Sem. Wave Resist., Tokyo-Osaka. 1976, pp. 93-106, disc. 418-419.

Eggers, K. W. H.; Choi, H. S. On the calculation of stationary ship flow components. Proc. 1st Internat. Conf. Numer. Ship Hydrodyn., Oct. 1975, pp. 455-479.

Evans, D. V. The transmission of deep-water waves across a vortex sheet. J. Fluid Mech. 68 (1975), 389-401.

Gadd, G. E. An interaction between surface water waves and a turbulent boundary layer and wake. Trans. Roy. Inst. Naval Arch. 117 (1975), 269-276, disc. 276-278.

Gadd, G. E. Wave pattern measurement. Proc. 14th Internat. Towing Tank Conf., Ottawa, 1975, vol. 3, pp. 21-42.

Gadd, G. E. Wave theory applied to practical hull forms. Internat. Sem. Wave Resist. Tokyo-Osaka, 1976, pp. 149-158, disc. 426-429.

Gadd, G. E. A method of computing the flow and surface wave pattern around full forms. Trans. Roy. Inst. Naval Arch. 118 (1976), 207-215, disc. 215-219.

Grollius, Walter. Untersuchung des Strömungsfeldes analytischer Schiffsformen auf flachem Wasser im Geschwindigkeitsbereich geringer Wellenbildung. Schiff u. Hafen 27 (1975), 743-753.

Hatano, Shuji; Mori, Kazuhiro; Tamashima, Masahiro; Ito, Masamitsu. On a method to obtain the equivalent singularity distributions of a ship by the aid of wave-analysis and its applications. Trans. West-Japan Soc. Naval Arch. No. 51 (1976), 287-296.

Hearn, Grant E. Alternative methods of evaluating Green's function in three-dimensional ship-wave problems. J. Ship Res. 21 (1977), 89-93.

Hershey, Allen V. Computation system for surface wave trains. Proc. 1st Internat. Conf. Numer. Ship Hydrodyn., Oct. 1975, pp. 503-515.

Himeno, Y. Displacement effect of three-dimensional turbulent boundary layer and wake of ship. Internat. Sem. Wave Resist., Tokyo-Osaka, 1976, pp. 299-303, disc. 451-452.

Hirata, Miguel Hiroo. The flow near the bow of a steadily turning ship. J. Fluid Mech. 71 (1975) 283-291.

Hirata, M. H. The line integral term in the wave resistance. Internat. Sem. Wave Resist., Tokyo-Osaka, 1976, pp. 245-248, disc. 444.

Hogben, N. Routine measurement of wave pattern resistance. Proc. 14th Internat. Towing Tank Conf., Ottawa, 1975, vol. 3, pp. 249-258.

Hogben, N. Routine measurement of wave pattern resistance. Proc. 14th Internat. Towing Tank Conf., Ottawa, 1975, vol. 3, pp. 249 - 258.

Hogben, N. Wave analysis: a review of experience at the National Physical Laboratory (NPL). Internat. Sem. Wave Resist., Tokyo-Osaka, 1976 pp. 305-309, disc. 452-453.

Hogben, N.; Standing, R. G. Wave pattern resistance from routine model tests. Trans. Roy. Inst. Naval Arch. 117 (1975), 279-295, disc. 295-299.

Hong, Young S. Numerical calculation of second-order wave resistance. J. Ship Res. 21 (1977), 94-106.

Inui, T. Introductory remarks. Internat. Sem. Wave Resist., Tokyo-Osaka, 1976, pp. 7-18; disc. 393.

Inui, T.; Kajitani, H. Hull form design, its practice and theoretical background. Internat. Sem. Wave Resist., Tokyo-Osaka, 1976, pp. 159-183, disc. 430-434.

Inui, T.; Kajitani, H. A study on local non-linear free surface effects in ship waves and wave resistance. Colloquium, 25th Anniv. Inst. Schiffbau Univ. Hamburg, June 1977. 46 pp.

Inui, T.; Kajitani, H.; Kusaka, Y. Analysis of hydrodynamical source singularities for surface ships. Proc. 14th Internat. Towing Tank Conf., Ottawa, 1975, vol. 3, pp. 238-244.

Inui, T.; Kajitani, H.; Okamura, H. Propagation of ship waves on a non-uniform flow. Proc. 14th Internat. Towing Tank Conf., Ottawa, 1975, vol. 3, pp. 231-237.

Jinnaka, T., Tsutsumi, T. and Ogiwara, S. Hull form design derived from wave analysis. Internat. Sem. Wave Resist. Tokyo-Osaka, 1976, pp. 125-147, disc. 422-425.

Keller, Joseph B. Wave patterns of non-thin or full-bodied ships. 10th Symp. Naval Hydrodynamics, Cambridge, Mass., 1974, pp. 543-545; disc. 546-547.

Keller, Joseph B.; Ahluwalia, Daljit S. Wave resistance and wave patterns of thin ships. J. Ship Res. 20 (1976), 1-6.

von Kerczek, C. H.; Salvesen, N. Numerical solutions of two-dimensional nonlinear wave problems. 10th Symp. Naval Hydrodynam., Cambridge, Mass., 1974, pp. 649-663, disc. 664-666.

Kinoshita, T. Wave resistance in viscous fluid derived from momentum analysis. Internat. Sem. Wave Resist., Tokyo-Osaka, 1976, pp. 295-298, disc. 451.

Kinoshita, Takeshi. Ship resistance in viscous fluid with free surface. I. (Japanese) J. Soc. Naval Arch. Japan 140 (1976), 31-37.

Kitazawa, T. and Takagi, M. On the second order velocity potentials of the thin ship. Internat. Sem. Wave Resist., Tokyo-Osaka, 1976, pp. 255-261, disc. 448-449.

Kitazawa, T.; Inui, T.; Kajitani, H. Velocity field measurements applied for analysis of ship's wave-making singularities. 10th Symp. Naval Hudrodynam., Cambridge, Mass., 1974, pp. 549-561, disc. 562-564.

Kurylev, B. V. On the motion of a catamaran in fluid of finite depth. (Russian) Trudy Leningrad. Korablestroit. Inst., vyp. 89 (1974), 83-89.

Kurylev, B. V. Computational determination of the features of the wave resistance of a catamaran. Trudy Leningrad. Korablestroit. Inst., vyp. 89 (1974). 91-95.

Kusaka, Y. On the contribution of line integral to the wave resistance of surface ships. Internat. Sem. Wave Resist., Tokyo-Osaka, 1976, pp. 249-254, disc. 444-448.

Kusaka, Yuzo; Inui, Takao; Kajitani, Hisashi. On the hydrodynamical source singularities for surface ships with special reference to Line Integral. (Japanese) J. Soc. Naval Arch. Japan 138 (1975), 12-22.

Lyakhovitskii, A. G. Investigation of the wave resistance of a three-hulled ship on deep water. Trudy Leningrad. Inst. Vod. Transp., vyp. 153 (1976), 14-24.

Maruo, H. Ship waves and resistance in a viscous fluid. Internat. Sem. Wave Resist., Tokyo-Osaka, 1976, pp. 217-238, disc. 438-442.

Maruo, H. On the separation of resistance components. Internat. Sem. Ship Technol., Seoul, 1976, pp. 4-1—4-23.

Maruo, Hajime. Wave resistance of a ship with finite beam at low Froude numbers. Yokohama Nat. Univ., rep., 1976, 22 pp.

Maruo, Hajime; Kasahara, Kazuko; Suzuki, Kazuo; Kawamura, Takehiko. On the ship form of minimum wave resistance with a bow bulb. (Japanese) J. Soc. Naval Arch. Japan 138 (1975), 1-11.

Matsui, M. On source distributions obtained from measured wave-making resistance. Internat. Sem. Wave Resist., Tokyo-Osaka, 1976, pp. 311-314, disc. 453.

Matsuura, Masami; Maruo, Hajime. On the propagation of surface waves across a uniform wake. J. Soc. Naval Arch. Japan 139 (1976), 56-63.

Mei, Chiang C. Flow around a thin body moving in shallow water. J. Fluid Mech. 77 (1976), 737-751.

Messerschmidt, Walter. Untersuchungen über den Wellenwiderstand ausgewählter Schiffsformen. Schiffbauforschung 13 (1974), Sonderheft, 23-31.

Moreno, M.; Perez-Rojas, L.; Landweber, L. Effect of wake on wave resistance of a ship model. Iowa Inst. Hydraul. Res. Univ. Iowa, IIHR Rep. No. 180 (Aug. 1975), i + 32 pp.

Mori, K. Calculation of velocity distributions in ship wake. Internat. Sem. Wave Resist., Tokyo-Osaka, 1976, pp. 355-362, disc. 455-456.

Nakmura, S. Added resistance and propulsive performance of ships in waves. Internat. Sem. Wave Resist., Tokyo-Osaka, 1976, pp. 199-216, disc. 435-438.

Nakatake, K. Free surface effect on propeller thrust. Internat. Sem. Wave Resist., Tokyo-Osaka, 1976, pp. 363-367, disc. 456-457.

Nakatake, Kuniharu; Inoue, Hiroshi. Ship side wave profile and wave-making resistance. Trans. West-Japan Soc. Naval Arch. No. 50 (1975), 19-28.

Narita, S. Some research on the wave resistance of a trimaran. Internat. Sem. Wave Resist., Tokyo-Osaka, 1976, pp. 381-388, disc. 457.

Newman, J. N. Linearized wave resistance theory. Internat. Sem. Wave Resist., Tokyo-Osaka, 1976, pp. 31-43, disc. 393-401.

Newman, J. N. Blockage with a free surface. J. Ship Res. 20 (1976), 199-203.

Nichols, B. D.; Hirt, C. W. Methods for calcualating multi-dimensional, transient free surface flows past bodies. Proc. 1st Internat. Conf. Numer. Ship Hydrodynamics, Oct. 1975, pp. 253-277.

Noblesse, F. The near-field disturbance in the centerplane Havelock source potential. Proc. 1st Internat. Conf. Numer. Ship Hydrodyn., Oct. 1975, pp. 481-501.

Noblesse, F. A note on second-order thin-ship theory by centerplane source distributions. Internat. Sem. Wave Resist., Tokyo-Osaka. 1976, pp. 263-266, disc. 449.

Noblesse, F., The fundamental solution in the theory of steady motion of a ship. J. Ship Res. 21 (1977), 82-88.

Noblesse, F.; Dagan, G. Nonlinear ship-wave theories by continuous mapping. J. Fluid Mech. 75 (1976), 347-371.

Ogilvie, T. F. On nonlinear wave resistance theory. Internat. Sem. Wave Resistance, Tokyo-Osaka, 1976 pp. 57-73, disc. 405-412.

Ogilvie, T. Francis Wave-length scales in slender-ship theory. Internat. Sem. Ship Technol., Seoul, 1976, pp. 5-1-5-22.

Ohring, Samuel. A fast fourth-order Laplace solver for application to numerical three-dimensional water wave problems. Proc. 1st Internat. Conf. Numer. Ship Hydrodyn., Oct. 1975, pp. 641-663.

Okamura, Hidekuni; Inui, Takao; Kajitani, Hisashi. Analysis of ship waves propagating on a non-uniform flow. (Japanese) J. Soc. Naval Arch. Japan 138 (1975), 37-45.

Pien, P. C. Catamaran hull-form design. Internat. Sem. Wave Resist., Tokyo-Osaka, 1976, pp. 185-198, disc. 434-435.

Plisov, N. B. On a method of measuring wave resistance. Trudy Leningrad. Korablestroit. Inst. vyp. 96 (1975), 85-89.

Pustoshnyi, A. F. Properties of the flow about a body and the structure of the resistance of ships of full lines. Probl. Prikl. Gidromekh. Sudna, pp. 54-92. Sudostroenie, Leningrad, 1975.

Salvesen, N.; von Kerczek, C. H. Numerical solutions of two-dimensional nonlinear body-wave problems. Proc. 1st Internat. Conf. Numer. Ship Hydrodyn., Oct. 1975, pp. 279-293.

Salvesen, Nils; von Kerczek, C. Comparison of numerical and perturbation solutions of two-dimensional nonlinear water-wave problems. J. Ship Res. 20 (1976), 160-170.

Sharma, S. D. and Bellows, G. E. Experiments on the wave-making of a drifting ship. Internat. Sem. Wave Resist., Tokyo-Osaka, 1976, pp. 369-380.

Shen, Hung-Tao; Farell, César. Numerical calculation of the wave integrals in the linearized theory of water waves. J. Ship Res. 21 (1977), 1-10.

Smorodin, A. I. The development of methods of the theory of wave resistance and their practical application in problems of ship hydrodynamics. Probl. Prikl. Gidromekh. Sudna, pp. 108-128. Sudostroenie, Leningrad, 1975.

Standing, R. G. Experience in computing the wavemaking of source/sink models. Nat. Phys. Lab., Ship Div., NPL Rep. Ship 190 (Sept. 1975), iii + 52 + 14 pp.

Standing, R. G. Experience in computing the wavemaking of hovercraft. Nat. Phys. Lab., Ship Div., NPL Rep. Ship 191 (Sept. 1975), iii + 56 + 24 pp.

Starobinskii, V. B. Wave resistance of ships on an air cushion of skeg type. Trudy Leningrad. Inst. Vod. Transp., vyp. 153 (1976), 25-29.

Suzuki, Katsuo. The representations of the velocity potential in the theory of wave resistance of ships. Mem. Defense Acad. (Yokosuka) 16, no. 3, 101-116 (1976).

Suzuki, K. Effects of wake and wave-breaking on wavemaking resistance. Internat. Sem. Wave Resist., Tokyo-Osaka, 1976, pp. 287-294.

Takahei, T.; Sakao, M.; Nagamatsu, N. and Shimoyama, N. On the wave resistance of a ship on the stream of which velocity varies with depth. Internat. Sem. Wave Resist., Tokyo-Osaka, 1976, pp. 349-353, disc. 455.

Takekuma, K. Some problems on the applications of linearized wave making resistance theory to hull form design. Internat. Sem. Wave Resist., Tokyo-Osaka, 1976, pp. 325-331, disc. 454.

Taniguchi, Kaname; Tamura, Kinya; Baba, Eiichi. Reduction of wave-breaking resistance by "MHI-Bow". Japan Shipbuldg. Marine Engrg. 7 (1973), no. 1, 7-14.

Tatinclaux, J. C. Effect of pressure drop at the bow and stern of an otherwise uniform pressure distribution on the induced wave resistance. Internat. Sem. Wave Resist., Tokyo-Osaka, 1976, pp. 389-390, disc. 457-458.

Timman, R. Small parameter expansives in ship hydrodynamics. 10th Symp. Naval Hydrodynam., Cambridge, Mass., 1974. pp. 439-447.

Tolefson, D. C.; Boichot, L. Free-surface linear water-wave problems by the finite element method. Proc. 1st Internat. Conf. Numer. Ship Hydrodyn., Oct. 1975, pp. 71-94.

Tsutsumi, Takayuki. On the wave resistance of ships represented by sources distributed over hull surface. Trans. West-Japan Soc. Naval Arch. No. 51 (March 1976), 269-285.

Tsutsumi, Takayuki; Ogiwara, Seiko. On the principal particulars of ship hull form and wave pattern resistance III. (Japanese) J. Soc. Naval Arch. Japan 138 (1975), 23-36.

Tsutsumi, T.; Ogiwara, S; Jinnaka, T. Comparison between calculated and directly measured wave resistance. Proc. 14th Internat. Towing Tank Conf., Ottawa, 1975, vol. 3, pp. 163-172.

Tuck, E. O. An approximation to Michell's Integral. Internat. Sem. Wave Resist., Tokyo-Osaka, 1976, pp. 239-244, disc. 443-444.

Ursell, F. Note on the refraction of head seas by long ships. 10th Symp. Naval Hydrodynam., Cambridge, Mass., 1974, pp. 565-568, disc. 569-571.

Ursell, F. The refraction of head seas by a long ship. J. Fluid Mech. 67 (1975), 689-703.

Ward, Lawrence W.; van Hooff, Richard W. The effect of probe location on a model wave resistance along a longitudinal cut. J. Ship Res. 20 (1976), 7-21.

Wehausen, J. V. A bibliography of wave resistance of ships. Internat. Sem. Wave Resist., Tokyo-Osaka, 1976, pp. 19-29.

Yamaguchi, M. On wave making resistance of asymmetrical ship hull forms generated by singularity distributions. Internat. Sem. Wave Resist., Tokyo-Osaka, 1976, pp. 315-323.

Yim, B. A variational principle associated with a localized finite-element technique for steady ship wave and cavity problems. Proc. 1st Internat. Conf. Numer. Ship Hydrodyn., Oct. 1975, pp. 137-153.

Yim, B. The sheltering effect of ship waves. Internat. Sem. Wave Resist., Tokyo-Osaka, 1976, pp. 271-276.

Yokoo, K. and Tanaka, H. Application of wave analysis to tank experiment. Internat. Sem. Wave Resist., Tokyo-Osaka, 1976, pp. 107-124, disc. 420-421.

Zaitsev, A. A.; Odulo, A. B. Motions in a layer of rotating fluid caused by a pressure applied to a free surface. Izv. Akad, Nauk SSSR. Mekh. Zhidk. Gaza 1974, no. 6. 52-57.

STILL WATER RESISTANCE OF SINGLE–STEP PLANING HULL

BY

CHUN–TSUNG WANG

INSTITUTE OF NAVAL ARCHITECTURE, NTU

INTRODUCTION

Figure 1 shows the separation and reattachment phenomenon of a single step planing hull. At planing, the forebody of the hull carries most of the loading. Due to the relative large aspect ratio of the forebody, the lift coefficient is increased. At the same time, frictional resistance is trimmed due to the relative small wetted surface after flow separation. Based on Shuford's equations (1958), Clement and Pope (1961) introduced method to select suitable step position. From lifting coefficient equation

$$C_{LS} = C_{LL} + C_{LC}$$

$$= \frac{0.02741\, A\tau}{1 + A} \cos^2\tau \,(1 - \sin\beta) + 4/3\, \sin^2\tau \cos^3\tau \cos\beta$$

where C_{LL} is lifting line term, C_{LC} is cross flow term, A is aspect ratio, β is deadrise angle at midship, and τ is trim angle.

The center of pressure location, l_p, measured from aft end of planing surface is

$$\frac{\ell_P}{\ell_m} = \frac{0.875\, C_{LL} + 0.50\, C_{LC}}{C_{LS}}$$

where l_m is mean wetted length.

The relationship between drag and lifting force is

$$\frac{R}{\Delta} = \tan\tau + \frac{C_f}{C_{LS}} \left(\frac{V_1}{V}\right)^2$$

where C_f is Schoenherr turbulent friction coefficient

$$\frac{0.242}{\sqrt{C_f}} = \log\,(C_f \times R_N{}')$$

and

$$R_N{}' = \frac{1}{\nu}\sqrt{\frac{2\Delta\cos\beta}{C_{LS}\,A}}\left(1-\frac{C_{LS}}{\cos\tau\cos\beta}\right)$$

ν is the kinematic viscosity, Δ is the boat load, V_1 is the mean velocity over bottom of planing surface, V is the horizontal velocity of planing surface. Assuming that the forebody carries 90% of boat load at fully planing range, Clement and Pope were able to obtain suitable step position at given design speed.

It is always desired to know resistance and trim characteristics of a single step planing hull besides step position. The purpose of the president paper is thus to study the still water resistance characteristics of a single step planing hull both analytically and experimentally, considering the variation of step positions, step heights, L. C. G. positions and loadings.

ANALYTICAL APPROACH

Assuming that the forebody of a single step planing hull carries Y portion of the dynamic component of the lift (at fully planing, Y=1), and utilizing the hydrodynamic results presented by Savitsky (1964), the governing equations for a single step planing hull at planing could be formulated (Wang & Lu, 1976) as followes:

The lift coefficient of a deadrise surface is

$$C_{L\beta} = \frac{\Delta}{\frac{1}{2}\rho V^2 b^2} = C_{LO} - 0.0065\,\beta\, C_{LO}{}^{0.6}$$

where lifting coefficient of a flat plate is

$$C_{LO} = \tau^{1.1}\left[\frac{1}{Y}0.012\left(\lambda-\frac{x}{b}\right)^{0.5} + 0.0055\,(\lambda-\lambda_H)^{2.5}/C_V{}^2\right]$$

and λ is the mean wetted length-beam ratio, $\lambda_H = \frac{ch}{b}$ when $x > ch$, $\lambda_H = \frac{x}{b}$ when $x < ch$, and c is observed to be around 8, $C_V = \frac{V}{\sqrt{gb}}$ b is the maximum beam with spray strip (Blound and Fox, 1976), and ρ is the water density. The center of pressure location is

$$\frac{\ell_P}{\lambda b} = \frac{0.012\left(\lambda-\frac{x}{b}\right)^{0.5}\left[\left(0.75+0.25\frac{x}{\lambda b}\right)Y+(1-Y)0.75\left(\frac{X-Ch}{\lambda b}\right)\right]+0.005(\lambda-\lambda_H)^{2.5}\frac{Y}{3}\left(1-\frac{\lambda_H}{\lambda}\right)/C_V{}^2}{0.012\left(\lambda-\frac{X}{b}\right)^{0.5}+0.0055\,(\lambda-\lambda_H)^{2.5}\,Y/C_V{}^2}$$

When $x < ch$, flow separated from the step and reattachment did not occur, thus Y=1. In general l_p is close to L. C. G. postion and they are assumed to be the same in the present study.

The mean velocity over the bottom of planing surface is

$$V_1 = V\left\{1-\frac{0.012\left(\lambda-\frac{X}{b}\right)^{0.5}\frac{\tau^{1.1}}{Y} - 0.0065\,\beta\left[0.012\frac{\tau^{1.1}}{Y}\left(\lambda-\frac{X}{b}\right)^{0.5}\right]^{0.6}}{\lambda\cos\tau}\right\}^{0.5}$$

And total drag-lift ratio is

$$\frac{R}{\Delta} = \tan\tau + \frac{D_f}{\Delta\cos\tau}$$

where the frictional component is

$$D_f = \frac{\rho}{2} V_1^{\,2}\,(\lambda - \lambda_H)\,b^2\,C_f / \cos\beta$$

and

$$\frac{0.242}{\sqrt{C_f}} = \log_{10}(R_N \times C_f)$$

$$R_N = \frac{V_1\,b\,\lambda}{\nu}$$

with given Δ, l_p (or L. C. G.), b, β, ρ, ν, h and x, the above equations could be used to solve R and τ of a single step planing hull at given speed. It should be pointed out that at h=x=0 and Y=1, i.e. planing hull without step, the above equations are identical to those shown by Savitsky (1964).

EXPERIMENTAL APPROACH

The basic model selected for the present study is that of series 62–4667–1 (Clement and Blount, 1963). Lines with a typical step are shown in Fig. 2. Model length is 3 ft and is made of wood. Spray strip is added along chine line. The maximum beam with spray strip is 0.75ft. Deadrise angle at midship is 13°. 0.04 in. diameter strip wire is added at a position 3 in. from bow. And two 0.5 in. diameter tubes open to air are connected to the step position.

Six sets of model test with different step positions, step hights and loadings are tested (Wang and Lu, 1976). Drag is measured by a free-trim, free-heaving resistance gauge (Liu, Wang and Hu, 1975), while trim and heaving are measured by a mechanic device (Wang et. al., 1972).

RESULTS AND CONCLUSIONS

For a stepless planing hull, Figure 3 shows that still water resistance and trim results obtained analytically and experimentally tend to confirm with each other at fully planing range ($V \geqslant 4$ m/s or $F_\nabla = \frac{V}{\sqrt{g\,\nabla^{1/3}}} \geqslant 3.25$).

For planing hulls with single step, Figures 4 and 5 show that still water resistance and trim data check with the analytical results at planing range for step conditions $x/L_p = 29.25\%$, $h/L_p = 1\%$ and $x/L_p = 36\%$, $h/L_p = 2\%$.

Figure 6 shows analytical relationships between drag-loading ratio and F_∇ at four different test conditions. It could be seen that at fully planing range, Say $F_\nabla = 6$, trim angle increases as step position moves forward, whereas drag-loading ratio decreases. But at relative lower planing speed, say $F_\nabla = 3.5$, drag-loading ratio tends to be small at $x/L_p = 22.5\%$. These conclusions could also be obtained if Clement and Pope's method were used to select suitable step positions for relative lower drag at different given speed.

REFERENCE

Blount, D.L. and D.L.Fox (1976), Small Craft Power Prediction, Marine Technology, V. 13, p. 14.

Clement, E.P. and J.D.Pope (1961), Stepless and Stepped Planing Hull Graphs for Performance Prediction and Design, DTMB Rept. 1490.

Clement, E.P. and D.L.Blount (1963), Resistance Tests of a Systematic Series of Planing Hull Forms, Trans. SNAME, V.71, p. 491.

Liu, C.Y., C.T. and T.U.Hu,(1975), Resistance Tests of a 36ft Planing Boat, NTU–INA–33.

Savistky, D. (1964), Hydrodynamic Design of Planing Hull, Marine Technology, V.l, p.71.

Shuford, C.L.(1958), A Theoretical and Experimental Study of Planing Surface Including Effects of Cross Section and Plan Form, NASA Rept. 1355.

Wang, C.T. et. al (1972), On the Ship Model Basin of NTU, NTU–SHL–11.

Wang, C.T. and C.Y.Lu (1976), Still Water Resistance of Single Step Planing Hull, NTU–INA–Tech. Rept.49.

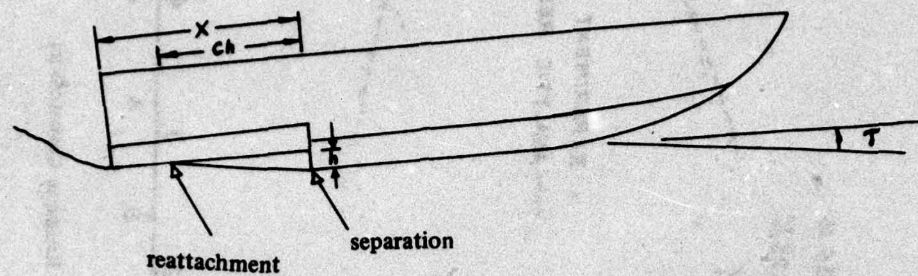

Fig. 1 Flow Separation and Reattachment along Single Step Planing Hull

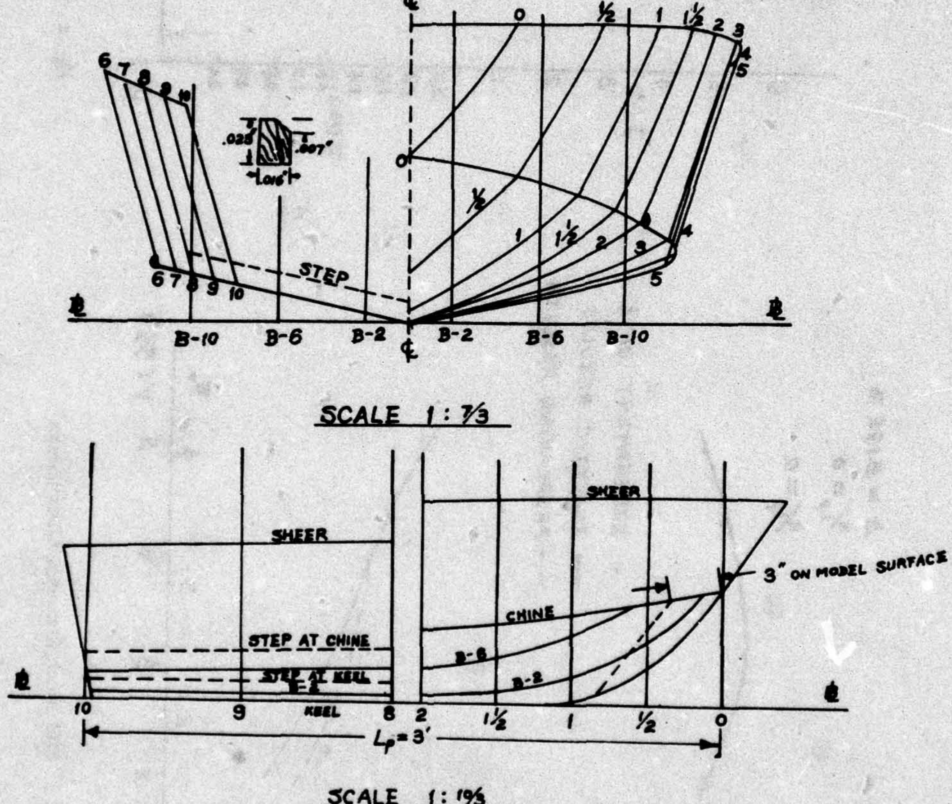

Fig. 2 Planing Hull Form Lines

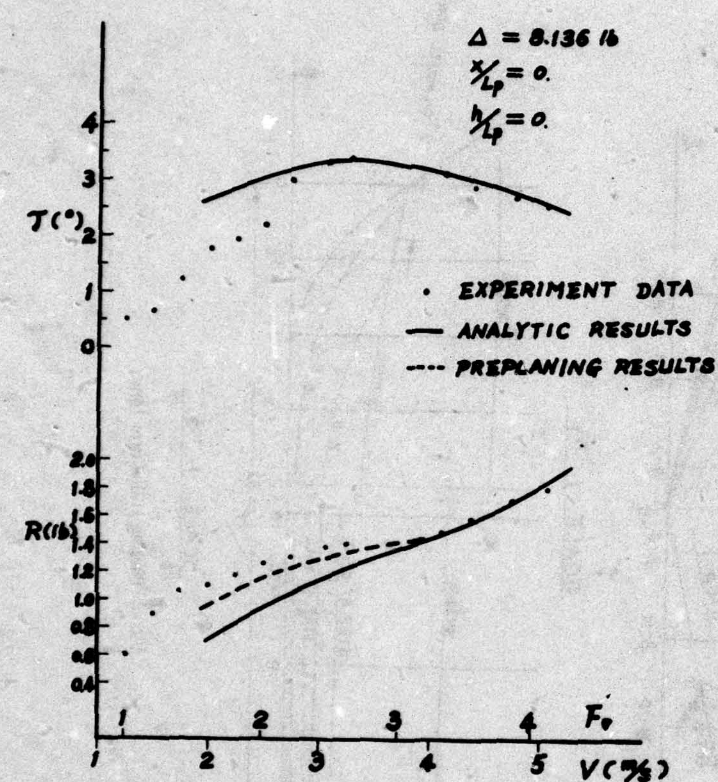

Fig. 3 Still Water Resistance Characteristics

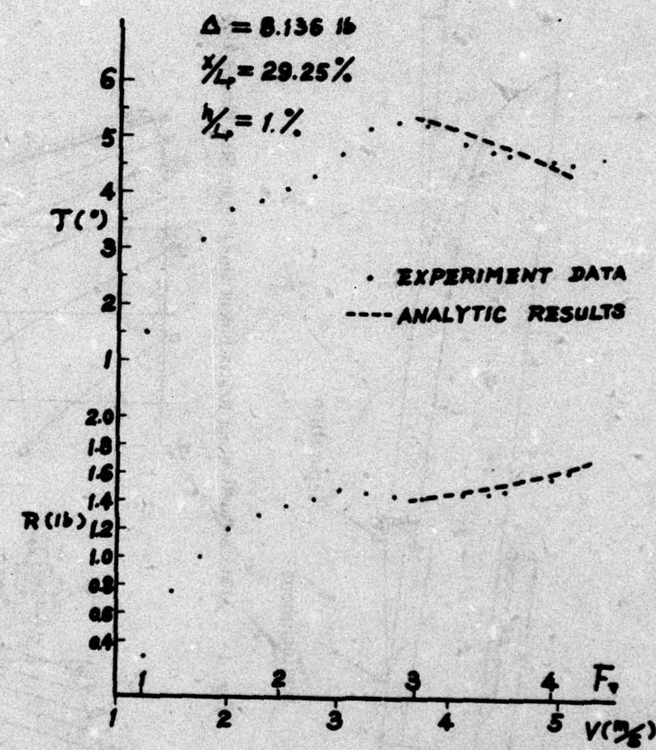

Fig. 4 Still Water Resistance Characteristics

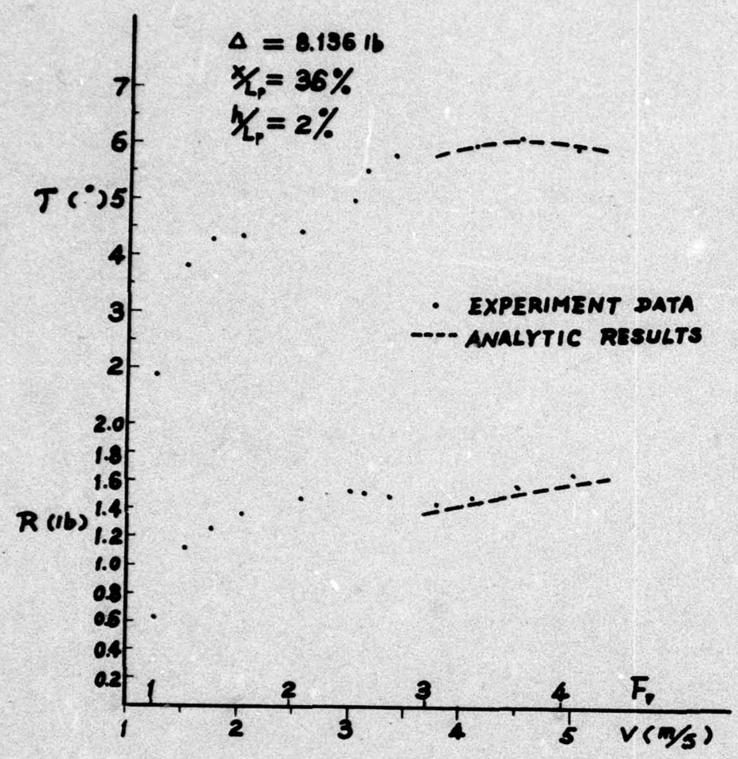

Fig. 5 Still Water Resistance Characteristics

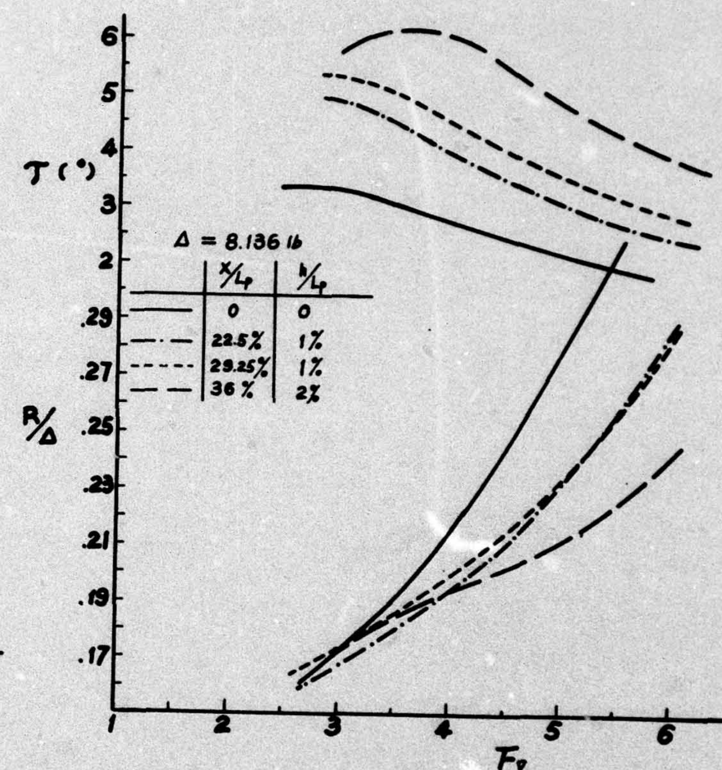

Fig. 6 Resistance Characteristics at Different Step Positions

A PREDICTION METHOD FOR THE VISCOUS DRAG OF SHIPS AND UNDERWATER BODIES WITH SURFACE ROUGHNESS AND/OR DRAG-REDUCING POLYMER SOLUTIONS

by

Paul S. Granville
David W. Taylor Naval Ship Research and Development Center

ABSTRACT

The viscous drag of ships and of underwater bodies including two-dimensional foils with surface roughness and/or drag-reducing polymer solutions may be readily predicted by the use of a proposed form-factor formula derived from boundary-layer theory. The effect of shape on drag is supplied by the form factor while the effect of surface roughness and/or drag-reducing polymer solution is given by existing flat-plate formulas which are summarized.

INTRODUCTION

The viscous drag or resistance of ships and of underwater bodies, including two-dimensional foils, with surface roughness and/or drag-reducing polymer solutions may be readily predicted by form factors in conjunction with a flat-plate drag. The form factors accommodate only the effect of shape while the flat-plate drag supplies the remaining effects of Reynolds number, surface roughness and/or drag-reducing polymer solutions. The use of form factors has obvious engineering advantages of simplified calculations and of indications of the magnitude of the effect of shape on viscous drag.

Methods exist for predicting the drag of flat plates with roughness[1] and/or drag-reducing polymer solutions[2] from boundary-layer similarity-law characteristics. There remains the problem of determining suitable form factors.

Analytical relations have been derived for form factors for smooth bodies in ordinary fluids from boundary-layer theory by means of a local skin-friction relation

NOTATION

A	Boundary-layer factor; slope of inner similarity law in natural logarithms
$\tilde{A}$	Cross-sectional area of ship hull to waterline
C	Concentration of polymer in solution
C_F	Flat-plate drag coefficient
C_v	Viscous drag coefficient
C_w	Concentration of polymer at wall downstream of injection
D_v	Viscous drag of body
f	Partial form factor
g	Separation form factor
H	Two-dimensional shape parameter for boundary-layer velocity profiles
h	Axisymmetric shape parameter
$\mathcal{I}$	Drag effect due to nonuniform polymer concentration
k	Characteristic length of roughness
L	Length of body
ℓ	Characteristic polymer length
m	Constant in formula for local skin friction, Equation (9)
$\tilde{m}$	Characteristic polymer mass
$\mathcal{P}$	Type of polymer including molecular weight
$\tilde{P}$	Perimeter of hull cross section up to waterline
q	Wake factor
$\tilde{q}$	Slope of linear logarithmic characterization of polymer solution
$\mathcal{R}$	Type of roughness configuration
R_L	Reynolds number
r	Radius of body of revolution
r_A	Radius of equivalent body of revolution based on cross-sectional area
r_p	Radius of equivalent body of revolution based on cross-sectional perimeter
S	Wetted surface area of body
$\mathcal{S}$	Shape of body
t	Characteristic polymer time
x	Axial distance from body nose
U	Velocity outside of boundary layer
U_∞	Forward speed of body
$\overline{(U/U_\infty)}$	Average value of velocity ratio U/U_∞
$(U/U_\infty)_A$	Value of U/U_∞ determined from cross-sectional area of equivalent body of revolution of a ship hull
u_τ	Shear velocity
α	Slope of meridian contour of body of revolution
ΔB	Similarity-law characterization

$\Delta(\overline{U/U_\infty})$	Deviation of $(\overline{U/U_\infty})$
ζ	Constant in formula for local skin friction, Equation (9)
$\bar{\zeta}$	Average value of ζ
θ	Two-dimensional boundary-layer momentum thickness
ν	Kinematic viscosity of fluid
ρ	Density of fluid
τ_w	Shear stress at wall

<u>Subscripts</u>

e	Tail end of body
i	Conditions at injection slot of polymer solution
o	Inception of drag reduction by polymer solution
r	Condition of fully-developed roughness flow
s	Condition of hydraulic smoothness
sp	Condition of special formula for form factor of smooth surfaces
u	Condition of universal formula for form factor

for smooth surfaces in ordinary fluids.[3,4] Such form-factor formulas obviously cannot apply to rough surfaces and/or drag-reducing polymer solutions.

Since the local skin friction for rough surfaces and/or drag-reducing polymer solutions cannot be characterized by any simple relations, the expedient of an average value has been adopted which is based on that for the equivalent flat plate itself. Formulas for form factors result which are generally applicable even for smooth surfaces in ordinary fluids. This allows a comparison with the more stringent formula for smooth surfaces in ordinary fluids which after an analysis shows only a small difference.

Form factors are considered for bodies of revolution in axisymmetric flow, for two-dimensional symmetric foils at zero angle of attack and for ship hulls by means of equivalent bodies of revolution.

To complete the presentation, existing formulas are summarized for the drag of flat plates with roughness and/or drag-reducing polymer solutions.

FORM FACTORS

General

For a smooth body in ordinary fluids, the coefficient of viscous drag or resistance C_v may be stated as a function of Reynolds number R_L and shape $\mathcal{S}$ or

$$C_v = f\left[R_L, \mathcal{S}\right] \tag{1}$$

and

$$C_v = \frac{D_v}{\frac{1}{2}\rho U_\infty^2 S} \tag{2}$$

$$R_L = \frac{U_\infty L}{\nu} \tag{3}$$

where

D_v = viscous drag or resistance
U = forward speed of body
S = surface area of body
L = length of body
ρ = density of fluid
ν = kinematic viscosity of fluid

For smooth streamlined bodies in ordinary fluids (no appreciable flow separation), the viscous drag coefficient C_v has been related to the drag coefficient of an equivalent flat plate C_F empirically[5] and theoretically[6] by means of a form factor f so that

$$C_v\left[R_L, \mathcal{S}\right] = \left(1 + f\left[\mathcal{S}\right]\right) C_F\left[R_L\right] \tag{4}$$

Form factor f as stated does not vary with Reynolds number R_L but only with body shape

For smooth, non-streamlined bodies in ordinary fluids (with appreciable flow separation), the Landweber Hypothesis[6] adds an additional separation form factor g to accommodate the added pressure drag due to flow separation or

$$C_v[R_L, \mathcal{S}] = (1 + f[\mathcal{S}])\, C_F[R_L] + g[\mathcal{S}] \tag{5}$$

Here form factor f is reduced to a partial form factor[7] for obvious reasons. Form factor g also is not considered to vary with Reynolds number R_L but only with body shape $\mathcal{S}$. Dependence on Reynolds number has been then transferred to an equivalent flat plate which is defined as a plate with the same surface area and length as the body in question. An ordinary fluid is defined as one without drag-reducing properties.

The Landweber Hypothesis[6] was proposed for the extrapolation of the viscous drag of ship hulls from model scale to full scale. It is a compromise between the traditional Froude method of extrapolation where f = 0 and the Hughes Hypothesis that considers g = 0. It is reasonable to consider the Landweber Hypothesis as originally stated to be applicable to all smooth bodies in ordinary fluids.

The concept of form factors is now to be extended to rough bodies, smooth bodies in drag-reducing polymer solutions, and rough bodies in drag-reducing polymer solutions. Uniform concentrations of polymer solutions and nonuniform concentrations from injection through the body surface are included.

For the general analytical consideration to follow, injection through one slot will represent the condition of nonuniform polymer concentration. Then a rough body with injection of drag-reducing polymer solution through a slot at position x_i may have a viscous drag coefficient with the following functional relationship

$$C_v = f\left[R_L, \mathcal{S}, \frac{k}{L}, \mathcal{R}, P, C_{w,e}, \frac{x_i}{L}\right] \tag{6}$$

where

- k = characteristic length of roughness
- $\mathcal{R}$ = roughness configuration
- P = type of drag-reducing polymer and molecular weight distribution
- $C_{w,e}$ = wall concentration of polymer at tail end

As stated here, a characteristic length ℓ for drag-reducing polymers may be substituted for characteristic length of roughness k. Also, a characteristic time t or characteristic mass $\tilde{m}$ drag-reducing polymers may be substituted for characteristic length ℓ such that

$$\ell = \sqrt{\frac{t}{\nu}} = \left(\frac{\tilde{m}}{\rho}\right)^{\frac{1}{3}} \tag{7}$$

For streamlined bodies, a form-factor representation is proposed as

$$C_v\left[R_L, \mathcal{S}, \frac{k}{L}, \mathcal{R}, P, C_{w,e}, \frac{x_i}{L}\right] = (1 + f[\mathcal{S}])\, C_F\left[R_L, \frac{k}{L}, \mathcal{R}, P, C_{w,e}, \frac{x_i}{L}\right] \tag{8}$$

which is a generalization of that for smooth surfaces in ordinary fluids, Equation (4).

For non-streamlined bodies, it is proposed that the Landweber Hypothesis be extended to rough surfaces and/or drag-reducing polymer solutions such that

$$C_v\left[R_L, \mathcal{S}, \frac{k}{L}, \mathcal{R}, P, C_{w,e}, \frac{x_i}{L}\right] = \left(1 + f[\mathcal{S}]\right) C_F\left[R_L, \frac{k}{L}, \mathcal{R}, P, C_{w,e}, \frac{x_i}{L}\right] + g[\mathcal{S}] \quad (9)$$

which is a generalization of Equation (5).

As for smooth bodies in ordinary fluids, form factors f and g are still considered only functions of body shape. All other parameter functional dependence is relegated to flat-plate drag coefficients.

Smooth Bodies in Ordinary Fluids

A formula for partial form factor f has been derived[3] for smooth bodies in ordinary fluids from the boundary-layer momentum equation for bodies of revolution in axisymmetric flow. A key ingredient is a power-law representation for local skin friction which may be stated as

$$\frac{\tau_w}{\rho U^2} = \frac{\zeta}{\left(\frac{U\theta}{\nu}\right)^m} \quad (10)$$

where

τ_w = wall shear stress

U = velocity outside boundary layer

θ = momentum thickness

ζ, m = constants

The resulting viscous-drag coefficient C_v for bodies of revolution without flow separation is given by

$$C_v = \frac{4\pi}{S/L^2}\left[\frac{(1+m)\zeta}{R_L^{\,m}} \int_0^1 \left(\frac{r}{L}\right)^{1+m} \left(\frac{U}{U_\infty}\right)^{(1+m)(h+2)-m} \sec\alpha \; d\left(\frac{x}{L}\right)\right]^{\frac{1}{1+m}} \left(\frac{U}{U_\infty}\right)_e^{\frac{1-h}{1+q}} \quad (11)$$

where

α is the angle between the tangent to the meridian contour and longitudinal axes

h is the average value of an axisymmetric boundary-layer shape parameter

x is the axial distance from the nose of the body of revolution,

r is the radius of the body of revolution

q is a constant

e is a subscript denoting conditions at the tail and

An equivalent flat-plate drag coefficient C_F is given by considering (U/U_∞) equal to unity in Equation (11)

or

$$C_F = \frac{4\pi}{S/L^2}\left[\frac{(1+m)\zeta}{R_L^m}\int_0^1\left(\frac{r}{L}\right)^{1+m}\sec\alpha\; d\left(\frac{x}{L}\right)\right]^{\frac{1}{1+m}} \tag{12}$$

Here for nonseparating conditions

$$1+f = \frac{C_V}{C_F} \tag{13}$$

or

$$1+f = \left[\frac{\int_0^1\left(\frac{r}{L}\right)^{1+m}\left(\frac{U}{U_0}\right)^{(1+m)(h+2)-m}\sec\alpha\; d\left(\frac{x}{L}\right)}{\int_0^1\left(\frac{r}{L}\right)^{1+m}\sec\alpha\; d\left(\frac{x}{L}\right)}\right]^{\frac{1}{1+m}}\left(\frac{U}{U_0}\right)_e^{\frac{1-h}{1+q}} \tag{14}$$

where f is the partial form factor for bodies of revolution in axisymmetric flow.

Using a ratio of C_V and C_F, both obtained from a power-law relation for local skin friction, tends to minimize any deviations arising from the use of a simplified method. The reference flat-plate drag formula to be used in Equation (4) is a more accurate logarithmic formula[8] such as

$$C_F = \frac{0.0766}{(\log_{10} R_L - 1.88)^2} + \frac{60}{R_L} \tag{15}$$

There is at present no simple analytical method for determining separation form factor g.

For <u>two-dimensional symmetric foils</u>, at zero angle of attack the form factor f is given by Equation (14) after r is considered constant and h = H, a two-dimensional shape parameter,

$$1+f = \left[\frac{\int_0^1\left(\frac{U}{U_0}\right)^{(1+m)(H+2)-m}\sec\alpha\; d\left(\frac{x}{L}\right)}{\int_0^1 \sec\alpha\; d\left(\frac{x}{L}\right)}\right]^{\frac{1}{1+m}}\left(\frac{U}{U_0}\right)_e^{\frac{1-H}{1+q}} \tag{16}$$

For ship hulls, an equivalent body of revolution is defined with two radii, r_p, based on perimeter and r_A based on cross-section area or

$$r_p = \frac{\tilde{P}}{\pi} \tag{17}$$

and

$$r_A = \sqrt{\frac{2\tilde{A}}{\pi}} \tag{18}$$

where

$\tilde{P}$ = perimeter of ship hull at a station to the water line

$\tilde{A}$ = cross-sectional area of a ship hull at a station to the water line

The cross-sectional area radius r_A is used to determine the longitudinal distribution of pressure which also determines $(U/U_\infty)_A$. The perimeter radius r_p is used explicitly in the formula for form factor such that

$$1+f = \left[\frac{\int_0^1 \left(\frac{r_p}{L}\right)^{1+m} \left(\frac{U}{U_\infty}\right)_A^{(1+m)(h+2)-m} \sec\alpha \; d\left(\frac{x}{L}\right)}{\int_0^1 \left(\frac{r_p}{L}\right)^{1+m} \sec\alpha \; d\left(\frac{x}{L}\right)}\right]^{\frac{1}{1+m}} \left(\frac{U}{U_\infty}\right)_{A,e}^{\frac{1-h}{1+q}} \tag{19}$$

Values of m = 0.169 and h = H = 1.4 are recommended. For the body of revolution q = 7 and for two-dimensional foils q = 1.

Rough Bodies and/or Drag-Reducing Polymer Solutions

As shown for smooth bodies in ordinary fluids, the derivation of a partial form factor from the boundary-layer momentum equation depends on the use of a local skin friction formula as a power-law relation. The situation for rough bodies and/or drag-reducing polymer solutions is quite different. The local skin friction coefficient varies not only with local Reynolds number but with a variety of other parameters such as local relative roughness, type of roughness, type of drag-reducing polymer, concentration, etc. There is no simple formulation. One way out of the impasse is to consider an average local skin-friction coefficient which is invariant along the boundary layer and which has a value commensurate with the roughness and/or drag-reducing polymer situation in question. Such a value is given by the average local skin friction of an equivalent flat plate with the same condition of roughness and/or polymer solution.

If an average of local skin-friction coefficient $\frac{\tau_w}{\rho U^2}$ is represented by $\bar{\zeta}$,

then from flat plates

$$\bar{\zeta} = \frac{C_F}{2} = f\left[R_L, \frac{k}{L}, \varrho, P, C_{w,e}, \frac{x_i}{L}\right] \tag{20}$$

The viscous drag coefficient C_v of a body of revolution with roughness and/or drag-reducing polymer solution is given by Equation (14) with $\zeta = \bar{\zeta}$ and $m = 0$ or

$$C_v = \frac{4\pi}{S/L^2}\left[\bar{\zeta}\int_0^1 \left(\frac{r}{L}\right)\left(\frac{U}{U_\infty}\right)^{h+2} \sec\alpha \; d\left(\frac{x}{L}\right)\right]\left(\frac{U}{U_\infty}\right)_e^{\frac{1-h}{1+q}} \tag{21}$$

and the drag coefficient of an equivalent flat plate is given by

$$C_F = \frac{4\pi}{S/L^2}\left[\bar{\zeta}\int_0^1 \left(\frac{r}{L}\right) \sec\alpha \; d\left(\frac{x}{L}\right)\right] \tag{22}$$

This ratio gives the partial form factor for <u>bodies of revolution in axisymmetric flow</u> or

$$1 + f = \left[\frac{\int_0^1 \left(\frac{r}{L}\right)\left(\frac{U}{U_\infty}\right)^{h+2} \sec\alpha \; d\left(\frac{x}{L}\right)}{\int_0^1 \left(\frac{r}{L}\right) \sec\alpha \; d\left(\frac{x}{L}\right)}\right]\left(\frac{U}{U_\infty}\right)_e^{\frac{1-h}{1+q}} \tag{23}$$

This is the same formula, Equation (14) with $m = 0$.
For <u>two-dimensional symmetric foils at zero angle of attack</u>, the partial form factor is given by

$$1 + f = \left[\frac{\int_0^1 \left(\frac{U}{U_\infty}\right)^{H+2} \sec\alpha \; d\left(\frac{x}{L}\right)}{\int_0^1 \sec\alpha \; d\left(\frac{x}{L}\right)}\right]\left(\frac{U}{U_\infty}\right)_e^{\frac{1-H}{1+q}} \tag{24}$$

For <u>ship hulls</u>, the partial form factor is given by

$$1 + f = \left[\frac{\int_0^1 \left(\frac{r_0}{L}\right)\left(\frac{U}{U_\infty}\right)_A^{h+2} \sec\alpha \; d\left(\frac{x}{L}\right)}{\int_0^1 \left(\frac{r_0}{L}\right) \sec\alpha \; d\left(\frac{x}{L}\right)}\right]\left(\frac{U}{U_\infty}\right)_{A,e}^{\frac{1-h}{1+q}} \tag{25}$$

As formulated here, the partial form factor f is a <u>universal</u> form factor which in principle also applies to smooth bodies in ordinary fluids.

FLAT-PLATE DRAG COEFFICIENTS FOR ROUGH SURFACES AND/OR DRAG-REDUCING POLYMER SOLUTIONS

<u>General</u> Since the formulas for flat plates with rough surfaces and drag-reducing polymer solutions are scattered in the literature, it will be useful to assemble them here. In general, drag coefficients for flat plates with rough surfaces and/or drag-reducing polymer solutions vary not only with Reynolds number but with a variety of other factors or

$$C_F = f\left[R_L, \frac{k}{L}, \mathcal{R}, P, C_{w,e}, \frac{x_i}{L}\right] \tag{26}$$

The specific variation of C_F with roughness and/or polymer solution is obtained from a similarity-law characterization ΔB such that

$$\Delta B = f\left[\frac{u_\tau k}{\nu}, \mathcal{R}, P, C\right] \tag{27}$$

where u_τ = shear velocity, $u_\tau = \sqrt{\frac{\tau_w}{\rho}}$

As stated before, a characteristic polymer length ℓ may be substituted for characteristic roughness length k when polymer solutions are involved.

The ΔB- characterization is usually obtained empirically from the viscous losses in pipe flow[2,9] and the torques of rotating disks.[10] Pipe-flow tests or rotating-disk tests are usually more convenient than the direct towing of flat plates.

<u>Rough Surfaces in Ordinary Fluids</u>

Here

$$C_F = f\left[R_L, \frac{k}{L}, \mathcal{R}\right] \tag{28}$$

For a given roughness configuration $\mathcal{R}$, the drag coefficient C_F is a function of two dimensionless ratios, a Reynolds number R_L and relative roughness k/L. The C_F values are obtained from a ΔB-characterization

$$\Delta B = f\left[\frac{u_\tau k}{\nu}, \mathcal{R}\right] \tag{29}$$

Although regular roughness configurations have been well studied, problems remain for the irregular roughness found in engineering applications. There is still no satisfactory method for geometrically characterizing such roughness in an hydrodynamically meaningful way.

There is a limiting case of fully-developed roughness flow where C_F is no longer a function of Reynolds number or

$$C_F = f\left[\frac{k}{L}, \mathcal{R}\right] \quad \text{for} \quad \frac{u_\tau k}{\nu} \geq \left(\frac{u_\tau k}{\nu}\right)_r \tag{30}$$

Here

$$\left(\frac{u_\tau k}{\nu}\right)_r = f\left[\mathcal{R}\right] \tag{31}$$

Another limiting case is that of hydraulic smoothness where C_F is only a function of Reynolds number or

$$C_F = f\left[R_L\right] \quad \text{for} \quad \frac{u_\tau k}{\nu} \leq \left(\frac{u_\tau k}{\nu}\right)_s \tag{32}$$

Here

$$\left(\frac{u_\tau k}{\nu}\right)_s = f\left[\mathcal{R}\right] \tag{33}$$

The full variation of C_F with roughness occurs only for

$$\left(\frac{u_\tau k}{\nu}\right)_s \leq \frac{u_\tau k}{\nu} \leq \left(\frac{u_\tau k}{\nu}\right)_r$$

A general formula for the drag coefficient of flat plates with rough surfaces is given by

$$\frac{1}{\sqrt{C_F}} = 4.13 \log_{10}(C_F R_L) + \frac{(\Delta B)_e}{\sqrt{2}} \tag{34}$$

which reduces to the Schoenherr formula for smooth surfaces for $\Delta B = 0$ or

$$\frac{1}{\sqrt{C_F}} = 4.13 \log_{10}(C_F R_L) \tag{35}$$

For fully-developed roughness flow of the Nikuradse-type sand roughness

$$\frac{1}{\sqrt{C_F}} = 4.13 \log_{10}\left(\sqrt{C_F}\,\frac{L}{k}\right) + 4.52 \tag{36}$$

Smooth Surfaces in Drag-Reducing Polymer Solutions

In this case,

$$C_F = f\left[R_L, \frac{\ell}{L}, P, C\right] \tag{37}$$

A characteristic time t or characteristic mass m may be substituted for characteristic length ℓ .

For a given polymer type P and concentration C, the drag coefficient C_F is a function of a Reynolds number R_L and length ratio ℓ/L.

The C_F-values are obtained from a ΔB-characterization

$$\Delta B = f\left[\frac{u_\tau \ell}{\nu}, P, C\right] \tag{38}$$

There is a limiting case of maximum drag reduction[11,12] where C_F is just a function of Reynolds number R_L or

$$C_F = f\left[R_L\right] \tag{39}$$

There is another limiting case of drag-reduction inception where for $\frac{u_\tau \ell}{\nu} \leq \left(\frac{u_\tau \ell}{\nu}\right)_o$ there is no drag reduction.
In general

$$\left(\frac{u_\tau \ell}{\nu}\right)_o = f\left[P, C\right] \tag{40}$$

A general formula for the drag coefficient of flat plates in a uniform polymer concentration is given by

$$\frac{1}{\sqrt{C_F}} = 4.13 \log_{10}\left(C_F R_L\right) + \frac{(\Delta B)_c}{\sqrt{2}} \tag{41}$$

which reduces to the Schoenherr formula for ordinary fluids.

For the case of maximum drag reduction which is another limiting case

$$\frac{1}{\sqrt{C_F}} = 11.33 \log_{10}(C_F R_L) - 32.44 \tag{42}$$

Finally for a linear ΔB-characterization of type

$$\Delta B = \tilde{q}\left[\log_{10}\left(\frac{u_\tau \ell}{\nu}\right) - \log_{10}\left(\frac{u_\tau \ell}{\nu}\right)_0\right] \tag{43}$$

where

$$\tilde{q} = f\,[C, P] \tag{44}$$

The drag coefficient[2,13] becomes

$$\frac{1}{\sqrt{C_F}} = 4.13\left(1 + \frac{\tilde{q}}{5.84}\right)\log_{10}(C_F R_L) - \frac{\tilde{q}}{\sqrt{2}}\log_{10}\frac{L}{\ell} - \frac{\tilde{q}}{\sqrt{2}}\log_{10}\left[\sqrt{2}\left(\frac{u_\tau \ell}{\nu}\right)_0\right] \tag{45}$$

Rough Surfaces in Drag-Reducing Polymer Solutions

Here

$$C_F = f\left[R_L, \frac{k}{L}, \ell, P, C\right] \tag{46}$$

or

$$C_F = f\left[R_L, \frac{\ell}{L}, \ell, P, C\right] \tag{47}$$

Rough surfaces tend to increase the drag while polymer solutions tend to reduce the drag. Hence, there is a mutually antagonistic result for both effects.

It has been found that there is no drag reduction for the condition of fully-developed roughness flow outside some transient viscoelastic effect.

The ΔB-characterization[2] is

$$\Delta B = f\left[\frac{u_\tau k}{\nu}, \ell, P, C\right] \tag{48}$$

or

$$\Delta B = f\left[\frac{u_\tau l}{\nu}, R, P, C\right] \tag{49}$$

A general formula for drag coefficient is

$$\frac{1}{\sqrt{C_F}} = 4.13 \log_{10}\left(C_F R_L\right) + \frac{(\Delta B)_e}{\sqrt{2}} \tag{50}$$

<u>Injection of Polymer Solution through a Slot</u>

Injection of concentrated polymer solution through a slot results in a nonuniform concentration of polymer downstream of which the value of the wall concentration determines the degree of drag reduction. Downstream of the slot, a concentration layer grows until it reaches the full thickness of the boundary layer. Afterwards, the concentration layer and the boundary layer coexist with the same thickness. There is an interaction between the growth of the boundary layer and the dilution of the drag-reducing polymer solution.

A prediction[14] of the development of the boundary layer and the resulting concentration of the polymer may be obtained semigraphically from a plot of $C_w e^{-\frac{\Delta B}{A}}$ against $\frac{u_\tau l}{\nu}$ for fixed values of C_w for the region where the momentum boundary layer and the concentration layer coexist. Here A is a boundary-layer parameter. The drag coefficient is given by[15]

$$\frac{1}{\sqrt{C_F}} = 4.13 \log_{10}\left(C_F R_L\right) + \frac{(\Delta B)_e}{\sqrt{2}} + \frac{\ell}{\sqrt{2}} \tag{51}$$

where

$$\ell = C_{w,e} \int_{C_{w,e}}^{C_{w,i}} \frac{1}{C_w^2} \frac{\partial(\Delta B)}{\partial(\ln C_w)}\, dC_w \tag{52}$$

An alternate form is

$$\ell = -(\Delta B)_e + C_{w,e} \int_{C_{w,e}}^{C_{w,i}} \frac{\Delta B}{C_w^2}\, dC_w \tag{53}$$

$C_{w,i}$ is the initial concentration.

COMPARISON OF FORM FACTORS

The partial form factor f for smooth bodies in ordinary fluids has been formulated in two ways: a universal form, Equation (23) depending on an average local skin friction coefficient and a specific form, Equation (14), depending on a power-law local skin friction coefficient for smooth surfaces. It is interesting to compare the two.

If an average value of $\frac{U}{U_\infty}$, $\left(\frac{\bar{U}}{U_\infty}\right)$, is considered constant along the body, then the universal relation gives a form factor f_u as

$$1 + f_u = \left(\frac{\bar{U}}{U_\infty}\right)^{h+2+\frac{1-h}{1+q}} \tag{54}$$

and the special smooth relation gives a form factor f_{sp} as

$$1 + f_{sp} = \left(\frac{\bar{U}}{U_\infty}\right)^{h+\frac{2+m}{1+m}+\frac{1-h}{1+q}} \tag{55}$$

If

$$\left(\frac{\bar{U}}{U_\infty}\right) = 1 + \Delta\left(\frac{\bar{U}}{U_\infty}\right) \tag{56}$$

then

$$f_u = \left(h+2+\frac{1-h}{1+q}\right)\Delta\left(\frac{\bar{U}}{U_\infty}\right) \tag{57}$$

and

$$f_{sp} = \left(h+\frac{2+m}{1+m}+\frac{1-h}{1+q}\right)\Delta\left(\frac{\bar{U}}{U_\infty}\right) \tag{58}$$

Finally

$$\frac{f_u}{f_{sp}} = \frac{h+2+\frac{1-h}{1+q}}{h+\frac{2+m}{1+m}+\frac{1-h}{1+q}} \tag{59}$$

For h = 1.4, m = 0.169, and q = 7

$$\frac{f_u}{f_{sp}} = 1.046 \tag{60}$$

A 4.6 percent deviation in form factor is suprisingly small when considering the differences in local skin friction coefficient used to derive the form factors.

Overall checks of the proposed method would involve measurements of the drags of bodies and flat plates with the same roughness and/or same polymer solutions at same concentration. Such measurements do not seem to be in evidence.

REFERENCES

1. Granville, P.S., "The Frictional Resistance and Turbulent Boundary Layer of Rough Surfaces," Journal of Ship Research, Vol. 2, No. 3, pp. 52-74 (Dec 1958).

2. Granville, P.S., "The Frictional Resistance and Velocity Similarity Laws of Drag-Reducing Polymer Solutions," Journal of Ship Research, Vol. 12, No. 3, pp. 201-212 (Sep 1968).

3. Granville, P.S., "A Modified Froude Method for Determining Full-Scale Resistance of Surface Ships from Towed Models," Journal of Ship Research, Vol. 18, No. 4, pp. 215-223 (Dec 1974).

4. Granville, P.S., "Elements of the Drag of Underwater Bodies," David Taylor Naval Ship R&D Center Report SPD-672-01 (Jun 1976).

5. Hoerner, S.F., "Fluid-Dynamic Drag," published by author, Midland Park, N.J. (1958).

6. Granville, P.S., "The Viscous Resistance of Surface Vessels and the Skin Friction of Flat Plates," Transactions of Society of Naval Architects and Marine Engineers, Vol. 64, pp. 209-240 (1956).

7. Granville, P.S., "Partial Form Factors from Equivalent Bodies of Revolution for the Froude Method of Predicting Ship Resistance," Proceedings of First Ship Technology and Research Symposium, Aug 1975, Society of Naval Architects and Marine Engineers, New York, NY.

8. Granville, P.S., "The Drag and Turbulent Boundary Layer of Flat Plates at Low Reynolds Numbers," Journal of Ship Research, Vol. 21, No. 1, pp. 30-39 (Mar 1977).

9. Huang, T.T., "Similarity Laws for Turbulent Flow of Dilute Solutions of Drag-Reducing Polymers," Physics of Fluids, Vol. 17, No. 2, pp. 298-309 (Feb 1974).

10. Granville, P.S., "The Resisting Torque and Turbulent Boundary Layer of Rotating Disks with Smooth and with Rough Surfaces in Ordinary Fluids and in Drag-Reducing Polymer Solutions," Journal of Ship Research, Vol. 17, No. 4, pp. 181-195 (Dec 1973).

11. Granville, P.S., "Limiting Conditions to Similarity-Law Correlations for Drag-Reducing Polymer Solutions," Naval Ship R&D Center Report 3635 (Aug 1971).

12. Granville, P.S., "Maximum Drag Reduction at High Reynolds Number for a Flat Plate Immersed in Polymer Solution," Journal of Hydronautics, Vol. 6, No. 1, pp 58-59 (Jan 1972).

13. Granville, P.S., "Hydrodynamic Aspects of Drag Reduction with Additivies," Marine Technology, Vol. 10, No. 3, pp. 284-292 (Jul 1973).

14. Granville, P.S., "Drag Reduction of Flat Plates with Slot Ejection of Polymer Solution," Journal of Ship Research, Vol. 14, No. 2, pp. 79-83 (Jun 1970).

15. McCarthy, J.H., "Flat-Plate Frictional-Drag Reduction with Polymer Injection," Journal of Ship Research, Vol. 15, No. 4, pp. 278-288 (Dec 1971).

THE EFFECT OF INITIAL ACCELERATION
ON SHIP WAVE
PATTERN AND WAVE SURVEY METHODS

by

S. M. CALISAL
U. S. Naval Academy

INTRODUCTION

The wave resistance of a ship moving at a constant speed can be calculated using information obtained from its wave pattern (1), (2), (3). Different methods which exist for wave resistance calculations are based on the existence of a linearized free-wave velocity potential and the conservation of momentum or energy in a control volume. One of the basic assumptions in the above mentioned methods is the requirement of a constant model speed.

The effect of initial acceleration upon the wave resistance of ships was studied by Wehausen (4). This work shows that the wave resistance calculated for a ship model with initial acceleration will have an oscillating and decaying behavior, and that the "mean" value of the oscillation will correspond to Michell's wave resistance. An immediate conclusion from previously mentioned work might be that the measured "wave resistance" values for a ship model moving at a constant speed but with initial acceleration might show a scatter of data about a "mean" value.

This paper presents a study to evaluate the effect of initial acceleration on the various existing wave survey methods and to determine which one is least affected by this possible source of error. The ship is represented by a distribution of sources and sinks. The wave spectrum for large cT values is calculated using the theorems in (4). The calculations indicate that for large cT values the initial acceleration will generate an additional two dimensional wave ζ_T superimposed on the ship's free waves. The form of ζ_T is given by

$$\zeta_T = \frac{A}{cT} \sin \left(\frac{1}{4} k_o(x-cT) + \phi(t)\right) + o(cT)^{-2}$$

It is also determined that this wave will have no influence on longitudinal cut methods but that transverse cut methods on the other hand will be affected.

Wave resistance calculations are usually made with nondimensional variables. We will use unbarred variables to represent dimensional variables and barred variables to represent dimensionless variables. As fundamental units we take ship speed, c, density of fluid, ρ, and gravitational acceleration, g. One can use $k_o = \frac{g}{c^2}$, which has the dimension (L^{-1}) to nondimensionalize lengths. The resistance can be nondimensionalized

by $\bar{R} = R\, k_o^2/\rho c^2$.

THEORY

The representation of a ship for ship wave resistance calculations can be made by a source and sink distribution. Even though the original wave resistance problem is nonlinear, linearization permits the superposition of the elementary effects of each source. The wave pattern can then be obtained as a sum of the waves generated by each source. The velocity potential of a source moving under the free surface is given by Lunde [5]. For a source moving in +x direction this potential can be written as:

$$\phi(x,y,z,t) = \frac{m(t)}{r_1} - \frac{m(t)}{r_2} + \frac{g^{1/2}}{\pi} \int_0^t m(\tau)\, d\tau \int_{-\pi}^{\pi} d\theta \int_0^{\infty} \sin\,[\sqrt{kg}\,(t-\tau)]$$

$$\exp\,(k[(z-f) + i\bar{w}\,])\, k^{1/2}\, dk \qquad (1)$$

in a coordinate system moving with the source. The variables in the equation are the source strength m, $r_1^2 = x^2 + y^2 + (z+f)^2$, $r_2^2 = x^2 + y^2 + (f-z)^2$ and $\bar{w} = (x + \int_\tau^t c(\tau)d\tau)$ $\cos\theta + y\sin\theta$. The coordinate system is given in figure 1. The coordinate of the source is (o, o, -f) and the velocities can be calculated from $v = -\nabla\phi$.

The surface wave elevation ζ can then be calculated from the linearized free-surface condition given by

$$\zeta\,(x,y,t) = \frac{1}{g}\,(\phi_t - c\phi_x)\Big|_{z=0} \qquad (2)$$

As ζ is the input for all calculations in wave survey methods, it will be calculatec first from a given velocity potential ϕ . The velocity potential contains the effects of the variation of the velocity from time t = 0 to t = t. A velocity-versus-time diagram will then be required for the calculation of velocity potential. Figure 2 shows a possible diagram for a ship reaching a constant velocity c_o at $t = t_o$ and maintaining that velocity for $t > t_o$. This might very well represent the towing-tank procedures where the velocity is kept constant during a particular experiment after the initial acceleration. Once the c(t) function is defined, as in Figure (2), one can obtain the velocity potential ϕ and wave height records

The integral (1) with respect to time can be separated into two terms as follows:

$$\int_0^t m\,(\tau)\, d\tau \int_{-\pi}^{\pi} d\theta \int_0^{\infty} \sin\,[\sqrt{kg}\,(t-\tau)]\, \exp\,\{k[z-f + i\bar{w}\,]\}\, k^{1/2}\, dk =$$

$$\int_0^{t_o} m\,(\tau)\, d\tau \int_{-\pi}^{\pi} d\theta \int_0^{\infty} \sin\,[\,\sqrt{kg}\,(t-\tau)]\, \exp\,\{k[z-f + i\bar{w}]\,\}\, k^{1/2}\, dk\; +$$

$$\int_{t_o}^{t} m\,(\tau)\, d\tau \int_{-\pi}^{\pi} d\theta \int_0^{\infty} \sin\,[\sqrt{kg}\,(t-\tau)]\, \exp\,\{k[z-f + i\bar{w}\,]\}\, k^{1/2}\, dk \qquad (3)$$

It can easily be seen that the third term represents the velocity potential due to a velocity function $c = c\cdot s(t-t_o)$ where s(t) is a step function. This term will be studied first and it will represent a test in which the ship model is brought to the desired velocity instantaneously. The effect of the second integral in (3) can be

studied separately.

WAVE PATTERN FOR AN IMPULSIVE START

The second integral on the right hand side of equation (3) can be integrated with respect to time variable t. The result is then expressed as the sum of a time-dependent and time independent term. The time independent term can be written as:

$$\phi_1(x,y,z) = \frac{4k_o m}{\pi} \int_0^{\pi/2} d\theta \sec^2\theta \int_0^\infty \frac{\exp(k(z-f)) \cdot \cos(k\, x \cos\theta) \cdot}{k - k_o \sec^2\theta} \cos(ky \sin\theta)\, dk. \tag{4}$$

The time dependent term on the other hand is

$$\phi_2(x,y,z,t) = \frac{g^{\frac{1}{2}} m}{\pi c^2} \int_0^{\pi/2} d\theta \sec^2\theta \int_0^\infty \{(kc \cos\theta + \sqrt{kg}) \exp[it(kc\cos\theta - \sqrt{kg})] - (kc\cos\theta - \sqrt{kg}) \exp[it(kc\cos\theta + \sqrt{kg})]\}$$

$$\frac{\exp\{k[(z-f) + i(x\cos\theta \pm y\sin\theta)]\}\, dk}{k^{\frac{1}{2}}(k - k_o \sec^2\theta)} \tag{5}$$

Except for the first $\sec^2\theta$ term, this equation is the same as given by Lunde [5].

The $\pm$ signs in equation (5) indicate that contributions of the $-$ and $+$ signs should be calculated separately and added. At this point it is difficult to write a simple expression for ϕ_2 for all values of time t. An expression for large t on the other hand is not difficult. Remembering that the velocity potential we are interested in for wave-survey methods corresponds to a relatively large t, an asymptotic expansion is calculated for the potential ϕ_2 for t=T.

Calisal (1976) gives the form of the time dependent term for large $\frac{k_o cT}{4}$ values as:

$$\phi_{2T} = \frac{4\sqrt{2m}}{(cT)} \exp\left(\frac{k_o}{4}(z-f)\right) \cos\left[\frac{ko}{4}(x-cT)\right] + o(cT)^{-2}$$

<u>Time-Dependent Wave System</u>

ϕ_{2T} will therefore generate a wave system superimposed on the steady wave pattern of the source. Since the total wave height is recorded, a time dependent error will be introduced. The contribution of ϕ_{2T} to the wave generated by a source is:

$$\zeta_T = \frac{1}{g}(\phi_{2T,t} - c\phi_{2T,x})|_{z=0}$$

or

$$\zeta_T = \frac{A}{cT}\sin\left(\frac{1}{4}k_o(cT-x)\right) + o(cT)^{-2}$$

where

$$A = \frac{2\sqrt{2m}}{c}\exp\left(-\frac{kof}{4}\right) \tag{17}$$

We can therefore conclude that the amplitude of the time-dependent wave will decrease linearly with time, and that the wave number will be constant and equal to $\frac{k_o}{4}$. As the ζ_T waves are moving with respect to the source or to the ship, the ship is in fact sailing not on a smooth surface but on her own acceleration waves. This would generate an unsteady wave resistance. The decaying amplitude will ensure that the

effect of ζ_T will be zero as $T \to \infty$.

As far as wave-height or wave-slope records are concerned, this effect can be looked upon as a "noise" superimposed on a signal. We will next try to see the form of this noise as seen by a fixed wave height or wave slope transducer and a stereo-photographic measurement, and their implications on wave-resistance calculations.

ERROR IN WAVE SURVEY METHODS

a - Longitudinal-cut methods.

One of the widely used techniques in ship wave-height measurement is the stationary sonic or electronic wave-height probe. Usually a time record is obtained and this record is later interpreted, based on the assumption of a constant model speed. The record generally begins after the model reaches a certain location $x = X$, or on the time scale at time $T = \frac{X}{c}$. The asymptotic form of the wave due to initial acceleration as seen by a fixed probe can be expressed as

$$\bar{\zeta}_T = \frac{A\, k_o^2}{\bar{L}-\bar{x}} \sin\left(\frac{1}{2}\bar{x} - \frac{\bar{L}}{4}\right)$$

where L is the distance between the probe and starting line, and the barred variables denote nondimensional values. The numerical operations required for the calculation of wave resistance from wave height records can be summarized as follows. First the Fourier transform of the longitudinal cut is obtained as

$$C(s,\bar{y}) + i\, S(s,\bar{y}) = \int_{-\infty}^{+\infty} \bar{\zeta}\,(\bar{x},\bar{y}) \exp\,(is\bar{x})\; d\bar{x}.$$

The value $(C^2 + S^2)^{1/2}$ is usually called the amplitude. The wave pattern is assumed to be transversely symmetric and the wave-resistance calculation is based on this transform. Wave resistance is then calculated as [2].

$$\bar{R}_W = \frac{1}{\pi} \int_0^\infty \frac{s^2 - 1}{s^2(2s^2-1)}(C^2 + S^2) \quad du$$

where $s = \sec\theta$, $u = \sec\theta \tan\theta$, θ is the direction of the propagation of the free waves. s and u are longitudinal and transverse wave numbers and are kinematically connected. The limits of integration in terms of the u variable are 0 and ∞ while the limits of integration in terms the s variable will be 1 and ∞ which is a direct consequence of the assumed free wave spectrum. One can easily see that this assumption eliminates the contribution of any wave with a dimensionless wave number $s < 1$ on the wave resistance calculation of the ship. Therefore, even though the wave record has an error, standard wave resistance calculations based on the previous formulas will not be affected by it.

The wave-resistance values obtained from a wave-slope record will similarly not be influenced by initial acceleration, as the transverse waves generated by the initial acceleration will have a transverse slope equal to zero up to this order of approximation.

The Fourier transform of the wave-height record on the other hand provides a

possibility of detecting the existence of the initial acceleration effects in the wave system. To give a graphical representation the effect of an imaginary acceleration is superimposed on an experimental record. The acceleration effect as reflected by a fixed wave-height probe shows a relatively high peak around $s=\frac{1}{2}$.

Another possible method for measuring the waves generated by a ship is the stereo-photographic technique. This type of measurement records the shape of the free surface at a given time. The photograph usually covers only the range of interest. As there is no interpretation of the length scale from a time scale, in contrast to the previous measurements, the calculations are straight forward. Figure 3 shows a relatively high value for the amplitude around $s = \frac{1}{4}$, instead of a Dirac delta function, which one would theoretically expect.

The numerical differences between amplitude values with initial-acceleration effects and amplitude values obtained from experimental data assumed free of initial acceleration effects decrease as the s value increases. For this numerical calculation the distance L is taken to be 1200' or two ship lengths for the sources at midship section. One can claim, therefore, that the wave resistance calculations based on fixed probes and longitudinal cuts are not affected by initial acceleration, even though the wave spectrum is.

b - Transverse cut methods.

The effect of initial acceleration on a transverse-cut method will correspond to a shift in the original free-surface level. If a stereo-photographic method is used, this shift will be a constant quantity for a given transverse-cut location. Theoretically the error introduced to wave height can be corrected very easily if enough information is available on the time history of the events.

Eggers [1] gave the formulas for calculating the wave resistance for a symmetric disturbance in a rectangular tank. The assumed free wave surface is expressed as

$$\zeta(x,y) = \sum_{\nu=0}^{\infty} \varepsilon_\nu \, [a_\nu \cos (s_\nu x) + b_\nu \sin (s_\nu x)] \cos (\frac{2\pi\nu}{b} y)$$

and the resistance is

$$R_\omega = \frac{b}{4} \sum_{\nu=0}^{\infty} \varepsilon_\nu \, (a_\nu{}^2 + b_\nu{}^2) \, (2 - \frac{1}{s_\nu{}^2})$$

where $\varepsilon_\nu = \frac{1}{2}$ for $\nu = 0$ and 1 otherwise, the tank walls are at $y = \pm b$ and $u = \frac{\pi\nu}{b}$. The values of a_ν and b_ν are obtained by evaluating the integral $\int_{-b}^{+b} \zeta(x, y) \begin{matrix}\cos\\ \sin\end{matrix} \frac{2\pi\nu}{b} dy$. One can easily see that the terms a_0 and b_0 will be influenced by the effect on initial acceleration, as $\zeta(x,y)$ will be changed locally by a constant value at a given x location. As two parallel transverse cuts are required for the calculation of a_ν and b_ν, a general conclusion cannot be given. An obvious solution is to locate the transverse cuts in such a way that the expected change in free surface elevation due to initial acceleration is equal to zero for two such cuts. However, the transverse cut method requires a special choice of spacing between cuts to minimize the numerical error in the calculations. This requirement is contradictory to the possible solution referred to above.

Results and Conclusion

Direct determination of the wave resistance value through wave survey analysis increased the understanding of the wave resistance concept and offered a new method to towing tanks. The wave-resistance values calculated by using such methods usually predict a wave resistance value less than the residual resistance. One of the assumptions used in the wave-survey methods namely constant ship velocity, is analyzed here. The results of the effect of the initial acceleration to the first order in $(\frac{1}{cT})$ can be summarized as follows:

a. The initial acceleration will not affect the wave resistance calculations based on longitudinal wave height or wave slope records.

b. Wave-resistance calculations based on transverse cut methods will be affected by initial acceleration effects. This influence will be limited to the first term of the series representing the wave resistance.

c. It is possible to determine the existence of the initial-acceleration effects in the wave spectra from the form of the amplitude spectrum calculated for the range $0 < s < 1$. The linearized wave-resistance problem predicts zero amplitude in this interval, and the influence of the initial acceleration to the first order in $(\frac{1}{cT})$ is confined to the same range. As there is no guarantee for the absence of non-linear effects in problems involving gravity waves it might be desirable to check the existence of initial-acceleration waves in the recorded spectra.

NOMENCLATURE

c	velocity of the ship
$-f$	z coordinate of the source
g	gravitational acceleration
$k_o = \frac{g}{c^2}$	wave number
m	source strength
R_W	wave resistance value
s	longitudinal nondimensional wave number
t	time variable
T	a large value for time
u	transverse nondimensional wave number
ζ	free surface elevation
ζ_T	waves generated by initial acceleration
ϕ	velocity potential
$(\bar{\ })$	barred variables represent nondimensional variables, whereas unbarred variables represent dimensional variables

BIBLIOGRAPHY

1. Eggers, K., "uber die Ermittlung des Wellenwiderstandes eines Schiffsmodells durch Analyse seines Wellensystems, I, II, "Schiffstechnik, Vol. 9, (1962), pp. 79-85; Vol. 10 (1963), pp. 93-106.
2. Sharma, S. D. (1966), "An Attempted Application of Wave Analysis Techniques to Achieve Bow-Wave Reduction, "Sixth Symposium on Naval Hydrodynamics, Washington, D. C., U. S. Printing Office, pp. 231-773.
3. Ward, L. W. (1964), "Experimental Determination of Ship Wave Resistance from the Wave Pattern, "Webb Institute of Naval Architecture, Glen Cove, N. Y., viii + 68 pp.
4. Wehausen, J. V., "Effects of Initial Acceleration Upon the Wave Resistance of Ship Models, "J. Ship Res. 7, No. 3, 38-50 (1964).
5. Lunde, J. K., "On the Linearized Theory of Wave Resistance for Displacement Ships in Steady and Accelerated Motion, "Trans, Sol. Nav. Architects Mar. Engr., 59 (1951a), 25-76; disc. 76-85.
6. Erdelyi, A., Asymptotic Expansions, Dover Publications, Inc., New York, N. Y., 1956.
7. Adee B. H., Harvey, P. J. An analyin of ship Resistance Report UWME - BHA - 75 - 01 March 1975 Department of Mechanical Engineering University Washington.
8. Calisal, S.M., "The Effect of Initial Acceleration on Ships Wave Pattern and Wave Survey Methods", Division of Engineering and Weapons Report, 2-76, April 1976.

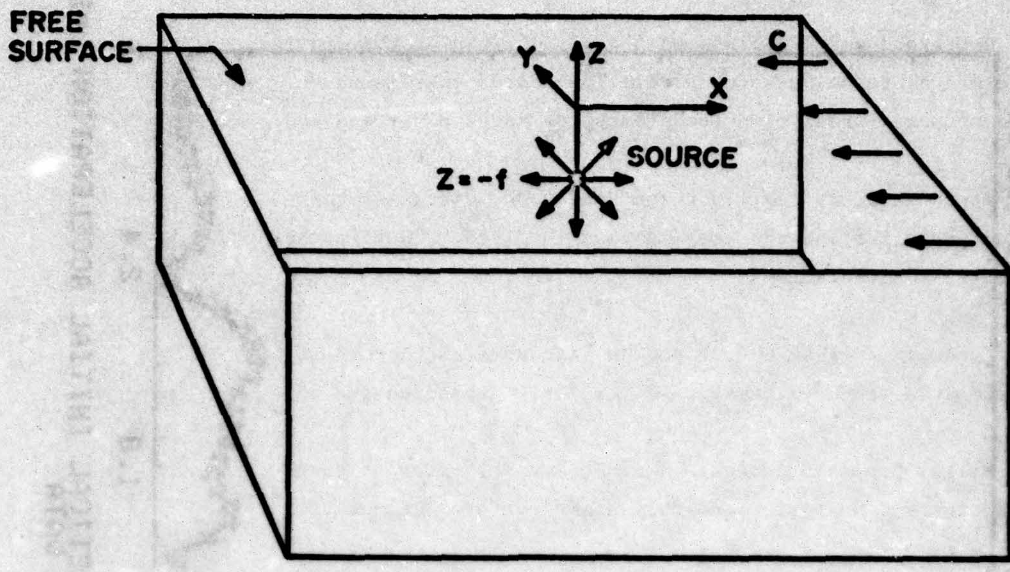

COORDINATE SYSTEM AND THE LOCATION OF THE SOURCE
FIGURE 1.

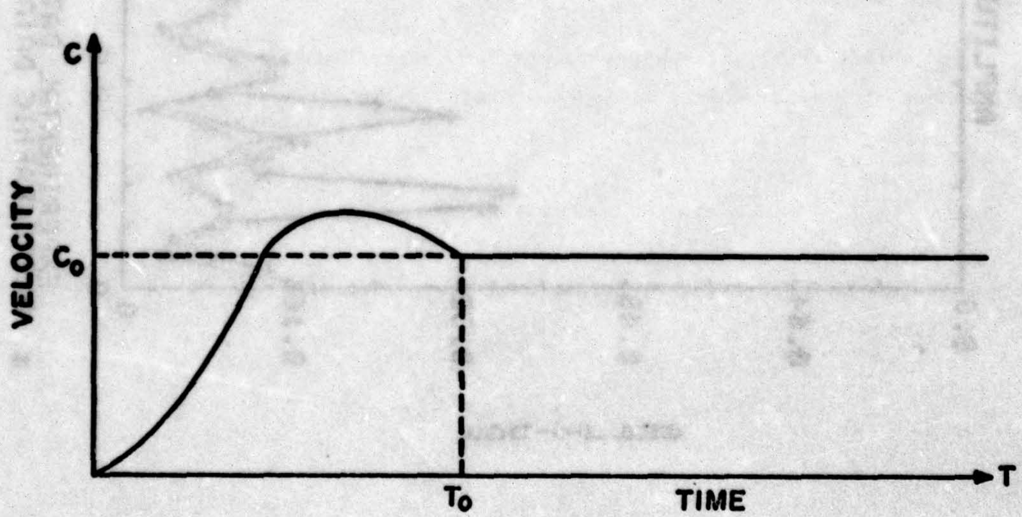

VELOCITY-TIME DIAGRAM
FIGURE 2

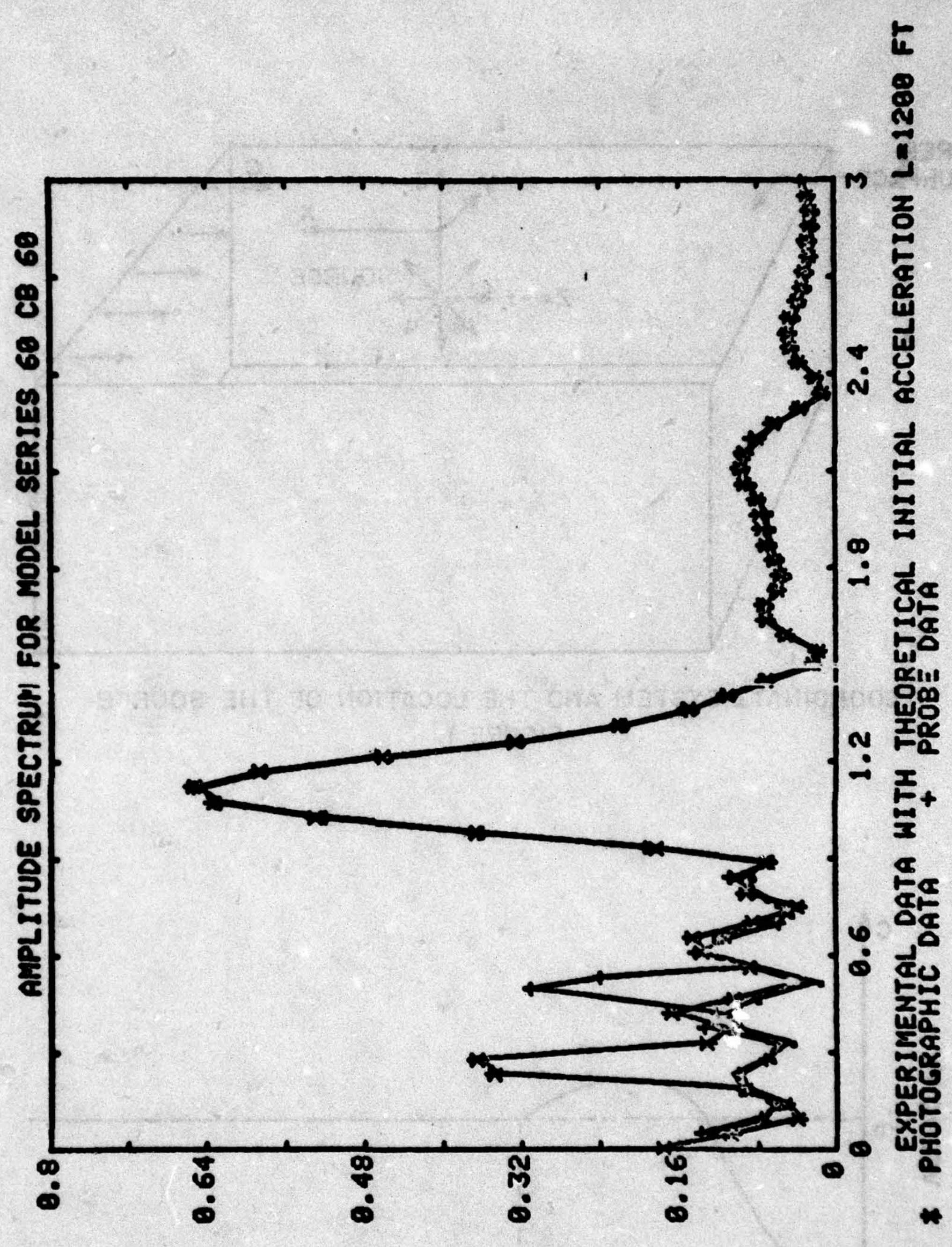
AMPLITUDE SPECTRUM FOR MODEL SERIES 60 CB 60
AMPLITUDE
0.8
0.64
0.48
0.32
0.16
0
0
0.6
1.2
1.8
2.4
3
EXPERIMENTAL DATA WITH THEORETICAL INITIAL ACCELERATION L=1200 FT
* PHOTOGRAPHIC DATA + PROBE DATA

FIGURE 3

AD-A062 506 NAVAL ACADEMY ANNAPOLIS MD F/G 5/11

PROCEEDINGS OF THE GENERAL MEETING (18TH) OF THE AMERICAN TOWIN--ETC(U)

1977 B JOHNSON, B NEHRLING

UNCLASSIFIED NL

2 OF 4

AD
A062506

EFFECT OF WAKE ON WAVE RESISTANCE

by

L. Landweber
Iowa Institute of Hydraulic Research

Introduction

Recent advances in higher-order ship wave theory, and the resulting improvement in the agreement between the computed wave resistance and the residuary, have led to the suggestion that the wave resistance can be satisfactorily calculated on the basis of irrotational flow alone. In an attempt to resolve the question of the influence of the wake, the total viscous and wavemaking resistance of a Series 60 ship model was measured, with the wetted surface first smooth, and then rough, in order to modify the wake. This work was reported in Theses by Moreno [1] and Perez-Rojas [2], and in a report by Moreno, Perez-Rojas, and Landweber [3].

Previous work

In the aforementioned study, a 3.05 m Series-60 model of 0.60 block coefficient was used. The surface was roughened by means of plastic pins of 0.64 cm diameter, 0.16 cm in height, at a spacing of 1.91 cm. It was found that the roughening approximately doubled the viscous resistance (as determined by wake-survey measurements) and appreciably decreased the wave resistance (determined from longitudinal-cut measurements); by 40% at a Froude number F = 0.25, by 50% at F = 0.28, by 30% at F = 0.31, and by 15% at F = 0.34. This indicates that the effect of the boundary layer and the wake on wave resistance should be included in the development of mathematical models for computing the wave resistance of a ship form.

A by-product of this work was the discovery that both the wake-survey and the longitudinal-cut measurements were affected by a long period surge in the towing tank. It was concluded that the affect of the surge was negligible for the determination of wave resistance. A procedure for measuring and correcting for the surge was presented.

Theoretical study

An attempt to calculate the wave resistance of a body, with the boundary layer and wake (BLW) taken into account by replacing the vorticity in BLW by Betz sources, such that the irrotational flow exterior to BLW is undisturbed, is under way. One can

show that the flow exterior to BLW can be exactly reproduced by source distributions M_o and M_1 on the surface of the body and on the outer boundary Σ of BLW, respectively which satisfy the boundary conditions that the normal component of the fluid velocity is zero on the body surface, and a "known function" of position along Σ, with this known function expressible in terms of the displacement thickness of the boundary layer and wake. These boundary conditions yield a pair of integral equations with M_o and M_1 as the unknown functions.

The form selected for this study is the thin body for which total resistance measurements are available and Weinblum, Kendrick and Todd [4] have computed the wave resistance by means of the Michel integral. This body, although of finite draft, may be considered essentially as a thin two-dimensional strut with fine parabolic ends and a long parallel middle body. Because of its fineness, higher-order corrections to linearized wave theory should be unnecessary, thus enabling the effects of the BLW to be more distinguishable.

Since the variation of the displacement thickness δ^* with downstream distance is required as input in the integral equations, and the values of δ^* near the stern and the near wake cannot be estimated with sufficient accuracy by existing theory or data, boundary-layer measurements on this form have been undertaken in a wind tunnel.

Because the modification of M_o by M_1 has been found to be small, it has been necessary to calculate these source strengths accurately, with special care near the wedgelike bow and stern, where the Michell formula for the source strength cannot match the proper analytical behavior. The wave resistance at low Froude numbers would then be calculated by means of the Lagally theorem, applied to the source distribution M_o. This result would be affected by the wake in two ways, one by the influence of the source distribution M_1 on M_o through the pair of integral equations, the other by the velocity induced at a source element of M_o by M_1, as applied in the Lagally theorem.

References

1. M. Moreno, "Experimental Study of the Influence of the Wake on the Wavemaking Resistance of a Ship Model," M.S. Thesis, The University of Iowa, 1975.

2. L. Perez-Rojas, "Effect of Surface Roughness on the Viscous Resistance of a Ship Model Determined by a Wake Survey," M.S. Thesis, The University of Iowa, 1975.

3. M. Moreno, L. Perez-Rojas, and L. Landweber, "Effect of Wake on Wave Resistance of a Ship Model," IIHR Report No. 180, August 1975.

4. G. Weinblum, J. Kendrick and A. Todd, "Investigation of Wave Effects Produced by a Thin Body," TMB Report 840, 1952.

Acknowledgement

This work is supported by the Office of Naval Research under Contract Number N00014-76-C-0012.

Discussion of Committee Report & Contributions

Professor Ward (of Webb Institute) made the following comments:

1. Concerning the Committee report, recommendation 2, which considered the effect of hull wake on wave survey results, he inquired as to the necessity for this action. He agreed that the production of waves by the hull would be influenced by the hull wake, but did not see how the waves, once produced, would be affected between the point of production and the measuring location. (Measurement by longitudinal cut methods was intended here.)

2. Regarding Professor Wehausen's contribution, he pointed out that we might be approaching a theoretical prediction of wave resistance that was reliable in a practical range of speeds (Baba et al). He recalled some very interesting optimized hulls produced at Berkeley, and asked whether the new theory would lend itself to a similar analysis. He reported that the Society of Naval Architects and Marine Engineers had recently, through an Advanced Planning Committee, placed renewed emphasis on energy conservation by the ship, and commented that such studies on optimized hull forms would be of interesting practical importance.

3. In regard to the contribution by Professor Calisal, he was encouraged by the advantage of using slope data in minimizing errors due to transients and said that he might have been the only actual user of such data. However, he also warned that this type of data (at least in a "narrow" tank such as Webb's) would be susceptible to side-wall errors (due to a kind of channeling effect). So Nature gives and takes away!

4. Regarding the contributions by Messrs. McCarthy and Granville, he remarked that neither had mentioned the importance of considering the effect of the free surface on the viscous flow and boundary layer separation problems in the stern area. This should be considered, despite the difficulties arising.

Professor Wu (of Cal Tech) commented on the contribution by Professor Landweber. He remarked that the shear flow, in general, would affect the passing of waves. In a uniform flow, waves would pass along a straight ray, while in a shear flow the ray would bend. This phenomenon must be the main source of the wake effect on the wave resistance.

Professor Wehausen also amplified the remarks made by Professors Ward and Wu and expressed his opinion that a longitudinal wave cut taken at a distance sufficiently remote from the model should be free from the shear flow of the model wake. On the other hand, a transverse wave cut is usually taken across the model wake where the

usual linearized wave theory is not satisfactory; therefore, shear flow effects should be taken into account. Hence, the results from the two different wave cuts should exhibit some discrepancies.

Mr. Lackenby (of BSRA) commented, on the idea of applying the equivalent-body-of-revolution technique to full forms. Since the cross flow would be considerable with a full form, whereas there would be no cross flow present for a body of revolution, he asked how this problem might be reconciled.

Professor Landweber remarked that the equivalent-body-of-revolution technique would not be useful in obtaining detailed information such as the local shear stress. However, for certain types of application, such as the prediction of total viscous drag, the technique could be very useful.

The following written discussion of the Committee Report was submitted by Mr. Michailidis.

"As a member of the Propulsion Committee, I was asked to report on the developments in the field of navigation of ships in ice covered and ice infested waters and the associated problem of increase of resistance in such circumstances. Since the nature of the problem is the increase of drag due to ice-ship interference, its approach in the towing tank level has been to m-asure the resistance of the model operating in such an environment primarily from which the delivered power can be derived. To avoid conflict of interests, it was subsequently suggested that it was more apropriate for the Resistance and Flow Committee to report on the matter. Unfortunately, this was not done.

Clearly, in a time when operations in ice covered waters are gaining importance and a new generation of powerful and expensive ships are being developed, would it not be wise to devote some of our efforts to this subject?

Development of new facilities (ice tanks) to experimentally study this complex phenomenon of ice-ship interference, both in North America and the rest of the world is an indication of the importance of the problem. The previous A.T.T.C. discussed the subject and the I.T.T.C. has appointed a Panel to report on this work."

18th
AMERICAN TOWING TANK CONFERENCE
Annapolis, Maryland, USA

REPORT OF
PROPULSION COMMITTEE

August 1977

United States Naval Academy

REPORT OF THE PROPULSION COMMITTEE

The Propulsion Committee held two meetings in the past year, one on 2 December 1976, the other on 4 May 1977. The Committee consists of the following members:

Richard A. Cumming
William G. Day, Jr., Reporter
Walter Gearhardt
Robert Henderson
Michael Michailidis
Eugene Miller
Otto Sherer
Raymond Wermter, Chairman

During these meetings, it was decided that the state of the art report would be presented as a series of Appendices on selected topics. It was also decided that the work of the Committee would be presented in two themes.

The first of these themes consists of reports of the activities of the ITTC Committees that parallel the mission of our Propulsion Committee along with three associated papers concerning scaling and predictions.

These appendices are as follows:

1. Activities of ITTC Performance Committee
2. A Review of the Activities of ITTC Propeller Committee
3. Scale Effect and Propeller Induction of the Wake
4. Recent Developments in the Analytical Prediction of Thrust Deduction
5. Experimental and Prediction Techniques for Estimating Added Power Requirements in a Seaway

These topics are those that are generally considered in depth by both the ATTC and the ITTC with extensive documentation in Reference 1.

Not so extensively covered in the literature are the subjects of our second theme, experimental problems associated with either unusual or high performance types of propulsions. There are therefore 5 more presentations in the following areas:

6. Performance of Ducted Propellers Fitted to Surface Craft
7. Partially Submerged and Supercavitating Propeller Systems
8. State of the Art Report on Waterjet Propulsion System Performance Analysis
9. A Survey of Propulsor-Vehicle Interaction on High Performance Marine Craft
10. Waterjet Propulsor Thrust Measurement using a Reaction Elbow

Because it was the feeling of the Committee that the subjects of the second group are beset with many tank problems such as multiple scaling laws, inadequate facilities, etc., it was thought advisable to feature them as the major theme of the session. Therefore these subjects will be presented first.

The subject matter contained in the body of this report is summarized as the following:

Appendix 1 is by Wermter and discusses the Model Ship Correlation Program proposed by the ITTC Performance Committee with the recommended approaches for use of form factors, AC_f, wake scaling and so on. Further work of the committee extends the use of the program to slender forms, twin screw ships and ships with ducted propellers.

Appendix 2 was prepared by Cumming and in addition to reporting on the previous activities of the ITTC Propeller Committee, he outlines the tasks being addressed for the 15 ITTC. These include wake scale effects, theoretical prediction of propeller performance , propeller induced vibratory forces, effects of cavitation performance and model techniques for thrusters on dynamical positioning vessels.

Huang prepared Appendix 3 wherein he reviews the many contributions made to our state of knowledge of the wake scaling laws over the past several years. He further discusses the effect of propeller action on wake and the interaction of the propeller and the axisymmetric boundary layer upstream of the propeller.

Appendix 4 is by Cox and gives a review of recent advances in the analytical prediction of thrust deduction and some applications of these data.

Day, Reed and Lin prepared Appendix 5. In it they review the standard experimental techniques for predicting added power in waves. They further discuss three proposed prediction techniques for added power and added resistance in waves.

Appendix 6, by Gearhardt and Henderson, discusses the model evaluation of ducted propeller and the scaling laws involved. They further suggest some ducted propeller configurations.

Appendix 7 is by Sherer and he discusses the nature of the scaling problems in predicting the performance of partially submerged and supercavitating propellers.

Miller prepared Appendix 8 and discusses waterjet configuration, model testing procedures and analysis, and full scale performance measurement.

Wilson discusses high performance craft interaction problems in Appendix 9. He does this by applying the various types of propulsors to various craft and talks to these configurations and the associated problems.

Finally, Appendix 10 by Eilers and Shrout, describes a new facility for the determination of full scale waterjet propulsion thrust.

It is felt these various appendices form a representative basis for the assessment of marine vehicle propulsion state of the art.

REFERENCES

1. Proceeding of Fourteenth International Towing Tank Conference, Ottawa September 1975.

ACTIVITIES OF ITTC PERFORMANCE COMMITTEE

by

Raymond Wermter

David W. Taylor Naval Ship Research and Development Center

The work of the Performance Committee has dealt largely with developing a rational Trial Prediction Computer Program and has concentrated very heavily on the detailed elements making up that program. First discussed before the 13th ITTC in Berlin, the calculations involved in correlation of ship and model data which are contained in the computer program, provide for a variety of options in the application of form factors, roughness allowances, wake, propeller corrections, and other factors.

The details of the computer program can be found in Reference 1. The work performed by the Committee for the 14th ITTC concentrated on exercising the program and examining in detail the many options available for the evaluation of the various factors mentioned above. This was done by soliciting the cooperation of a number of tanks to apply the program to their model/full-scale data base in correlation studies. The tanks that participated are listed below:

Bassin d'Essais des Carenes, Paris, France
Ishikawajima-Harima Heavy Ind., Co. Yokohama, Japan
Nagasaki Techn Inst MHI, Nagasaki, Japan
DTNSRDC, Washington, USA
NSMB, Wageningen, the Netherlands
NSFI, Trondheim, Norway
The Shipbuilding Research Centre of Japan, Tokyo, Japan
Ship Division, NPL, Feltham, England
Skibsteknish Laboratorium, Lyngby, Denmark
SSPA, Göteborg, Sweden
Versuchsanstalt für Wasserbau und Schiffbau, Berlin, Germany

There were 212 ships involved in these correlation studies with 833 data points. Ship types were as follows:

Types of Ships	Number of Ships	Number of Data Points
Ore and oil tankers, VLCC	127	498
Product Carriers	13	42
LNG-LPG-ships	1	4
Cargo Ships	43	150
Container Ships	16	71
Passenger Liners	1	1
Ferries	2	4
Tugs	1	1
Trawlers	-	-
Others	8	62

Reference 2 presents the results of this study. Details will not be given here, it will be sufficient to say that Method 55 appears to produce the best results.

The various methods and the factors that make them up are given in References 1 and 2. It should be of some interest to list the techniques used for determining the various factors in Method 55.

Figure 1 reproduces the flow chart of the logic incorporated in the computer program. Several elective factors are indicated on this diagram and are described below for Method 55:

1) Form Factor is determined using data from model resistance tests obtained at low speeds and the frictional formulation used by the experimenter. Analytical methods are not used to calculate the form factor in Method 55.

2) Roughness Allowance is calculated using the following formula:

$$\Delta C_F = \left\{105 \left(\frac{\alpha}{L_{WL}}\right)^{1/3} - 0.64\right\} 10^{-3}$$

where α = hull roughness, typically 150 x 10^{-6} m. (0.006 in.)

3) Viscous resistance is calculated using the form factor, k, obtained in (1) above, in the equation

$$C_{VS} = (1+k)\, C_{FS} + \Delta C_F$$

4) Full Scale Wake is computed by the application of a displacement wake:

$$w_d = t_m + \Delta t$$

where $\Delta t = 0.04$

5) Propeller open-water characteristics are corrected for blade section drag using the values determined by Lerbs' analysis method where $C_{DL} = C_D$ at the 0.75 radius and the blade roughness is assumed to be 30×10^{-6} m. (0.001 in.).

6) Lift corrections to propeller open-water characteristics are not made in Method 55.

Having reported on the results of the above work in great detail the Committee failed to recommend a standard procedure to the Conference. Item 2.1 incorporates the reasons for the decision. Findings and recommendations of the Committee are given in Reference 3 and are reproduced in their entirety below:

1. Findings

1.1 The experimental determination of the form effect on the viscous resistance is superior to any of the empirical formula examined by the Committee. The method proposed by Prohaska for determining the form factor is recommended.

2. Recommendations

2.1 Prediction Methods

2.1.1 At present the Conference is not ready to recommend an analytical prediction method for general acceptance. Method 55, described in Appendix 2 of the Committee report represents the best of the methods studied and it should be a starting point for further investigations.

2.1.2 It is important to complete the test material with data for more slender ships.

2.1.3 Prediction methods for unconventional propulsion devices should be examined.

2.2 Form Factors

2.2.1 Further work should be carried out on the influence of separation effects on form factors.

2.3 Separation

2.3.1 Further studies of flow patterns at the stern of full ship forms are required, including studies of flow conditions in self-propulsion tests, studies of scale effects in flow patterns and full scale comparisons.

2.4 Propulsion Factors

2.4.1 Further examination of the flow conditions on the propeller blades in the open and behind conditions is of the utmost importance. The interpretation of the propulsion factors, including the scaling of propeller characteristics, wake and relative rotative efficiency, is closely related to this investigation.

2.4.2 Adequate knowledge of the lift and drag for ship propellers is still lacking and investigations should continue. It is important to determine which type of roughness characterizes the propeller surface and how it affects K_T and K_Q.

2.5 Hull Deterioration and Fouling

2.5.1 Information on hull roughness has been made available by only a few institutions and more data are required. It is hoped that the development of automated roughness gages will encourage the measurement and analysis of roughness effects.

2.6 Wind, Waves and Steering

2.6.1 More efforts should be applied to the study of the added resistance due to drift angle, rudder angle, and steering. The resistance increment associated with the diffraction of waves at small sea-states should also be examined.

Since the Conference, work continues in all areas listed above. The original data base was largely biased toward high block ships and an effort is being made now to introduce a sample of slender ships as well. Various propulsor types and configurations such as twin screw, controllable-reversible pitch propellers and ducted propellers are also being introduced.

With regard to the more novel types of propulsors, there are some difficulties in establishing correlation between ship and model data. For example, frequently the pitch of a CP propeller is not always accurately known for full-scale trial conditions due to difficulties in measurement or even definition of pitch angle. Another example of novel propulsor scaling problems concerns ducted propellers. Work done by Minsaas in Norway indicates that it is necessary to use the rudder during open-water experiments of the ducted propeller in order to achieve reasonable values of propulsive coefficients. The scaling of shroud drag and its effect on propulsor characteristics has also become an important consideration for ducted propellers.

Work also continues in the Committee with regard to form factor determination, flow separation and the scaling of propulsion factors as a function of model and propeller scale.

With the further consideration of all factors above and the additional data being processed it is hoped that a firm recommendation as to an approved method can be made to the 15th ITTC.

REFERENCES

1. Proceedings of Fourteenth International Towing Tank Conference, Volume 3, Performance Committee Report, Appendix 1, September 1975.

2. Proceedings of Fourteenth International Towing Tank Conference, Volume 3, Performance Committee Report, Appendix 2, September 1975.

3. Proceeding of Fourteenth International Towing Tank Conference, Volume 1, Performance Committee Findings and Recommendations, September 1975.

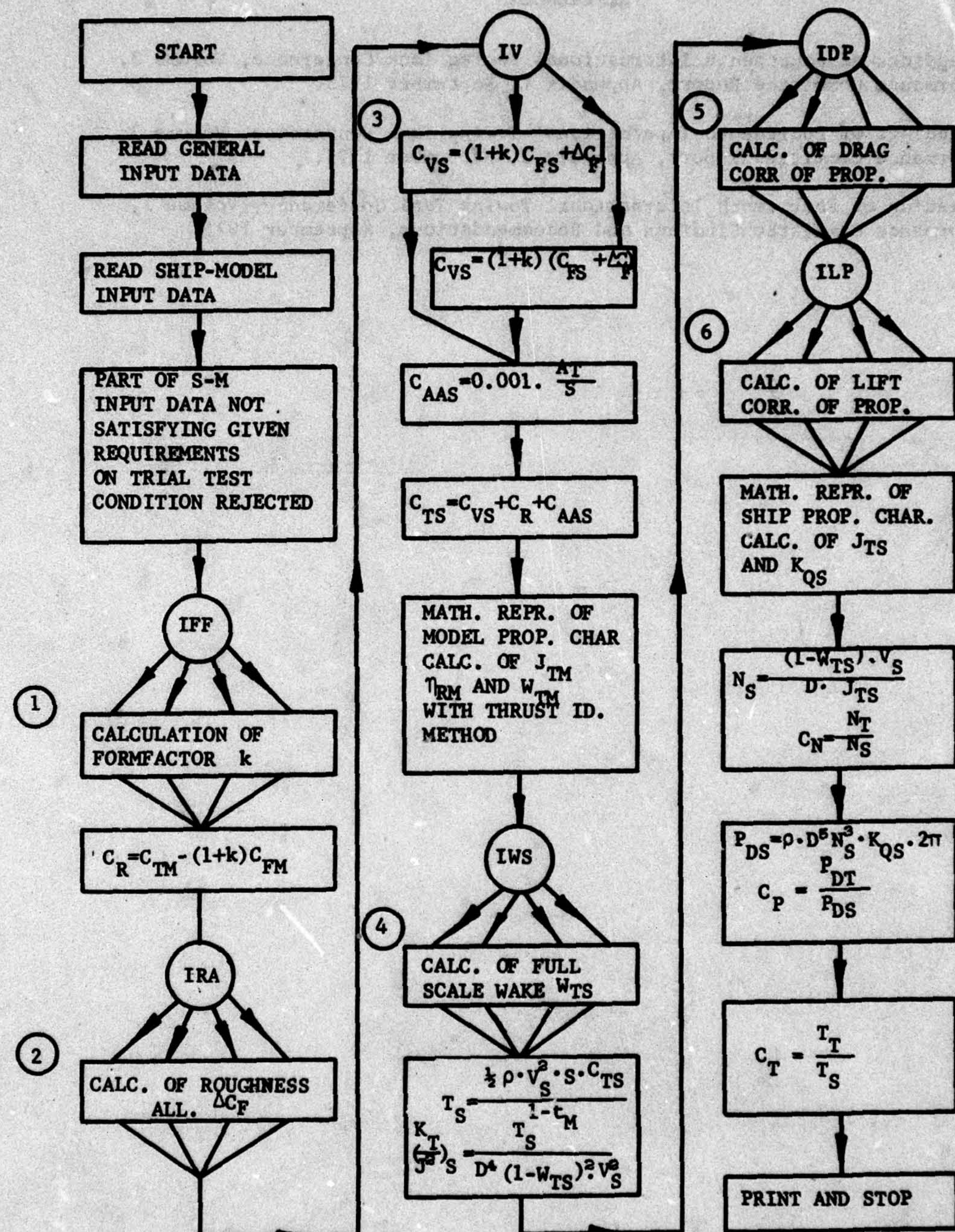

Figure 1 - ITTC Trial Prediction Test Program Flow Diagram

A Review of the Activities of the 15th ITTC Propeller Committee

by

Richard A. Cumming

David W. Taylor Naval Ship Research and Development Center

A review of the activities of the 15th ITTC Propeller Committee through approximately 15 June 1977 is presented. The findings and recommendations of the 14th ITTC Propeller Committee are included as background information and results of recent work at the David W. Taylor Naval Ship Research and Development Center (DTNSRDC), which bear upon the activities of the Propeller Committee are discussed.

The FINDINGS of the 14th ITTC Propeller Committee as they appear in Volume 1 of the Proceedings of the 14th ITTC are shown below.

"1. Findings

1.1 From the comparative propeller vibratory shaft force calculations that have been made it is concluded that several of the methods have given satisfactory results. It is expected that these methods will be satisfactory in other situations but no final conclusions can be drawn with respect to their validity in cases when high reduced frequencies are involved.

1.2 From limited experimental data the effect of cavitation on the forces in 1.1 appears to be small.

1.3 Propeller vibratory shaft forces, mean lateral and vertical forces and bending moments, and propeller blade fluctuating stresses have been found to be proportional to the product of propeller speed of rotation and the ship speed, assuming that the mean wake and its distribution are independent of ship speed. This is the preferred method of plotting these data.

1.4 When comparing ducted propeller and conventional propeller tests the rudders should be installed in both the behind and open water tests. Duct and screw thrust should be measured and scaled separately. Hull factor analysis should be based on the total thrust of the system.

1.5 The prediction of full-scale wake distributions from model distributions has met with some success but more work is considered necessary in this area.

1.6 Wake scale effect is important in the case of propeller cavitation induced pressures in some situations.

1.7 A method for the experimental determination of cavitation tunnel wall effect due to pressure wave reflections has been developed, but verification in a number of test facilities must be made before this method can be generally adopted."

These findings deal with propeller vibratory forces, wake distribution scale effect, and model test techniques for ducted and open propellers. A significant amount of work has been reported since the 14th ITTC in both of the first two areas and some unexpected results have been obtained which will be discussed in the following paragraphs. The RECOMMENDATIONS made by the 14th ITTC Propeller Committee as they appear in Volume 1 of the 14th ITTC Proceedings are shown below.

"2. <u>Recommendations</u>

2.1 Work should be continued to produce acceptable methods of scaling model wake distributions and theoretically calculating wakes. In conjunction with this attempts should be made to account for propeller induction on the wake. To aid with this work it is recommended that instrumentation be developed capable of measuring unsteady and turbulent flow, and propeller induction. Mean wake scale effect is excluded.

2.2 Methods of calculating pressure distributions on propeller blades in uniform and nonuniform flow should be evaluated and compared with the aim of giving guidance to the Conference on the applicability of these methods. Consideration should also be given to calculating secondary flows, boundary layer development, scale effect and cavitation patterns. In connection with this recommendation appropriate instrumentation and experimental techniques should be developed and confirmatory experiments performed.

2.3 Methods should be developed for the accurate and reliable prediction of propeller induced fluctuating pressure forces for full-scale ships based on model measurements and theoretical techniques. Together with existing methods for the calculation of unsteady shaft forces this should lead to the production of criteria for acceptable levels of propeller induced excitation. In this

connection the Committee should contact the ISSC with a view to cooperating with them on the question of hull response.

2.4 The effect of cavitation and air drawing on ship hull propulsion factors and propeller performance should continue to be studied. Also attempts should be made to obtain experimental information on the effect of cavitation on propellers operating in transitory modes such as when accelerating or decelerating ships in various manoeuvering situations.

2.5 The operation of thrusters on dynamically positioned vessels have associated interaction and noise problems and the Committee should consider and report on model experiment techniques for assessing these aspects of performance.

2.6 The Committee, should continuouly review the performance prediction techniques of marine propulsion devices other than conventional screw propellers. Particular attention should be paid to special testing problems associated with the following devices: ducted propellers, controllable pitch propellers (spindle torque), vertical axis propellers, overlapping propellers, contra-rotating propellers and high-speed propulsion devices."

These recommendations continued to emphasize the problems of wake distribution scale effect, but the emphasis on propeller vibratory forces shifted from shaft forces to the so-called pressure forces or surface forces acting on the hull and appendages. Emphasis was also placed on the development of criteria for the acceptable level of propeller-induced vibratory forces based on the principle that towing tank superintendents should be able to advise the customer with regard to whether the excitation measured or predicted by his establishment are likely to cause problems for the ship operator. Considerable discussion of this recommendation took place at the final session of the 14th ITTC with the result that the members voted to adopt the recommendation even though the task is likely to be a difficult one.

As is almost invariably the case, a certain amount of overlap between the work of the Propeller Committee and two other ITTC Committees, the Cavitation Committee and the Performance Committee, was found to exist. This overlap is shown in Table 1. Three of the Propeller Committee recommendations are seen to overlap four of the Performance Committee recommendations and five of the Propeller Committee recommendations overlap five of the Cavitation Committee recommendations. The recommendations of the 14th ITTC Propeller Committee to develop methods for calculating secondary flows, boundary layer development, scale effect, and cavitation patterns (see Recommendations 2.2 above) was not included in Table 1. It was subsequently decided, however, that the Cavitation Committee would take the responsibility for the prediction of

cavitation patterns. The descriptions of the tasks ultimately selected by the 15th ITTC Propeller Committee are presented in Table 2. A review of the work of the Propeller Committee to date on these tasks follows and is supplemented by a description of recent related work at DTNSRDC as well as commentary on selected topics.

TABLE 1 - PROPOSED TASKS FOR THE PROPELLER COMMITTEE OF THE 15TH ITTC

Tasks	Covering Recommendations		
	Prop	Perf	Cav
I. Wake Scale Effects			
A. Effect of propeller induction on the wake	2.1		
B. Scaling propeller performance in a model wake to propeller performance full-scale	2.1	6	
C. Testing techniques regarding producing full-scale wakes in model testing facilities	2.1	5	
D. Theoretical prediction of full-scale wakes	2.1		
E. Evaluation of instrumentation for measuring wake at the propeller	2.1		
II. Theoretical Prediction of Propeller Performance			
A. Evaluation and comparison of methods for predicting propeller blade pressure distributions	2.2		4
B. Evaluation of prediction techniques for single blade forces, bending moments, and spindle torques, including both steady and unsteady	2.2		
III. Propeller Induced Vibratory Forces			
A. Assessment of theoretical procedures for predicting propeller induced pressure forces	2.3		
B. Assessment of model experimental procedures for predicting propeller induced pressure forces	2.3		8
C. Development of criteria for acceptable levels of propeller induced excitation	2.3		
D. Evaluation of cavitation tunnel wall effect due to pressure wave reflections (method of Huse)	1.7 2.3		

Task	Covering Recommendations		
	Prop	Perf	Cav
IV. Effect of Cavitation and Air Drawing on Ship Hull Propulsion Factors and Propeller Performance			
A. Interaction of a cavitating propeller with a ship's hull and the effect on thrust deduction and wake fraction	2.4		
B. Effect of cavitation on conventional and ducted propeller performance	2.4		2
C. Effect of air drawing on propeller performance	2.4		
D. Effect of cavitation on propellers operating in transitory modes, i.e., manoeuvers, acceleration, deceleration, etc.	2.4		
V. Thrusters on Dynamical Positioning Vessels			
A. Assessment of model experimental techniques for predicting full-scale thruster performance on dynamical positioning vessels	2.5	3	
B. Model experimental techniques for assessing interaction of thrusters on dynamical positioning vessels	2.5	3	
C. Model experimental techniques for assessing noise of thrusters on dynamical positioning vessels	2.5	3	7
VI. Marine Propulsion Devices Other Than Conventional Screw Propellers			
A. Assessment of special testing problems associated with:			
1. Ducted propellers	2.6		
2. Controllable-pitch propellers	2.6		
3. Cycloidal propellers (Vertical Axis)	2.6		
4. Overlapping propellers	2.6		
5. Contrarotating propellers	2.6		
6. High-speed propulsion devices	2.6		5
7. Highly-skewed propellers	2.6		
VII. Other			
A. Effect of blade roughness on propeller lift and drag		7	

TABLE 2 - TASKS FOR THE PROPELLER COMMITTEE OF THE 15TH ITTC

I. <u>Wake scale effects</u>

A. Effect of propeller induction on the wake.

B. Predicting full scale nominal and effective wake distributions from the model wake (Nominal wake distribution is the distribution without the propeller. Effective wake distribution is the distribution with the propeller, but with the propeller-induced velocities subtracted out). This task includes theoretical prediction of wakes.

C. Testing techniques and instrumentation for model and full-scale wake measurement, and testing techniques for producing full-scale wakes in model-testing facilities.

II. <u>Theoretical prediction of propeller performance</u>

A. Evaluation and comparison of methods for predicting propeller blade pressure distributions.

B. Evaluation of prediction techniques for single blade forces, bending moments and spindle torques, including steady as well as unsteady.

III. <u>Propeller induced vibratory forces</u>

A. Assessment of theoretical procedures for predicting propeller induced pressure forces.

B. Assessment of model experimental procedures for predicting propeller induced pressure forces, including problems with tunnel wall effects.

C. Development of criteria for acceptable levels of propeller induced excitation.

IV. <u>Effect of cavitation and air drawing on ship hull propulsion factors and propeller performance</u>

A. Interaction of a partially cavitating propeller with a ship's hull and the effect on thrust deduction and wake fraction (ship speeds $\leq$ 30-35 knots).

B. Scaling of air injection on ducted propellers.

V. <u>Thrusters on dynamical positioning vessels</u>

A. Assessment of model experimental techniques for predicting full-scale thruster performance on dynamical positioning vessels, including problems of air drawing

B. Model experimental techniques for assessing interaction of thrusters on dynamical positioning vessels.

VI. **Marine propulsion devices other than conventional screw propeller-special testing problems**

A. Ducted propellers

B. Controllable-pitch propellers

C. Cycloidal propellers

D. Overlapping propellers

E. Contrarotating and tandem propellers

F. Highly-skewed propellers

G. Very low rpm, semi-ducted propellers

H. Ducted air propellers

I. Propellers in ice

VIII. **Other**

A. Effect of viscosity and blade roughness on propeller lift and drag

Task I. - **Wake Scale Effects (Including Propeller Induction Effects)**

The problem of wake scale effect due to differences in model and full scale Reynolds number and surface roughness has been of concern for a long time and the associated problem of the effect of propeller induction on the wake is of similar concern to naval architects and propeller designers. The Propeller Committee has compiled a list of some of the literature on the subject[(1)-(24)]. The first 16 of these deal with the effect of the propeller on the wake while the last 8 are primarily Japanese works on various aspects of the wake field.

Different characteristics of the wake are important to various propeller performance characteristics. If one thinks of the harmonic analysis of the wake, then the zeroth harmonic or circumferential mean velocity is important in determining the radial distribution of pitch and camber to give the desired time average thrust and torque characteristics. The first harmonic determines the steady side forces and shaft bending moments, the blade number harmonic and its multiples determine the blade frequency thrust and torque, and the harmonics immediately above and below the blade number harmonics determine blade frequency side forces and bending moments. Cavitation and the unsteady stresses in individual blades are determined by all the harmonics, i.e., by the total variation in velocity around the propeller disc.

The measured velocity at any point in the propeller disc is usually repeatable to within ±1 percent or perhaps ±2 percent of the free stream (ship) speed, some region of the wake being more unsteady than others. This level of precision (repeat-

1. Numbers in parentheses denotes references listed on page 11.

ability) is generally sufficient for the calculation of those propeller characteristics which depend on either the total variation in velocity (radial load distribution, mean and unsteady stress, cavitation) or the larger amplitude harmonics (steady side forces, blade frequency forces and moments for 2, 3, or 4 bladed propellers). However, the data available to date indicates that a significant improvement in the precision of wake survey techniques will be necessary in order to properly determine that amplitude and phase angle distribution of the low amplitude harmonics and the effects of Reynolds number, roughness, and propeller induction on these harmonics.

Task II. - Theoretical Prediction Of Propeller Performance

A. Propeller Blade Pressure Distribution

The Propeller Committee is presently in the process of gathering theoretical predictions of propeller blade pressure distributions from a number of institutions. Pressure distribution measurements on a three-bladed, 610 mm diameter propeller are being conducted in the high speed towing basin at DTNSRDC in uniform flow and with the shaft inclined to the flow. The pressure transducers are of the strain gage type and are recessed into the blade surface. A 1 mm diameter hole the gage to sense the surface pressure. The blades can be adjusted to any desired pitch setting and all four combinations of speed of advance and rpm ($\pm V, \pm N$) can be run. The results of these measurements should prove very useful in developing methods for the prediction of propeller blade loading in all four quadrants of propeller operation and in explaining the discrepancies between theory and experiment in the prediction of single blade forces in inclined flow to be discussed in the following section.

B. Single Blade Forces, Bending Moments, and Spindle Torque

A review of the state of the art in this area has been conducted by Prof. Dr. -Ing H. Jarzyna in which a number of references are cited [(25)-(54)]. The basic conclusion is that the available theoretical models are adequate for the prediction of bending moments and spindle torque in the design condiiton, but that problems may be encountered at off design conditions, particularly when the pitch of controllable-pitch propeller blades is being rapidly changed.

Recent work conducted at DTNSRDC has indicated that the unsteady blade forces and moments are predicted reasonably well by theoretical methods and that they are proportional to the product of propeller rotational speed and advance speed when the velocity variation is due to the axial component of velocity (Findings 1.1 and 1.3 of the 14TH ITTC Propeller Committee). However, this same work indicates that

these quantities are not well predicted by theory for propellers operating in inclined flow where the tangential velocity variation is primarily responsible for the variation in angle of attack and loading. This work is discussed briefly in the next paragraphs.

The first work at DTNSRDC in measuring single blade forces in inclined flow was done by Boswell[55,56], in which the six components of force and moment acting on a single blade behind a model hull were measured. The measured results in terms of the bending moment at the 40 percent radius are shown in Figure 1 and are compared to full scale data obtained from strain gages mounted on the blade surface. The wave forms are not identical but the peak-to-peak amplitude is approximately the same in the ship and model. Figure 2 shows a comparison of the same model data with theoretical predictions using the quasi-steady method of McCarthy[57] and the unsteady lifting surface method of Tsakonas[58]. Both methods predict significantly lower peak-to-peak amplitudes.

This was initially thought to be due to a propeller hull interaction mechanism which was not being accounted for inasmuch as the wake field used to make the prediction of the unsteady forces is always measured without the propeller. However, subsequent experiments with a propeller in open water with a shaft inclination angle of 10 degrees showed that the discrepancy between theory and experiment still existed. A thin, flat plate aligned with the flow direction had little effect on the unsteady forces when brought near the propeller (to within approximately 1 cm of the blade tip). The forces measured over a range of advance coefficient were not proportional to the product of rotational speed and advance speed. Efforts are currently underway to determine why the theoretical prediction methods are not correctly predicting the experimental results.

Task III. - Propeller-Induced Vibratory Forces

A. Assessment of Theoretical Procedures for Predicting Propeller Induced Pressure forces

No work in this area has been reported as yet by the Committee. Some exploratory experimental work has been conducted at DTNSRDC (sponsored jointly by the U.S. Maritime Administration and the American Bureau of Shipping) in which the blade-frequency force and pressures acting on the upstream and of an ellipsoidal body due to a nearby propeller were measured. The experimental results were in reasonable agreement with the theoretical prediction made by Dr. Vorus[59] of the University of Michigan. Dr. Breslin of the Stevens Institute of Technology is currently in the process of making predictions for the same body. This work has not yet been completed. It is hoped to extend it to more realistic shapes and to include cavitation effects in the future.

B. Assessment of Model Experimental Procedures for Predicting Propeller Induced Pressure Forces, Including Problems with Tunnel Wall Effects

The work of the Committee on this task is continuing and a survey of the literature on the subject(60)-(89) will be prepared. A recent paper by Chiba and Hoshino(90) on the same subject was also noted.

C. Development of Criteria for Acceptable Levels of Propeller Induced Vibration

The Committee has sent sixty-eight inquiries requesting information on this topic and twelve replies had been received at the time of the March 1977 Committee meeting, but at least six or seven more are expected.

Task IV. - Effect of Cavitation and Air Drawing on Ship Hull Propulsion Factors on Propeller Performance

A. Interaction of a Partially Cavitating Propeller with a Ship's Hull

This task is being prepared by the Propeller Committee for the Cavitation Committee, but little information on the subject has been found to date. Further inquiries are being made.

B. Scaling of Air Injection on Ducted Propellers

Dr. Huse (Trondheim) has prepared a report on this topic based on the model and full scale work that has been completed. Dr. Huse reports that more than 10 ships have had duct air injection systems installed. A scaling law is derived based on the assumption that the relative volume increase of the cavity should be the same for model and ship. If this is true, then the scaling law is:

$$Q_s = Q_m \cdot (n_s/n_m)^3 \cdot \lambda^5$$

where Q = volume flow rate of air,

n = propeller rotational speed,

λ = scale ratio between model and ship, and

s,m = subscripts indicating ship and model, respectively.

Dr. Huse reports that full scale experience has indicated that this scaling law appears to slightly over estimate the amount of air required to avoid erosion in full scale, that there is no effect on propulsive efficiency, that high frequency noise is attenuated, and that low frequency exciting forces and vibration showed a slight increase. Two references to work in this field are cited[91,92].

Experiments will be conducted in the near future at DTNSRDC to explore the feasibility of extending this concept to conventional propellers.

Task V. - Thrusters on Dynamical Positioning Vessels

A state of the art report on model experimental techniques for these thrusters is being prepared by Dr. English of the National Physical Laboratory. Dr. English cites a large volume of literature on this subject[93]-[117].

Task VI. - Marine Propulsion Devices Other Than Conventional Screw Propeller - Special Testing Problems

The Committee members are in the process of preparing statements on this task and no definite results are available at this time.

Task VII. - Effect of Viscosity and Blade Roughness on Propeller Lift and Drag

Mr. Rader is preparing this report and no definite results are available at this time.

REFERENCES

1. Wertbrecht, H.M., "Vom Sog, ein Versuch Seiner Berechnung," Jahrbuch Schiffbautechnische Gesellschaft, Vol. 42, 1941, pp. 147-204.

2. Hickling, R., "Propellers in the Wake of an Axisymmetric Body," Transactions of the Royal Institute of Naval Architects, Vol. 99, 1957, pp. 601-617.

3. Tsakonas, S. and Jacobs, W.R., "Potential and Viscous Parts of the Thrust Deduction and Wake Fraction for an Ellipsoid of Revolution," Journal of Ship Research, Vol. 4, No. 2, 1960, pp. 1-16.

4. Hucho, W. -H., "Uber den Einfluss einer Heckschraube auf die Druckverteilung und die Grenzschicht eines Rotationskorpers - Teil II: Untersuchungen bei hoheren Schubbelastungsgraden," Institut Fur Stromungsmechanik der Technischen Hockschule Branunschweig, Bericht 64/45, 1965.

5. Wald, Q., "Performance of a Propeller in a Wake and the Interaction of Propeller and Hull," Journal of Ship Research, Vol. 9, No. 1, 1965, pp. 1-8.

6. Hucho, W. -H., "Uber den Zusammenhang zwischen Normalsogn, Reibungssog und dem Nachstrom bei der Stromung um Rotationskorper," Schiff und Hafen, Heft 10, 1968, pp. 689-693.

7. Hucho, W. -H., "Untersuchungen uber den Einfluss einer Heckschraube auf die Druckverteilung und die Grenzschicht Schiffsahnlicher Korper," Ingenieur-Archiv Vol. XXXVII, 1969, pp. 288-303.

8. Nelson, D.M., "Development and Application of a Lifting-Surface Design Method for Counterrotating Propellers," Naval Undersea Center Technical Paper 326, November 1972.

9. Raestad, A.E., "Estimation of Marine Propeller's Induced Effects on the Hull Wake-Scale Effect on the Hull Wake Field," Det norske Veritas Report No. 72-3-M, Chapter 1, 1972.

10. Namimatsu, M. and Moraoka, K., "Wake Distribution of Full Form Ships," Ishikawajima-Harima Heavy Industries, Co., Ltd., Japan, Engineering Review, Vol. 7, No. 3, 1975.

11. Nagamatsu, T. and Sasajima, T., "Effect of Propeller Suction on Wake," Journal of the Society of Naval Architects of Japan, Vol. 137, 1975.

12. Titoff, I.A. and Otlesnov, Yu, P., "Some Aspects of Propeller-Hull Interaction," Swedish-Soviet Propeller Symposium Moscow, 1975.

13. Huang, T.T., Wang, H.T., Santelli, N., and Groves, N.C., "Propeller/Stern-/Boundary Layer Interaction on Axisymmetric Bodies: Theory and Experiment," David W. Taylor Naval Ship Research and Development Center Report 76-0113, December 1976.

14. Huang, T.T. and Cox, B.D., "Interaction of Afterbody Boundary Layer and Propeller," Symposium on Hydrodynamics of Ship and Off-Shore Propulsion Systems, The Veritas Center, HØVIK, Norway, 20-25 March 1977.

15. Huse, E., "Bilge Vortex Scale Effect," Symposium on Hydrodynamics of Ship and Off-Shore Propulsion Systems, The Veritas Center, HØVIK, Norway, 20-25 March 1977.

16. Hoekstra, M., "An Investigation into the Effect of Propeller-Hull Interaction on the Structures of the Wake Field," Symposium on Hydrodynamics of Ship and Off-Shore Propulsion Systems, The Veritas Center, HØVIK, Norway, 20-25 March 1977.

17. Hatano, S., et al, "Calculation of Velocity Distribution in Ship Wake," Journal of the Society of Naval Architects of Japan, Vol. 138, 1975. (2nd Report will be published this year.)

18. Tanaka, I., et al, "Calculation of Viscous Flow Field Around Ship Hulls With Special Reference to Stern Wake Distribution," Journal of Kansai Society of Naval Architects, Vol. 150, 1973.

19. Brard, R., "Viscosity, Wake and Ship Waves," Journal of Ship Research, Vol. 14, No. 4, 1970.

20. Tatinclaux, J.C., "Effect of a Rotational Wake on the Wavemaking Resistance of an Ogive," Journal of Ship Research, Vol. 14, No. 2, 1970.

21. Inui, T., et al, "Observation and Analysis on the Behaviour of Stern Vortices Shed from Wallsided Full Forms," Journal of the Society of Naval Architects of Japan, Vol. 138, 1975.

22. Kayo, Y., "Wake Survey Results of a Submerged Wake Generator," Journal of the Society of Naval Architects of Japan, Vol. 140, 1976.

23. Kato, N., et al, "An Approach to the Stern Flow of Full Hull Form by Vortex Singularity Distribution (No. 1)," Journal of the Society of Naval Architects of Japan, Vol. 140, 1976. (No. 2 will be published this year.)

24. Okuno, T., "Distribution of Wall Shear Stress and Cross Flow in Three Dimensional Turbulent Boundary Layer on Ship Hull," Journal of the Society of Naval Architects of Japan, Vol. 139, 1976.

25. Sparenberg, I.A., "Application of Lifting Surface Theory to Ship Screws," International Shipbuilding Progress, No. 67, 1960.

26. VanManen, J.D. and Bakker, A.R., "Numerical Results of Sparenberg's Lifting Surface Theory for Ship Screws," International Shipbuilding Progress, No. 104, 1963.

27. Verbrugh, P.J., "Unsteady Lifting Surface Theory for Ship Screws," Netherlands Ship Model Basin Report No. 68-036-AH, 1968.

28. Kuiper, G., "Some Preliminary Results of an Exact Treatment of the Linearized Lifting Surface Integral Equation," Netherlands Ship Model Basin Report No. 69-108-SP, 1969.

29. Kuiper, G., "Some Remarks on Lifting Surface Theory," International Shipbuilding Progress, No. 199, 1971.

30. Oossanen, P., "Profile Characteristics in Cavitating and Non-Cavitating Flows," International Shipbuilding Progress, No. 199, 1971.

31. Hylarides, S. and Van Gent, W., "Propeller Hydrodynamics and Shaft Dynamics," Netherlands Ship Model Basin Symposium on High Powered Propulsion of Large Ships, Wageningen, 1974.

32. Van Gent, W., "Unsteady Lifting Surface Theory for Ship Screws," Journal of Ship Research, Vol. 19, No. 4, 1974.

33. Oossanen, P., "Method of Assessment of the Cavitation Performance of Marine Propellers," International Shipbuilding Progress, No. 245, 1975.

34. Tsakonas, S. and Jacobs, W.R., "Unsteady Lifting Surface Theory for a Marine Propeller of Low Pitch Angle with Chordwise Loading Distribution," Journal of Ship Research, Vol. 9, No. 2, September 1965.

35. Tsakonas, S., Jacobs, W.R., and Rank, P., "Unsteady Propeller Lifting Surface Theory with Finite Number of Chordwise Modes," Stevens Institute of Technology Report 1133, December 1966; Journal of Ship Research, Vol. 12, No. 1, March 1968.

36. Breslin, J.P. and Eng, K.S., "A Method for Computing Propeller-Induced Vibratory Forces on Ships," Proceedings of the First Conference on Ship Vibration, Stevens Institute of Technology, January 1965.

37. Tsakonas, S., Breslin, J.P., and Miller, M., "Correlation and Application of an Unsteady Flow Theory for Propeller Forces," Transactions of the Society of Naval Architects and Marine Engineers, Vol. 75, 1967.

38. Tsakonas, S. and Jacobs, W.R., "Propeller Loading Distribution," Journal of Ship Research, Vol. 13, No. 4, December 1969.

39. Tsakonas, S, Jacobs, W.R., and Ali, M.R., "An Exact Linear Lifting Surface Theory for a Marine Propeller in Non-Uniform Flow field," Journal of Ship Research, No. 4, 1973.

40. Cummings, D.E., "Numerical Prediction of Propeller Characteristics," Journal of Ship Research, No. 3, 1972.

41. Tsakonas, S., Chen, C.Y., and Jacobs, W.R., "Exact Treatment of the Helicoidal Wake in the Propeller Lifting Surface Theory," Stevens Institute of Technology Report DL 1117, August 1966; Journal of Ship Research, Vol. 11, No. 3, September 1967.

42. Johnsson, C., "Pressure Fluctuation Around a Marine Propeller, Results of Calculation and Comparison with Experiment," Statens Skeppsprovningsanstalt Publication No. 63, 1971.

43. Raestad, A., "Computer Programme NV538: The Free Stream Pressure Field Induced by the Propeller," Det norske Veritas Report No. 70-22-M, 1970.

44. Søntvedt, T., "Theoretical Calculations of Hydrodynamic Loading on the Marine Propeller," Det norske Veritas Report 71-64-M, 1972.

45. Høiby, O.W., "Three Dimensional Effects in Propeller Theory," Skipsmodelltanken Publication No. 105, 1970.

46. Johnsson, C., "On Theoretical Predictions of Characteristics and Cavitation Properites of Propellers," Statens Skeppsprovningsanstalt Publication No. 64, 1968.

47. Johnsson, C., "Correlations of Predictions and Full Scale Observations of Propeller Cavitation," International Shipbuilding Progress, June 1973.

48. Huse, E., "Pressure Fluctuations on the Hull Induced by Cavitating Propellers," Skipsmodelltanken Publication No. 111, 1972.

49. Johnsson, C. and Søntvedt, T., "Propeller Excitation and Responce of 230.000 TBW Tankers - Full Scale Measurements and Theoretical Calculations," Statens Skeppsprovningsanstalt Report No. 70, 1972.

50. Tanibayashi, H., "Practical Approach to Unsteady Propeller Problems," International Shipbuilding Progress, No. 226, 1973.

51. Yamazaki, R., "On the Theory of Screw Propellers in Non-Uniform Flows," Memoirs of Faculty of Engineering, University of Kyushu, Vol. 25, No. 2, 1966.

52. Hanaoka, T., "Numerical Lifting Surface Theory of a Screw Propeller in Non-Uniform Flow," Report of Ship Research Institute of Japan, Vol. 6, No. 5, 1969.

53. Sugai, K., "Hydrodynamics of Screw Propellers Based on a New Lifting Surface Theory," Journal of the Society of Naval Architects of Japan, June 1965; June 1968.

54. Sugai, K., "A Method for Calculating the Hydrodynamic Characteristics of Marine Propellers," Journal of the Society of Naval Architects of Japan, December 1970.

55. Boswell, R.J., et al, "Experimental Determination of Mean and Unsteady Loads on a Model CP Propeller Blade for Various Simulated Modes of Ship Operation," Transactions of the Eleventh ONR Symposium on Naval Hydrodynamics, Government Printing Office, 1976.

56. Boswell, R.J., Nelka, J.J., and Denny, S.B., "Experimental Unsteady and Mean Loads on a CP Propeller Blade on a Model of the FF1088 for Simulated Modes of Operation," David W. Taylor Naval Ship Research and Development Center Report 76-0125, October 1976.

57. McCarthy, J.H., "On the Calculation of Thrust and Torque Fluctuations of Propellers in Nonuniform Wake Flow," David Taylor Model Basin Report 1533, October 1961.

58. Tsakonas, S., et al, "An Exact Linear Lifting Surface Theory for Marine Propeller in a Nonuniform Flow Field," Journal of Ship Research, Vol. 17, No. 4, December 1974.

59. Vorus, W.S., "A Method for Analyzing the Propeller-Induced Vibratory Forces Acting on the Surface of a Ship Stern," Transactions of the Society of Naval Architects and Marine Engineers, Vol. 82, 1974, pp 186-210.

60. Garguet, M. and Lepeix, R., "The Problem of Influence of Solid Boundaries on Propeller-Induced Hydrodynamic Forces," Symposium on "High Powered Propulsion of Large Ships," Wageningen, 1974.

61. Isay, W.H., "Uber die Wechselwirkung Zwischen Shiffsruder und Schraubenpropeller," Shiffstechnik Heft 62, Bd. 12, 1965.

62. Schwanecke, H., "State of the Art on Propeller-Excited Vibrations," Propeller Committee Report, The Eleventh International Towing Tank Comference, 1966.

63. Pohl, K.H., "Das Instationare Druckfeld in der Ungebung eines Schiffspropellers und die von ihm auf benachbarten Platten erzeugten periodischen Krafte," Schiffstechnik, Heft 32, Bd. 6, 1959.

64. Pohl, K.H., "Die durch eine Shiffsschraube auf benachbarten Platten erzeugten periodischen hydrodynamische Krafte," Schiffstechnik, Heft 35, Bd. 7, 1960.

65. Takahashi, ------

66. Oosterveld, M.W.C., et al, "Some Propeller Cavitation and Excitation Considerations," West European Conference on Marine Technology, The Hague, 1974.

67. Noordzij, L., "A Method to Calculate the Pressure Field Induced by a Cavitating Propeller," Netherlands Ship Model Basin Symposium on "High Powered Propulsion of Large Ships," 1974.

68. Oossanen, P. van, "Calculation of Performance and Cavitation Characteristics of Propellers Including Effects of Non-Uniform Flow and Viscosity," Netherlands Ship Model Basin Publication No. 457, 1974.

69. Huse, E., "The Magnitude and Distribution of Propeller-Induced Surface Forces on a Single-Screw Ship Model," Norwegian Ship Model Experiment Tank Publication No. 100, 1968.

70. Huse, E., "Trykkimpulser fra kaviterende Propell," Paper Presented at "Nordisk Skipsteknisk Møte," Abo, Finland, 1971.

71. Huse, E., "Pressure Fluctuations on the Hull Induced by Cavitating Propellers," Norwegian Ship Model Experiment Tank Publication No. 111, 1972.

72. Søntvedt, T. and Frivold, H., "Low Frequency Variation of the Surface Shape of Tip Region Cavitation on Marine Propeller Blades and Corresponding Disturbances on Nearby Solid Boundaries," The Eleventh ONR Symposium on Naval Hydrodynamics, 1976.

73. Høilund, A.P., Holden, K.O., and Søntvedt, T., "Propeller Cavitation as a Source of Vibrations," Jahrbuch STG, Bd. 67, 1973.

74. Johnsson, C.-A. and Søntvedt, T., "Propeller Cavitation and Response of 230.000 TDW Tankers," The Ninth ONR Symposium on Naval Hydrodynamics, 1972.

75. Johnsson, C.-A., "Pressure Fluctuations Around a Marine Propeller, Results of Calculations and Comparison with Experiment," Statens Skeppsprovningsanstalt Publication No. 69, 1971.

76. Johnsson, C.-A., et al, "Vibration Excitation Forces From a Cavitating Propeller, Model and Full Scale Tests on a High Speed Container Ship," The Eleventh ONR Symposium on Naval Hydromechanics, 1976.

77. Denny, S.B., "Comparison of Experimentally Determined and Theoretically Predicted Pressures in the Vicinity of a Marine Propeller," Naval Ship Research and Development Center Report 2349, 1967.

78. Vorus, W.S., "Calculation of Propeller-Induced Vibratory Hull Forces, Force Distributions, and Pressures, Free-Surface Effects," Journal of Ship Research, Vol. 20, No. 2, 1976.

79. Vorus, W.S., "A Method for Analyzing the Propeller-Induced Vibratory Forces Acting on the Surface of a Ship Stern," Transactions of the Society of Naval Architects and Marine Engineers, Vol. 82, 1974.

80. Breslin, J.P. and Tsakonas, S., "Marine Propeller Pressure Field Due Loading and Thickness Effects," Transactions of the Society of Naval Architects and Marine Engineers, Vol. 67, 1959.

81. Jacobs, W.R., Mercier, J., and Tsakonas, S., "Theory and Measurements of Propeller-Induced Vibratory Pressure Field," Stevens Institute of Technology Report SIT-DL-1485, 1970.

82. Tsakonas, S., Jacobs, W.R., and Ali, M.R., "Propeller-Rudder Interactions Due to Loading and Thickness Effects," Stevens Institute of Technology Report SIT-DL-1589, 1972.

83. Breslin, J.P., "Review of Theoretical Prediction of Vibratory Pressures and Forces Generated by Ship Propellers," The Second International Ship Structures Conference, Delft.

84. Breslin, J.P., "Report on Vibratory Propeller, Appendage and Hull Forces and Moments," Propeller Committee Report," The Twelfth International Towing Tank Conference, 1969.

85. Breslin, J.P. and Kowalski, T., "Experimental Study of Propeller-Induced Vibratory Pressures on Simple Surface and Correlation with Theoretical Predictions," Stevens Institue of Technology, Davidson Laboratory Report 973, 1973.

86. Breslin, J.P., "Review and Extension of Theory for Near-Field Propeller-Induced Vibratory Effects," The Fourth Symposium on Naval Hydrodynamics 1962.

87. Breslin, J.P., "The Pressure Field Near a Ship Propeller," Journal of Ship Research, Vol. 1, 1958.

88. Tsakonas, S., Breslin, J.P., and Jacobs, W., "The Vibratory Force Produced by a Marine Propeller on a Long, Rigid Strip," Journal of Ship Research, March 1962.

89. Bavin, V.F., Vashkevich, M.A., and Miniovich, I.Y., "Pressure Field Around a Propeller Operating in Spatially Non-Uniform Flow," The Seventh Symposium on Naval Hydrodynamics, 1968.

90. Chiba, N. and Hoshino, T., "Effect of Unsteady Cavity on Propeller-Induced Hydrodynamic Pressure," Journal of the Society of Naval Architects of Japan, Vol. 139, 1976.

91. Huse, Erling, "Air Injection to Avoid Cavitation Erosion in Propeller Ducts," Ship Research Institute of Norway Report R-49.75, 1975.

92. Okamoto, H., et al, "Cavitation Study of Ducted Propellers on Large Ships," Transactions of the Society of Naval Architects and Marine Engineers, Vol. 83, 1975.

93. Bond, R., "Dynamic Ship Positioning Systems and Their Power Requirements," Conference on Electrical Propulsion and Shaft Generators for Ships, Institute of Marine Engineers, London, 1975.

94. Pronk, C. and Schneiders. C.C., "Propulsion for Off-Shore Vessels," Third LIPS Propeller Symposium, 1976.

95. Pronk, C. and Schneiders, C.C., "Performance of Thrusters," LIPS Technical Report 1003-7501; Also Paper OTC 2230, Off-Shore Technology Conference 1975, Houston, Texas.

96. Made, A. vd and Bussemaker, O., "Thrusters for Dynamic Positioning," The Second International Off-Shore Craft Conference, Thomas Reed Publications, September 1976.

97. Brown, N.A. and Norton, J.A., "Thruster Design for Acoustic Positioning Systems," Journal of Marine Technology, April 1975.

98. Brix, J.E. and Bussemaker, O., "Lateral Thrusters with Anti-Suction Tunnels," ---

99. English, J.W. and Wise, D.A., "Hydrodynamic Aspects of Dynamic Positioning," North East Coast Institution of Engineers and Shipbuilders, December 1976.

100. Ardenaes, O., "Alternative Thruster Systems," Symposium on Safety and Reliability of Dynamic Positioning Systems, Symposium Proceedings No. 1, Det norske Veritas, Oslo, 1975.

101. Minsaas, K., "Hydrodynamical Design of Thrusters for Safe and Reliable Dynamic Positioning," Symposium on Safety and Reliability of Dynamic Positioning Systems, Symposium Proceedings No. 1, Det norske Veritas, Oslo, 1975.

102. Lindahl, C.A., "Consideration on Thruster Desidn, Maintenance and Installation," Symposium on Safety and Reliability of Dynamic Positioning Systems, Symposium Proceedings No. 1, Det norske Veritas, Oslo, 1975.

103. Oosterveld, M.W.C. and van Oortmerssen, G., "Thruster Systems for Improving the Manoeuverability and Position-Keeping Capability of Floating Objects," The Fourth Annual Off-Shore Technology Conference, Paper No. OTC 1625, Houston, Texas, 1972.

104. Nielsen, G.F., "On the Influence of the Propeller Race on Large, Towed Structures," Norwegian Maritime Research, No. 4, 1976.

105. Oosterveld, M.W.C., "Ducted Propeller Characteristics," Symposium on Ducted Propellers, Royal Institute of Naval Architecture, London, 1973.

106. Caster, E.B., "Ducted Propeller Designs for Improved Backing Performance," Symposium on Ducted Propellers, Royal Institute of Naval Architects, London, 1973.

107. English, J.W. and Rowe, S.J., "Some Aspects of Ducted Propeller Propulsion," Symposium on Ducted Propellers, Royal Institute of Naval Architects, London, 1973.

108. Anwar, H.O., "Prevention of Vortices at Intakes," Water Power, October 1968.

109. Deggett, L.L. and Keulegan, G.H., "Similitude in Free-Surface Vortex Formations," Journal of the Hydraulics Division, Proceedings of the American Society of Civil Engineers, Vol. 100, No. HY11, November 1974, pp. 1565-1581.

110. Kenn, M.J. and Zanker, K.J., "Aspects of Similarity for Air-Entraining Water Flows," Nature, 7 January 1967.

111. Quick, M.C., "Scale Relationships Between Geometrically Similar Free Spiral Vorticies, Part 1," Civil Engineering and Public Works Review, September 1962.

112. Quick, M.C., "Scale Relationships Between Geometrically Similar Free Spiral Vortices, Part 2," Civil Engineering and Public Works Review, October 1962.

113. Denny, D.F., "An Experimental Study of Air-Entraining Vortices in Pump Sumps," Proceedings of the Institute of Mechanical Engineers, Vol. 170, December 1970, pp. 106-125.

114. Quick, M.C., "Efficiency of Air-Entraining Vortex Formation at Water Intake," Journal of the Hydraulic Division, Proceedings of the American Society of Civil Engineers, Vol. 96, No. HY7, July 1970.

115. Chang, E., "Review of Literature on Drain Vortices in Cylindrical Tanks," British Hydromechanics Research Association, TN 1342, March 1976.

116. Berge, J.P., "A Study of Vortex Formations and Other Abnormal Flow Effects in a Tank With and Without a Free Surface," Houille Blanche, 21, 1, pp 13-40, 1966 (In French)(BSRA Translation 3166).

117. Amphlett, M.B., "Air-Entraining Vortices at a Horizontal Intake," Hydraulic Research Station, Report No. OD/7, April 1976.

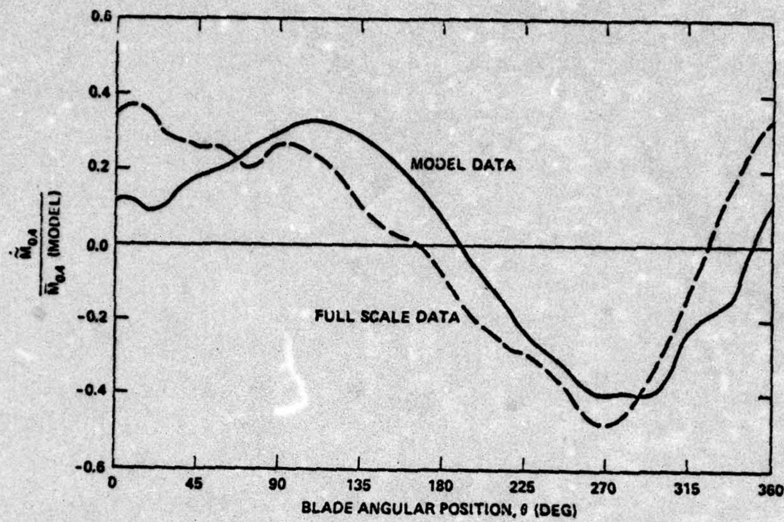

Figure 1 - Variation of Bending Moment at 40 Percent Radius With Blade Angular Position, Comparison of Model Data and Scale Data (Figure 29 of Reference 56)

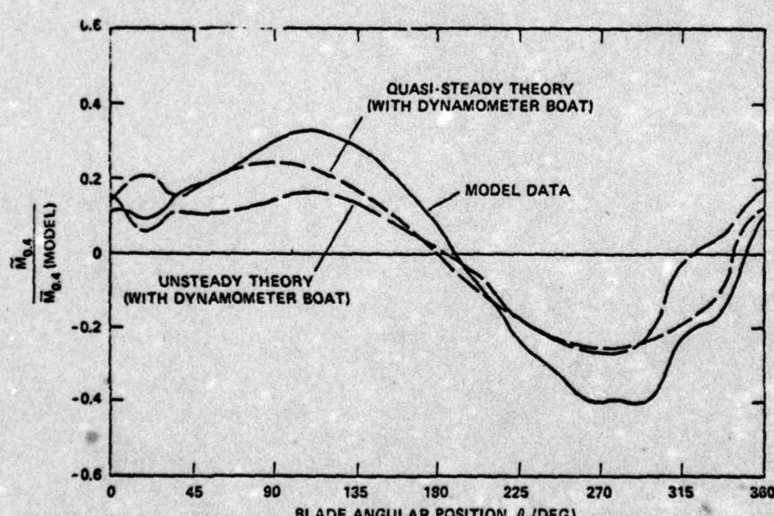

Figure 2 - Variation of Bending Moment at 40 Percent Radius With Blade Angular Position, Comparison of Model Data With Theory (Figure 31 of Reference 56)

SCALE EFFECT AND PROPELLER INDUCTION ON THE WAKE

A State-of-the-Art Review

by

Thomas T. Huang
David W. Taylor Naval Ship Research and Development Center

INTRODUCTION

Powering characteristics of a full-scale ship - propeller thrust, shaft horsepower, and the rate of revolution - are usually derived from the results of model tests. The ship models are tested in the towing tank at Reynolds numbers which are typically two orders of magnitude less than those occurring at full-scale. Furthermore, if the radius of the propeller is less than the boundary-layer thickness at the propeller location, the nominal wake distribution for the full-scale ship is expected to be different from the nominal wake distribution on the model. This difference is called the scale effect of the wake. The nominal wake distribution is measured in the absence of the propeller by a standard wake rake.

With a propeller operating the flow over the ship stern is normally accelerated. The mutual interaction of the propeller and the nominal wake results in a new resultant velocity distribution. An effective velocity distribution is defined to be the resultant velocity distribution with the propeller in operation minus the propeller-induced potential flow velocity profile. The effective wake is an important input to propeller design and is essential for the correct prediction of powering, cavitation performance, and unsteady forces.

The present review covers two subject areas: (1) scale effect on the wake, and (2) propeller induction on the wake. Although there has been extensive literature devoted to these two topic areas, only a few papers advance our basic understanding of the physics of the ship wake. Much more research work remains to be done in order to predict the full-scale ship wake from the measured model nominal wake.

SCALE EFFECT ON SHIP WAKE

The mean nominal wake fraction measured in the absence of the propeller and mean effective wake fraction derived from the propeller open-water and behind-the-hull experiments on six different scale models of Victory Ships were found by Van Manen and Lap[1] to decrease with increasing scale. Significant scale effect on the wake fraction of eleven super-tankers was found by Yazaki and Yokoo[2]. The mean effective wake fractions derived from the standardization speed trials of these super-tankers were found to be smaller than those measured on the models by values scattered between 0.05 and 0.15. Nilsson and Raestad[3] reported that the trial results of the propeller rpm of their fleet of 35,000-ton tankers were about 8% higher than the results derived from the model tests. In eight classes of large tankers built at Kockums[3] (40,000 to 350,000 tons), model tests always under-predicted propeller rpm. The measured higher full-scale rpm than that predicted from the model test may be partially caused by the scale effect on the wake. The difference in wake distribution between full-scale and model may also present serious problems to the prediction of full-scale cavitation and vibratory forces from the corresponding model tests[3] if no appropriate correction is made to account for this difference.

Most towing tanks have their own empirical approaches to account for the scale effect on the wake between the model and full-scale. Some empirical methods were published in the proceedings of the ITTC and a comprehensive review of various approaches was made by Dyne[4]. The empirical method proposed by Sasajima and Tanaka[5] was the first attempt to extrapolate the nominal wake distribution measured on the model to the full-scale ship. Their method assumed that the frictional component of the wake varied linearly with the flat-plate frictional coefficient, which is a rough two-dimensional approximation. The method of Sasajima and Tanaka[5] is to derive an approximated full-scale nominal wake from the measured model nominal wake. The effect of propeller induction was not considered in their method. However, most applications (i.e. Dyne[6]) used the derived nominal wake as the effective wake distribution for the full-scale ship.

A brief outline is repeated below of the derivation of a simplified wake-scaling formula used by Sasajima and Tanaka[6] given by Huang and Cox[7]. Strictly speaking, even for a turbulent boundary layer along a flat-plate, the well-known laws of the wall and wake[8] cannot be brought into a power law. However, for a given value of Reynolds number, the velocity profile of a two-dimensional flat-plate turbulent boundary layer can be crudely approximated by:

$$\frac{u_x}{V_s} = 1-w(y) = \left(\frac{y}{\delta}\right)^{\frac{1}{n}}$$

where u_x is the longitudinal velocity along x, w is the wake fraction, V_s is the ship speed; y is the transverse distance, δ is the boundary-layer thickness, and the constant n increases slightly with increasing Reynolds number. In this case the total (functional) resistance coefficient becomes

$$C_F = \frac{\delta}{2x} \int_0^1 \left(1 - \frac{u_x}{V_s}\right) \frac{u_x}{V_s}\, d\left(\frac{y}{\delta}\right) = \frac{n}{(n+1)(n+2)} \frac{\delta}{x} \qquad (2)$$

which implies that δ is proportional to C_F for a fixed value of n. Therefore, a similarity form of the solution for the $\frac{1}{n}$ - power velocity profile when n is fixed may be approximated by

$$\frac{u_x}{V_s} = 1 - w = f\left(\frac{y}{x}\frac{x}{\delta}\right) = g\left(\frac{y}{x}\frac{1}{C_F}\right) \qquad (3)$$

If the velocity profile is known (either from measurement or computation) at a given Reynolds number, the velocity profile can be obtained for other Reynolds numbers if n is assumed to have a fixed value. For a given value of u_x/V_s or w, Equation (3) states that the coordinate of the velocity profile is shifted by

$$\left(\frac{y}{x}\right)_s = \frac{\left(\frac{\delta}{x}\right)_s}{\left(\frac{\delta}{x}\right)_m} \left(\frac{y}{x}\right)_m = \frac{C_{F_s}}{C_{F_m}} \left(\frac{y}{x}\right)_m \qquad (4)$$

where the subscripts m and s denote the values corresponding to the model and full-scale ship, respectively.

As for the flat plate, if the frictional component of the axisymmetric nominal velocity profile at the propeller disk is assumed to follow a $\frac{1}{n}$ - power law, then the frictional resistance coefficient is related to boundary-layer thickness by

$$C_F = \frac{\delta^2}{S} \int_0^1 \left(1 - \frac{u_x}{V_s}\right) \frac{u_x}{V_s} \frac{r}{\delta}\, d\left(\frac{r}{\delta}\right) = \frac{n}{(2n+1)(2n+2)} \frac{\delta^2}{x^2} \frac{x^2}{S} \qquad (5)$$

where r is radial distance and S is the surface area (the value of x^2/S is identical for model and ship). In demonstrating gross axisymmetric effect, we have neglected the variation of static pressure across the boundary layer and pressure resistance. In this case the radial distance of the full-scale nominal velocity profile is shifted from the radial distance of the measured model nominal velocity profile by

$$\left(\frac{r}{x}\right)_s = \frac{\left(\frac{\delta}{x}\right)_s}{\left(\frac{\delta}{x}\right)_m} \left(\frac{r}{x}\right)_m = \sqrt{\frac{C_{F_s}}{C_{F_m}}} \left(\frac{r}{x}\right)_m \qquad (6)$$

Accurate turbulent boundary-layer computation methods do exist for two-dimensional and axisymmetric flow. The Douglas CS[9] differential boundary-layer method, modified to account for the effects of transverse curvature, and boundary-layer and wake displacement[10,11] have been used to check the validity of the simple empirical relationships of equations (4) and (6) by Huang and Cox[7]. Figure 1 shows the comparison of the computed profiles by the Douglas CS[9] method and the empirical method. Equation (4) was used to calculate the profile for $R_{n_s} = 3 \times 10^9$ from the profile predicted by the Douglas CS method at a lower model Reynolds number $R_{n_m} = 6 \times 10^6$. If the flat-plate empirical method were adequate, then Curve II should be a good approximation of Curve I which was computed by the Douglas CS[9] method. Figure 2 shows the comparison of the theoretically computed and empirically calculated profiles for an axisymmetric body. It is obvious from Figure 2 that the flat-plate empirical method (Equation (4)) is not suitable for calculating the scale effect on an axisymmetric thick stern boundary layer. The axisymmetric empirical method (Equation (6)) yields a somewhat better approximation of the theoretically computed profile.

The scale effect for U-shaped ships with significant bilge vortex formation was investigated by Huse[12]. The bilge vortices were considered as a separate contribution to the total wake distribution. Huse[12] simulated the full-scale stern flow by applying boundary-layer suction at the ship stern. Under this condition the bilge vortices were displaced downward and toward the center plane in comparison with the flow without suction.

Three-dimensional boundary-layer computation methods applicable to the ship stern are in the development state[13,14,15]. A satisfactory method should contain a proper account of the free surface, large cross flow, transverse curvature, and boundary-layer-wake displacement effects. In the absence of appropriate 3-D boundary-layer computation methods, empirical methods have been and will continue to be used to estimate the scale effect on the nominal wake distribution. Wake patterns differ from ship to ship. In some cases when the lines of iso-wake are more similar to circles with center at the propeller shaft center line, the axisymmetric empirical method would appear to be more appropriate. In other cases when the lines of iso-wake are more similar to straight lines with ship center plane as the boundary, the flat-plate empirical method would appear to be more appropriate. In other cases when the iso-wake lines are not so simple, perhaps a linear combination of flat-plate and axisymmetric empirical methods may be employed.

PROPELLER INDUCTION ON SHIP WAKE

The wake distribution measured by a standard wake rake in the absence of the propeller is called the nominal wake. As stated earlier, the most critical

information for the wake-adapted propeller design and propeller performance prediction is the knowledge of the effective wake which is different from the nominal wake. The resultant velocity profile, as the result of the propeller/stern boundary layer interaction minus the propeller induced potential flow velocity profile, is the effective velocity profile which is experienced by the propeller blades in producing the local thrust and torque. Sometimes the effective wake distribution for the model propeller is scaled up or down from the nominal wake distribution measured in the absence of the propeller by a constant factor which is the ratio of the Taylor thrust-identity wake fraction to the measured volume-mean nominal wake fraction.

The influence of a stern-mounted propeller on the pressure coefficient and the flow field past different bodies of revolution and a flat plate was measured by Hucho[16,17,18], although no attempt was made to actually calculate the effective wake distribution from the nominal wake. The Hucho data[16,17,18] contain a lot of valuable information but proper analyses and comparison with theories need to be made. Estimation of effective wake was made by Raestad[19], Nagamatsu and Sasajima[20], and Titoff and Otlesnov[21]. Raestad[19] takes into account the streamline contraction due to the propeller induced velocity but not the local conservation of energy, and the effective wake is not properly defined. Since the propeller induced velocity has not been subtracted out of the resultant velocity, the Raestad[19] procedure yields too large an effective velocity. For a propeller operated in open water, the limiting stream annulus with the radius R_o at far upstream is contracted to the propeller radius R_p. This contraction was approximated by the momentum theory by Nagamatsu and Sasajima[20], e.g.,

$$(\frac{R_o}{R_p}) = \tfrac{1}{2}\,[1 + \sqrt{1+\tilde{C}_T}] \tag{7}$$

where $\tilde{C}_T$ is the thrust loading coefficient,

$$\tilde{C}_T = 8T/[\rho V_s^{\,2}(1 - w\ )^2\ \pi R_p^{\,2}) = C_T/(1 - w\ )^2;$$

w is the volume-mean wake fraction which was assumed to be the volume-mean average of the measured nominal wake over the radius R_o instead of R_p as normally done. The computed w was found to agree satisfactorily with the effective mean wake derived from the self-propulsion experiments of a tanker model at full load, and a cargo ship model at full and ½ load; agreement was less satisfactory for the tanker model at ballast condition. The estimation method of Nagamatsu and Sasajima[20] yields the effective mean wake fraction only. The circumferential-average radial distribution of the wake, which is an important input to the wake-adapted propeller design, cannot be obtained by this method.

Titoff and Otlesnov[21] formulated a procedure to derive the three-dimensional distribution of effective propeller inflow from the measured distribution of resultant inflow immediately upstream of an operating propeller. The method makes use of the open water propeller characteristics and a quasi-steady approximation to subtract the propeller induced velocity from the measured resultant velocity to obtain the effective velocity. The resultant inflow velocity distribution with the propeller in operation is not measured in current towing tank practice, and the quasi-steady method of determining the velocities induced forward of a propeller through open water tests will give too high induced velocities in the high wake regions and too low in the low wake regions.

Hoekstra[22] used a stern-mounted diffuser to simulate the influence of the propeller suction on the nominal inflow (similar to actuator disk representation). The resultant velocity distribution at the propeller plane was measured by a five-hole pitot tube. Effective velocity fields were derived from the measured resultant velocity field with the diffuser-induced velocity field subtracted out. The diffuser-induced velocity field was solved approximately by potential-flow approximation. The diffuser was represented by an axisymmetrical vortex sheet of a finite length in a uniform onset flow (nominal inflow was assumed to be uniform). The vorticity distribution on the sheet was uniquely determined by the zero-normal-velocity condition at the sheet and the Kutta Condition at the trailing edge. The velocity field induced by the vortex sheet was solved by the law of Biot and Savart. For the purpose of relating the action of a given diffuser to that of the simulated propeller, a fictitious thrust, equal to the thrust of an actuator disk which produced the same upstream flow induction as the diffuser, was introduced. This method can at best approximate the average propeller induction and cannot represent the radial distribution of the propeller induction. The cost of manufacturing the diffuser may also hinder further practical application.

The only known previous effort to theoretically address the problem of the propeller/stern boundary layer interaction is due to Nelson, who developed an unpublished computer program for calculating the effective wake from the measured nominal wake and static pressure distribution across the boundary layer.

Both the nominal velocity profile in the absence of a propeller and the resultant velocity profile at small distances upstream of an operating propeller were measured by Laser Doppler Velocimeter by Huang[10] et. al.. An inviscid approximation was also made to describe the hydrodynamic interaction between a propeller and a thick axisymmetric boundary layer upstream of the propeller. The inviscid theory[7,10] takes into account the contraction of the stream annulus and assumes that the total energy within the same stream annulus remains constant with and without the propeller in operation (Figure 3). The resultant velocity profiles were obtained from the measured circumferential-average nominal velocity profile and the

circumferential-average propeller-induced axial velocity profile calculated by using a field-point velocity program[23]. In current propeller design and performance prediction practice only the measured nominal velocity profile is available. The full-scale nominal velocity profile is then estimated from the measured model nominal profile as discussed in the previous section. In order to compute the effective velocity profile, either for the model propeller or for the full-scale propeller, the inviscid theory[7,10] can be applied in an iterative procedure. A computer program[24] has been written for this application.

The inviscid theory for propeller/boundary-layer interaction so far is limited to axisymmetric flow and can only be applied to the circumferential-average wake. Further research is necessary to solve the three-dimensional propeller/wake interaction. The comparisons[7,10] of inviscid theory and LDV measurements have been made so far for relatively lightly loaded propellers ($C_T < 1$). Additional experiments are required to validate and to imporve the inviscid theory so that applications to more heavily loaded propellers can be made with confidence.

REFERENCES

1. Van Manen, J.D., and A.J.W. Lap, "Scale-Effect Fxperiments on Victory Ships and Models," Part II in Transactions of the Institution of Naval Architects, Vol. 100, pp. 374-395 (1958); Parts III and IV in Transactions of the Royal Institution of Naval Architects, Vol. 104, pp. 23-25 (1962).

2. Yazaki, A., and K. Yokoo, "On the Roughness Allowance and the Scale Effect on the Wake Fraction of Super Tankers," Proceedings, Eleventh International Towing Tank Conference, Tokyo, Japan, Performance Session, pp. 161-164 (1966).

3. Nilsson, G., and K. Raestad, "Problems in Full Scale Propulsion from a Shipbuilder's Viewpoint," Shipbuilding Progress, Vol. 23, No. 266, pp. 342-352 (Oct 1976).

4. Dyne, G., "On the Scale Effect on Wake and Thrust Deduction," Proceedings, Thirteen International Towing Tank Conference, Berlin, Hamburg, West Germany, Appendix 6, Report of Performance Committee, Vol. 1, (1972).

5. Sasajima, H., and I. Tanaka, "On the Estimation of Wake of Ships," Proceedings, Eleventh International Towing Tank Conference, Tokyo, Japan, Appendix X, Performance Session, pp. 140-143 (1966).

6. Dyne, G., "A Study of the Scale Effect on Wake, Propeller Cavitation and Vibratory Pressure at Hull of Two Tanker Models," Transactions, The Society of Naval Architects and Marine Engineers, Vol. 82, pp. 162-185 (1974).

7. Huang, T.T., and B.D. Cox, "Interaction of Afterbody Boundary Layer and Propeller," presented at the Symposium on Hydrodynamics of Ship and Offshore Propulsion Systems, Høvik outside Oslo, Norway, (March 20-25, 1977).

8. Schlichting, H., Boundary-Layer Theory, Sixth Edition, McGraw-Hill Book Co., New York (1968).

9. Cebeci, T., and A.M.O. Smith, Analysis of Turbulent Boundary Layers, Academic Press, New York, 1974.

10. Huang, T.T., H.T. Wang, N. Santelli, N.C. Groves, "Propeller/Stern/Boundary Layer Interaction on Axisymmetric Bodies: Theory and Experiment," DTNSRDC Report 76-0013, (Dec 1976).

11. Wang, H.T., and T.T. Huang, "User's Manual for a Fortran IV Computer Program for Calculating the Potential Flow/Boundary Layer Interaction on Axisymmetric Bodies," DTNSRDC Ship Performance Departmental Report SPD-737-01 (Dec 1976).

12. Huse, E., "Bilge Vortex Scale Effect," presented at Symposium on Hydrodynamics of Ship and Offshore Propulsion System, Høvik outside Oslo, Norway, 20-25 March, 1977.

13. Cebeci, T., K. Kaups, and J. Ransey, "Calculation of Three-Dimensional Boundary Layers on Ship Hulls," Proceedings of the First International Conference on Numerical Ship Hydrodynamics, Gaithersburg, Maryland, pp. 409-433, 20-22 (Oct 1975).

14. Larsson, L., "A Calculation Method for Three-Dimensional Turbulent Boundary Layers on Shiplike Bodies," Proceedings of First International Conference on Numerical Ship Hydrodynamics, Gaithersburg, Maryland, pp. 385-408, 20-22 (Oct 1975).

15. Tanaka, I., and T. Suzuki, "Examples of Calculation of Stern Flow Field Using Boundary Layer Theory Approach," Presented at Symposium on Hydrodynamics of Ship and Offshore Propulsion Systems, Høvik outside Oslo, Norway, 20-25 (March 1977).

16. Hucho, W.-H, "Über den Einfluss einer Heckschraube auf die Druckverteilung und die Grenzschicht eines Rotationskörpers-Teil II: Untersuchungen bie hoheren Schubbelastungsgraden, "Institut Für Stromungsmechanik der Technischen Hochschule Branunschweig, Bericht 64/45 (1965).

17. Hucho, W.-H, "Über den Zusammenhang zwischen Normalsog, Reibungssog und dem Nachstrom bei der Strömung um Rotationskörper," Schiff und Hafen, Heft 10, pp. 689-693 (1966).

18. Hucho, W.-H, "Untersuchungen über den Einfluss einer Heckschraube auf die Druckverteilung und die Grenzschicht Schiffsähnlicher Körper," Ingenieur-Archiv Vol. XXXVII, pp. 288-303 (1969).

19. Raestad, A.E., "Estimation of Marine Propeller's Induced Effects on the Hull Wake Field," Det Norske Veritas Report No. 72-3-M, Chapter 1 (1972).

20. Nagamatsu, T. and Sasajima, T., "Effect of Propeller Suction on Wake," Journal of the Society of Naval Architects of Japan, Vol. 137, pp. 58-63 (1975).

21. Titoff, I.A. and Otlesnov, Yu, P., "Some Aspects of Propeller-Hull Interaction," Swedish-Soviet Propeller Symposium, Moscow (1975).

22. Hoekstra, M., "An Investigation into the Effect of Propeller Hull Interaction on the Structures of the Wake Field," presented at Symposium on Hydrodynamics of Ship and Offshore Propulsion System, Høvik outside Oslo, Norway, 20-25 (March 1977).

23. Kerwin, J.E., and R. Leopold, "A Design Theory for Subcavitating Theory," Transactions of the Society of Naval Architects and Marine Engineers, Vol. 72, pp. 294-355 (1964).

24. Huang, T.T., "User's Manual for a Fortran IV Computer Program for Calculating Propeller/Stern Boundary-Layer Interaction on Axisymmetric Bodies," DTNSRDC Ship Performance Department Report SPD-737-02 (Dec 1976).

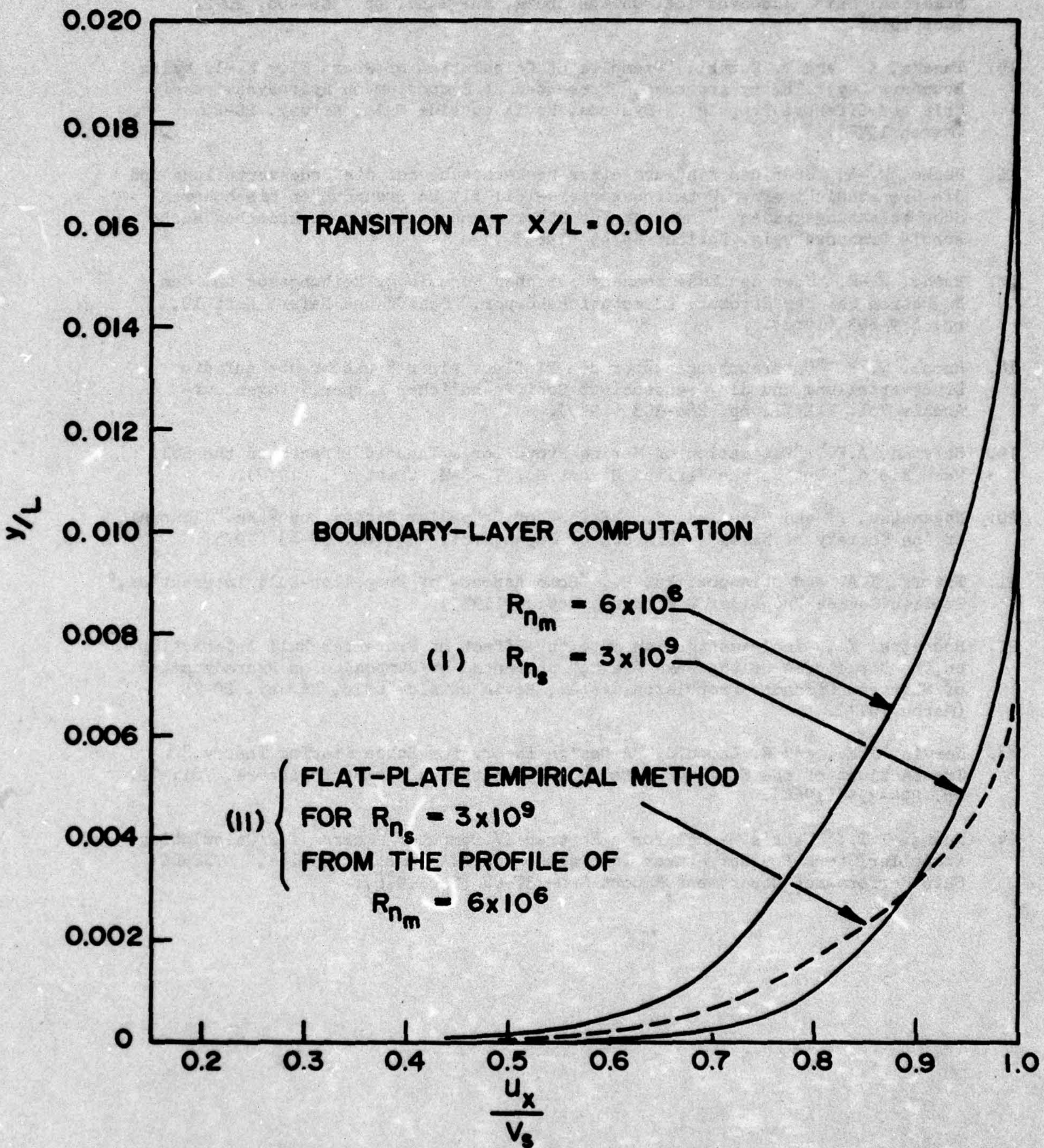

Figure 1 —Theoretically Computed and Empirically Calculated Scale Effect on Axial Velocity Profile on Flat-Plate.

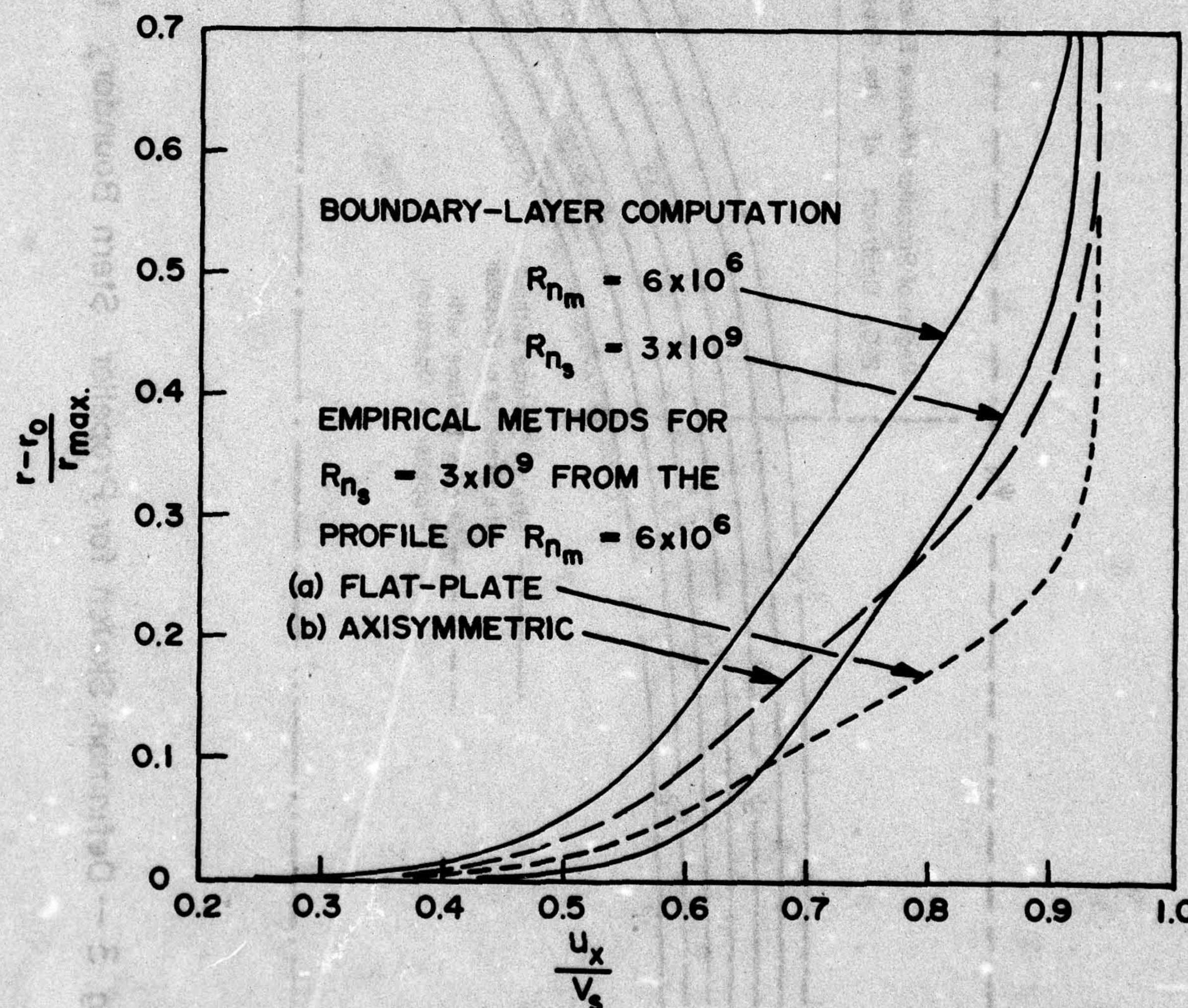

Figure 2 — Theoretically Computed and Empirically Calculated Scale Effect on Nominal Axial Velocity Profile on Afterbody 1.

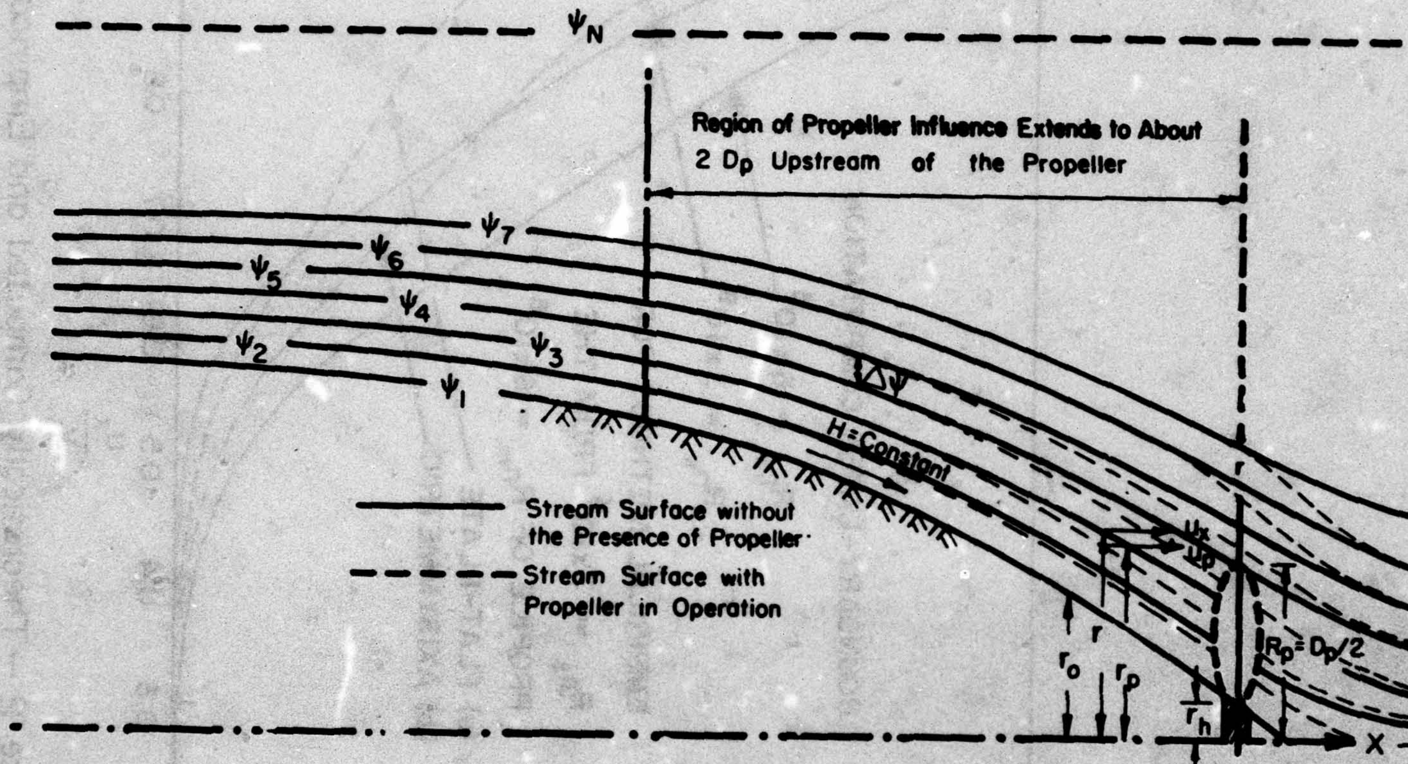

Fig. 3 — Definition Sketch for Propeller Stern Boundary Layer Interaction

RECENT DEVELOPMENTS IN THE ANALYTICAL PREDICTION OF THRUST DEDUCTION

by

Bruce D. Cox

David W. Taylor Naval Ship Research and Development Center

INTRODUCTION

The added resistance arising from propeller-hull interaction is a familiar concept to naval architects. Propellers operating in close proximity to ship sterns normally act to accelerate the flow over the hull afterbody. For sufficiently fine forms where flow separation effects are minimal, the reduction in afterbody pressure increases the hull pressure drag. The flow acceleration also increases the wall shear stress, and hence, the frictional resistance. The net result is that the delivered propeller thrust must be greater than the hull resistance in the absence of the propeller.

This increase in resistance due to propeller-hull interaction is defined in terms of the thrust deduction fraction t,

$$t = (T-R_T)/T$$

where R_T is the bare hull resistance and T is the propeller thrust. The thrust deduction must be known in advance for a propeller design to meet specified propulsion requirements. Pending the development of adequate theoretical techniques for predicting the thrust deduction, it has been traditional practice to conduct model scale resistance and propulsion tests using a stock propeller with principal characteristics similar to the envisioned design. This approach has proven reasonably satisfactory for many conventional designs. However, a large number of experiments would be required to determine the effects of different afterbody forms, propeller locations, blade geometries, and loading characteristics. Thus, analytical methods are desireable both from the standpoint of evaluating a given propeller and hull design and for economically investigating higher efficiency propeller-hull configurations.

The present note reviews progress in developing the theory and numerical techniques for calculating the thrust deduction. Early concepts are briefly outlined followed by a description of recent developments based on propeller lifting surface theory. The usefulness of these techniques is illustrated by results obtained for deeply submerged bodies. Finally, the possibility of extending the analysis to surface ship applications and different propulsor types is discussed.

SUMMARY OF EARLY THEORETICAL DEVELOPMENTS

Various techniques for the analysis and prediction of thrust deduction have been reported during the past forty years, as cited in the comprehensive bibliography

by Nowacki and Sherma[1]. Dickmann[2] was the first investigator to provide a reasonable analysis of the interaction force between a hull and propeller based on potential flow considerations. To represent an axisymmetric body, he applied the method of discrete singularties on the body axis together with a single point sink to represent the propeller. With this model it was possible to relate the thrust deduction to the thrust loading coefficient, C_T, and potential wake fraction, w_p, in the form

$$t = (2w_p)/(1+\sqrt{1+C_T})$$

During the 1940's some of Dickmann's ideas were extended, as outlined by Weinblum[3] in his survey paper. Korvin-Kroukovsky[4] also used the method of singularities, but represented the propeller by a constant-strength sink disc and corrected the body sources to account for the propeller induced flow and the boundary layer displacement thickness. Breslin[5] derived a relatively simple relationship between thrust deduction and afterbody form using a doublet distribution based on slender-body theory.

Further developments have logically followed from advances in propeller theory and the advent of high-speed digital computing capability. Thus, Beveridge[6] was the first to apply the Douglas-Neumann three-dimensional flow calculation to represent the body. In a later investigation, Beveridge[7] introduced a sink-disc with radially varying strength derived from propeller lifting-line theory. Based on this method, predictions for three different realistic hull forms, including one surface ship, compared reasonably well with experimental data. Similar techniques have also been applied to contrarotating propellers[8,9].

APPLICATION OF PROPELLER LIFTING SURFACE THEORY

Recently an extended treatment of the potential flow analysis has been developed[10,11] which differs in two fundamental respects from previous approaches. First, a more comprehensive and realistic representation of the propeller is introduced, based on a lifting surface formulation. This overcomes the limitations of the sink-disc approximation by including the additional effects of blade thickness, skew, rake, and chordwise load distributions. As such, the propeller calculation is comparable in scope and accuracy to currently available lifting-surface design methods.

Heretofore, the propeller has been approximated as a sink-disc, in which the diameter, axial location, and radial distribution of loading are explicitly represented. In fact, it can be shown[11] that a sink-disc of strength $\sigma(r)$,

$$\sigma(r) = (Z/2\pi) \int_r^R (d\Gamma/dr')(1/r'\tan\beta_i(r')\, dr'$$

generates the circumferential average velocity field of a moderately loaded lifting-line representation of a propeller with tip radius R, bound circulation $\Gamma(r)$, pitch angle $\beta_i(r)$, and Z symmetrically spaced blades. The lifting surface effects may be conveniently regarded as corrections to this lifting line representation. These

corrections are based on the theory and numerical method developed by Kerwin[12,13] in which blade thickness and chordwise loading are represented by discretized source and vortex singularities distributed over the surface of the blade.

In previous investigations the thrust deduction has been derived (in an elegantly simple manner) by applying the Lagally steady-flow theorem to the propeller sink disc singularities. In the lifting surface formulation, it is more convenient to consider the body flow directly. Thus, time-averaged propeller induced velocities[12] and modified hull pressure distributions are computed, including appropriate corrections to the body singularity strengths. The interaction force, F_x, may then be found by integrating the hull pressure,

$$F_x = \vec{e}_x \cdot \oint_{\substack{\text{Body} \\ \text{Surface}}} (P_{\substack{\text{with} \\ \text{propeller}}} - P_{\substack{\text{without} \\ \text{propeller}}})\vec{n}\, dA(\vec{r}_B)$$

or by applying Lagally's theorem to the hull singularities $\sigma(\vec{r}_B)$,

$$F_x = -\rho \oint_{\substack{\text{body} \\ \text{surface}}} \sigma(\vec{r}_B)\, V_x(\vec{r}_B)\, d\,A(\vec{r}_B)$$

where V_x is the propeller induced velocity at the hull boundary, $\vec{r}=\vec{r}_B$.

The foregoing analysis has been successfully applied to deeply submerged bodies of revolution[10,11,14] where comparisons with direct force measurements (model resistance and propulsion tests) and with measurements of afterbody pressure distribution show excellent agreement. As an illustrative example, the results for an appended Series-58 model are summarized in Table 1. Calculations for several propeller-body configurations show that the significant contribution is over the last 20 to 30 percent of the body with more than half of the interaction force concentrated within a distance of one propeller diameter. Conventional stern appendages contribute up to 25 percent of the total thrust deduction. It is also found that for conventional propellers the lifting-surface representation predicts 10 to 20 percent lower thrust deduction than the sink-disc approximation. For highly raked propellers, the correction is much larger. It can be concluded from these comparisons that the potential flow analysis is a sound approach, at least for application to non-separating hull forms. Boundary layer measurements by Huang[14] also indicate that for streamlined axisymmetric bodies, the increase in frictional resistance contributes less than 5 percent of the interaction force. This suggests that the thrust deduction is essentially <u>independent</u> <u>of</u> <u>scale</u> for fine forms.

For a selected body, parameteric calculations have been carried out to determine the role of propeller diameter, axial position, and radial distribution of loading[15]. The results show that propeller diameter has less influence on thrust deduction than previously inferred from stock propeller experiments. Aft displacement of the blades, as obtained by moving the propeller aft and/or by raking the blades, causes marked reductions in the thrust deduction, as illustrated in the example of Figure 1. It is also possible to reduce the thrust deduction by loading the

propeller more heavily toward the tip. Additional calculations are planned to study the effect of afterbody form and to identify high efficiency propeller-hull configuraitons.

PROSPECTS FOR EXTENSIONS OF THE THEORY

The analytical method has been developed with a view to more general ship-propeller configurations. For ducted, contrarotating, and tandem propulsors, the calculation of induced velocities on the hull surface may be derived in the same manner as for the single, open propeller. For example, in the case of a ducted propeller, the distribution of duct loading and thickness is established in the course of design. Based on appropriate distributions of source and vortex singularities, the velocity at arbitrary field points can be computed. The potential flow interaction analysis should be equally successful in these applications as for the open propeller.

Recent progress in the computation of the potential flow about surface ships[16] suggests that the problem of propeller-hull interaction in the presence of a free surface can be addressed in the near future. As an initial step it is recommended that the analysis be applied in the low Froude number range where, as a first approximation, the free surface can be represented by a rigid wall. In this case the thrust deduction can be derived using simple images of the hull and propeller about the waterline plane. It will also be necessary to conduct flow visualization experiments and obtain detailed boundary layer measurements to clarify the role of viscosity and flow separation effects, and to establish the limitations of the potential flow analysis.

REFERENCES

1. Nowacki, H. and Sharma, S.D., "Free Surface Effects in Hull Propeller Interaction," The University of Michigan College of Engineering Report 112, September 1971.

2. Dickmann, H.E., "The Interaction between Propeller and Ship with Special Consideration to the Influence of Waves," Jahrbuch der Schiffbautechnischen Gesselschaft, 40, 1939.

3. Weinblum, G., "The Thrust Deduction," American Society of Naval Engineers, Vol. 63, 1951.

4. Korvin-Kroukovsky, B.V., "Stern Propeller Interaction with a Streamline Body of Revoluti International Shipbuilding Progress, Vol. 3, No. 17, 1956.

5. Breslin, J.P., "A Simplified Theory for the Thrust Deduction Force on a Body of Revolution," Midwest Conference on Solid and Fluid Mechanics at the University of Michigan, April 1957.

6. Beveridge, J.L., "Pressure Distribution on Towed and Propelled Streamline Bodies of Revolution at Deep Submergence," David Taylor Model Basin Report 1665, June 1966.

7. Beveridge, J.L., "Analytical Prediction of Thrust Deduction for Submersibles and Surface Ships," Journal of Ship Research, Vol. 13, No. 4, December 1969.

8. Nelson, D.M., "Development and Application of a Lifting-Surface Design Method for Counterrotating Propellers," Naval Undersea Center TP 326, November 1972.

9. Beveridge, J.L., "Thrust Deduction in Contrarotating Propellers," Naval Ship Research and Development Center Report 4332, November 1974.

10. Huang, T.T. and Cox, B.D., "Interaction of Afterbody Boundary Layer and Propeller," Symposium on Hydrodynamics of Ship and Offshore Propulsion Systems, Oslo, Norway, March 1977.

11. Cox, B.D. and Hansen, A.G., "A Method for Predicting Thrust Deduction Using Propeller Lifting Surface Theory," David Taylor Naval Ship Research and Development Center Report (In Preparation).

12. Kerwin, J.E. and Leopold, R., "A Design Theory for Subcavitating Propellers," Transactions of the Society of Naval Architects and Marine Engineers, Vol. 72, 1964.

13. Kerwin, J.E., "Computer Technique for Propeller Blade Section Design," International Shipbuilding Progress, Vol. 20, No. 227, July 1973.

14. Huang, T., et al, "Propeller/Stern/Boundary-Layer Interaction on Axisymmetric Bodies: Theory and Experiment," David Taylor Naval Ship Research and Development Center Report 76-0113, December 1976.

15. Cox, B.D., "A Theoretical Parametric Study of the Thrust Deduction on Deeply Submerged Bodies," David Taylor Naval Ship Research and Development Center Report (In Preparation).

16. Dawson, C., "A Practical Computer Method for Solving Ship Wave Problems," to be presented at the Second International Conference on Numerical Ship Hydrodynamics, University of California, Berkeley, September 1977.

Table 1

Measured and Computed* Values of Thrust Deduction for an Appended Series-58 Body (NSRDC Model 4620, Propeller 3638)[10,11]

Method			Thrust Deduction, t
Measured	Resistance and Self-Propulsion Experiments		0.150
Computed	Lifting Surface Method	Body Pressure Integration	0.135
		Lagally Theorem	0.133
	Lifting Line Method	Lagally Theorem	0.141
		Beveridge[7] (using approximate σ)	0.159

*Potential flow only; added frictional resistance is estimated to increase thrust deduction by 3 to 5 percent.

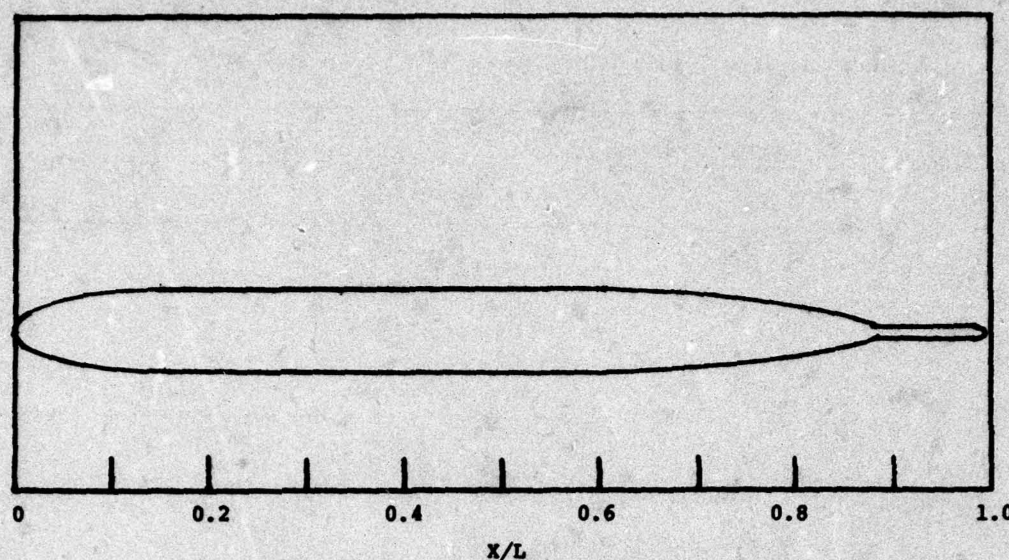

DTNSRDC Model 5225-1 (With 10 Percent Sting Added)

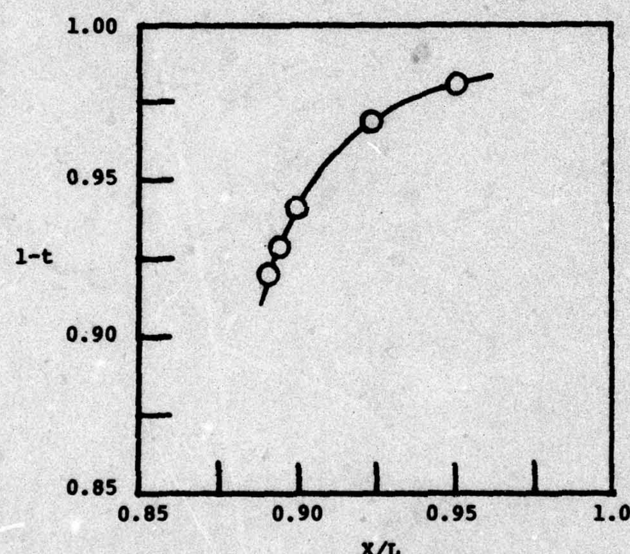

Figure 1 - Effect of Propeller Axial Location on the Thrust Deduction[15] (Computed Values)

Experimental and Prediction Techniques for Estimating Added Power Requirements in a Seaway

by

William G. Day, Jr., Arthur M. Reed and Wen-Chin Lin
David W. Taylor Naval Ship Research & Development Center

INTRODUCTION

Frequently towing tanks are tasked to provide powering predictions for new ship designs which will require a power margin to maintain speed in a seaway. The added power requirements are sometimes estimated by design margins or they may be defined through experimental procedures. In performing experiments to estimate the added power required to maintain speed in a seaway, several techniques may be used in both data analysis and extrapolation. This paper is intended to discuss techniques of conducting model experiments for the prediction of added power in a seaway and how such data should be extrapolated to full scale.

The paper will begin with a discussion of various prediction techniques for estimating added power in a seaway and their advantages and disadvantages. This will be followed by recommendation of an experimental procedure and review of the techniques used at the David W. Taylor Naval Ship Research and Development Center (DTNSRDC). Finally, we will conclude with a discussion of how data should be extrapolated to full scale and what data should be presented. A bibliography containing much of the literature relevant to added resistance and power is also included.

DISCUSSION OF PREDICTIVE TECHNIQUE FOR ADDED POWER IN WAVES

There are three basic methods for predicting the added power in a seaway from model experiments. The first method employs experiments to measure only added resistance in waves, the second uses added resistance in waves' experiments combined with calm water propulsion experiments and finally, the third method requires propulsion experiments both in calm water and waves.

Technique 1: Added Resistance in Waves, Still Water Propulsive Characteristics

An added resistance experiment is performed using a model of whatever scale is appropriate for a particular facility. The added power is then predicted from the added resistance by applying calm water propulsive coefficients to the added resistance data. The typical model for these experiments can vary from the 1.5 to 2.0-meter models which are frequently used for head seas experiments in facilities such as the DTNSRDC 140-foot tank, the University of California Richmond Station Towing Tank, and the Davidson Laboratory Towing Tank; to the 5.5 to 6.0-meter models which are towed in the DTNSRDC Carriage II Basin. These added resistance tests are usually performed in regular seas so that added resistance response operations can be determined; however, such tests are sometimes performed in irregular seas.

Technique 2: Added Resistance in Waves, Still-Water Overload Propulsive Characteristics

In this technique an added resistance experiment in waves similar to the experiment mentioned above is performed. However, in this approach a second experiment is also performed with a propulsion model in still water. This second experiment is an "overload" self-propulsion experiment in which the propulsion point of the model corresponds to the ship propulsion point including the additional load due to the added resistance in waves. This approach assumes that the propulsive coefficients for powering in waves will change from those in still water but that the change is only due to the increased loading of the propeller.

In principle, this technique does not necessarily require a powered model experiment. Increased loading calculations could be made using the propeller open water characteristics. This would result in a slightly more accurate version of the first technique.

Technique 3: Propulsion in Waves

In this technique, propulsion experiments are performed both in calm water and in waves. The difference in the required power between these two experiments is the added power in waves.

Propulsion in waves experiments are performed using larger models than those which may be used for added resistance experiments. The appropriate model size is generally governed by the selection of a model propeller which is sufficiently large to minimize Reynolds number scaling problems on the propeller blades. This choice of propeller size usually results in a model of 5.5 to 6.0-meters in length.

As in the case of added resistance in waves, added power tests can be performed in either regular waves or irregular waves. In terms of general usefulness, the data collected in regular waves is most useful because it allows simple extrapolation of model data to full-scale data in arbitrary irregular seas.

Discussion of the Various Techniques

Although there has been no comprehensive set of experiments on one model in which all three experimental methods have been employed and compared, it is still possible to make some definitive statements concerning the three techniques. It is intuitively obvious that Technique 1 would not give very accurate results (although for rough design margins it may be adequate) in that it does not even account for the effects of propeller loading increase. In particular, Figure 1 which gives data presented by Moor and Murdey (1970) shows that the propulsive coefficients do change in a seaway. The effects of propeller loading changes are not so clearly shown from these data. From this it can be concluded that Technique 1 should only be used if the effects of increased propeller loading are accounted for by use of at least the propeller open water characteristics with a resulting change in propeller efficiency.

Technique 2 is not as straight forward to evaluate. There is a large amount of data to show that technique 2 results in very reliable predictions of increased power, and yet other data shows that it is not at all reliable. Journee (1976) gives a large amount of data (see Figure 2) which shows that the added power is virtually identical with the increased power obtained from propeller overload tests in calm water applied to the resistance obtained in waves. In fact, Journee goes on to conclude, ".....there are no significant differences between these measurements and overload tests in still water even in the cases of extreme emerging of the propeller. This means that the propulsive efficiency is the same in both cases." On the other hand such work as that by Moor and Murdey (1968, 1970) states that such a method is not applicable. They go on to state [Moor and Murdey (1970)], "Such variations from the still water lines demonstrate that the effects of increasing resistance by a tow force in waves and of resistance being increased by the waves, are not the same as the effects of increasing resistance by a tow force in still water." However, upon examining the data which they present, it is obvious that either of the above conclusions could be drawn depending upon what model is being examined. This is illustrated by Figures 3 and 4 which are taken from Moor and Murdey (1970). Figure 3 shows data which varies significantly from the calm water data, while the data shown in Figure 4 is indistinguishable from the calm water data. In particular the data for full load conditions seem to be fairly consistent and some of it would definitely support Journee's conclusion, while the data for the ballast condition seem to vary widely and would definitely lend credence to Moor and Murdey's conclusions. The wide variation found in the ballast condition may be due to reduced propeller submergence, which may lead to emergence and ventilation in a seaway.

In conclusion we can state that Technique 2 is not always valid for use in predicting the power required in a seaway. This statement is supported by Nakamura (1976) who states, "It has been said that the propulsive performance in waves is explained fairly well by the overload effect on the propeller due to the added

resistance in waves. As mentioned above, however, the self-propulsion factors are affected considerably by ship motions, so it is considered that the results of the overload tests in still water are not always coincident with those of self-propulsion tests in waves."

The propulsion in waves' experiments of Technique 3 are the experiments which seem to come closest to representing the situation which a ship actually encounters. The propulsion in waves' experiments not only account for the actual loading on the propeller, but also account for the variation in the hull propulsion factors due to ship motions.

The one disadvantage of self-propulsion experiments in waves is the fact that such tests must of necessity be conducted at the model self-propulsion point. This means that the propeller is actually overloaded relative to the ship self-propulsion point. Such a disadvantage as this can be overcome by use of some type of external thruster designed to provide the appropriate amount of additional thrust to bring the propeller down from the model self-propulsion point to the ship self-propulsion point.

Recommendation

Of the three experimental techniques for obtaining added power in waves which have been discussed, the most appropriate would appear to be self-propulsion experiments in waves, i.e. Technique 3. All of the works discussed so far [Moor and Murdey (1970), Journee (1976) and Nakamura (1976)], along with many others, have obtained useful, consistent data by performing such experiments. There seems to be no question on the part of any author that using added resistance in waves' data with model calm water propulsion data, i.e. Technique 1, results in erroneous predictions.

Technique 2 in which added resistance data in waves is used with the data from overload self-propulsion tests in calm water is more controversial. Although the results of some experiments show this method to be quite good, other data shows it to be in error. Until a complete set of experiments which directly compare the techniques discussed herein is performed, no method can be said to be entirely satisfactory. For towing tanks without the capability to perform powering in waves' experiments, Technique 2 appears to be a reasonable compromise. The best state-of-the-art technique for properly accounting for both increased resistance and change in propulsive characteristics of a model in a seaway appears to be Technique 3. The authors therefore recommend this approach, model self-propulsion in waves, to be the standard for use.

CURRENT EXPERIMENTAL PROCEDURES AT DAVID TAYLOR NAVAL SHIP R&D CENTER

At DTNSRDC model experiments to determine the added power required in a seaway are generally performed using a propulsion model which was built for shaft horsepower predictions. However, the scale ratio for these models frequently gives too large a model for the capability of the wavemaker, in which case a compromise is generally reached between the two experiments. For powering-in-waves experiments the appropriate ship and appendage geometry as well as the design propeller geometry is scaled. More detail is usually unnecessary except for the addition of freeboard to the design sheer, if such was not the case for the original model. Decking is frequently required thereafter for protection of motors and dynamometry.

Although the external geometry is in all respects the same for powering in still water and in waves, the model ballasting is much more detailed. The total mass of the ballasted model is therefore centered at the appropriate point for the ship. In addition, the dynamic requirements for radius of gyration and metacentric height are also met. Generally the tolerance for these parameters are kept within ± 0.5% except for trim which can be even more carefully set. Typical values for model ballasting tolerances are:

Displacement	± 0.025% (e.g. ± 2N out of 8000N)
Trim	± 0.025% (e.g. + 2mm for LWL of 6m)
Longitudinal Center of Gravity	± 0.5%
Vertical Center of Gravity	± 0.5%
Radius of Gyration	± 0.02 LWL

Models are attached to the towing carriage by a single, counterbalanced heave staff for added resistance experiments. For powering in head waves experiments, the model is propelled in a free-running condition. Directional control is provided by an automatic feedback servo system to the rudder(s) from sonic transducers which operate on targets behind and beside the model. Data links to the model dynamometry from the towing carriage instruments are provided by umbilical cables which apply no force.

The powering in waves' experiments are generally performed in the long, linear, towing tank (Carriage 2 Basin) which is equipped with a pneumatic wavemaker capable of generating waves from 15 to 45 centimeters high. Irregular waves generally are produced by control of the intake/exhaust ports of the pneumatic air supply by means of a pre-programmed control tape. Most frequently the tape used in the experiments is that which generates wave heights most closely representing (producing) a Pierson-Moskowitz spectrum.

spectrum. Currently no control tapes are available at DTNSRDC which produce a two-parameter wave spectrum.

Added resistance experiments are performed at constant speed for a variety of wavelengths in regular head seas. Typically wavelength varying from nondimensional frequency of encounter (ω_e) of 1 to 10 are run with approximately 16 points for each wave height. Wave heights used in these regular wave experiments will generally vary between L/50 and L/20. Coincident still-water resistance experiments will be run in order to determine the added resistance coefficient, which according to current practice is defined as:

$$\sigma_{AW} = \frac{R_{T,AW} - R_{T,CW}}{\rho g \zeta_a^2 \; B^2/L}$$

Added power experiments are run necessarily at model self propulsion point. The model is free to surge, and therefore, the true speed of any given run in the towing tank is determined by adding the response of the surge measuring sonic transducer to the carriage speed. Propeller thrust, torque and revolutions per minute (n) are measured using the standand DTNSRDC model electronic transmission dynamometer.

The dynamometry which is used for the powering measurement has an accuracy of $\pm$ 0.5 percent of the design load. Typically for a 6m model this loading would be 5 newton-meters for torque and 100 Newtons for thrust. The dynamometers are capable of responding to the 0.10 hz range of dynamic signals encountered in the wave experiments. A 20 hz low-pass filter is generally used in the signal conditioning to minimize "noise" and to eliminate the 200 hz natural frequency of the dynamometer.

As in the added resistance experiments, still-water model self-propulsion experiments are performed during the same set of runs. Added power is then determined from the difference between these two results for a particular set of wave conditions.

Data are collected on board the towing carriage using a mini-processor and some preliminary calculations are performed there. All data are digitized and recorded on magnetic tape for later use, such as with the irregular sea spectra as mentioned above.

EXTRAPOLATION AND PRESENTATION OF DATA

As an initial step toward extrapolation we will take a brief look at dimensional analysis. The total resistance in waves may be written as a funcpion of ship length (L), mass (M), pitch moment of inertia (I_p) and speed (U). In addition we must include the physical constants: gravitational acceleration (g), water density (ρ), and kinematic viscosity (ν), along with the description of the waves given by the wave length (λ) and the wave amplitude (ζ_a). Using these quantities, we can say that the resistance is given by

$$R_T = R_T\,(L,\ M,\ I_p,\ U,\ g,\ \rho,\ \nu,\ \lambda,\ \zeta_a)$$

Upon performing dimensional analysis using ρ, g, and L as our fundamental variables, we obtain a nondimensional drag coefficient:

$$C_T = \frac{R_T}{\rho g L^3} = C_T\left(\frac{M}{\rho L^3}, \frac{I_P}{\rho L^5}, \frac{U}{\sqrt{gL}}, \frac{UL}{\nu}, \frac{\lambda}{L}, \frac{\zeta_a}{L}\right)$$

If we assume that we have fixed the geometry of the ship and model correctly, then $M/\rho L^3$ and $I_p/\rho L^5$ are both fixed and do not affect our results ; thus we have:

$$C_T = C_T\left(F_N, R_N, \frac{\lambda}{L}, \frac{\zeta_a}{L}\right)$$

If we fix ζ_a to be zero, then we are left with only the calm water drag on our ship and we can define an added resistance coefficient ΔC_T as follows:

$$\Delta C_T = C_T\left(F_N, R_N, \frac{\lambda}{L}, \frac{\zeta_a}{L}\right) - C_T\left(R_N, R_N, \frac{\lambda}{L}, 0\right)$$

Theoretical considerations lead us to the conclusion that ΔC_T is independent of the Reynolds number, even though C_T is not, and also that ΔC_T is a function of $(\zeta/\lambda)^2$; therefore we may write that as:

$$\Delta C_T = \Delta C_T\left(F_N, \frac{\lambda}{L}, \frac{\zeta_a}{L}\right) = \left(\frac{\zeta_a}{L}\right)^2 \Delta C_T\left(F_N, \frac{\lambda}{L}, \frac{\zeta_a}{L}\right)$$

We can easily relate the more usual added resistance coefficient σ_{AW}, to ΔC_T^1:

$$\sigma_{AW} = \frac{\Delta R_T}{\rho g (\zeta_a)^2 B^2/L} = \frac{\Delta C'_T}{(B/L)^2}$$

where B is the ship beam.

Repeating the same process for added power, we must consider the additional variables [propeller diameter (D), propeller submergence (h), propeller speed in revolutions per second (n), propeller torque (Q), and propeller thrust (T)] along with the atmospheric pressure (Pa) and the vapor pressure of the water (Pv). Performing additional dimensional analysis leads to the following additional parameters.

$$K_T = \frac{T}{\rho n^2 D^4}, \quad K_Q = \frac{Q}{\rho n^2 D^5}, \quad J = \frac{U}{n D}$$

$$F_P = n\sqrt{\frac{D}{g}}, \quad R_p = \frac{nD^2}{\nu}, \quad \sigma = \frac{\rho g h + P_a - P_\nu}{1/2\, \rho U^2} \quad \frac{h}{D}, \text{ and } \frac{L}{D}$$

We can now define an added power coefficient by taking the difference between the power required in waves and the power required in calm water. Upon neglecting the quantities which are ratios of geometric quantities and viscosity we obtain :

$$\Delta C_P = \frac{\Delta P_D}{\rho g\, L^3 \sqrt{gL}} = \Delta C_P \left(F_N, \frac{\lambda}{L}, \frac{\zeta_a}{L}, K_T, K_Q, J\right),$$

where we have neglected the effects of the changes in propeller Froude number and cavitation number.

From the nondimensionalization of ΔC_T and ΔC_P the usual Froude scaling determines how the data collected for a model should be extrapolated to ship scale. The added resistance data should be scaled by the scale ratio cubed times the ratio of the density of water for the ship to the density of water for the model. The same procedure applies to the added power except that the model added power is multiplied by an additional square root of the scale ratio.

There are many formats in which data for added resistance and added power in waves data can be presented. In the case of regular wave data these formats generally show a nondimensional added resistance or added power coefficient for a constant speed as a function of a non-dimensional wave length or frequency. In irregular seas the same coefficients are usually shown as a function of the modal period of the spectrum or as a function of ship speed for a given spectrum. Any of these formats are very satisfactory.

The same cannot be said for the presentation of data relating to propulsive coefficients. These data are generally broken down into the same coefficients which are presented for calm water propulsion, and no presentation of the propulsive efficiency (η_D) is given. It is this coefficient which is the most important to the understanding differences between propulsion in waves relative to resistance in waves.

It is therefore proposed that all future data presentations include a curve of the propulsive efficiency in waves defined as:

$$\eta_{D_W} = \frac{P_E + \Delta P_E}{P_D + \Delta P_D}$$

where P_E and ΔP_E are the calm water effective horsepower and added effective horsepower and added effective horsepower in waves respectively, and P_D and ΔP_D are similar quantities for shaft horsepower. Given the propulsive efficiency in a seaway we may even define the decrease in propulsive efficiency as $\Delta\eta_D = \eta_D - \eta_{DW}$ (a positive quantity). Using the above formula one can plot the change in shaft-horsepower against the change in effective horsepower (for constant change in efficiency) which results in a series of straight lines whose slope and intercept are functions of the change in efficiency. The case of no change in efficiency is the 45° line through the origin. Those cases in which efficiency decreases lie above this line while

those cases where efficiency increases lie below the line.

One reason for the difficulty in evaluating the effects of a seaway on propulsive efficiency comes from the lack of data at the same model scale. Frequently, powering experiments for models in a seaway are performed with the same model used for still water self-propulsion experiments mentioned in the previous section. However, the resistance values associated with the added power measurements may have come from resistance experiments in waves with a much smaller model. In some instances, the small model resistance experiments may even have been done with a bare hull model, leading to still more difficulties in comparisons. A case in point is the data which has been presented Yeh, et al (1973) and Strom-Tejsen, et al (1973). The added resistance values for the model identified as the destroyer form in Strom-Tejsen, et al were obtained principally from regular waves' experiments with a small (5-foot LWL) model. Propulsion data for this hull in head seas were obtained at a later time using a larger (18.2-foot LWL) geosim andare reported in Yeh, et al. Data from both sources have been compared in Figure 5.

The abscissa of Figure 5 reflects the increase in resistance (effective power) which has been non-dimensionalized by the still water resistance. The ordinate shows the increase in shaft power nondimensionalized by shaft power. If in fact the propulsive characteristics of this hull in a seaway are not substantially different from those in still water, the points for all Froude numbers and wave lengths should fall on the diagonal. If the propulsive efficiency decreases in the wave experiments, the points should fall above the diagonal. The fact that most points fall below the diagonal might be interpreted as an increase in propulsive efficiency, but in fact, it merely shows that when attempting to compare data from separate experiments using 2 models of different scales, the results prove inconclusive. It is not possible to perform a similar type analysis from the information presented in Moor and Murdey (1970), one would hope that the propulsive efficiencies shown in their figures do not contain such anamolies. Certainly, when attempting to use Techniques 1 and 2 for predicting added power, the danger of error from small model resistance data coupled with larger model propulsion data exists. This conclusion is further supported by Tasaki (1975) who states "In the propulsion tests in still water, 6m to 7m models are taken into consideration of the scale effect. In the tests in waves, however, 2m to 5m models are usually used for the convenience of the experiments. The above-mentioned variations of the propulsion factors, therefore, may contain partially the scale effect of hull and propeller."

Another point to be considered when presenting added power in a seaway is the sea state representation. The added power quantity which is desired is not a response amplitude operator as a function of wave length, but the response of the ship to a particular irregular seaway. Such a response could be obtained by performing propulsion tests in irregular seas having the desired spectrum. The disadvantage of this approach

is that the resulting data is applicable only to that particular irregular seaway.

Dalzell (1972, 1974, 1975, 1976) and Neal (1974) have shown some success at deriving a regular waves response operator from model experimental data in irregular waves by means of cross-bi-spectral analysis. However, such techniques still need additional validation and such tools are not yet at the point where they can be used for data analysis on a regular basis.

For making added power predictions in irregular seaway using model self-propulsion data from regular waves experiments, the technique proposed by Murdey (1972) in the 13th ITTC is considered to be the preferred method. Moor and Murdey (1972) give a substantial amount of excellent data comparing experiments in irregular waves to predictions made using this technique.

A brief description of the method which Murdey calls the Direct Power Method follows. Given model torque (Q) and propeller speed data (n), the added power in a wave of amplitude ζ_a is given as:

$$\Delta P_D\,(\omega) = \frac{2\pi}{550}\;\left[\, Q + \delta\, Q(\omega) \right]\;\left[n + \; n(\omega)\; \right] - Q\, n \;,$$

where $\delta Q(\omega)$ and $\delta h\;(\omega)$ are the added torque and added propeller revolutions at the given wave frequency ω . The mean added power in a sea spectrum is:

$$\Delta P_D = 2\,S(\omega)\,\frac{\Delta P(\omega)}{\zeta_a^{\,2}(\omega)}\;\delta\;(\omega)$$

where $S(\omega)$ is the model scale wave spectra.

CONCLUSIONS

Having reviewed these techniques for experiments and data analysis, four conclusions may be drawn:

1. The method described herein as Technique 3, that is model self propulsion in both still water and waves, is recommended as an experimental procedure. If this is not possible, Technique 2 considering an overload experiment in still water with added resistance in waves should be used.

2. It is desirable to use a large model which has been dynamically ballasted and which has propellers which will provide a minimum Reynolds number scale effect to perform powering in waves experiments. Regular wave experiments are preferred. Model self-propulsion as well as an overload propulsion experiment should be performed in still water in order to compare with the propulsion in waves' experiment.

3. In addition to added power, data should be presented for the added thrust, torque and propeller revolutions along with the added resistance coefficient σ_{AW}, for each condition tested. The comparable propulsive characteristics should be calculated based on the added resistance as well as added power experiments.

4. The calculations recommended by Murdey in the 13th ITTC for calculating added power in an irregular sea (the direct power method) are recommended.

Furthermore it is recommended that a comprehensive series of experiments be performed to adequately resolve the questions concerning the use of overload experimental propulsive characteristics with added resistance data to calculate added power requirements in waves. These experiments should also include an analysis of the effects of model scale on these predictions.

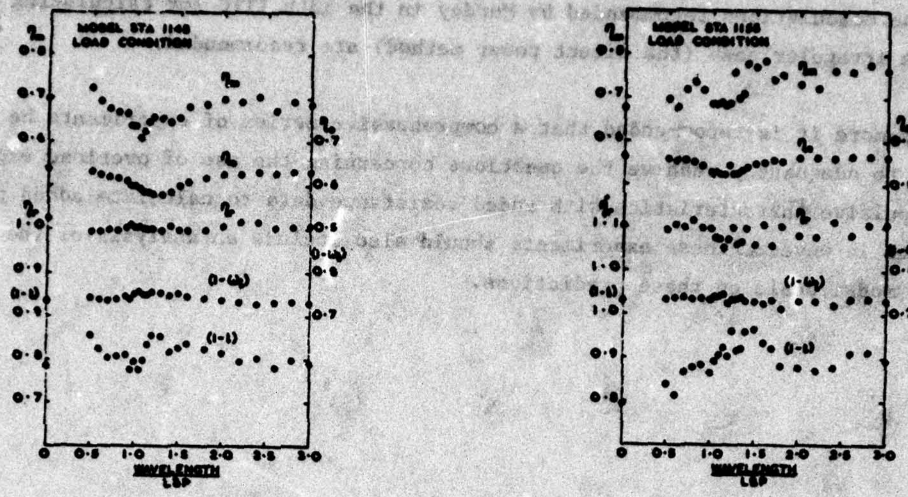

Figure 1 - Variation in Model Propulsive Coefficients with Wave Length [Figure 8, Moor & Murdey (1970)]

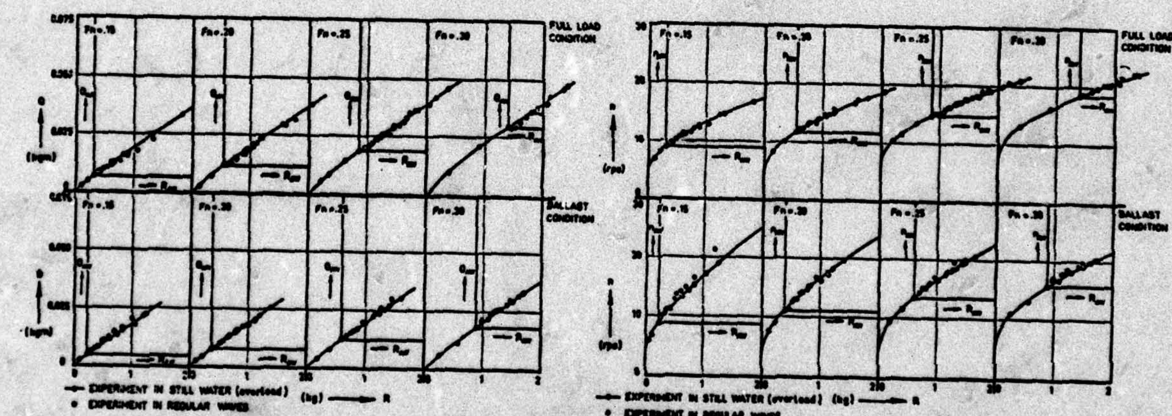

Propeller Torque **Propeller Revolutions**

Figure 2 - Propeller Torque and Revolutions as a Function of Overload and Added Resistance [Figures 27 & 25, Journée (1976)]

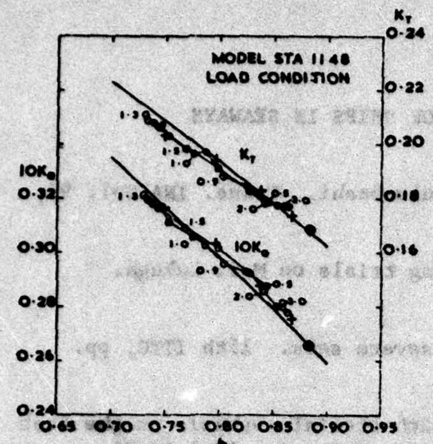

Figure 3 - Variation of Thrust and Torque Coefficients with Advance Coefficient with Lower K_T at $\lambda/L = 1.0$ [Figure 7, Moor & Murdey (1970)]

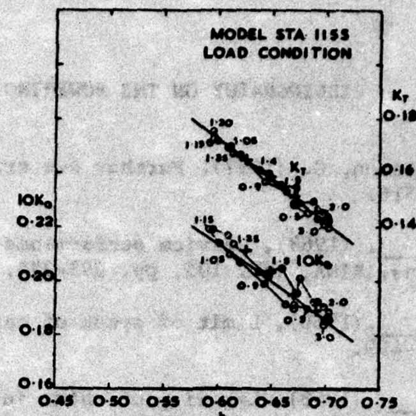

Figure 4 - Variation of Thrust and Torque Coefficients with Advance Coefficient with K_T agreement at $\lambda/L = 1.0$ [Figure 7, Moor and Murdey (1970)]

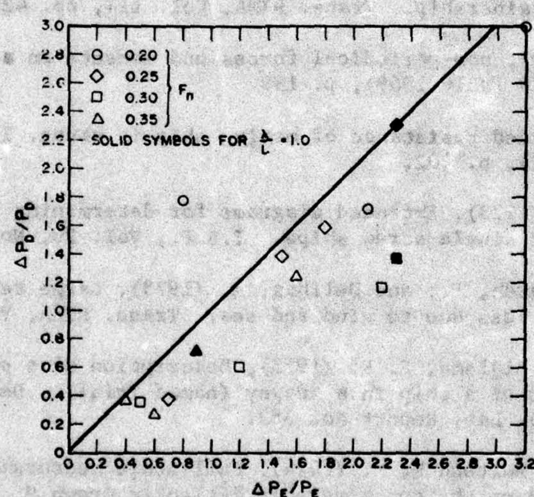

Figure 5 - Comparison of Added Power and Added Resistance for a Low Block Coefficient Hull Form

BIBLIOGRAPHY ON THE POWERING PERFORMANCE OF SHIPS IN SEAWAYS

1. Aertssen, G. (1957), Further sea trials on the Lubumbashi. Trans. INA Vol. 99, p. 516.

2. ______. (1963), Service performance and seakeeping trials on M.V. Lukuga. Trans. RINA, Vol. 105, pp. 293-335.

3. ______.(1966), Limit of speed of cargo ships in severe seas. 11th ITTC, pp. 456-459.

4. ______.(1968), Laboring of ships in rough seas with special emphasis on the fast ship. SNAME, Diamond Julilee International Meeting, N.Y., pp. 10.1-10.21.

5. ______.(1969), Service performance and trials at sea. Performance Committee, 12th ITTC.

6. ______. (1975), Speed loss due to weather on one class of container ships in the North Atlantic with reference to the relationship between wind and waves. 14th ITTC, Vol. 4, pp. 435-444.

7. Aertssen, G.; Ferdinande, V.; and De Lembre, R. (1965), Service performance and seakeeping trials on two conventional trawlers. Transactions, NECI, Vol. 81, p. 32.

8. Aertessen, G.; and Sluys, M. F. van (1972), Service performance and seakeeping trials on a large containership. Trans. RINA, Vol. 114, pp. 429-447.

9. Ankudinov, V. I. (1969), non-periodical forces and moments on a ship in waves. I.S.P. Vol. 16, No. 179 (July 1969), p. 199.

10. ______. (1972), The added resistance of moving ship in waves. I.S.P., Vol. 19, No. 220 (December 1972), p. 402.

11. Auf 'm Keller, W. H. (1973), Extended diagrams for determining the resistance and required power for single screw ships. I.S.P., Vol. 20, No. 225.

12. Berlekom, W. B.; Tragardh, P.; and Dellhag, A. (1975), Large tankers-- Wind coefficient and speed loss due to wind and sea. Trans. RINA, Vol. 117, pp. 41-58.

13. Beukelman, W. B.; and Bijlsma, E. F. (1973), Description of a program to calculate the behavior of a ship in a seaway (named Trial). Delft University of Technology, Ship Hydro. Lab. Report No. 383.

14. Beukelman, W. B.; and Buitenhek, M. (1974), Full scale measurements and predicted seakeeping performance of the containership "Atlantic Crown." I.S.P., Vol. 21, No. 243 (November 1974), p. 69. (Also TNO Report No. 185S).

15. Boese, P. (1970), Eine einfache Methode zur Berechnung der Widerstandserhohung eines Schiffes im Seegang. Schieffstechnik, Bd. 17, Heft 86 (1970), p. 29.

16. Buitenhek, M.; and Ooms, J. (   ), A phase locked loop servo system. Delft Ship Hydromechanics Laboratory.

17. Dalzell, J. F. (1972), Application of cross-bi-spectral analysis to ship resistance in waves. Davidson Laboratory, Stevens Institute of Technology, SIT-DL-1606, 141 pp.

18. ______. (1972), Some additional studies of the application of cross-bi-spectral analysis to ship resistance in waves. Davidson Laboratory, Stevens Institute of Technology. SIT-DL-72-1641.

19. ______. (1974), Cross-bi-Spectral analysis: Application to ship resistance in waves. Jour. of Ship Research, Vol. 18, No. 1, pp. 62-72.

20. ______. (1975), The applicability of the functional polynomial input-output model to ship resistance in waves. Davidson Laboratory, Stevens Institute of Technology, SIT-DL-1794, 137 pp.

21. ______. (1976), Application of the functional polynomial model to the ship added resistance problem. 11th Symp. on Naval Hydrodynamics, ONR (in print).

22. ______. (1976), A study of the feasibility of wave pulse techniques for experimental determination of added resistance. Davidson Laboratory, Stevens Institute of Technology, SIT-DL-76-1928, 69 pp.

23. Dalzell, J. F.; and Kim, C. H. (1976), Analytical investigation of the quadratic frequency response for added resistance. Davidson Laboratory, Stevens Institute of Technology, SIT-DL-76-1878, 66 pp.

24. Fujii, H.; and Takahashi, T (1976), On the resistance increase of a ship in regular head sea. Mitsubishi Heavy Industries Technical Review, Vol. 7, No. 2 (January 1967), p. 86 (in Japanese).

25. ______. (1975), Experimental study on the resistance increase of a ship in regular oblique waves. 14th ITTC, Vol. 4, pp. 351-360.

26. ______. (1975), Experimental study on the resistance increase of a large full ship in regular oblique waves. Jour. of Soc. of Naval Arch. Japan, Vol. 137 (June 1975), p. 132 (in Japanese).

27. ______. (1975), Experimental study on the resistance increase of a ship in regular oblique waves. Proceedings, 14th ITTC, Vol. 4, pp. 351-360.

28. Fukuda, J.; Ono, Y.; and Ogata, G. (L966), Determination of fore and after draught of ballasted bulkcarriers associated with the criteria of slamming and propeller-racing. 11th ITTC.

29. Geisler, O.; and Siemer, F. (1974), Dynamische Belastung von Schiffsdampfturbinenanlagen bei Umsteuer-Manovern. Schiff and Hagen, Heft 3.

30. Gerritsma , J.; Bosch, J. J. van den; and Beukelman, W. B. (1962), Propulsion in regular and irregular waves. I.S.P., Vol. 8, No. 82, p. 235.

31. Gerritsma , J. (1963), Propulsive performance in waves. 4th bi-annual seminar, Ship Behaviour at Sea, SIT (January 1963).

32. ______. (1969), Sustained sea speed. 12th ITTC.

33. ______. (1972), Some recent advances in the prediction of ship motions and ship resistance in waves. NSMB 40th Anniversary International Meeting, p. 171.

34. Gerritsma, J.; and Beukelman, W. B. (1972), Analysis of the resistance increase in waves of a fast cargo ship. Appendix 5 of Report Seakeeping Comm. Proc. 13th ITTC Vol. 2 (1972), p. 902; I.S.P., Vol. 19, No. 217 (September 1972), p. 285. (Also Netherlands Ship Research Centre Report No. 169S).

35. ______. (   ), Analysis of the modified strip theory for the calculation of ship motions and wave bending moments. Netherlands Ship Research Centre T.N.O., Shipbuilding Department, Report No. 96-S.

36. Goodwin, A. J. H.; et al. (   ), The practical application of computers in marine engineering.

37. Hanaoka, T. (1953), Non-uniform theory of wave resistance, Part 5. Journal Zosen Kyokai, Vol. 94, Vol. 94, pp. 27-34.

38. Hanaoka, T.; et al. (1963), Research in waves. "Researches on Seakeeping qualities of ships in Japan." Soc. of Naval Arch. of Japan, 60th Anniversary Series, Vol. 8, p. 216.

39. Havelock, T. H. (1942), The drifting force on a ship among waves. Phil. Magazine, Ser. 7, Vol. 33, pp. 467-475.

40. Harvald, S. A. (1950), Wake of merchant ships. Doctor's thesis, The Danish Technical Press, Copenhagen.

41. Haskind, M. D. (1946), The hydrodynamic theory of ship oscillations in rolling and pitching. Prikl. Mat. Mekh., Vol. 10, pp. 33-66 (Translation: (1953), The hydrodynamical theory of the oscillation of a ship in waves. SNAME Tech. and Res. Bull., No. 1-12, pp. 3-43).

42. Hosoda, R. (1973), The added resistance of ships in regular oblique waves. Jour. of Soc. of Naval Arch. Japan, Vol. 133 (June 1973), p. 7.

43. Ilyin, V. M.; Shapakoff, V. S.; and Smorodin, A. I. (1974), The estimation methods for ship added resistance and propulsive characteristics in seaway. Symp. of Dynamics of Marine Vehicles and Structures in Waves, London, p. 413.

44. Isherwood, M. A. (1973), Wind resistance of merchant ships. Trans. RINA Vol. 115, pp. 327-338.

45. Jinnaka, T. (1958), Some experiments on the exciting forces of waves acting on the fixed ship models. Jour. of Soc. Naval Arch. Japan, Vol. 103 (July 1958), p. 47 (in Japanese).

46. ______. (1960), Periodical source and its applications (continued). Jour. of Soc. of Naval Arch. Japan, Vol. 198 (December 1960), p. 1 (in Japanese).

47. Joosen, W. P. A. (1966), Added resistance of ships in waves. 6th Symp. on Naval Hydrodynamics, Washington, D.C.

48. Journee, J. M. J. (1976), Motions, resistance and propulsion of a ship in longitudinal regular waves. Report No. 428, Delft University of Technology, Ship Hydromechanics Laboratory, May 1976.

49. Kent, J. L. (1922), Experiments on mercantile ship models in waves. Trans. INA, Vol. 64, pp. 63-97.

50. ______. (1924), The effects of wind and waves on propulsion of ships. Trans. INA, Vol. 66, pp. 188-213.

51. ______. (1926), Experiments on mercantile ship models in waves. Trans. INA, Vol. 68, pp. 104-123.

52. ______. (1927), Propulsion of ships under different weather conditions. Trans. INA, Vol. 69, pp. 144-163.

53. ______. (1927), Average sea speeds of ships under winter weather conditions. Trans. INA, Vol. 69, pp. 290-313.

54. ______. (1931), The effect of rough water on the propulsion of single-screw ships. Trans. INA, Vol. 73, pp. 281-287.

55. Kent, J. L.; and Cutland, R. S. (1935), Resistance experiments in smooth and rough water made with models of high speed ships. Trans. INA, Vol. 77, pp. 81-91.

56. ______. (1936), Self-propelled experiments in smooth and rough water made with models of high speed ships. Trans. INA, Vol. 78, pp. 110-124.

57. ______. (1938), Further resistance and propeller experiments with models of coasters. Trans. INA, Vol. 80, pp. 107-135.

58. ______. (1942), The effect upon ship propulsion in rough water of alterations in the shape of propeller blades. Trans. INA, Vol. 84, pp. 34-51.

59. Kholodilin, A. N.; and Yurkov, N. N. (1975), on added resistance of ship in head waves. 14th ITTC, Vol. 4, pp. 286-301.

60. Lap, A. J. W. (1954), Diagrams for determining the resistance of single screw ships. I.S. P., Vol. 1, No. 4.

61. Lin, W. C.; and Reed, A. M. (1976), The second-order steady force and moment in an oblique seaway. 11th Symp. on Naval Hydrodynamics, 15 pp. (in print).

62. Lipis, V. B. (1966), Calculation from vortex theory of the action of a propeller during pitching of a vessel. Trudy Tsentral'nogo Nauchno- Issledovatel'skogo Instituta Morskogo Flota (TsNIIMF), Gidromekhanika, (English Translation).

63. Loukakis, T. A. (1972), Theoretical calculation of ship resistance in waves. MIT Report No. 72-17.

64. Maruo, H. (1957), The excess resistance of ship in rough seas. I.S.P., Vol. 4, No. 35, pp.

65. ______. (1952), Modern developments of the theory of wave-making resistance in the non-uniform motion, Part 1. Soc. Naval Arch. Japan, 60th Anniversary Ser., Vol. 2, pp. 1-82.

66. ______. (1957), On the increases of the resistance of a ship in rough seas (I). Jour. of Soc. Naval Arch. Japan, Vol. 101 (August 1957), p. 33 (in Japanese).

67. ______. (1960), On the increase of the resistance of a ship in rough seas (II). Jour. Soc. Naval Arch. Japan, Vol. 108 (December 1960), p. 5. (in Japanese).

68. ______. (1960), The drift of a body floating on waves. Journ. Ship Research, Vol. 4, No. 1, pp. 1-10 (December 1960).

69. McCarthy, J. R.; Norley, W. H.; and Obler, G. I. (1961), The performance of a fully submerged propeller in regular waves. DTMB Report 1440, 34 pp.

70. Moens, W. D. (   ), Meterological routeing (in Dutch).

71. Moor, D. I. (1970), Effects of performance in still water and waves of some geometric changes to the form of a large twin-screw ship. Trans. SNAME, Vol. 78, pp. 88-150.

72. Moor, D.I.; and Murdey, D.C. (1968). Motions and propulsion of single screw models in head seas. Trans. RINA, Vol 110, pp 403-446.

73. ______. (1970), Motions and propulsion of single screw models in head seas, Part II. Trans. RINA, Vol. 112, P. 121.

74. Murdey, D.C. (1972), On predictions of power increase in irregular waves from model experiments in regular waves. 13th ITTC, pp. 882-901.

75. Nakamura, S. (1969), Various factors on seakepping qualities. Symposium on Seakeeping Qualities of Ships, Soc. Naval Arch. Japan (July 1969).

76. ______. (1974), Experiments of the resistance increment and propulsive performance on the swells. JTTC-II, SK39-21, (in Japanese).

77. ______. (1976), Added resistance and propulsive performance of ships in waves. International Seminar Wave Resistance, Tokyo, 18 pp.

78. Nakamura, S.; ET.AL. [Committee SR-125] (1974), The calculation of the nominal speed loss in a seaway. Ship-Building Research Association of Japan, Report No. 188, (in Japanese).

79. Nakamura, S.; Hosoda, R.; and Shintani, A. (1969), Propulsive performance of a series 60, CB = 0.70 ship model in regular head waves. 12th ITTC, p. 783.

80. ______. (1969), On propulsive performance of a ship in regular head waves. Jour. Kansai Soc. Naval Arch. Japan, No. 134 (December 1969), p. 23 (in Japanese).

81. Nakamura, A,; Hosoda, R.; and Naito, S. (1975), Propulsive performance of a container ship in waves (1st Report). Jour. Kansai Soc. Naval Arch. Japan, No. 156 (March 1975), p. 31 (in Japanese).

82. Nakamura, S.; Hosoda, R.; and Nema, K. (1975), Propulsive performance of a container ship in waves (2nd Report). Jour. Kansai Soc. Naval Arch. Japan, No. 157 (June 1975) (in Japanese).

83. Nakamura, S.; Hosoda, R; and Naito, S. (1975), Propulsive performance of a container ship in eaves (3rd Report). Jour. Kansai Soc. Naval Arch. Japan, No. 158 (September 1975), p. 37 (in Japanese).

84. Nakamura, S.; Hosoda, R.; Naito, S.; and Inoue, M. (1975), Propulsive performance of a container ship in waves (4th Report). Jour. Kansai Soc. Naval Arch. Japan, No. 159 (December 1975) (in Japanese).

85. Nakamura, S.; Naito, S.; and Inoue, R. (1975), Open-water characteristics and load fluctuations of a propeller in waves. Jour. Kansai Soc. Naval Arch. Japan, No. 159 (December 1975) (in Japanese).

86. Nakamura, S.; and Tasaki, R. (1963), Model experiments in waves, researches of seakeeping qualities of ships in Japan. Soc. Naval Arch. Japan, 60th Anniversary Series, Vol. 8, Chap. 6 (1963), p. 103.

87. Nakamura, S.; and Shintani, A. (1965), On ship motions and resistance increase of mathematical ship form in regular waves. Journ. Soc. of Naval Arch. Japan, Vol. 118 (December 1965), p. 24 (in Japanese).

88. Neal, E. (1974), Second-order hydrodynamic forces due to stochastic excitation. 10th Symp. on Naval Hydrodynamics, ONR, pp. 517-539.

89. Newman, J. N. (1959), The damping and wave resistance of a pitching and heaving ship. Jour. of Ship Research, Vol. 3, No. 2, pp. 1-19 (June 1959).

90. Newman, J. N. (1967), The drift force and moment on ships in waves. Jour. of Ship Research, Vol. 11, No. 1, pp. 51-60 (March 1967).

91. Ochi, M. K. (1964), Prediction of occurrence and severity of ship slamming at sea. 5th Symp. on Naval Hydrodynamics, Bergen, Norway.

92. ______ (1968), Statistical properties of powering characteristics in waves. 15th ATTC, Vol. 1.

93. Ochi, M. K.; and Motter, E. (1974), Prediction of extreme ship responses in rough seas of the North Atlantic. International Symposium on the Dynamics of Marine Vehicles and Structures in Waves, London, pp. 199-209.

94. Ooosterveld, M. W. C.; and Oossanen, P. Van (1972), Recent developments in marine propeller hydrodynamics. International Jubille Meeting 1972, N.S.M.B. Wageningen.

95. Pershin, V. I., and Vosnezzensky, A. E. (1957), Study of ship speed decrease in irregular sea. Proc. Symp. on Behavior of Ships in a Seaway, Wageningen.

96. Salvesen, N. (1974), Second-order steady-state forces and moments on surface ships in oblique regular waves. International Symp. on the Dynamics of Marine Vehicles and Structures in Waves, London, pp. 225-239.

97. Shintani, A. (1970), On the comparison between calculations and experiments on the resistance increase in waves. Jour. Kansai Soc. Naval Arch. Japan, No. 137 (September 1970), p. 44 (in Japanese).

98. ______. (1971), Influence of ship form particulars on resistance increase in regular waves. Jour. Kansai Soc. Naval Arch. Japan, No. 139 (March 1971), p. 35 (in Japanese).

99. ______. (1973), Some notes on approximate methods of the calculation of resistance increase of ships in waves. Jour. Kansia Soc. Naval Arch. Japan, No. 150, (September 1973), p. 27 (in Japanese).

100. ______. (1973), Towing tank experiments on propulsive efficiency in regular head waves (1st Report). JTTC-II, SK 36-12.

101. Sibul, O. J.,(1964), Ship resistance in uniform waves. University of California, Berkeley, College of Engineering Report NA-64-1.

102. ______. (1966), An experimental study of ship resistance and motions in waves--A test for linear superposition. University of California, Berkeley, College of Engineering, Report NA-66-3.

103. ______. (1967), Increase of ship resistance in waves. University of California, Berkeley, College of Engineering Report, NA-67-2.

104. ______. (1969), Ship resistance in irregular waves. University of California, Berkeley, College of Engineering, Report NA-69-5.

105. ______. (1971), Constant thrust vs. constant velocity method for resistance measurement in waves. University of California, Berkeley, College of Engineering, Report NA-71-1.

106. ______. (1971), Measurement and calculation of ship resistance in waves. College of Engineering, University of California, Berkeley, Report No. NA-71-2.

107. Sluijs, M. F. Van (1972), Performance and propeller load fluctuations of a ship in waves. Netherlands Ship Research Centre TNO Report No. 163S.

108. ______. (1972), Propeller load fluctuation and performance in regular and irregular waves. 13th ITTC, pp. 208-218.

109. Sluijs, M. F. Van; and Tan, Seng Gie (1972), Behavior and performance of compact frigates in head seas. I.S.P., Vol. 19, No. 210, (February 1972).

110. Spens, P. G.; and Lalangas, P. A. (1962), Measurements of the mean lateral force and yawing moment on a series 60 Model in oblique regular waves. Stevens Institute of Technology, Davidson Laboratory Report 880.

111. Strom-Tejsen, J.; Yeh, H.; and Moran, D. D. (1973), Added resistance in waves. Trans. SNAME, Vol. 81, p. 109.

112. Swaan, W. A. (1960), A short nate on the power prediction of ships in waves. 9th ITTC, pp. 502-511.

113. Takagi, M.; Hosoda, R.; and Shimasaki, H. (1971), An improvement for the calculation of added resistance in waves. Jour. Kansai Soc. Naval Arch. Japan, No. 141 (June 1971), p. 33 (in Japanese).

114. Taniguchi, K. (1961), Propulsion of ships in waves. Bulletin of Soc. Naval Arch. Japan, No. 383 (August 1961), p. 315 (in Japanese).

115. Taniguchi, K.; and Watanabe, K. (1956), Self-propulsion tests in rough water of large ship-models. Jour. Soc. Naval Arch. Japan, Vol. 98, pp. 23-30 (in Japanese).

116. Tasai, F.; Takagi, M.; Ganno, M.; Arakawa, H.; and Kurihara, M. (1971), A study on the seakeeping qualities of high speed single screw container ships in head waves. Jour. Soc. Naval Arch. West Japan, No. 41 (March 1971), p. 45 (in Japanese).

117. Tasaki, R. (1957), On the characteristics of the driving machine in self-propulsion test among waves, Jour. Soc. Naval Arch. Japan, Vol. 10, pp. 25-32, (in Japanese).

118. ______. (1963), Effect of characteristics of driving machine in self-propulsion tests in waves. Soc. Naval Arch. Japan, 60th Anniversary Series, Vol. 8, Chapt. 6.6, pp 162-166.

119. ______. (1963) On shipment of water in head waves. 10th ITTC, London.

120. ______. (1975), Propulsion factors and fluctuating propeller load in waves. 14th ITTC, Vol. 4, pp. 224-236.

121. Tasaki, R.; Kitagawa, H.; Okamoto, H.; and Tanaka, A. (1976), Model experiments of high speed container ships in regular head waves. Jour. Kansai Soc. Naval Arch. Japan, (in Japanese).

122. Todd, G. H. (1969), Ship power prediction in waves. 12th ITTC.

123. Vassilopoulos, L.A. (1967), The application of statistical theory of non-linear systems to ship motion performance in random seas. I.S.P., Vol. 14, No. 150, (February 1967).

124. Vedeler, S. (1970), A note on wave influence on propulsion systems. European Shipbuilding, Vol. 6, pp. 79-85.

125. Vossers, G. (1961), Fundamentals of the behavior of ships in waves. NSMB, Publication 151a.

126. Wahab, R. (1967), Observations made on board of dutch ships. Netherlands Ship Model Basin Report 67-090-WO.

127. Wahab, R.; and Moss, L. W. (1971), On the added drag of destroyers in regular head waves. NSRDC Report No. 3704.

128. Yeh, H. Y. H.; Schutz, H.; and Plaia, P. (1973), Powering characteristics of a low-block displacement hull form in head seas. NSRDC Report 4059, 26 pp.

129. Yoshino, T. (1973), The results of model experiment of container carrier (L/B = 8, one and twin screw ship) in oblique waves. JTTC-I, SK 36-11, (in Japanese).

130. Yoshino, T., Saruta, T. and Yoshino, Y. (1974), Model tests on thrust and torque increase and fluctuations acting on propeller shaft of high-speed container ship with single or twin screws in oblique waves. Report of SRI, Vol. 4, pp. 217-232, (in Japanese).

131. Yuasa, H. (1974), Calculation of the fluctuations of propeller load induced by ship motions in oblique wave (Part 1). Jour. Soc. Naval Arch. Japan, Vol. 136 (December 1974), p. 69 (in Japanese).

132. ______. (1975), Calculation of the fluctuations of propeller load induced by ship motions in oblique waves (Part 2). 14th ITTC, Vol. 4, pp. 381-389.

PERFORMANCE OF DUCTED PROPELLERS FITTED TO SURFACE CRAFT

by

W. S. Gearhart[(1)] and R. E. Henderson[(2)]
Applied Research Laboratory
The Pennsylvania State University

INTRODUCTION

The primary difference between the propeller and the ducted propeller involves the shape of the slipstream that passes through the propulsor. In the ducted propeller, the shape of the slipstream can be controlled by proper shaping of the shroud or duct which surrounds the blade rows while the slipstream through a propeller is always contracting and hence the fluid accelerates as it approaches the propeller disk. The ducted propeller provides the designer with the option of either accelerating or decelerating the flow before it enters the rotating blade row. The slipstream pattern of a propeller and that of a ducted propeller having both an accelerating and a decelerating shroud arrangement are shown in Figure (1). The velocity of the slipstream at various stations through each propulsor is also shown schematically in Figure (1). The propeller and converging ducted propeller accelerate the flow into the disk and, therefore, it is apparent that the blade surface velocities at the blade tips will be higher and the local static pressure lower than that of the ducted propeller with a decelerating duct.

Model Evaluation of Ducted Propeller Performance

The evaluation of a ducted propeller design by a series of model tests is as important a step in the development of a new design as is the model evaluation of open propellers. However, the model evaluations of a ducted propeller must be approached in a different light than the evaluation of open propellers. For example, the evaluation of the ducted propeller must be conducted using the entire unit, i.e., the duct, hull, rudders, and the propeller combined. While many designers consider the duct and the propeller as separate enities, it is in fact the combination which provides the propulsive advantages realized in many prototype applications [1].

---

(1) Associate Professor of Engineering Research

(2) Associate Professor of Mechanical Engineering

The performance of a ducted propeller is measured by the net thrust, propeller plus duct, and net power required by the unit. Several authors [2] have taken the approach that model evaluations can be conducted with and without the duct installed and the contribution of each element determined. This is erroneous since the propeller and duct operate in combination and an interaction exists between the forces produced by each element.

The question of open water versus behind-a-model hull tests is perhaps more crucial for a ducted propeller than for an open propeller. This is of course a function of the wake flow in which the propulsor is operating. If the ducted propeller is subjected to flow nonuniformities when operated behind a hull, the model tests should include these nonuniformities. If these are not modelled, the duct will be subjected to an unreal flow field which means both the duct and the propeller within the duct will not model the prototype performance. Therefore, in addition to the forces which exist on the duct and propeller, an important item in model evaluations is the measurement of the flow field within the duct.

A most important observation made by several investigators, [3], [4], is the importance of including the model rudders when investigating the propulsive characteristics of a ducted propeller. This is particularly true when the rudders are located in the propulsive slipstream of the ducted propeller. Since the slipstream will contain fluid rotation, the rudders act to remove this rotation and thereby decrease the propulsive losses. A similar effect is observed with an open propeller.

The determination of the flow field, velocities and pressures within the ducted propeller, can aid significantly in the evaluation of the ducted propeller performance. An example of the use of such data is described in [5].

<u>Scaling of Model Performance to Prototype</u>

Since the ducted propeller has not seen as extensive use as the open propeller, there is not a large quantity of data available which relates model and prototype performance. It is only since the advent of VLCC's that such data have appeared in the open literature. Recent publications [6], [7] deal primarily with the scaling of cavitation performance rather than powering performance.

In general, the conclusions reached regarding the powering performance of ducted propeller is that they provide a more efficient and faster means of propulsion that the equivalent open propeller [1]. However, the experiences in scaling model powering data to full scale are not discussed. In addition to the usual scaling corrections applied to model propeller data, it is necessary to correct for the difference in Reynolds number on the model and prototype propeller duct. This correction can be appreciable due to the large wetted area of most propeller ducts.

With respect to the scaling of model cavitation performance, some very extensive model and full scale observations have been conducted [6], [7]. These studies report the results of model tests in both cavitation tunnel and vacuum towing

tank tests. Correlation of these results with full scale observations lead the authors to conclude: (a) there is satisfactory correlation of cavitation patterns between the vacuum tank tests and full scale; (b) at full scale the extent of the cavitation patterns are slightly larger than on the model; (c) the presence of a model hull in front of the ducted propeller is very important for cavitation testing; and (d) tip cavitation is more important than blade surface cavitation because of its influence on erosion of the duct inner surface.

ESTIMATION OF DUCTED PROPELLER PERFORMANCE

Influence of Duct Geometry

The duct geometry typically used with a ducted propeller is shown in Figure (2a). A variety of studies [5], [8], [9], [10] have been directed toward developing duct shapes with diffusing type of ducts downstream of the rotor, Figure (2b). It was concluded in [5] that it is difficult to find firm evidence of any significant improvement in the performance of a ducted propeller as a result of the use of diffusing ducts aft of the rotor.

This conclusion can be supported by a simplified one-dimensional analysis of the flow through a ducted propulsor. A great deal of basic information can be derived regarding the total thrust generated and the power required by a given propulsor geometry on the basis of one-dimensional momentum considerations.

Such an approach assumes a uniform flow in the propulsor slipstream upstream of the unit as depicted at station (1) in Figure (2). The flow downstream of this station shall be assumed to be <u>inviscid</u> and <u>nonseparating</u>. Typical of an actuator disk analysis, it shall be assumed that <u>no rotation</u> exists in the downstream slipstream. In a later discussion, the importance of this assumption will be considered. It is also assumed that the static pressure which exists at stations (1) and (5) equals the free stream value P_∞. Additionally, it is assumed for each of the two propulsors shown in Figure (2a) and (2b) that the rotor diameters are equal and are designed to ingest the same rate of mass flow and place the same energy per unit mass flow into the fluid. Based on these assumptions, the relation of total energy per unit mass flow between stations (1) and (5) can be written as:

$$P_{T_1} = P_{T_5} - \gamma \overline{H}$$

or

$$p_\infty + \rho \frac{V_\infty^2}{2} = p_\infty + \rho/2(V_\infty + \overline{\Delta V})^2 - \gamma \overline{H} \quad , \tag{1}$$

where $(\overline{H})$ represents the energy per unit mass flow placed in the fluid by the rotor and is equivalent for both rotors. The parameters with bars overhead represent

mass-averaged quantities. The nondimensional rotor head, $\overline{H}$, can be expressed in terms of the change in velocity between stations (1) and (5) as:

$$\frac{\overline{H}}{\frac{V_\infty^2}{2g}} = 2\left(\frac{\overline{\Delta V}}{V_\infty}\right) + \left(\frac{\overline{\Delta V}}{V_\infty}\right)^2 . \qquad (2)$$

This relation indicates that the change in nondimensional energy between stations (1) and (5) is the same for propulsors having the same value of $(\overline{\Delta V})$.

The nondimensional mass flow rate shall be defined as:

$$C_m = \frac{\rho A_5}{\rho A_3}\left(\frac{V_\infty + \overline{\Delta V}}{V_\infty}\right) = \frac{\overline{V_3}}{V_\infty} \qquad (3)$$

and is equivalent for both propulsors. The nondimensional energy per unit time placed in the flow can be expressed as:

$$\frac{\text{Power}}{\rho\,\frac{V_\infty^3}{2}\,A_3} = \left(\frac{\overline{H}}{\frac{V_\infty^2}{2g}}\right)\left(\frac{\overline{V_3}}{V_\infty}\right)$$

$$= \left(\frac{\overline{H}}{\frac{V_\infty^2}{2g}}\right) C_m . \qquad (4)$$

Equation (4) indicates that fluid power for both propulsors is equivalent since the mass flow rate and head of each propulsor are the same.

The total, or net, propulsor thrust, based of the impulse-momentum relationship, is:

$$T_T = \rho\,\overline{V_3}\,A_3\,\overline{\Delta V} \quad ,$$

and nondimensionally the total propulsor thrust coefficient can be defined as:

$$C_{T_T} = \frac{T_T}{\rho \frac{V_\infty^2}{2} A_3} = 2\, C_m \left(\frac{\Delta \bar{V}}{V_\infty}\right) \quad . \tag{5}$$

The mass flow coefficient and change in velocity between stations (1) and (5) are the same for both propulsor arrangements. It is concluded that the two propulsors will generate equal total thrust for the same shaft power.

The preceding indicates that diffusing ducts will not produce any gains in overall performance as compared to nondiffusing ducts. In summary, assuming an ideal or inviscid flow, the same fluid power is required in both cases to produce the same total thrust. In practice, real flow effects cause both types of ducts to suffer from an internal blockage. Boundary layer growth on the inner surface, coupled with the lower velocity tip clearance flow, [5], results in duct blockage. On this basis, moderate divergence of the duct downstream of the rotor would compensate for the blockage and provide a lower velocity discharge jet. Only on this basis, could some minor gain in the propulsive coefficient or efficiency be obtained.

In contrast, claims of gains in efficiency by the use of diffusing ducts most probably result from changes in mass flow through the propulsor when various diffuser angles are used. Unfortunately, experimental measurements to confirm this are lacking and it is doubtful that the controversy of the merits of diffusing ducts will not be resolved until the details of the flow field are more throughly recorded. A method to perform such tests is discussed later.

Influence of Advance Ratio

Experimental results indicate considerable differences in propulsor performance with and without the presence of rudder appendages. The reason for the differences in powering performance with and without appendages present, has been suggested in [3] to result from the differences in the amount of swirl in the downstream flow. Should the presence of rudder appendages reduce the amount of swirl, then it can be surmised that the kinetic energy loss, as well as the drag associated with a low pressure region in the wake, will be reduced. Both of these mechanisms contribute to increased power requirements as the amount of swirl in the downstream wake increases. The kinetic energy loss associated with swirl in the discharge slipstream is discussed in [11] and is represented by the propulsive coefficient or propulsive efficiency. For application with zero swirl in the far wake the propulsion coefficient η_p is:

$$\eta_p = \frac{1}{1 + \frac{1}{2}\frac{\Delta \bar{V}}{V_\infty}} \quad , \tag{6}$$

and for cases with swirl in the far wake the propulsive coefficient is:

$$\eta_p = \frac{1}{1 + \frac{1}{2}\left(\frac{\overline{\Delta V}}{V_\infty}\right)\left[1 + \left(\frac{\overline{V}_\theta}{\overline{\Delta V}}\right)^2\right]} . \tag{7}$$

On the basis of impulse-momentum and actuator disc relations, Reference [11] indicates that:

$$\frac{\overline{V_3}}{\overline{U}} = \frac{\overline{V}_\theta}{\overline{\Delta V}} . \tag{8}$$

The duct geometries typically used in ducted propeller arrangements result in $\overline{V}_3/V_\infty = 1 + \overline{\Delta V}/V_\infty$. Substitution of this quantity and equation (8) into equation (7) gives:

$$\eta_p = \frac{1}{1 + \frac{1}{2}\frac{\overline{\Delta V}}{V_\infty}\left[1 + \left(\frac{V_\infty}{\overline{U}}\right)^2 + 2\left(\frac{\overline{\Delta V}}{\overline{U}}\right)\left(\frac{V_\infty}{\overline{U}}\right) + \left(\frac{\overline{\Delta V}}{V_\infty}\right)^2\right]} . \tag{9}$$

With reference to a given mass flow, the above indicates that for a given change in velocity the propulsive coefficient decreases as shaft speed decreases or advance ratio increases. The reason for this behavior is that more swirl remains in the far wake as the design advance ratio of the propulsor is increased, which thereby results in a higher kinetic energy loss.

The kinetic energy loss is not the only loss to be considered. A region of low pressure, lower than p_∞, exists in the downstream propulsor slipstream if rotation is present and results in added drag that must be overcome by the propulsor. On this basis, more power is required for propulsion than if rotation did not exist. The existence of the added drag due to the presence of rotation in the downstream slipstream is recorded and discussed in [12]. A more detailed discussion shall be presented here to provide a means of estimating the drag increment due to rotation as a function of design advance ratio.

For simplicity in illustrating the origin of the added drag due to slipstream rotation, a propeller operating on the aft of a body of revolution shall be considered as shown in Figure (3). A control volume shall be selected to provide boundaries parallel and perpendicular to the axis of revolution and the viscous forces acting on the external surface of the control volume shall be neglected. The momentum

addition to the fluid by the propulsor shall be assumed to exactly fill the axial momentum deficit of the wake downstream of the propulsor. On this basis there is no difference in axial momentum between stations (1) and (2) and the axial momentum equation associated with the control volume can be written as:

$$p_\infty A_{ab} - \bar{p}_{ab} A_{ab} - D_{BB} + T = 0 \quad . \tag{10}$$

The axial momentum term on the right side of equation (10) is zero since the axial momentum in and out of the control volume are equal under the assumption that the body wake deficit is entirely filled by the action of the propeller. The reaction forces of propeller thrust and bare body drag acting on the fluid of the control volume have the directions shown in Figure (3). Ambient static pressure, p_∞, acts over the entire face of the control volume at station (1); however, this is not the case in the far wake at station (2).

This becomes apparent from the equation of radial equilibrium which expresses the static pressure gradient as:

$$\frac{1}{\rho}\frac{dp}{dr} = \frac{V_\theta^2}{r/\cos_\phi} + \frac{V_m^2}{R_m} \tag{11}$$

where V_θ and V_m represent the components of peripheral and meridional velocity in the far wake and ϕ is the angle between the axisymmetric streamwise direction and the axis of revolution. At station (2) the cosine of ϕ is unity and R_m, the radius of curvature of the axisymmetric streamlines at station (2), is infinite. In this case, equation (11) reduces to:

$$\frac{1}{\rho}\frac{dp}{dr} = \frac{V_\theta^2}{r} \quad . \tag{12}$$

From this relation at station (2), it is apparent that there can be no gradient in static pressure outside the region designated (a-b), which is the slipstream of the flow through the propeller. Outside the region of the propeller slipstream the static pressure is ambient, but inside the slipstream it is less than ambient decreasing as the axis of rotation is approached.

The static pressure $\bar{p}_{ab}$ which represents an average over the region (ab) will be less than p_∞. Utilizing equation (10) the effective net propeller thrust, represented as the sum of the body drag and propeller shaft thrust as shown below, is negative and the body is underpropelled.

$$(T_{prop} - D_{BB}) = - A_{ab}(p_\infty - \bar{p}_{ab}) \quad . \tag{13}$$

As indicated by equation (13), to obtain a self-propelling condition, the propeller shaft thrust must be greater than body drag to compensate for the effects of rotation in the slipstream.

An engineering evaluation of the magnitude of this added drag term due to swirl in the far wake can be obtained by considering Figure (3) and assuming a small hub radius and no meridional curvature of the streamlines at station (2). The nondimensional radial equilibrium equation can be written as:

$$\frac{p(r) - p_\infty}{\rho \frac{V_\infty^2}{2}} = 2 \int_{1.0}^{r/r_T} \left(\frac{V_\theta}{V_\infty}\right)^2 \left(\frac{r_T}{r}\right) d\left(\frac{r}{r_T}\right) \quad . \tag{14}$$

The swirl placed in the flow shall be assumed to have a radial distribution of constant angular momentum (free vortex) which can be expressed as:

$$\frac{V_\theta}{V_\infty} = K \left(\frac{r_T}{r}\right) \quad . \tag{15}$$

Substituting equation (15) into equation (14), the static pressure distribution as a function of radial distance across the slipstream can be obtained as:

$$\frac{p(r) - p_\infty}{\rho \frac{V_\infty^2}{2}} = - K^2 \left[\left(\frac{r_T}{r}\right)^2 - 1.0\right] \quad . \tag{16}$$

The increment of additional drag associated with the reduced pressure in the slipstream can now be obtained by integrating the pressure over the slipstream area

$$\Delta C_D = \frac{\text{Drag}}{\rho \frac{V_\infty^2}{2} \pi r_T^2} = 2 \int_{r/r_T}^{1.0} \frac{(p(r)-p_\infty)}{\rho \frac{V_\infty^2}{2}} \left(\frac{r}{r_T}\right) d\left(\frac{r}{r_T}\right)$$

$$= - 2 K^2 \left\{ \ln \frac{r_T}{r} - \frac{1}{2}\left[1 - \left(\frac{r}{r_T}\right)^2\right]\right\} \quad . \tag{17}$$

The limiting value of (r) shall be set equal to the hub radius and (K) evaluated from either measurements of slipstream rotation similar to those in [1] or evaluated based on the relation given by equation (8) which can be written in terms of the advance ratio as:

$$\overline{V}_\theta/V_\infty = \frac{J}{(0.707)\pi}\left[\frac{\overline{\Delta V}}{V_\infty} + 1.0\right]\frac{\overline{\Delta V}}{V_\infty} \quad . \tag{18}$$

The preceding assumes small values of (r_h/r_T) and that the mean disk diameter is based on the mean area of the disk. It is apparent from equation (18) that $(\overline{V}_\theta/V_\infty)$, or (k), increases directly with advance ratio. Therefore, if $(\Delta V/V_\infty)$ is held constant, then the added drag due to rotation in the slipstream increases as design shaft speed decreases. The presence of the rudder in the slipstream tends to reduce the swirl in the slipstream and thereby reduce the added drag. The power required for propulsion would therefore decrease with the presence of the rudder. This performance has been measured with and without rudders present as reported in [5]. The twin-rudder arrangement reported in [4] indicated significant gains in efficiency by their use. A twin-rudder configuration is undoubtably more effective in reducing slipstream swirl and would explain a good portion of the efficiency gain.

In any event, the use of the rudders as a means to reduce the swirl in the slipstream is an ineffective means of recovering the energy and reducing the added drag component. Flow separation about the rudders certainly occurs and if sufficient gains in efficiency and power reduction can be achieved, the added cost and complexity of a stationary vane system might be justified.

<u>Example</u>

The evaluation of the magnitude of the efficiency and power losses associated with swirl in the slipstream shall be estimated using the velocity measurements of the ducted propeller arrangement reported in [5]. Flow measurements as reported in [5] for ducted propellers are very scarce, and it is therefore suggested that future research and development on ducted propellers would benefit a great deal from similar measurements on other ducted configurations.

The velocity surveys at the duct exit, [5], indicate an average value of $\overline{V}_3/V_\infty$ approaching 2.40, if corrections are included for area change between the measuring station and the plane of the rotor. The indicated advance ratio at which the data was obtained is 0.356. This data results in a value of $\overline{\Delta V}/V_\infty$ of 1.40 and a $\overline{V_\theta}/V_\infty$, evaluated from equation (18), of 0.523. This computed value is in close agreement with a $\overline{V_\theta}/V_\infty$ of 0.500 measured at a nondimensional radius of 0.7 in [5].

The total propulsor thrust coefficient can be computed from equation (5) and results in a C_{T_T} of 6.72. The added drag increment ΔC_D resulting from rotation in the wake was computed by graphical integration of equation (17) using the experimental tangential velocity distribution given in [5]. The resulting ΔC_D was 0.336 which is 5.0 percent of the total propulsor thrust. Using a computed value of $\overline{V_\theta}/V_\infty$ of 0.523 and a inner radius limit of 0.1 in equation (17), a value of ΔC_D of 0.494, or 7.3 percent of the total propulsor thrust is obtained. This is good agreement considering the assumptions made in the development of equation (17). It is also noted that the tangential velocity distribution measured in [5] deviates somewhat from a free vortex, contrary to the assumptions used in deriving equation (17).

The above analysis indicates that the added drag resulting from rotation in the slipstream amounts to between 5-7 percent of total propulsor thrust and that power losses of this same percentage could result. From equation (17), it was previously indicated that these losses are directly proportional to the square of the change in advance ratio.

The kinetic energy loss associated with slipstream rotation is represented by the changes in propulsive coefficient, computed by equations (6) and (7). The propulsive coefficients computed, using a $\overline{\Delta V}/V_\infty = 1.4$ and $\overline{V_\theta}/V_\infty = 0.500$ based on the experimental data of [5], result in $\eta_p = 58.8\%$ assuming zero rotation and $\eta_p = 55.9\%$ including the effects of rotation.

The combined effect of kinetic energy losses and added drag due to slipstream rotation amounts to predicted power losses of between 8-10 percent. It is of significance that these losses would increase substantially with relatively small increases in design advance ratio; however, an increase in design advance may be desirable for reasons of cavitation resistance.

Suggested Ducted Propeller Configurations

The potential gains in efficiency that can be realized by eliminating the rotation in the propulsor slipstream could justify the use of a stationary set of vanes. Two alternatives exist:

(1) A set of vanes could be located upstream of the rotor and place swirl in the flow counter to that placed in by the rotor. The resulting discharge from the duct nozzle would be axial with no rotation.

(2) A set of vanes could be located downstream of the rotor to reduce the swirl to zero before discharge of the slipstream from the duct.

These two configurations are depicted in Figure (4) and would result in a slightly longer duct than commonly used. The wetted frictional drag of the ducted propulsor in [5] amounts to approximately 0.5 percent of total propulsor thrust and therefore small increases in length would result in small losses in power.

The vanes in front of the rotor offer a better configuration for backing and stopping operation of the propulsor and could result in a more uniform inflow to the rotor. This configuration would tend to increase the velocity relative to the rotor blades and decrease cavitation resistance; however, if flow distortions are attenuated by their action, this would tend to improve cavitation resistance. As such, it is possible that little loss in cavitation resistance would occur with the ducted propulsor with vanes upstream of the rotor. Additionally, the elimination of a cavitating hub vortex by either of these arrangements would result in a more effective rudder action and conceivably less vibration.

A potential advantage of these arrangements is the capability of decreasing design shaft speed to provide improved cavitation resistance. This can be achieved without increasing the diameter of the propulsor or increasing the kinetic energy loss or added drag due to rotation in the far wake.

Experimental Evaluation of Ducted Propeller Flow Fields

The importance of a knowledge of velocities and pressure throughout a ducted propeller cannot be overemphasized. Such measurements should include flow surveys at the inlet and exit of the propeller, at the exit of the duct, and at a station approximately one duct diameter downstream of the exit. These measurements can best be conducted with a five-hole probe giving three components of velocity, together with the distributions of total and static pressure. The use of these data in the analysis of ducted propeller performance has been discussed earlier. Care must be exercised in the use of these probes near the duct walls as significant errors can arise from the probe wall interference. This interference can be minimized by proper calibration of the probes near a wall in a known flow. With the advent of the Laser Doppler Velocimeter (LDV) surveys of the velocity field in the absence of probe interference can be conducted. However, the use of a LDV still requires the flow to be probed to obtain the distribution of total pressure. The total pressure can be obtained more easily and accurately with conventional probes than the static pressure. The presence of a probe in a three dimensional rotational flow field will cause a disturbance which results in inaccurate static pressure readings.

A Laser Velocimeter system as shown by Figure (5) has been used in conjunction with the large 48-inch diameter water tunnel at the Applied Research Laboratory at The Pennsylvania State University. This system has been used to obtain the flow field at a number of stations through various propulsor arrangements mounted on axisymmetric bodies.

SUMMARY AND RECOMMENDATIONS

The literature indicates that the powering performance, cavitation and flow field within ducted propellers are strongly effected by the presence of the hull and rudder appendages. On this basis, the value of performance data obtained in the absence of the hull and appendages is limited.

Divergence of the duct aft of the rotor and the intended beneficial results suggested by the use of the diffusion is shown to compensate only for duct blockage caused by real flow effects. Reported results to the contrary, should be accepted with caution until supporting data indicating the details of the flow field inside the duct with varying degrees of divergence are obtained.

The limited amount of data available describing the flow field at the discharge from a ducted propeller has been reviewed and indicates that relatively high jet velocities exist. These jet velocities are far higher than those typical of an open propeller. The tangential swirl present in the slipstream is also relatively high and preliminary analysis indicates that reductions in shaft power of 8-10 percent could be achieved by its elimination.

The recent development of the laser velocimeter offers a convenient means of obtaining the details of the flow field at various stations through the ducted propeller and open propeller. By this means, the propeller and ducted propeller can be studied and data obtained indicating mass flow, slipstream swirl and velocity as a function of propulsor geometry and advance ratio. The combination of these data with force measurements provide a basis to develop improved propulsor configurations for large surface craft.

NOMENCLATURE

$A_{1,2,3,4,5}$	flow area (stations listed on Figures 1, 2, 3, 4)(ft^2,m^2)
C_m	mass flow coefficient
C_{T_T}	total propulsor thrust coefficient
H	fluid head (ft,m)
J	advance ratio = V_∞/nD_3
D_3	rotor or propeller disk diameter (ft,m)
n	shaft speed (rpm)
p	static pressure (psf, pascals)
P	total pressure (psf, pascals)
p_∞	ambient static pressure (psf, pascals)
R_m	change in radius of curvature of streamlines (ft,m)
r	radius from axis of rotation (ft,m)
r_T	tip radius of rotor (ft,m)
η_p	propulsive coefficient
U	wheel velocity (ft/sec, m/sec)
V	velocity (ft/sec, m/sec)
V_∞	forward velocity of ship (ft/sec, m/sec)
V_θ	tangential velocity (ft/sec, m/sec)
V_m	meridional velocity (ft/sec, m/sec)
ΔV	change in velocity (ft/sec, m/sec)

REFERENCES

(1) Andersen, O. and Tani, M., "Experience with the S. S. 'Golar Nichu'" Royal Institute of Naval Architects (RINA), Proceedings of Symposium on Ducted Propellers, London, 1973.

(2) Minsaas, K., Jacobsen, G. M., and Okamoto, H., "The Design of Large Ducted Propellers for Optimum Efficiency and Maneuverability," RINA, Proceedings of Symposium on Ducted Propellers, London, 1973.

(3) English, J. W., "Report of Propeller Committee," Appendix 2, 14th International Towing Tank Conference, 1975.

(4) Gibson, I. S. and Van Gunsteren, "Optimization of Nozzle - Propeller - Rudder for High Powered Large Ships," Symposium on High Powered Propulsion of Large Ships," Wageningen, December 1974.

(5) English, J. W., Rowe, S. J., "Some Aspects of Ducted Propeller Propulsion," Paper No. 3, p. 20, RINA Symposium on Ducted Propellers, London, 1973.

(6) Narita, H., Kunitake, Y., and Yagi, H., "Correlation Results of Model and Full Scale Ducted Propeller Observations," NSMB Symposium on High Powered Propulsion of Large Ships, December 1974.

(7) Okamoto, H., Okada, K., Saito, Y. and Masai, K., "Full Scale Cavitation Observations on Tankers Fitted with Ducted Propellers," NSMB Symposium on High Powered Propulsion of Large Ships, December 1974.

(8) Longhouse, R. E. and Loth, J. L., "Experimental Investigation of an External Aerodynamic Diffuser," Aerospace Engineering TR-29, West Virginia University, Department of Aerospace Engineering, Morgantown, West Virginia, USA.

(9) Morel, M. P. and Lissaman, P. B. S., "The Jet Flap Diffuser: A New Thrust Augmenting Device," AIAA Paper No. 69-77, July 1969.

(10) McDonald, A. T., Fox, R. W. and van Dowoestine, R. V., "Effects of Swirling Inlet Flow on Pressure Recovery in Conical Diffusers," AIAA Paper No. 71-84, January 1971.

(11) Wislicenus, G. F., Fluid Mechanics of Turbomachinery, Volumes 1 and 2, Dover Publications, Inc., (New York), 1965.

(12) Van Lammeran, W. P. A., Troost, L., Koning, J. C., Resistance, Propulsion and Steering of Ships, Volume II, The Technical Publishing Company, H. Stam-Haarlem-Holland, 1948.

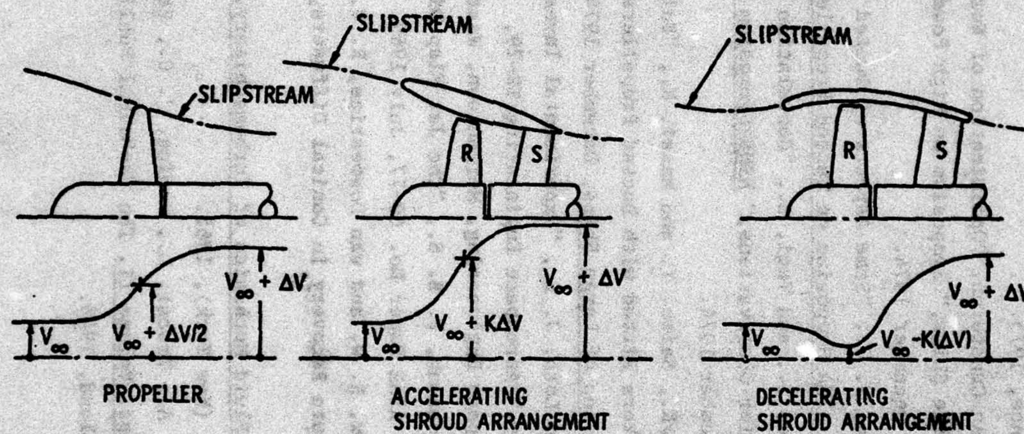

Figure 1 - Different Propulsor Slipstreams

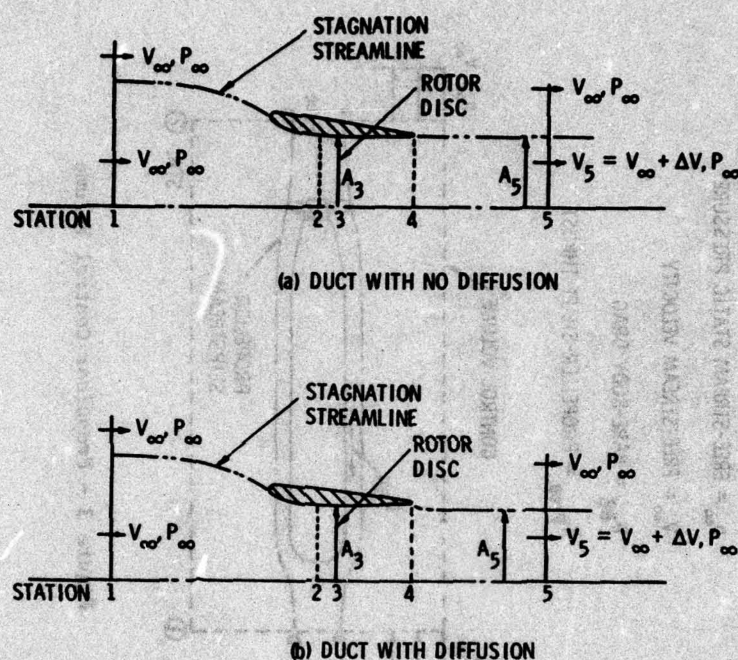

Figure 2 - Ducted Propeller with and without Duct Diffusion

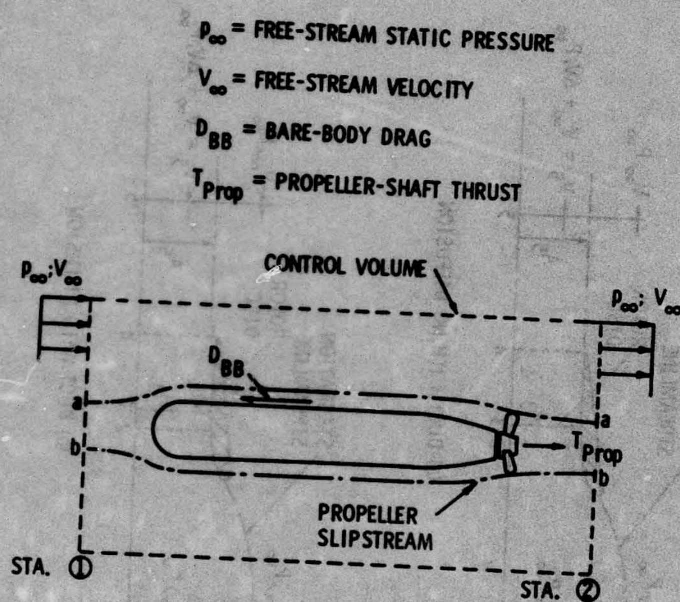

Figure 3 - Propulsor Control Volume

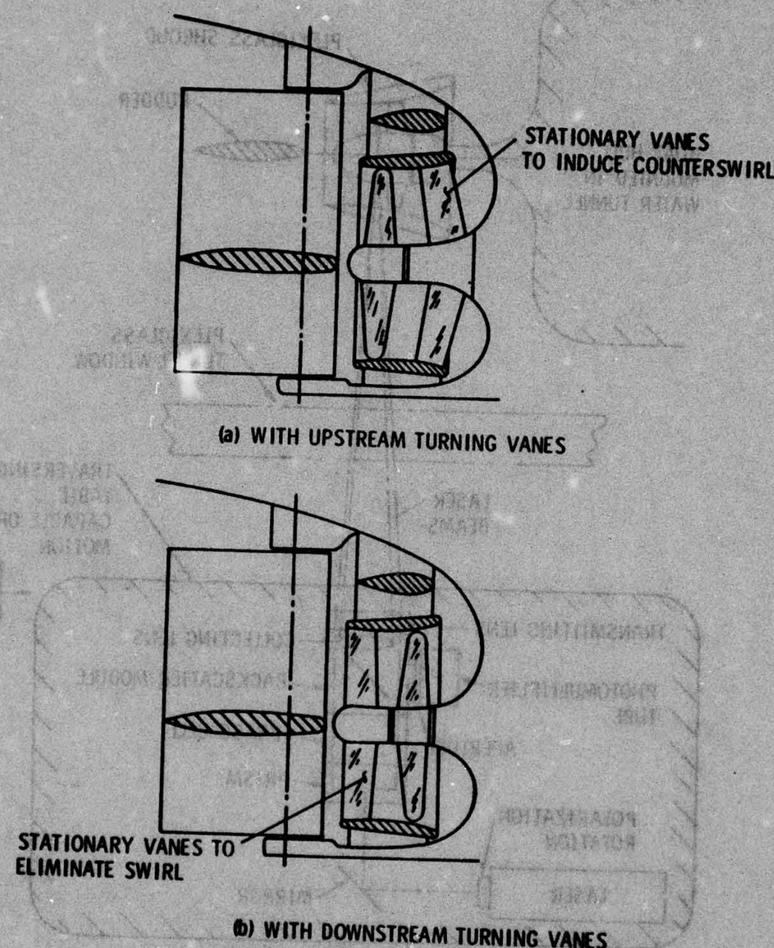

Figure 4 - Possible Ducted Propeller Configurations

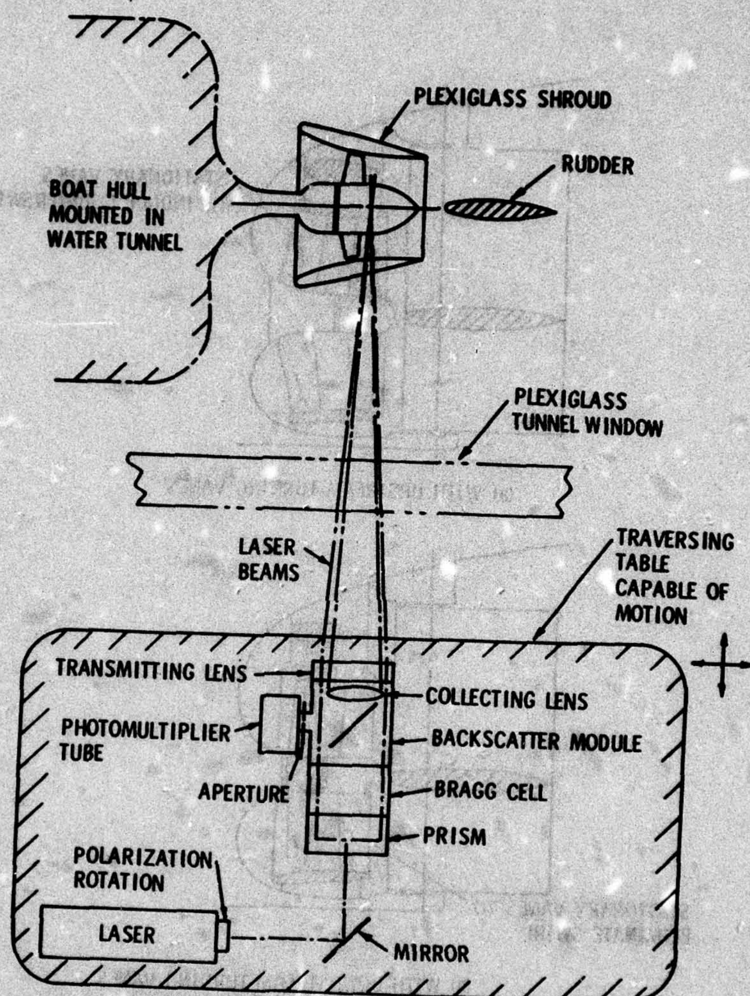

Figure 5 - Schematic of Laser Doppler Velocimeter Setup

PARTIALLY SUBMERGED AND SUPERCAVITATING PROPELLER SYSTEMS

by

J. O. Scherer
HYDRONAUTICS, Incorporated

INTRODUCTION

Scaling problems for ventilated propellers have been dealt with in previous reports (References 1, 14 and 25) and summarized in the ATTC report of 1974 (Reference 24). This paper will not repeat these discussions, but rather will deal with one special scaling problem for which some information has been developed as a consequence of tests performed on a series of partially submerged supercavitating propellers in the past few years. (Reference 1).

The problem is that of determining propeller thrust at bollard and near bollard conditions (i.e., low advance ratio). This is of particular concern with regard to surface effect ships which must be able to accelerate through a low speed "hump" in their resistance curve.

Historically high speed propeller testing has been conducted in variable pressure water tunnels without a free surface. Bollard tests cannot normally be conducted in such a facility for a variety of reasons, the most important being that the running propeller will drive water around the tunnel loop and thus prevent equilibrium conditions from being attained.

However, in the past, bollard data has been of little interest as planing boats and hydrofoils have no difficulty obtaining adequate low speed thrust. It is the SES, with its low speed resistance hump combined with the poor low speed performance of ventilated propellers that has recently focused attention on this region of a propeller performance curve.

NATURE OF SCALING PROBLEM

In the following discussion, the term "supercavitating" will be used to describe the general operating conditions of a propeller in which a cavity is shed from the leading edge, covers the entire chord of the blade section, and collapses downstream of the trailing edge of the blade. Under such conditions, the low-pressure back of each blade is limited in its thrust producing capability to levels determined by its projected

area and the cavity pressure, while the thrust produced by the high pressure face is controlled by hydrodynamics. Previously, designers and experimenters have "corrected" propeller performance predictions for differences in cavity pressure by assuming that the blade performance would be changed in a manner similar to that of an isolated foil and that the propeller inflow conditions would not be significantly altered. Recent studies (Reference 1) have shown that this is not a good assumption at low advance ratios and that, under some operating conditions, the cavity pressure becomes the dominant parameter in controlling the inflow and thus the propeller performance. Under these conditions, the correct scaling of cavity pressure in water tunnel or towing basin tests becomes vital if these data are to represent full scale performance - date cannot be "corrected" to reflect differences between model and full scale cavitation numbers.

Under normal operating conditions, the minimum cavity pressure which can exist is about equal to vapor pressure. However, the cavity pressure will generally be higher than this value due to the inclusion of air or other gas into the blade cavities. Such air may come from entrained bubbles or may occur through the diffusion of disolved gas from the surrounding water; it may be ingested from the free surface or from other nearby cavities shed by struts, rudders, or underwater engine exhaust; or it may be purposefully injected into the cavities to "ventilate" them.

Cavity pressure is expressed nondimensionally as the "cavity cavitation number", σ_c:

$$\sigma_c = \frac{P_{static} - P_{cav}}{\frac{1}{2}\rho\, V^2} \qquad [1]$$

The reference velocity "V" is either the advance velocity of the propeller through the surrounding water V_a or the mean relative velocity seen by a blade section V_m, depending on the phenomenon being described (see Figure 1). Note that σ_c is maximum when the static pressure is vapor pressure and is then equal to the vapor cavitation number of the flow σ_v:

$$\sigma_v = \frac{P_{static} - P_{vapor}}{\frac{1}{2}\rho\, V^2} \qquad [2]$$

Note also that there is a relationship between σ_c and Froude number in that the static pressure is a function of depth. In the case of a naturally ventilated propeller with atmospheric pressure in the cavities:

$$P_{static} = P_{atm} + P_{depth} \qquad [3]$$

$$P_{cav} = P_{atm} \qquad [4]$$

$$\sigma_c = \frac{P_{depth}}{\frac{1}{2}\rho\, V^2} = \frac{2\,g\,h}{V^2} = \frac{2}{Fr^2} \qquad [5]$$

The implication of Equation 5 is that, for a naturally ventilated propeller, the cavitation number will never be zero. It will be seen this is of great importance for partially submerged propellers at low advance ratios or near bollard operation.

In general the cavity will not be at atmospheric pressure, even for a ventilated propeller, but will have higher than atmospheric pressure owing to pressure losses of air flowing into the cavities.

NEAR BOLLARD PERFORMANCE

Figures 2 and 3 taken from date of References 7 and 1, are typical curves of propeller performance showing thrust coefficient (K_T) and efficiency (η) as a function of advance ratio (J). These figures are for a partially submerged propeller operating with naturally ventilated cavities. Five operating regimes are shown on Figure 2 which indicate the dominate feature of the flow governing performance in each regime. Of concern here is the region of lowest advance ratios indicated as "Thrust Dominated by Blade σ_c".

The flow in this region is characterized by blade cavities so large that they impinge on the following blade or, in some cases, actually engulf the following blade. The appearance of the flow behind the propeller changes from one of discrete helical cavities to one of an unstructured "muff" of cavities as the advance ratio is reduced to near bollard conditions.

Figure 3 shows performance for a large range in pitch angle settings from 5 degrees above design pitch (D+5) to 15 degrees below design pitch (D-15). Note that, although reduced pitch results in improved low advance ratio efficiency, it has almost no effect on K_T at the lowest advance ratios for which data was obtained in this experiment. In fact, systematic model tests have shown that propeller geometry has almost no impact on achievable K_T values at and near bollard operation, although geometry does influence efficiency. This includes such gross parameters as blade profile, section shape, blade area, design and/or operating pitch, and even the number of blades. The only parameters which seem to be able to change the thrust capability in this regime are cavity pressure and RPM. Nondimensionally, these combine into one parameter at bollard, and that is σ_c based on the mean relative velocity of a blade section V_m. This influence can be seen on Figure 2 where, at very low values of "J" there are two sets of data shown for K_T. The upper set was obtained at constant RPM with decreasing advance velocity, the lower set was obtained with constant advance velocity and increasing RPM as zero J (bollard) was approached. This latter set resulted in much lower values of σ_c (based on V_m) and thus lower values of K_T at bollard. At higher advance ratios, the two sets of data merge together and this effect is lost. This dependence of K_T on cavity pressure is further illustrated in Figure 4, from Reference 25, for the case of zero advance velocity and varying depths of submergence. Here again, an increase in σ_c, either through a drop in cavity pressure or by a reduction in blade velocity, results in an increase in K_T.

It should be recognized that if the cavity pressure were actually equal to the static pressure of the surrounding fluid, there could be no pressure gradiant ahead of the propeller to accelerate the flow. Then, at zero advance speed, there would be no flow through the propeller disk. Fortunately, as has been explained, the cavity pressure is always slightly less than the fluid pressure, even for a partially submerged propeller, because of the increase in pressure with depth. That is, the Froude number, and thus the cavitation number can never be exactly zero over the entire propeller disk (Equation 5).

The level of thrust generated at bollard and near bollard conditions is thus very sensitive to cavitation number and this parameter <u>must</u> be scaled if test data are to be meaningful for these conditions. Altmann (Reference 25) states that:

> "Unless both full scale and model scale ratios of static cavity pressure to dynamic streamline pressure (which are characterized by σ_c) are matched exactly, neither the inflow, section performance, cascade effect, or outflow of the propeller model will be correct. Without exaggeration it may be stated that blade section shape might just as well not be "scaled" if σ_c is not also correct. The plight of the propeller designer is serious; with the exception of air-filled semi-submerged propellers, the static pressure in cavities of full scale propellers is not known and, in fact, has not ever been measured".

Froude scaling may not be adequate to insure correct cavitation number matching even for ventilated propellers. Froude scaled, low advance ratio tests on the SES 100B propeller indicated that the propeller would be marginal in its ability to produce adequate thrust at "hump" speed. Yet the prototype accelerates through hump speed without difficulty. Thus other parameters may have effects on low advance ratio performance in that they indirectly affect cavity pressure. These would include dissolved and undesolved air content, Reynolds number, Weber number (when spray is present), and the ratio of air density to water density (ADR) in a depressurized test facility. In the case of the SES 100B, it is believed that the full scale propeller does not ventilate as readily as the model did, and therefore operates with higher cavity cavitation number, and thus produces more thrust than predicted by the model tests.

CONCLUSION

It is clear that, under conditions where it is important to obtain accurate performance estimates of a supercavitating propeller at or near bollard conditions, the cavity cavitation number must be scaled. In order to insure that this scaling is accomplished it will be necessary to measure the cavity pressure for both model and prototype propellers under operating conditions. It is not adequate to assume that the cavity pressure will be atmospheric for a ventilated propeller or vapor pressure for a fully

submerged propeller as there are many parameters which influence the cavity pressure.

REFERENCES

1. Bohn, J., and Altmann, R., "Analysis of Supercavitating Propeller Model Test Data", HYDRONAUTICS, Incorporated Technical Report 7307-3, April 1975.
2. Auslaender, J., "The Linearized Theory of Supercavitating Hydrofoils Operating at High Speeds Near a Free Surface", HYDRONAUTICS, Incorporated Technical Report 001-5, June 1961.
3. Auslaender, J., "Low Drag Supercavitating Hydrofoil Sections", HYDRONAUTICS, Incorporated Technical Report 001-7, April 1962.
4. Hsu, C.C., "Some Remarks on the Progress of Cavity Flow Studies", Paper Presented at the ASME Fluids Engineering Conference, Minneapolis, May 1975.
5. Scherer, J.O., Bohn, J., and Altmann, R., "The Design of Supercavitating Propellers", HYDRONAUTICS, Incorporated Technical Report 7307-6, August 1976.
6. Bohn, J., and Altmann, R., "Two Supercavitating Propeller Designs for Hydrofoil Ships", HYDRONAUTICS, Incorporated Technical Report 7607.01-1, May 1976.
7. Hecker, R., and Altmann, R., "High Performance Marine Propellers - An Overview", Paper Presented at the Winter Annual ASME Meeting, Marine Propulsion Section, New York, December 1976.
8. Barr, R., "Supercavitating and Superventilated Propellers", Transactions of the Society of Naval Architects and Marine Engineers, Volume 78, 1970.
9. Tulin, M., "Supercavitating Propellers - Momentum Theory", HYDRONAUTICS, Incorporated Technical Report 121-4, September 1964.
10. Staff Report, "Model Tests of Supercavitating Propellers for Surface Effect Ships", HYDRONAUTICS, Incorporated Technical Report 7307-2, May 1974.
11. Hecker, R., Peck, J., and McDonald, N., "Experimental Performance of TMB Supercavitating Propellers", David Taylor Model Basin Report 1432, January 1964.
12. Newton, R., and Rader, H., "Performance Data of Propellers for High Speed Craft", Paper Presented at R.I.N.A. Annual Meeting, London, 1960.
13. Barr, R., "Selection and Design of a Partially Submerged Propeller System for a 100 Ton SES", HYDRONAUTICS, Incorporated Technical Report 7016-1, January 1970.
14. Hecker, R., and Morgan, W., "Scale Effect Studies on Partially Submerged Propeller 4281", NSRDC Report 249-H-06, December 1968.
15. Mercier, J., "Optimum Propellers with Finite Hubs", HYDRONAUTICS, Incorporated Technical Report 127-1, June 1962.
16. Etter, R., and Hsu, C.C., "An Investigation of Tandem Row High Head Pump Inducers", HYDRONAUTICS, Incorporated Technical Report 703-8, February 1970.
17. Yim, B., "Investigation of Gravity and Ventilation Effects in Water Entry of Thin Foils", Paper Presented at IUTSM Symposium, Leningrad, USSR, June 1971.
18. Yim, B., "Linear Theory on Water Entry and Exit Problems of a Ventilating Thin Wedge", Journal of Ship Research, Volume 18, Number 1, March 1974.

AD-A062 506 NAVAL ACADEMY ANNAPOLIS MD F/G 5/11

PROCEEDINGS OF THE GENERAL MEETING (18TH) OF THE AMERICAN TOWIN--ETC(U)

1977 B JOHNSON, B NEHRLING

UNCLASSIFIED NL

3 OF 4

AD A062506

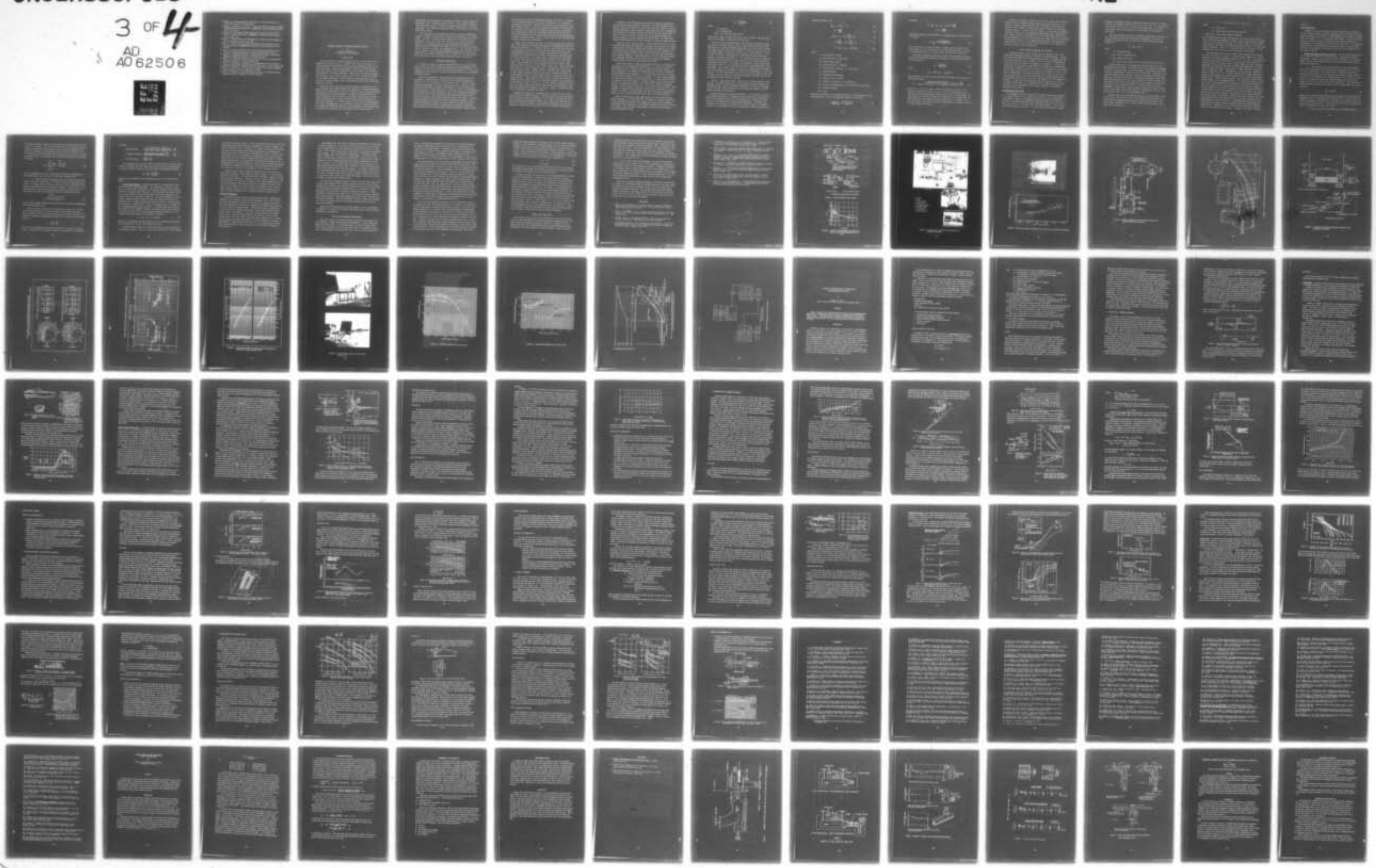

19. Wang, D.P., "A Linearized Theory of Water Entry of a Fully Ventilated Foil", In Publication, Journal of Fluid Mechanics.

20. Altmann, R., Schaefer, K., and Bohn, J., "Non-Steady Performance Features of Semi-Submerged Supercavitating Propellers", HYDRONAUTICS, Incorporated Technical Report 7307-5, August 1975.

21. Altmann, R., "Non-Steady Performance Measurements on Model Supercavitating Propellers for Surface Effect Ships", HYDRONAUTICS, Incorporated Technical Report 7307-4, December 1974.

22. Dobay, G., "Unsteady Blade Force Measurements on a Skewed Partially-Submerged Propeller", NSRDC Report 392-H-01, June 1970.

23. Barr, R., "Design Studies for SES Supercavitating Propeller Systems; Volume II - Measured Performance", HYDRONAUTICS, Incorporated Technical Report 816-1 (II), May 1969.

24. Shen, Y.T., "General Scaling Problems on Fully Cavitating and Ventilated Flows", 17th American Towing Tank Conference Cavitation Committee Report, June 1974.

25. Altmann, R., "Performance Features of Supercavitating Propellers", Draft Report submitted to SNAME for Presentation at 1977 Annual Meeting.

26. Shields, C.E., "Open-Water Performance Characteristics of Several Semi-Submerged Propellers", NSRDC Report 193-H-01, December 1966.

27. Crown, D., and Hecker, R., "The Effect of Blade Thickness on the Performance of a Supercavitating Partially-Submerged Propeller", NSRDC Report 249-H-04, November 1968.

28. Crown, D., and Hecker, R., "Inclined Shaft Performance of Two Partially-Submerged Propellers Behind a Test Boat", NSRDC Report 249-H-14.

29. Crown, D. and Hecker, R., "The Steady-State Performance of Two Skewed Partially-Submerged Propellers", NSRDC Report 249-H-08, June 1969.

WATERJET PROPULSION SYSTEM PERFORMANCE ANALYSIS

by

E. R. Miller, Jr.
HYDRONAUTICS, Incorporated

INTRODUCTION

Waterjet propulsion systems continue to find limited applications in commercial and naval vessels. In general the overall efficiency of a waterjet propulsion system will be lower than a propeller system for the same application. Thus waterjet propulsion systems find applications when other factors such as transmissions, draft limits, etc. outweigh considerations of overall efficiency. Some recent and proposed waterjet applications to naval vessels include the SES 100A, the PHM, the 3KSES and the OSPREY conversion. Recent commercial applications include the Jetfoils, a class of ferries for San Francisco Bay and a high speed planning hull crew boat.

Relative to more conventional marine propulsion systems, waterjet systems present some unique problems with respect to performance analysis. This is particularly true in the area of model and full scale experimental determination of system performance. A complete self-propelled model test, analogous to such tests for a conventional propeller driven ship, cannot be conducted due to scale effect problems with the pump and internal flow passages. As a result, both for theoretical and experimental evaluation of performance, it is convenient to divide a waterjet propulsion system into different elements. The performance of each element can be determined and based on their performance; the overall system

performance can be determined. The typical elements include propulsion appendages, inlet, diffuser, pump and nozzle. This approach requires a valid theoretical model of overall system performance based on element performance and a rigorous accounting system to keep track of all of the interaction effects.

The literature on the design and analysis of waterjet propulsion systems is extensive and the basic concepts and theories are well understood. Reference 1 presents a good overview and an extensive list of references. Thus, this report will concentrate on the more limited aspects of the techniques used for the experimental determination of waterjet system performance, both model and full scale, and the analysis used to interpret and apply the experimental data. The following sections of this report provide additional background information, describe the techniques and equipment typically used for model and full scale experiments and discuss the interpretation and application of the data.

BACKGROUND INFORMATION

In order to provide a clearer understanding of the role of experiments in the evaluation of waterjet propulsion system performance, it is useful to briefly review some of the problems associated with each of the elements in the system and to review the equations which describe overall system performance.

Propulsion Appendages: Waterjet propulsion appendages are those structures or modifications to the basic craft geometry necessary or desirable for the installation of the waterjet inlet. The most common propulsion appendages include the strut and pod for a strut-pod inlet or the fairing necessary to provide a horizontal surface for the installation of a flush or a semi-flush inlet. Strut-pod inlets are most commonly used on hydrofoil vessels although the SES 100A was originally equipped with such an inlet. The strut and pod have significant drag and may affect the stability and control characteristics of the vessel. At high speeds cavitation on the strut and pod are potential problems. Theoretical and empirical methods are used to design the strut and pod but model testing has been found to be necessary to determine cavitation characteristics and to obtain reliable drag predictions. Flush or semi-

flush inlets are used on planing boats and SES. The hull of a planing boat is normally suitable for an inlet installation so no propulsion appendages are required. For SES, which usually have significant side-hull deadrise angles, a fairing is required to provide a horizontal surface which will not ventilate at significant yaw or cross flow angles. The theoretical and empirical information available for the design of flush inlet fairings is very limited and as a result considerable reliance is placed on model testing. This is particularly true for the prediction of inlet ventilation and broaching.

Inlet: Both strut-pod and flush or semi-flush type inlets have been used. Each type has significant advantages and disadvantages which are outlined in Reference 1. In general, flush or semi-flush inlets are used on craft which have hulls in contact with the surface because of their lower appendage drag. The inlet design is governed by the inflow requirements as a function of craft speed. Many waterjet propelled craft have high drag at both a low speed (hump or takeoff) and at top speed. As a result, the system flow rate is about the same over a wide speed range. This requires the inlet to operate over a wide range of inlet velocity ratios (IVR's) or to have variable inlet area. Low and moderate speed craft, for which cavitation is not a problem, have fixed area inlets which operate over a range of IVR's. Operation over a wide range of IVR's implies large variations in the inlet lip angle of attack, and at high speed a large lip leading edge radius is required for cavitation free operations. This large lip radius results in high inlet drag and creates a venturi effect within the inlet which requires a low design IVR at high speed to avoid cavitation. A low IVR further increases the inlet drag. For these reasons many recent high speed waterjet propelled craft have been equipped with variable area inlets. Figure 1 illustrates some of the concepts for variable area inlets.

Design methodologies are reasonably well developed for both strut-pod and flush or semi-flush inlets. Strut-pod inlets for very high speeds cause the most problems. References 2 to 7 provide representative examples of the design methodologies now in use. Model tests were used extensively in the development of these design methodologies and are still required to confirm inlet drag predictions and cavitation performance.

Diffusers: The diffuser-ducting design is largely determined by inlet and pump imposed boundary conditions. The basic geometry of the diffuser system is determined by inlet location, area, aspect ratio and variable area factor; pump location, flange geometry, total discharge and flow coefficient, diffusion schedule selection, and splitting requirements. In strut-pod inlets the diffuser design and performance are closely related to external geometry and system drag. For flush inlet system diffuser geometry has little influence on external shape and drag.

Strut-pod inlets usually ingest a very uniform flow and as a result available theoretical and empirical procedures can be used for the cruise speed condition to design diffuser and turning vane geometry and to make the complex design tradeoffs which result from the need to balance internal losses against external drag. Model tests have been performed on final diffuser designs for strut-pod inlets to develop variable geometry for off-design conditions and to confirm the cavitation performance, energy recovery and flow distribution into the pump.

Flush inlets ingest a highly non-uniform flow due to the hull boundary layer and flow turning and prediffusion. As a result of velocity nonuniformities, the diffuser typically operates partially stalled. In many applications the diffuser is complicated by the need to transition from rectangular inlet geometry to a circular pump inlet and or to split the flow from one inlet to more than one pump. Data and design procedures for flush inlet diffusers are very limited and as a result model testing is essential in the development of diffuser geometry and performance prediction. A substantial amount of the flush inlet diffuser development testing to date has been carried out in wind tunnel type facilities. Flow channels are used when the potential occurrence of cavitation is a major concern. In either case measurements are made of pressure distributions, energy recovery, effectiveness and outlet flow velocity distribution.

Pumps: A wide range of pump types have been used in waterjet propulsion systems. It is desirable that the pumps in a waterjet propulsion system have high efficiency, light weight and operate without damage or significant thrust breakdown at the minimum operating Net Positive Suction Head (NPSH). Pump cavitation performance is usually characterized by suction specific speed N_{ss}

$$N_{ss} = \frac{N\sqrt{Q}}{(NPSH)^{3/4}} \quad (1)$$

where

N = Pump RPM

Q = Discharge GPM

NPSH = Net Positive Suction Head

The greatest danger of pump cavitation occurs at hump or takeoff speeds when the discharge is high and the NPSH is low.

Waterjet propulsion pumps based on conventional commercial design can operate cavitation free at values of N_{ss} between 8,000 and 12,000. Manufacturers of high performance pumps, which are derivatives of rocket fuel pumps and which may include inducers, claim that operation free of cavitation damage is possible at values of N_{ss} of about 25,000. A discussion of the many considerations in pump selection and preliminary design is presented in Reference 8. As a practical matter, for high performance waterjet propulsion system, there are only a limited number of pump designs available. These pumps have undergone a long evolutionary development based on the technology developed for high performance rocket fuel pumps. The critical issues faced by the propulsion system designer, from the standpoint of experimental validation of performance, include the prediction of cavitation damage from tests of sub scale pumps and the need to assure that the cavitation and pump performance are valid for the actual inflow velocity condition expected.

Nozzles: Fixed area nozzles, which have very high efficiencies (98 percent), are almost always used. Such nozzles are often integral with the pump casing. Nozzle calibration experiments for head vs. discharge and jet area are often conducted since such data are needed in overall system performance determination.

Thrust Available and Overall Efficiency: In the analysis of waterjet propulsion systems it is typical to use the bare hull resistance or EHP as the reference condition for determining the required net thrust available and defining the overall system efficiency. Following this convention and ignoring the presence of a boundary layer and assuming a horizontal jet discharge, the basic relationships required to define the

system performance are:

$$T_{gross} = \rho Q(V_j - U_o) \tag{2}$$

$$hp = \frac{\rho g Q H}{\eta_p \eta_t} \tag{3}$$

$$NPSH = h_o + (1-k)\frac{U_o^2}{2g} - \Delta h \tag{4}$$

$$H = \frac{V_j^2}{2g\eta_n} - (1-k)\frac{U_o^2}{2g} + \Delta h \tag{5}$$

$$Q = V_j A_j = V_i A_i = (IVR) U_o A_i \tag{6}$$

where

ρ = mass density of water

V_j = jet velocity, A_j = jet area

U_o = craft forward speed

g = acceleration due to gravity

V_i = average inlet velocity, A_i = inlet area

η_p = pump efficiency

η_t = transmission efficiency

h_o = ambient static pressure

k = diffuser or internal loss coefficient

Δh = elevation change between nozzle exit and water surface

η_n = nozzle efficiency

$IVR = V_i/U_o$

With minor variations in the characterization of system losses, the following approach is used in formulating propulsive efficiency.

$$\eta = \frac{T_{gross} U_o}{550 \times hp} = \frac{(V_j - U_o) U_o \eta_p \eta_t}{gH} \tag{7}$$

defining:

$$\bar{\eta} = \frac{\eta}{\eta_p}, \quad \eta_n = \eta_t = 1.0, \quad H^* = \frac{2gH}{U_o^2}$$

$$K = k + \frac{2g\Delta h}{U_o^2}$$

and substituting the relationship for V_j from equation (5) into equation (7) yields:

$$\bar{\eta} = \frac{\eta}{\eta_p} = \frac{2[\sqrt{1-K+H^*}-1]}{H^*} \tag{8}$$

This relationship, plotted in Figure 2, reveals that propulsive efficiency depends on the system loss and on the pump head, there existing an optimum pump head (jet velocity ratio) for each loss coefficient.

An overall propulsive coefficient based on net propulsor thrust is a better criterion than propulsive efficiency. Defining overall propulsive coefficient as

$$\text{opc} = \frac{T_{net} U_o}{550 \times hp} \tag{9}$$

where

$$T_{net} = \rho Q(V_j - V_m) - C_{D_i} A_i \tfrac{1}{2}\rho U_o^2 \tag{10}$$

and accounting for nozzle and transmission efficiency and the presence of the boundary layer:

$$\text{opc} = (\eta_p \eta_t) \times \frac{2[\sqrt{[V^*/U_o)^2 (1-K) + H^*]}\,\eta_n - (V_m/U_o)] - \frac{C_{D_i}}{IVR}}{H^*} \tag{11}$$

where V^* and V_m are the energy velocity and momentum velocity of the ingested boundary-layer flow, and C_{D_i} is the drag coefficient of the inlet and associated appendages, based on inlet area and ship speed. In this definition of overall propulsive coefficient it is assumed that the added drag due to the weight of water in the system is included in the bare hull drag. Care should be used in making system tradeoffs to account for these interaction effects.

Equation 11 provides a summary of the various factors which must be known in order to predict waterjet propulsion system performance. In addition to pump, transmission and nozzle efficiency, which should be available from component suppliers, the system designer must determine internal losses, K, external and inlet drag, C_{D_i}, and energy and momentum velocity, V* and V_m, of the ingested boundary layer flow. Experiments play a major role in the determination of this information as well as in the determination of cavitation performance and pump inlet flow conditions. The remaining sections of this paper describe typical experimental procedures which are used to measure these parameters and the analysis required to interpret these experiments.

MODEL TESTING PROCEDURES AND ANALYSIS

As indicated above, model testing plays an important role in the design and performance analysis of waterjet propulsion systems. In addition to the determination of pump performance, which is usually done by the pump manufacturer, model testing is used to determine appendage and inlet drag, inlet performance and diffuser performance. In the United States, most of the recent testing has been carried out by HYDRONAUTICS, Incorporated, DTNSRDC, California Institute of Technology and Rohr Marine. The discussion which follows in this section is presented in terms of the type of information to be developed rather than in terms of test facilities or model types. The three basic types of information needed are (1) Appendage and Inlet Drag, (2) Inlet Performance and (3) Diffuser Performance. In many cases the same model and test facility are used to determine all of these. It is assumed that the pump performance will be developed by the pump manufacturer so pump testing is not discussed further in this section.

Appendage and Inlet Drag

The appendage and inlet drag may be determined from tests conducted in a towing tank, in a free surface flow channel or in a closed throat water tunnel. There are limitations imposed by tests in each type of facility. In towing tank experiments appendage models tend to be small and thus subject to scale effects due to Reynolds number. Also, cavitation numbers cannot be scaled. In a free surface flow channel or water

tunnel the appendage models are larger and cavitation number is scaled. However, the complete external flow field of the craft is not represented and this may, in some cases, influence appendage drag. In a closed throat water tunnel the effects of a free surface on drag cannot be determined.

The usual procedure has been to determine appendage drag by tests of bare hull model and the model fitted with appendages. The inlet is blocked off and faired over and there is no flow through the system. Therefore:

$$D_A = D_{AH} - D_{BH} - K \tag{12}$$

where

D_A = appendage drag

D_{AH} = drag of appended hull

D_{BH} = drag of bare hull

K = calculated friction drag on the fairing over the inlet

In this definition the appendage drag includes drag due to the appendages and also changes in vehicle drag due to effects the appendage may have on lift and trim. This is usually not significant on the SES but may be significant on a hydrofoil or planing boat. Therefore, it is important that the tests include a range of trim angles and drafts and that D_A be determined on the basis of expected prototype trim and draft rather than constant model LCG, seal deflection, trim tab setting, etc. This type of test loses its meaning if the flow through the inlet can be expected to have a significant effect on the flow field around the appendages. A high speed, cavity running strut-pod inlet would be such a case. The drag of a strut-pod, which is independent of the hull, can be determined from a test of the appendage alone.

The inlet drag is the external drag which can be attributed to the inlet itself. The inlet drag tests are conducted with the inlet uncovered and the appropriate ramp and lip combination installed. The inlet drag is determined over a range of inlet velocity ratios. The inlet drag is defined by

$$D_i = D_m + \rho Q(V_j - V_m) - (D_{AH} - K) \tag{13}$$

where

D_i = inert drag

D_m = drag measured with the drag balance

$\rho Q(V_j - V_m)$ = thrust minus ingested momentum

By this definition the inlet drag includes the drag on the external surface of the lip and sideplates, if any, as well as any effects the inlet flow has on the overall craft drag. For an SES, where the inlet flow could cause an unwetting of the sidehull behind the inlet, the inlet drag could be negative. Again, it is important that D_i in equation (13) be determined on the basis of expected prototype trim and draft.

The experiments necessary to measure inlet drag with flow through the inlet are about on the order of magnitude more complex than the experiments to determine appendage drag with no inlet flow. The complexity results from the need to determine Q, V_j and U_m and the likely need to include a pump on the model to get a large enough Q to reach high IVR's. Experiments of this type have been carried out by DTNSRDC in a towing tank with large SES models (1/20 scale for 3KSES) and with a large (1/3 scale) planing hull model. HYDRONAUTICS, Incorporated has conducted a number of these tests in its variable pressure free surface High Speed Channel (HSC) using partial length sidehull models for SES and partial planing hulls. Figure 3 shows a typical test setup for a flush inlet on an SES sidehull in the HYDRONAUTICS HSC. An interesting feature of this test setup is the variable area "thrustless" nozzle shown in Figure 4. This device operates on the principle that if the flow is internally turned 90 degrees to the axial direction and ejected radially there will be zero thrust in the axial direction and the radial forces will cancel. With the flow emitting equally in all directions, the axial components at any yaw or pitch also cancel. Typical test results from an inlet drag test, performed on an SES flush type inlet, using the equipment illustrated above are shown in Figure 5. Substantial data scatter must be expected since the inlet drag is determined from small differences of large numbers. DTNSRDC has also conducted similar tests on strut-pod inlets in their 36-inch water tunnel. A typical test setup is shown in

Figure 6.

Inlet Performance

Measures of inlet performance include energy velocity, energy recovery, velocity profile, pressure distribution and cavitation inception. Inlet performance, as measured by these parameters, is usually determined from water tunnel tests at scaled cavitation number. The Cal Tech water tunnel, the 36-inch tunnel at DTNSRDC and the High Speed Channel at HYDRONAUTICS, Incorporated have been used for these tests. The following description of the measurement and analysis procedures used by HYDRONAUTICS, Incorporated for an SES type flush inlet are representative of the state of the art.

Energy Velocity and Recovery Profiles - Data are taken using pitot-static rakes in series with a scani-valve and differential pressure transudcers. The data are measured at three locations, i.e., boundary layer survey at ramp tangency point, inlet survey and circular outlet survey (see Figure 7).

1. The boundary layer survey located at the ramp tangency point uses three pitot-static probes spaced traversely at 0.3, 0.5 and 0.7 of the inlet width. The survey rake is transversed vertically through the flow field and data taken at the locations shown in Figure 7. Due to the non-uniformity of the boundary layer in the transverse plane caused by the fairing shape, the root mean square of the three data points per level is used for data reduction purposes. Thus, producing a single value for each vertical position which is then curve fit to the equation:

$$\frac{U}{U_o} = (y/\delta)^{1/n} \qquad (14)$$

where y is the vertical distance below the baseline, n the distribution parameter, and δ the boundary layer thickness which is used in the data reduction program to calculate the total head in the boundary layer (h_o) at each inlet velocity ratio. This total head is used as a reference on which to determine the losses in the inlet.

2. Inlet surveys are performed over a rectangular plane

positioned as nearly normal to both the upper and lower surfaces of the diffuser as possible. Five pitot-static probes are vertically traversed through each plane with data taken at five locations totaling 25 data points at each plane. The probe positions are shown in Figure 7. The 25 static and total head data points of each plane are curve fitted using a Fourier series. In principle, the total head integration is performed as follows:

$$h_1 = \frac{\int_0^A h_\ell v_\ell \, da}{\int_0^A v_\ell \, da} = \frac{\int_0^A h_\ell v_\ell \, da}{Q} \tag{15}$$

h_ℓ and v_ℓ represent the local total head and velocity corresponding to each differential area, da, and Q is the total ingested flow.

3. Outlet surveys are acquired over the circular outlet plane using a four probe rotary rake. Both total and static measurements are taken at 8 equally spaced positions around the outlet, providing 32 data points. The probe positions are shown in Figure 7. The total and static head measured at each of the 32 points are curve fit using a Fourier Series and the total head integrated using the following equation:

$$h_2 = \frac{\int_0^{2\pi} \int_0^R h_\ell v_\ell r \, dr \, d\theta}{Q} \tag{16}$$

where h_ℓ and v_ℓ again represent the local head and velocity corresponding to each differential area.

These total head values are then converted to ratios and corrected for the elevation losses to obtain Infinite Froude number recoveries. This is necessary since the elevation losses are not Froude scaled in the model and prototype. The general equation used to correct for the elevation is:

$$\eta = \frac{h_b}{h_a} + \frac{\Delta \ell}{q^*} \tag{17}$$

where $\Delta\ell$ is the differential elevation between the centroids of planes a and b. Performing this calculation using all three planes of measurement

provides:

$$\text{- Ramp Recovery} = \frac{\text{total head at the inlet } (h_1)}{\text{total head at ramp tangency } (h_o)} + \frac{\Delta \ell}{q^*}$$

$$\text{- Diffuser Recovery} = \frac{\text{total head at the outlet } (h_2)}{\text{total head at the inlet } (h_1)} + \frac{\Delta \ell}{q^*}$$

$$\text{- Total Recovery} = \frac{(h_2)}{(h_o)} + \frac{\Delta \ell}{q^*}$$

The integrated velocity (U_1) which is calculated at the inlet survey plane, u projected onto the normal inlet plane at the lip leading edge to obtain the inlet velocity ratio (IVR) using the following equation:

$$IVR = \frac{U_i}{U_o} = \frac{U_1}{U_o}\left(\frac{H_1}{H_i}\right) \tag{18}$$

where H_1 is the height of the survey plane and H_i is the normal inlet height.

Cavitation Inception - Cavitation inception is determined by both direct and video tape observations. The exterior and interior of the model are observed for cavitation as the ambient channel static pressure and IVR is increased and/or decreased. The principal areas where cavitation is most likely to occur are the ramp, inlet lip, sideplates, and diffuser throat as indicated in Figure 8. The basic procedure is to set a given channel pressure and then to raise or lower the IVR until the inception point is found, during which time the inlet is being monitored and recorded on a video system. Once the inception point is determined the following parameters were recorded: run number, pump rpm, nozzle Δp (for flow rate), and channel velocity and pressure which are integrated and reduced to obtain IVR and the incipient cavitation number σ_i. The incipient cavitation number is calculated as follows:

$$\sigma_i = (P_c + P_d - P_v)\, 2g/U_o^2 \tag{19}$$

where P_c is the ambient channel pressure, P_d is the hydrostatic pressure due to draft, and P_v is the vapor pressure of water.

A subject which is related to inlet cavitation is inlet ventilation and broaching in waves. This is of particular importance for SES equipped

with flush or semiflush inlets. Inlet ventilation occurs due to the flow field around the craft which tends to entrain air from the cushion and carry it under the inlet. Because it is related to the craft flow field, this type of inlet ventilation cannot be simulated in existing water channel facilities which have been used for inlet tests. To date, inlet ventilation has been investigated and empirical fixes developed using towing tank tests with models equipped with operating inlets. In these tests only measurements of total flow are made and no attempt is made to measure details of inlet performance. Lack of cavitation number scaling may effect the validity of these tests but insufficient full scale data are available to indicate the seriousness of the scaling problems.

Typical results from the velocity surveys at the inlet plane and the circular diffuser outlet plane are shown in Figure 9. The considerable flow distortion at the outlet plane is evident. Typical results for the energy recovery as a function of IVR are shown in Figure 10. The ramp recovery is the ratio of the energy at the ramp tangency point survey to the energy at the inlet survey and the diffuser recovery is the ratio of the energy at the inlet survey to the energy at the circular outlet survey. Typical results from the cavitation inception observations are shown in Figure 11 as a function of inlet velocity ratio.

Diffuser Performance

As indicated in the typical results presented above, diffuser performance can be obtained in the same water channel tests used to determine inlet performance. There are some practical problems associated with this approach particularly for systems with complex ducting systems such as an SES with multiple pumps. Limited space may be available in or around the water channel and, because of the loads involved, models become complex and expensive. This is a serious problem for diffuser design since the process depends heavily on model test data and flow visualization. For this reason there has been a tendency to do diffuser tests in simple wind tunnel facilities. Such facilities are in place at HYDRONAUTICS, Incorporated and Rohr Marine. To a limited extent larger wind tunnel facilities, such as the one at the University of Maryland have been used.

The diffuser test wind tunnel facility at HYDRONAUTICS, Incorporated is shown in Figure 12. For tests of an SES flush inlet a partial model of the sidehull with the inlet installed is mounted on one wall of the tunnel. The diffuser down stream of the inlet is modeled up to the pump inlet flanges. This is followed by long section of straight ducting which recombine into the inlet of a single blower. The inflow to the blower is controlled to obtain the desired IVR. Venturies at the downstream end of the straight ducting allow a simple measurement of total flow to be made. On a typical model, velocity surveys are made at the ramp tangency point, the inlet plane, the start of duct bifurcation, the end of duct bifurcation and the outlet plane. In addition, static pressure measurements are made along the ramp roof and inside and outside of the inlet. The wind tunnel tests are run at speeds of about 180 ft/sec and the model size is such that the Reynolds number is about 1/4 of that obtained in typical water channel tests.

The diffuser performance measures obtained from the wind tunnel tests include total energy recovery, static pressure recovery, flow velocity distribution, surface static pressures and qualitative flow visualization. The data analysis procedures described above in the section on inlet performance are also used for dissufer performance analysis. A major problem in a diffuser wind tunnel test is setting up the proper boundary layer characteristic at the ramp tangency point since this influences the diffuser performance. Various combinations of wake screens are developed on a trial and error basis until acceptable boundary layer characteristics are obtained.

Typical test results from wind tunnel diffuser tests are presented in Figures 13, 14 and 15 to illustrate the various ways in which diffuser performance is quantified.

FULL SCALE PERFORMANCE MEASUREMENT

Full scale waterjet propulsion system performance measurements are more difficult to make than comparable measurements on more conventional propeller driven craft. Direct measurements of speed and power (pump shaft torque and RPM) are no more difficult than for conventional craft and such measurements have been made on most types of waterjet propelled

craft. Although such measurments are of great value in determining overall craft performance, they do not provide direct information on the propulsion system performance. Variations from predicted speed-power could be due to errors in the estimated craft drag, the propulsion system performance or both. The problem results from the fact that, in general, it is not feasible to make a direct measurement of thrust in a fashion similar to a shaft thrust meter used on a propeller driven craft.

The most extensive full scale waterjet propulsion system performance trials have been carried out on the XR-1 and 100A SES test craft. The NAVSEC Norfolk Division has carried out some trials on planing hulls and, in one case Reference 9, a direct measurement of thrust was made by mounting the entire pump and inlet system on load cells. For the SES test craft the approach has been to determine thrust by measures of system flow, head rise, etc. and to measure the performance of individual system elements in a manner analogous to the model tests described above. For the SES 100A, basic parameters which are measured or will be measured include speed, RPM, flow rate, pump head rise, thrust, overall energy recovery, diffuser outlet flow distribution, ramp static pressure distribution, cavitation inception, boundary layer characterization and lip differential pressure coefficient. In order to determine some of these parameters a large number of individual measurements must be made and the resulting data acquisition system and data precessing system is quite complex. A description is provided in Reference 10.

One of the most important parameters, both for propulsion system performance and craft performance evaluation, is thrust. As noted above, a direct measurement of thrust cannot usually be made. Thus, the basic approach adopted is to determine thrust by measurement or determination of the parameters which appear in Equation (2). Basically, this means determining system flow rate, the jet velocity and the momentum velocity of the ingested flow. On the SES 100A two different procedures have been used. The first assumed that the nozzle characteristics (area, contraction coefficient and efficiency), pump performance (head and flow vs RPM) and the diffuser efficiency were known from analysis, model tests or pump acceptance tests. Direct measurements of craft speed, RPM and the momentum and energy velocities of the ingested flow were made. The thrust

calculation then proceeded in accordance with the flow diagram shown in Figure 16. The problem with this procedure is that the pump performance, diffuser efficiency and nozzle characteristics of the system when installed on the craft are not known with sufficient accuracy. For this reason, a more direct method was adopted. In this approach the flow rate through the nozzle and the jet velocity are correlated with a direct measurement of the static pressure in the nozzle according to:

$$Q = K \cdot P^{\frac{1}{2}} \tag{20}$$

$$V_j = Q/C_A A_j \tag{21}$$

The constants K and C_A were obtained from tests of a 1/2 scale nozzle and further refined from bollard thrust tests in which thrust was measured directly by load cells in the mooring lines.

One major activity associated with full scale measurement is correlation with predictions. Several correlation studies for waterjet propulsion system performance have been conducted or are now underway. NAVSEC Norfolk Division has compared the performance of waterjets installed on planing hulls with performance predictions supplied by the system manufacturer's (Reference 9). In general, the manufacturer's prediction of available thrust was higher than actually measured. The most extensive correlation studies are being conducted with the XR-1 and 100A SES test craft. Reference 11 reports excellent correlation for inlet and diffuser performance between tests on the XR-1B and about a 1/3 scale model tested in a water channel. It is still too soon to draw any conclusions about correlation between model test results and full scale performance for the inlet system fitted on the SES 100A. There is still clearly a need for additional model-full scale correlation data for all aspects of waterjet propulsion system performance.

SUMMARY AND CONCLUSIONS

This state of the art report has concentrated on the role of model and full scale experiments in waterjet propulsion system analysis. The basic theories for waterjet propulsion system per formance are well known and provide the framework which allows system performance to be determined from the performance of system elements. Almost all model

testing is directed at the evaluation of the performance of particular system elements rather than at overall system tests. The typical elements which are considered include appendages, inlet, diffuser and ducting, pump and nozzle. From the standpoint of the system designer, the most important information which comes from model testing includes appendage and inlet drag, inlet cavitation and ventilation and diffuser performance. This assumes that the pump performance is adequately determined by the pump manufacturer.

In usual practice inlet and appendage drag may be determined in towing tank or water channel tests. Inlet performance is determined in flow channel tests at scaled cavitation numbers. Diffuser performance is determined either in water channel tests or wind tunnel tests. To date, experimental facility capabilities have not limited the development of waterjet propulsion systems. Major scaling problems have not as yet been encountered although there is some concern about scaling inlet ventilation on SES's.

Full scale propulsion system performance evaluations are more complex than for conventional propeller systems because of the large number of parameters which must be measured and the fact that system thrust cannot be determined directly. Some detailed full scale measurements programs have been or are being carried out, particularly for SES test craft. The limited model to full scale correlations conducted to date for SES test craft have been encouraging.

REFERENCES

1. Barr, R. A. and Etter, R. J., "Selection of Propulsion System for High Speed Advanced Marine Vehicles," Marine Technology, January 1975, Volume 12, No. 1, pp 33.

2. Levy, J. and Meggitt, D. J., "Study of Waterjet Propulsion for 400-Ton Hydrofoil Ship," Aerojet Electrosystems Company Report No. 4366, October 1971.

3. Sherman, Peter M. and Lincoln, Frank W., "Ram Inlet Systems for Waterjet Propulsors," AIAA Paper No. 69-418, May 1969.

4. Development Sciences, Inc., "Theoretical Calculations of Pod Inlets for Surface Effect Ships," DSI Final Technical Report Contract No. N00024-720C-0901, February 1973, FOUO.

5. Chisholm, M. A., Kentis, D. H., and Reichert, G., "Analysis Report of Waterjet Inlet Hydrodynamics," Lockheed Missiles and Space Company Report LMSC/D313032, December 1974, FOUO.

6. Aerojet-General Corporation, Surface Effect Ships Division, "Waterjet Inlet Analysis Program Final Report," Report AGC-T-338, December 1972, FOUO.

7. Johnson, V. E., Jr. et al., "Design and Performance of Diffusers, Fixed-Area Inlets and Variable-Area Inlets in Integrated Inlet-Diffuser Subsystems," HYDRONAUTICS, Incorporated Technical Report 7152-1, August 1972, FOUO.

8. Wislicknus, G., "Hydrodynamic Design Principles of Pumps and Ducting for Waterjet Propulsion," NSRDC Report 3990, June 1973.

9. Hankley, D. W., "Full Scale Propulsion Characteristics of Two Marine Waterjets Rated at 500 HP and 1050 HP," NAVSEC NORDIV Report No. 6660-6, January 1971.

10. "SES-100A Test Craft Program Design Description Report (Update) Vol VI Data Acquisition Subsystem," AGC-T-373, Aerojet Surface Effect Ships Division, FOUO.

11. Poquette, G. M. and Etter, R. J., "Waterjet Inlet/Duct Development Phase II, XR-1B Correlation Tests," HYDRONAUTICS, Incorporated Technical Report 7244-2, March 1973, FOUO.

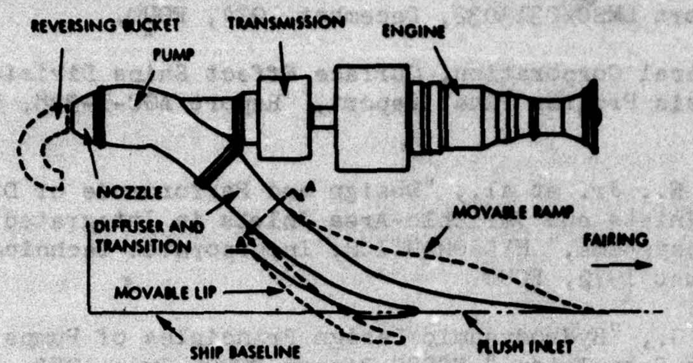

TYPICAL WATERJET SYSTEM SHOWING ALTERNATE VARIABLE-AREA FLUSH INLET SCHEMES

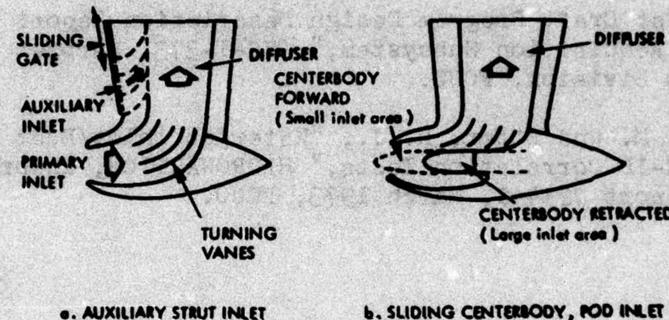

VARIABLE INLET AREA, STRUT-POD INLETS

FIGURE 1 - TYPICAL WATERJET INLET SYSTEMS

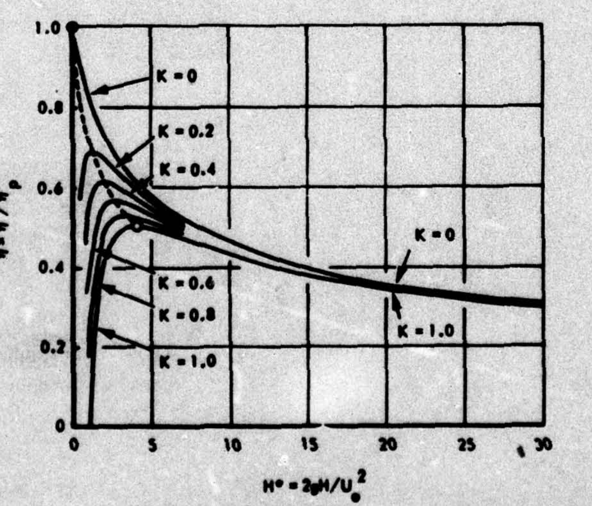

FIGURE 2 - WATER-JET SYSTEM PROPULSIVE EFFICIENCY BASED ON GROSS THRUST-EQUATION (8)

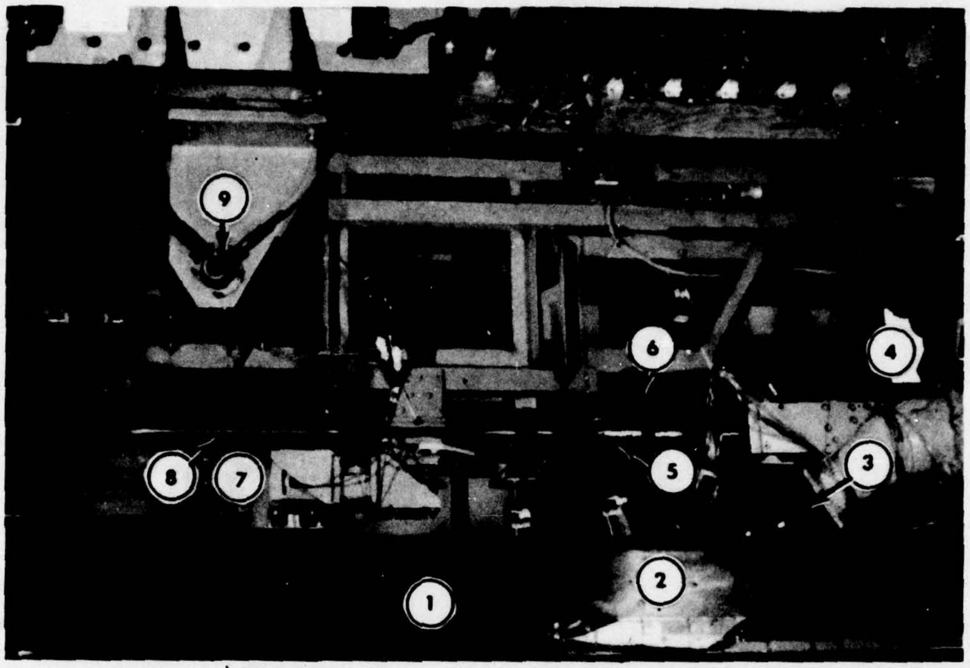

a) Yaw Rig

1. Fairing
2. Inlet
3. Outlet Flange
4. After Mount
5. Thrustless Coupling
6. Yaw Pivot Point
7. Forward Mount
8. Drive Shaft
9. Pitch Pivot Point

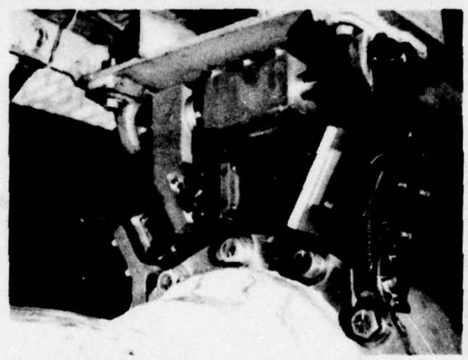

b) Enlargement of Aft Mount (4)

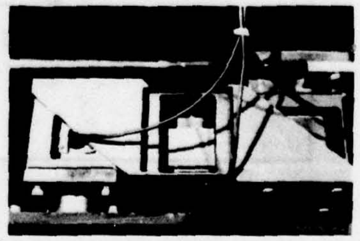

c) Enlargement of Forward Mount (7)

FIGURE 3 - WATERJET INLET TEST SETUP FOR HYDRONAUTICS HIGH SPEED CHANNEL

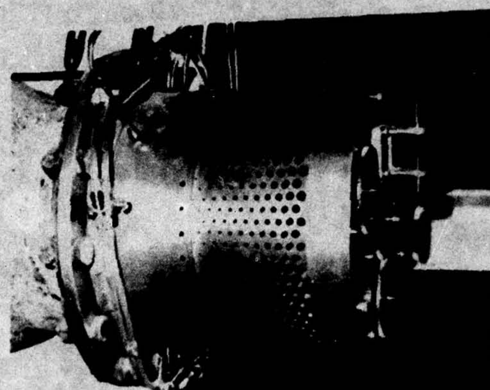

FIGURE 4 - THRUSTLESS NOZZLE

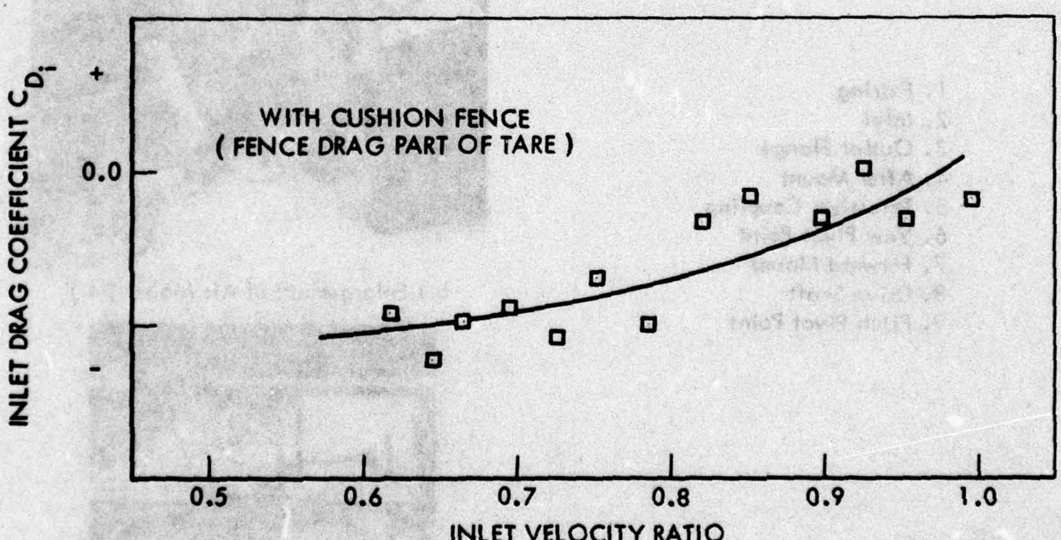

FIGURE 5 - TYPICAL INLET DRAG COEFFICIENT AS A FUNCTION OF INLET VELOCITY RATIO

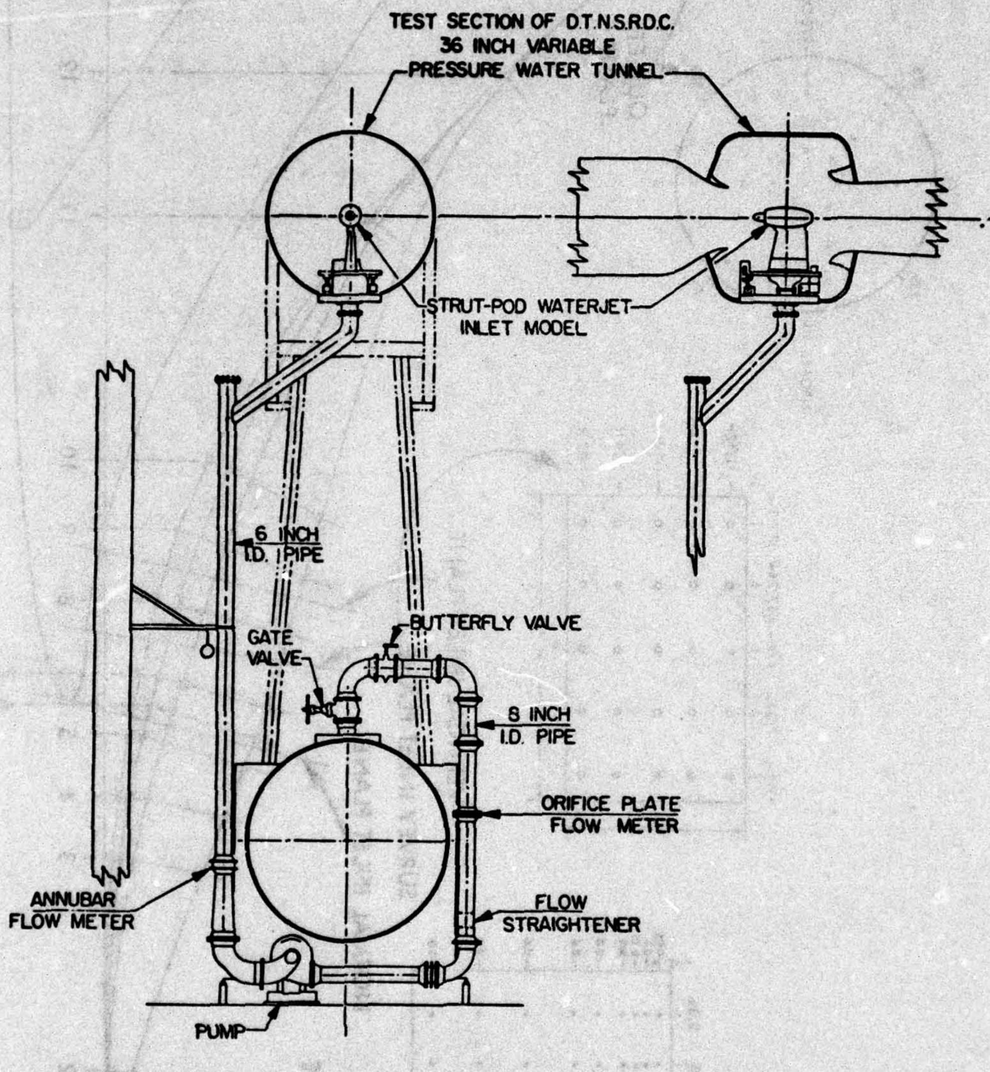

FIGURE 6 - SKETCH OF MODEL TEST SYSTEM IN DTNSRDC 36 INCH VARIABLE PRESSURE WATER TUNNEL

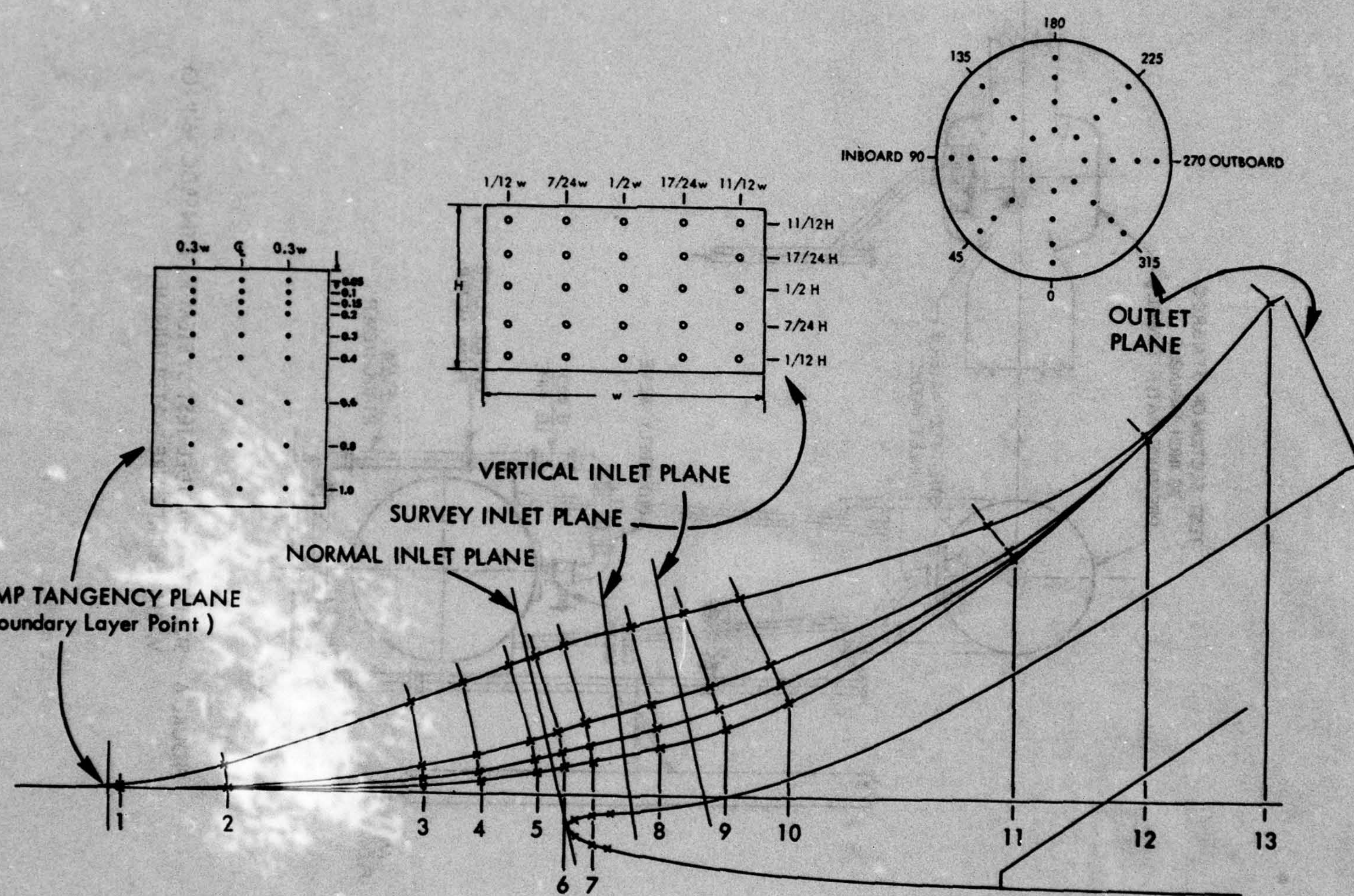

FIGURE 7 - LOCATION OF MAJOR SURVEY PLANES AND STATIC TAPS

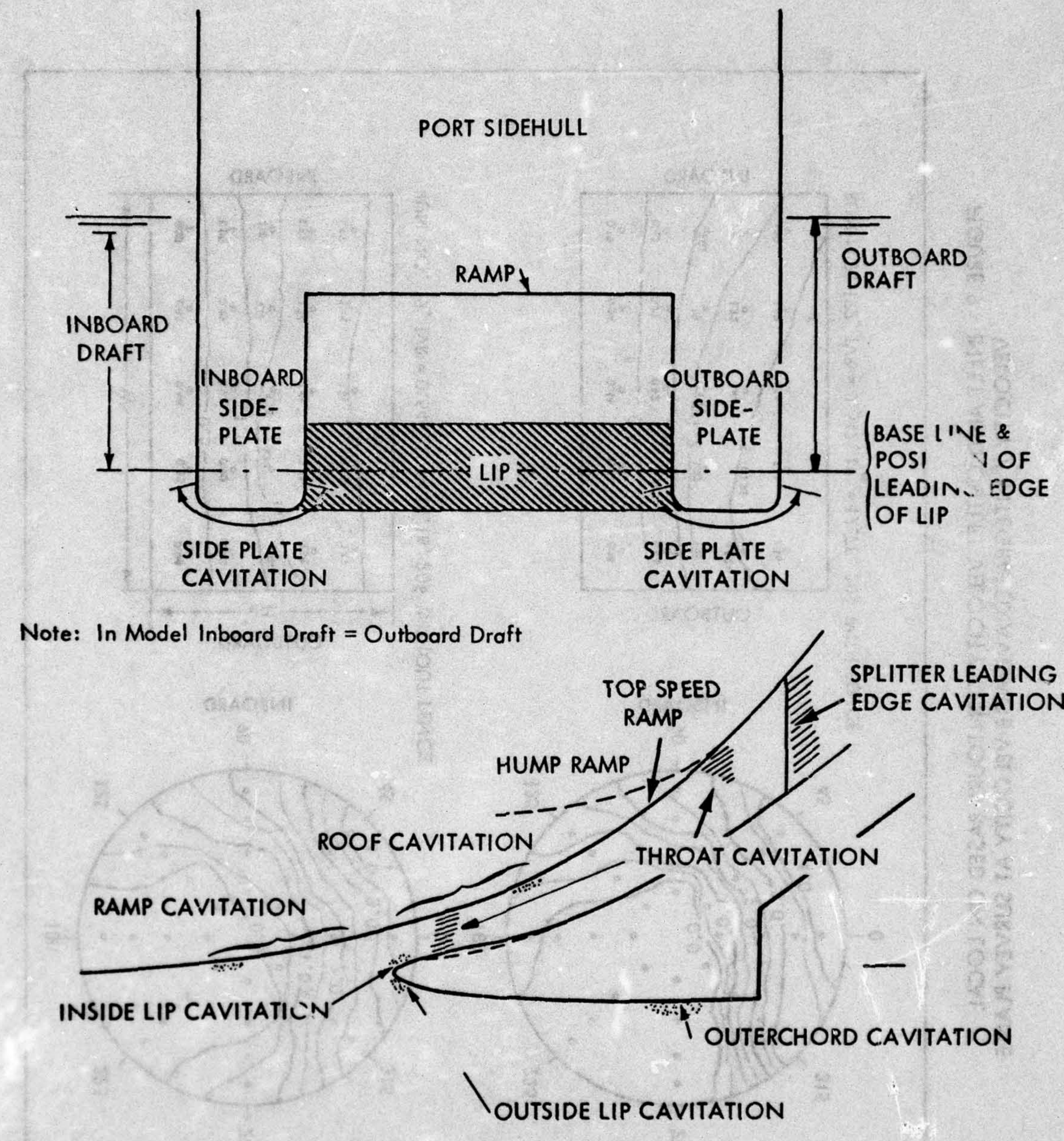

FIGURE 8 - LOCATION OF POSSIBLE CAVITATION INCEPTION ON A WATERJET INLET SYSTEM

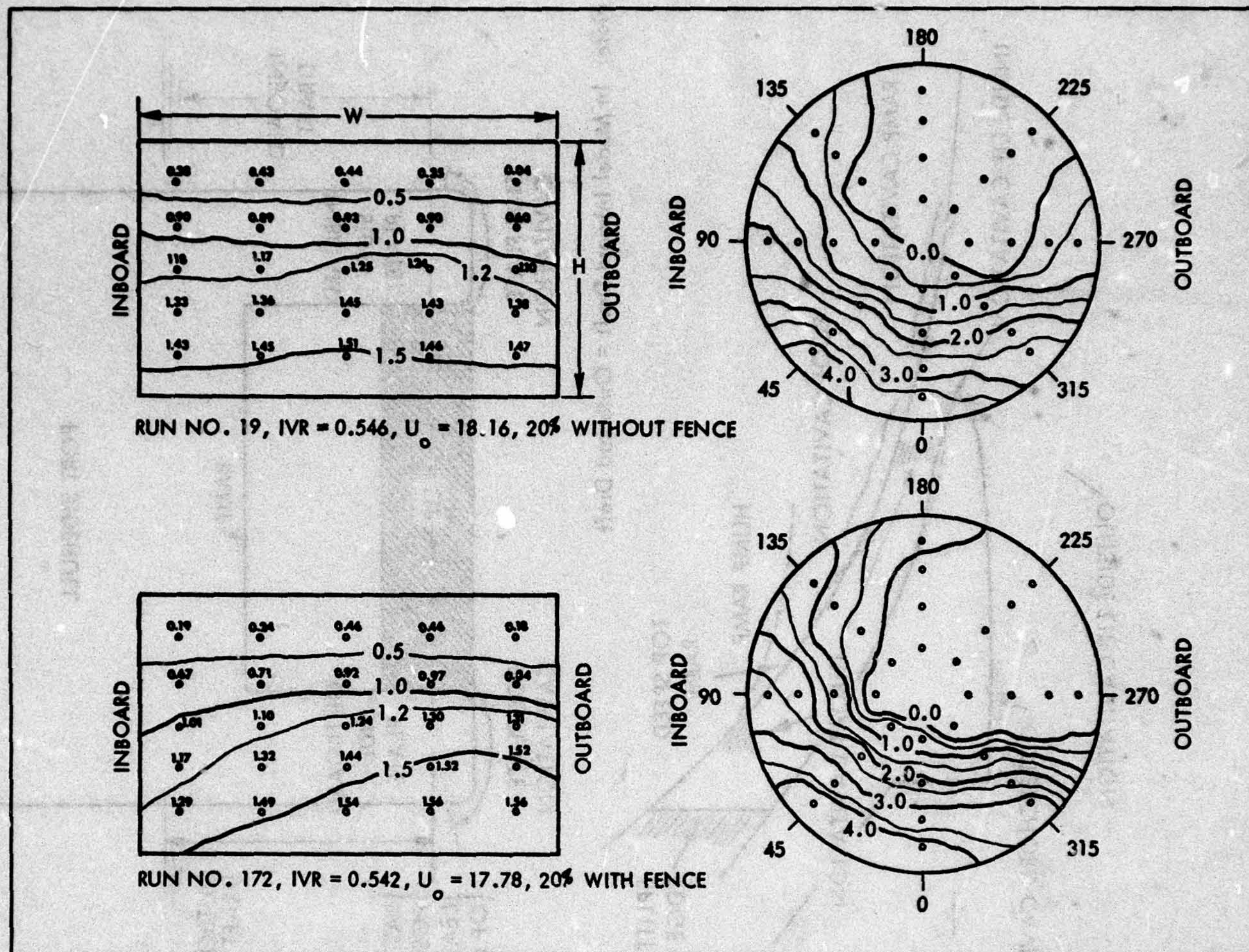

FIGURE 9 - INLET AND OUTLET VELOCITY CONTOURS BASED ON LOCAL VELOCITY / INTEGRATED AVERAGE VELOCITY AT SURVEY PLANE

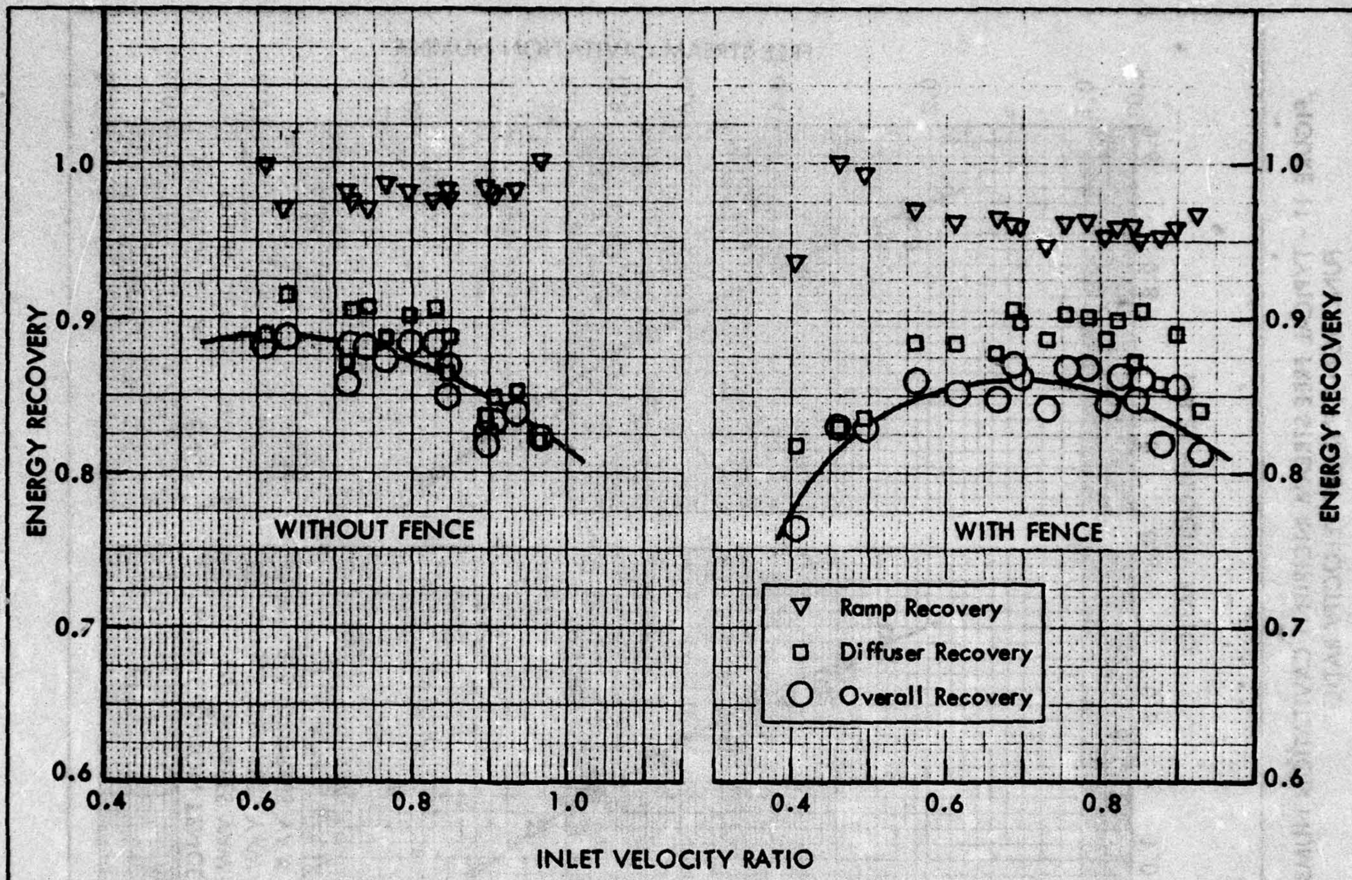

FIGURE10- ENERGY RECOVERY AS A FUNCTION OF INLET VELOCITY RATIO

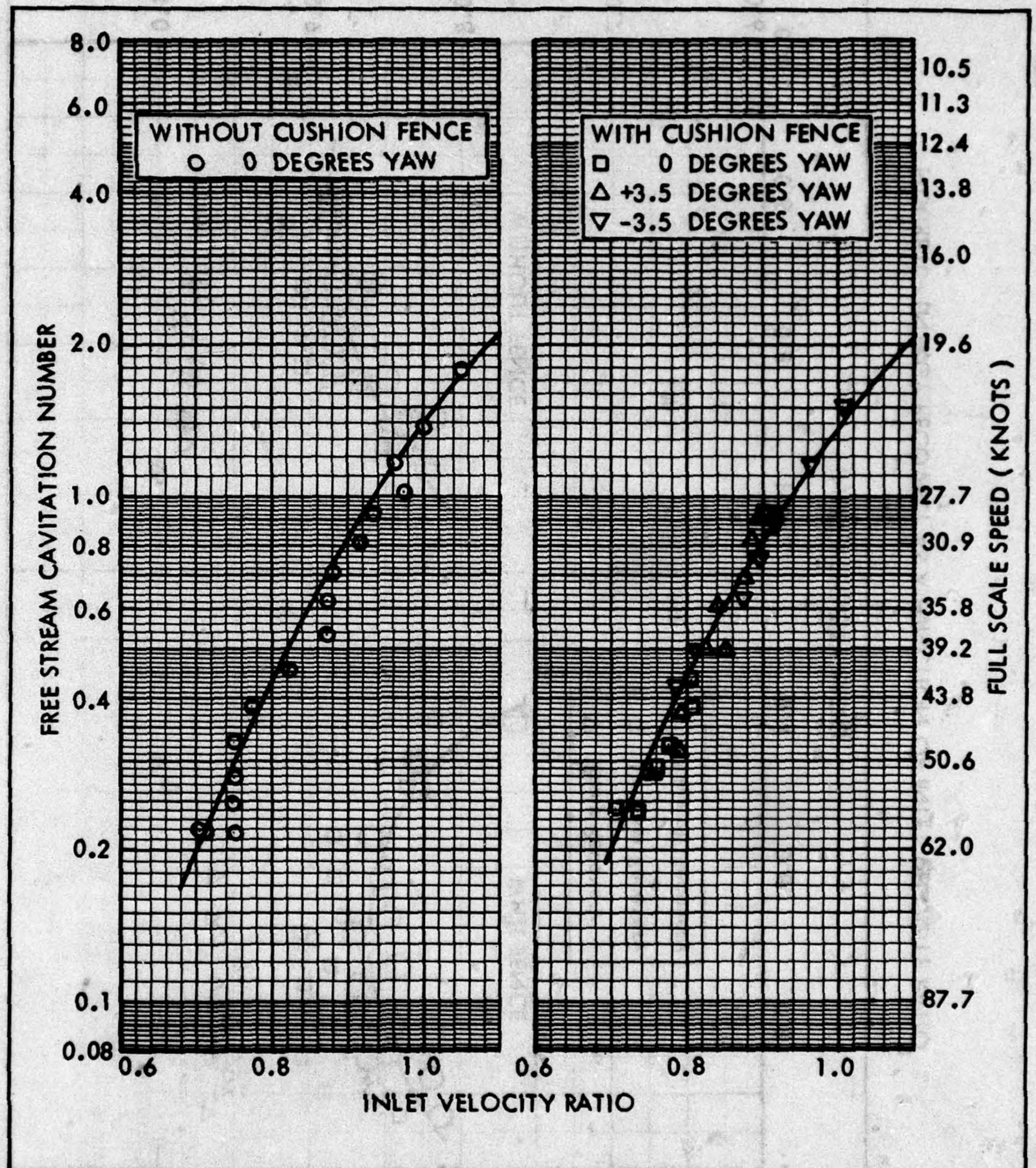

FIGURE 11 - TYPICAL FREE STREAM INCIPIENT CAVITATION NUMBER AS A FUNCTION OF INLET VELOCITY RATIO

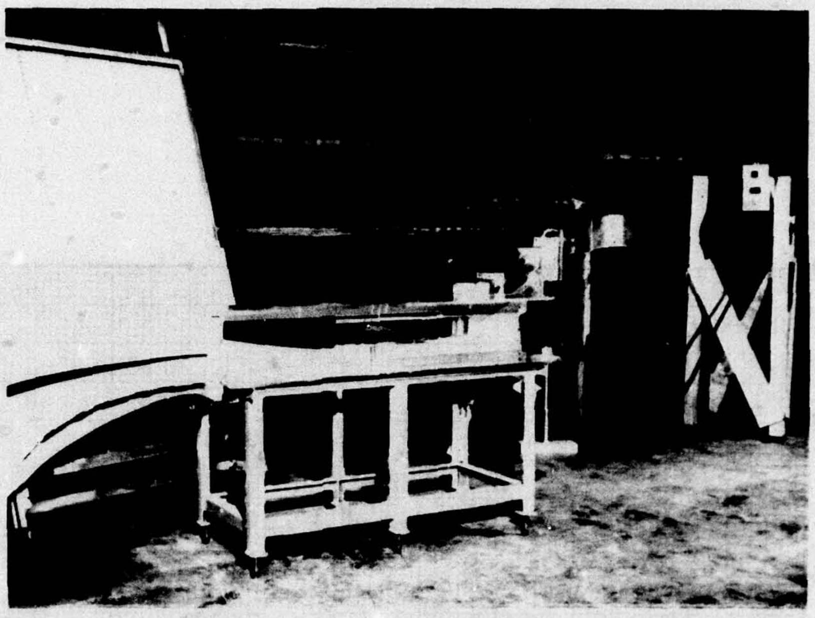

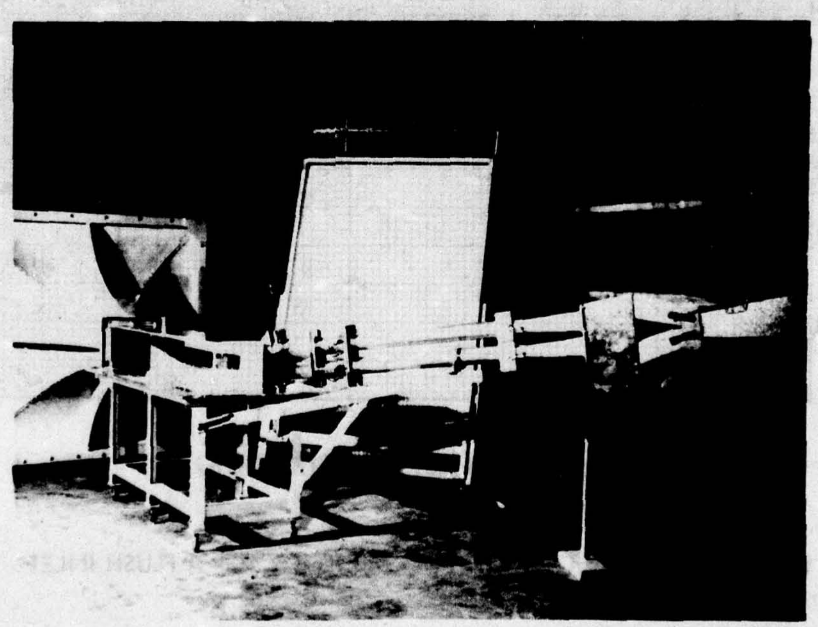

FIGURE 12 - INLET-DIFFUSER MODEL IN WIND TUNNEL TEST FACILITY

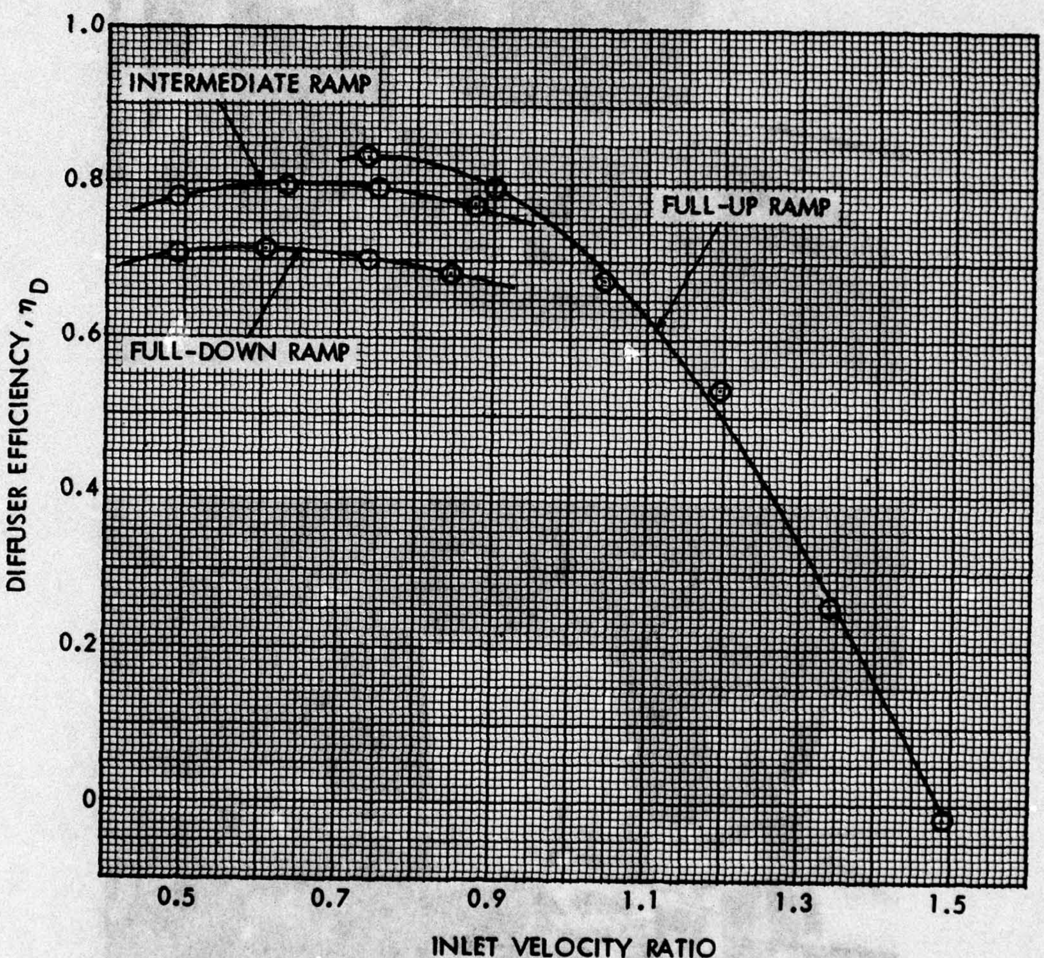

FIGURE 13 - DIFFUSER EFFICIENCY FOR A FLUSH INLET

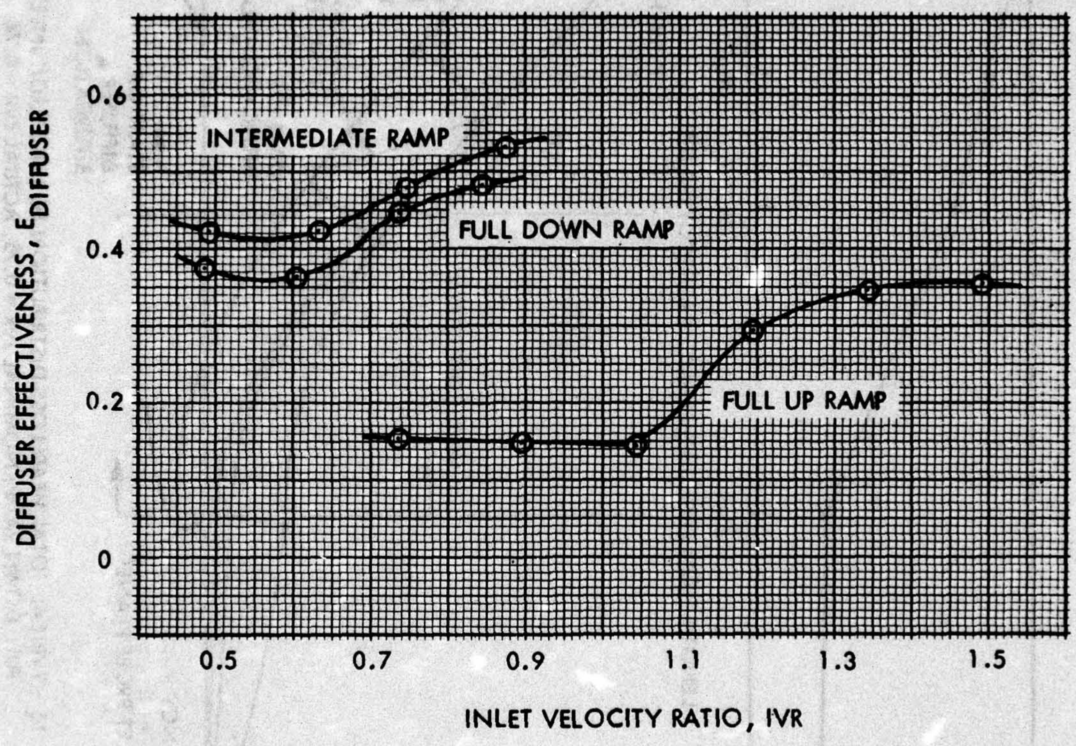

FIGURE 14 - DIFFUSER EFFECTIVENESS FOR A FLUSH INLET

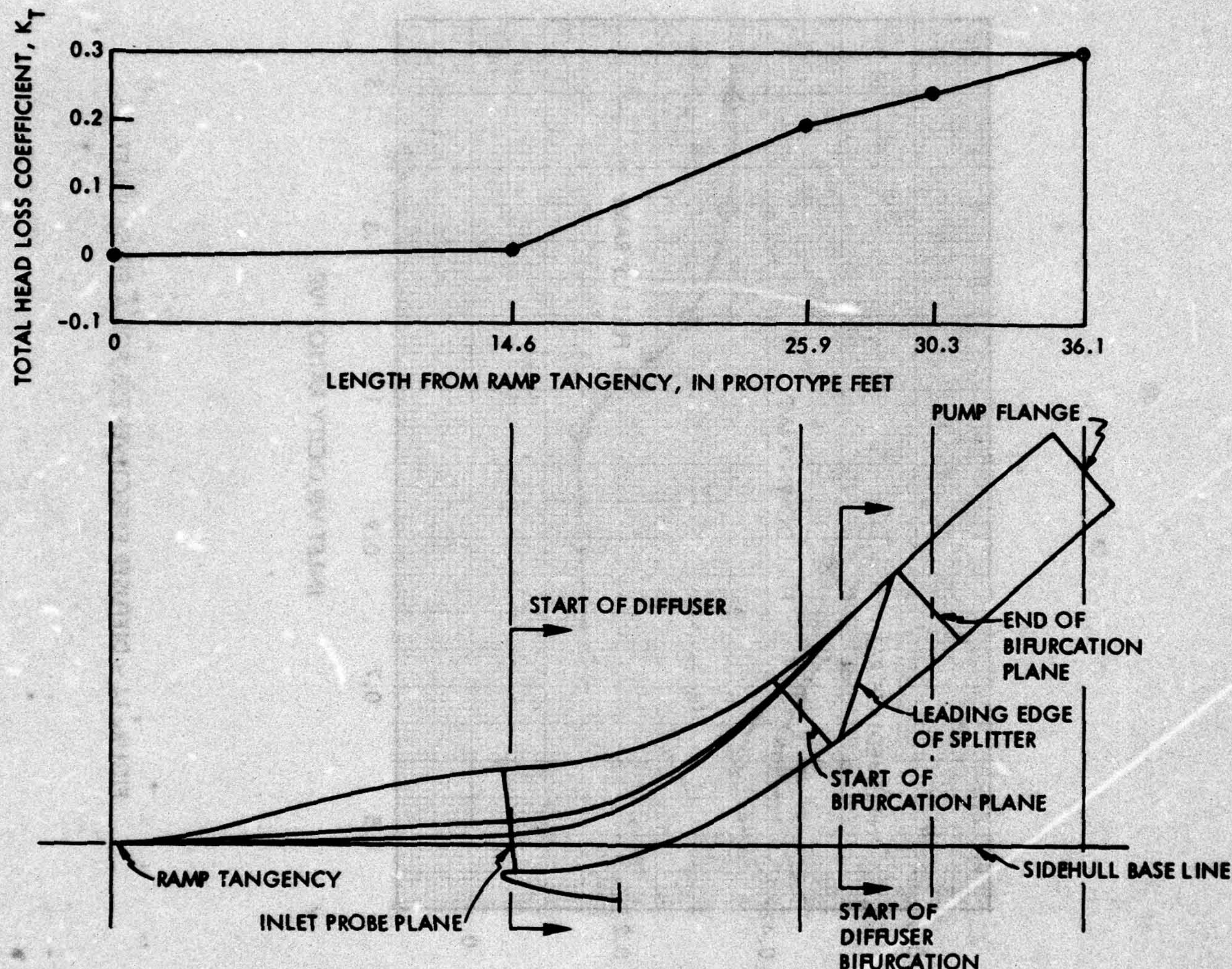

FIGURE 15 - TYPICAL TOTAL HEAD LOSS DISTRIBUTION FOR THE FLUSH INLET, FUIL DOWN RAMP; NOMINAL IVR = 0.75, ACTUAL IVR = 0.74

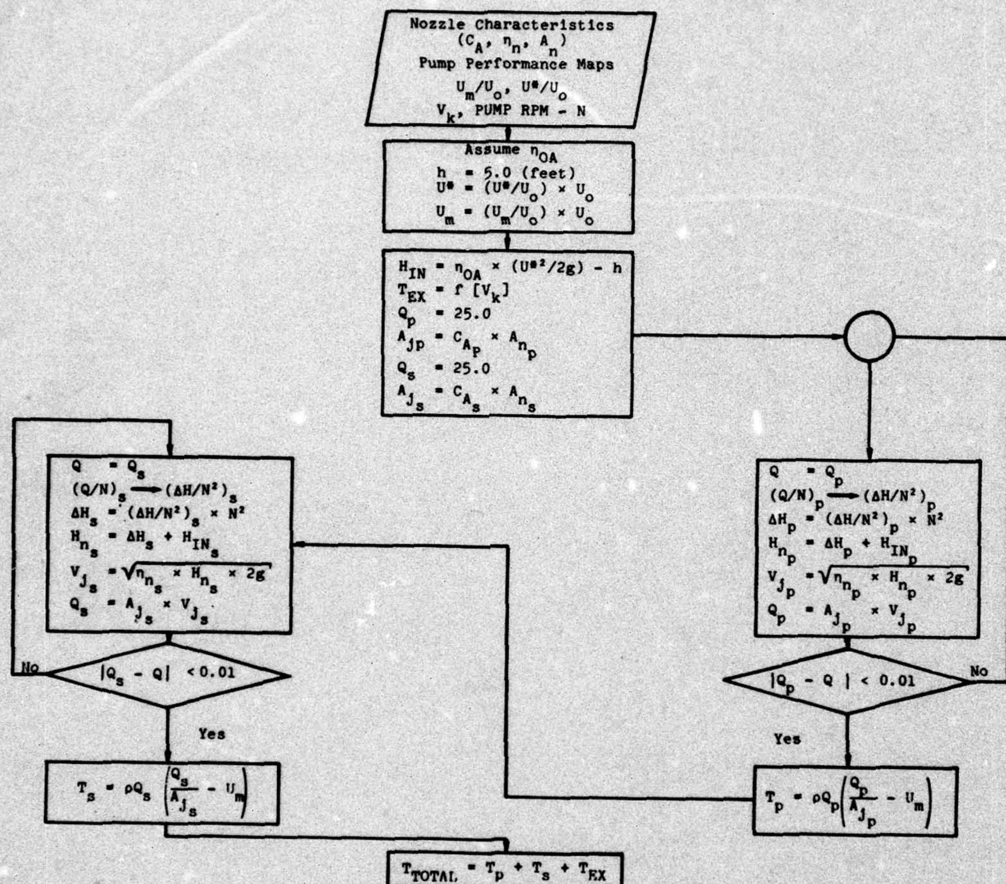

FIGURE 16 - ITERATIVE PROCEDURE FOR CALCULATING SES-100A THRUST

A SURVEY OF PROPULSION-VEHICLE INTERACTIONS ON HIGH-PERFORMANCE MARINE CRAFT

by

Michael B. Wilson
David W. Taylor Naval Ship Research and Development Center

ABSTRACT

This is a review of the literature and the state of current knowledge concerning propulsive interaction problems involved in the design of high-performance marine craft. A wide range of propulsor-vehicle combinations are discussed in a general fashion. Selected examples of experimental and analytical results are presented or mentioned when they are available, and gaps in our information base are noted.

INTRODUCTION

Interaction problems can be encountered at an early stage in the hydrodynamic design of a marine vehicle, and broadly speaking involve all the mutual influences exerted by the propulsor and vehicle geometries. For the most part, the concept of interaction is narrowed here to refer to those properties that influence the calm water <u>powering estimate</u> of a specified vehicle-propulsor combination. Physically, this involves the mutual interference of velocity fields and pressure distributions, and a determination of the ultimate consequences of these interferences on a vehicle's self-propelled performance. There can be interaction problems arising from straight-on flow over adjacent arrangements of a propulsor and body; or from propulsor operation at large vehicle trim or yaw angles; or due to transverse forces inherent to the propulsor mode of action. Expecially for high-performance vehicles, cavitation and ventilation will influence interference flows.

From an engineering point of view, the complexity of the combined flow must be distilled down to measurable, net effects that can be applied to predict thrust and power absorbed by a propulsion device installed in a vehicle. Propulsive factors serve this purpose.

A definition of a high-performance marine vehicle has been given by Dobay and Gregory (1974) as "any craft that exceeds the present norm of performance as regards speed, seakeeping, etc." Generally, high performance refers to high speed, although this is a relative term. There seems to be a natural division of these vehicles into two groups: (a) displacement craft whose speed-length ratio exceeds 1.5, and (b) vehicles with lift supplied partly or wholly from hydrodynamic, aerodynamic, or aerostatic forces in any portion of the speed range. This is a broad enough definition to encompass a host of hybrid vehicle concepts, but of course there exists presently a group of 'usual' high performance vehicles that includes:

- Planing Craft
- High-Speed Displacement
- Small Waterplane Twin Hull (SWATH)
- Hydrofoil
- Air Cushion Craft (includes ACV, SES, and WIGE)

Five main propulsor types are associated with these vehicles:

1. Subcavitating Submerged Propellers
2. Supercavitating, Submerged Propellers
3. Partially-Submerged Supercavitating Propellers
4. Waterjet Propulsors
5. Airpropulsors

Classical Propulsive Interaction

The familiar format for powering prediction of propeller-driven craft is the starting point for a discussion of propulsive interaction. It will prove inadequate for some propulsor types, yet it provides a simple structure for assembling the efficiencies of the components of a self-propelled vehicle. The power required to be delivered to the propeller shaft can be estimated from

$$P_D = R_T U_o / PC$$

$$P_D = (\eta_o \eta_H \eta_R \eta_A)^{-1} P_E,$$

where P_E = effective power (for bare, unappended vehicle) = $R_T U_o$

η_o = characterizing or 'open flow' propulsor efficiency; this should be determined at the prototype scale cavitation number

η_H = hull efficiency = $(1 - t)/(1 - w)$

η_R = relative rotative efficiency

η_A = appendage efficiency = $P_{E,\ bare}/P_{E,\ appended}$

R_T = bare hull drag

U_o = forward speed of vehicle

PC = $\eta_o \eta_H \eta_R \eta_A$ = propulsive coefficient

t = thrust deduction fraction

w = wake fraction

The essential ideas involved with interaction are contained in this representation, and are conveyed quantitatively in the factors t, w, η_A, and η_R.

The pressure field associated with the operation of the propulsor can increment the bare hull drag by the amount $\Delta D = T - R_T$. The thrust deduction fraction is $t = \Delta D/T$, where T = thrust of propulsor working on the vehicle.

The velocity field, wake, or boundary layer developing over the vehicle will present a modified flow to the propulsor, different or possibly Reynolds number-scaled from that used to characterize the propulsor by itself. There is, then, a net inflow velocity $V_A = (1 - w)U_o$, where w is the effective Taylor wake fraction.

There may be drag penalties due to appendages or modifications in the vehicle shape near the propulsor unit, and these can be lumped into an efficiency factor $\eta_A = R_{T,\ bare}/R_{T,\ appended}$.

For propulsors involving rotating propellers or inducers, the spatially distorted inflow created by the mutual action of vehicle and propulsor will give rise to a factor termed the relative rotative efficiency η_R = torque (open)/torque (combination); determined at the same thrust and rotational speed.

Scaling

Model testing is the main tool for determining the interaction properties. Ideally the three principal scaling coefficients --- Froude number, Reynolds number, and cavitation number --- should be modelled from the prototype scale, as well as geometric similarity and nondimensional thrust coefficient. As usual, satisfying all three of the fluid dynamic parameters simultaneously is impossible using a scale model. With a variable pressure water channel or a vacuum towing basin, simultaneous satisfaction of Froude and cavitation numbers can be accomplished. In such cases, however, care must be exercised with regard to too-small Reynolds numbers on the important components of scaled-down propulsors. Also, if ventilation is

important to the flow, reduced pressure over the water will not allow the ratio of air pressure-to-static water pressure to be satisfied.

The choice of the scaling parameter(s) that should be satisfied in experiments to determine interaction factors for a high-performance craft is somewhat of an art, and depends on the vehicle type, the actual speed range, and the test facilities available. For example, for planing boats or displacement hulls fitted with subcavitating propellers and operating at moderate speeds ($V_K \leq 30$ knots), cavitation-scaled open propeller characteristics and Froude-scaled self-propulsion tests on a towing basin should be performed for obtaining the interaction characteristics. For a SES propelled at 80 knots by waterjet or cavitating propeller, cavitation number scaling must be accomplished both for the open water tests (when applicable) and for the propulsion experiments. If at all possible, propulsion tests should also be performed at a scaled Froude number, and in some cases simultaneous cavitation and Froude scaling in a variable pressure water channel can be done with a proper choice of scale ratio.

In the discussions that follow the main emphasis is on experimental results from towing tank, water tunnel, water channel, or wind tunnel tests. The scaling procedures used will be noted. Contributions from analysis in the area of propulsive interactions for high performance vehicles are not plentiful. But an attempt has been made to find and comment on those that do exist.

1. SUBCAVITATING, SUBMERGED PROPELLERS

In the present context of high-performance marine vehicles, the term subcavitating propeller encompasses both non-cavitating and trans-cavitating free screw propulsors, but with no precise definition for the latter category. It may suffice to state that trans-cavitating propellers are essentially subcavitating designs capable of operating with substantial partial cavitation present without excessive performance losses. Partial cavitation covers a wide and nebulous range of conditions where blade cavity lengths are mostly less than one chord, and where only part of the blade sides, root to tip, are covered by the cavities.

High performance vehicles that are paired with sub- and partially-cavitating screw propellers include: planing hulls, high speed displacement ships, SWATH ships, and hydrofoil craft. At the speeds typical for these vehicles ($V_K \leq 50$ knots) an account of cavitation number must be given to the open water propeller characteristics. However, with the exception of a few hydrofoil-strut-pod-propeller experiments, the propulsive interaction factors for these propeller-vehicles combinations are determined in towing basin tests at Froude-scaled speeds.

The essential physical feature of propeller flow relating to interaction is the pressure field induced in the region ahead of the propeller disk or along a plane outside the propeller diameter and roughly parallel to the thrust axis. An

approximation to the net force acting on the boundary due to the operating propeller can be obtained by integrating the pressure changes over the exposed area and resolving the result into a longitudinal component (added drag) and a vertical component (producing added sinkage and trim).

A useful tool for understanding the average, induced velocity field due to thrust loading for a free, subcavitating propeller in a uniform stream has been developed, for example, by Hough and Ordway (1965). It has the advantage that complete flow velocity pictures (and therefore pressure distributions) can be obtained rather simply. However, no account of the hub or blade thickness is made. Also, the solution does not consider the presence of a nearby solid wall. Further calculations by Hough and Ordway (1967) show the mean flow streamlines and perturbation flow streamlines for a representative blade loading function. Particularly the latter indicates that outside the propeller radius, a sink disk characteristic of the propeller is very accurate. Figure 1 indicates the magnitude and sign of the approximate pressure distribution induced along an imaginary boundary by a free propeller, using the linearized nondimensional pressure

$$\left(\frac{p - p_o}{\frac{1}{2}\rho U_o^2}\right)\frac{1}{C_T} \approx -\frac{2\bar{u}}{C_T U_o}$$

where $\bar{u}$ = mean axial induced velocity. This shows the characteristic suction peak ahead of the propeller.

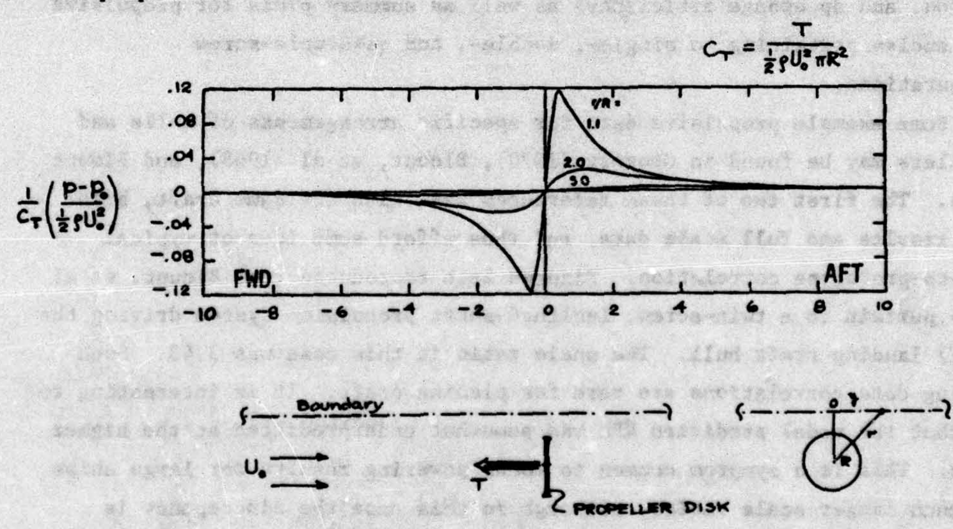

Figure 1 - Mean Induced Pressure Distribution Along a Plane Boundary Outside a Propeller Slipstream.

More accurate field point velocities for a propeller operating either in a uniform flow or in the non-uniform stream behind a ship form can be obtained with lifting line theories or with lifting surface calculations. An example of the latter is the work of Kerwin and Leopold (1964), which also provides the possibility of including blade thickness effects.

Near Hulls

There are three general hull types of interest: planing hulls, high speed displacement ships, and SWATH ships.

<u>Planing Hulls</u>. Propulsive interaction factors for planing hull-propeller combinations are obtained experimentally in self-propulsion tests conducted in a towing basin.

Typically the propulsive factors determined are the thrust deduction t, wake fraction based on thrust w_T, wake fraction based on torque w_Q, the relative rotative efficiency η_R, and when applicable, the appendage efficiency η_A. The propulsive interactions so represented are strictly Froude number-scaled. When applying these factors to the prototype scale, it is not customary to correct the wake fractions for Reynolds number. The usual practice is to use the wake fraction based on thrust directly from model tests.

Examples of synthesis reference works on planing hull powering problems are given by Hadler (1966), Blount and Fox (1976), and Hadler and Hubble (1971). A fair amount of propulsive interaction data is assembled in these. For instance, in the latter paper, a series of plots are presented of the various components of propulsive interactions (thrust deduction, wake fraction, and appendage efficiency) as well as summary plots for propulsive efficiencies pertaining to single-, double-, and quadruple-screw configurations.

Some example propulsive data for specific arrangements of hulls and propellers may be found in Gregory (1970), Blount, et al (1968), and Blount (1965). The first two of these references deal with the same craft, both model results and full scale data, and thus afford some idea of typical model-to-prototype correlation. Figures 2a,b reproduced from Blount, et al (1968) pertain to a twin-screw, inclined-shaft propulsion system driving the LCVP(T) landing craft hull. The scale ratio in this case was 3.43. Such powering data correlations are rare for planing craft. It is interesting to note that the model predicted RPM was somewhat underpredicted at the higher speeds. This is a symptom common to model powering results for large ships with much larger scale ratios, although in this case the discrepency is probably due to cavitation on the blades on the full scale. The disturbing discrepency is with trim.

Planing craft of all types and sizes often use inclined shaft propulsion arrangements. This can have an influence on the net thrust in the horizontal direction, especially in combination with craft trim, and of course there is a transverse force generated by inclined propeller operation.

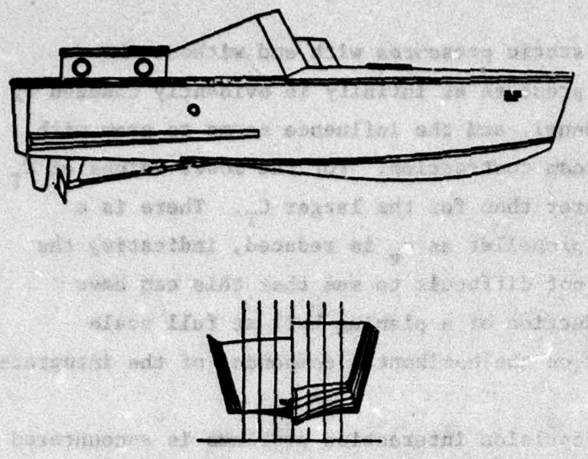

Figure 2a- Profile and Body Plan of LCVP(T) Planing Craft (From Blount, et al (1968))

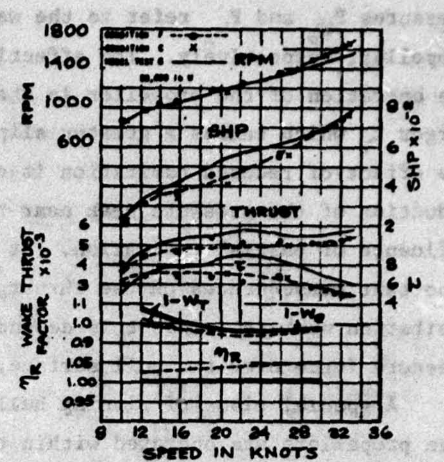

Figure 2b- Comparison of Model and Full-Scale Propulsion Data for the LCVP(T) (From Blount, et al (1968))

Hadler (1966) has provided an analysis of hull-propulsor interactions in his synthesis of angled propeller effects, including net suction forces and trimming moment on the boat due to propeller operation. Some experimentally determined force and moment data, including side force results are available for inclined propellers at various cavitation numbers in the report by Peck and Moore (1974).

Interaction effects arising from the propeller-induced pressure field on a nearby boundary are subject to important changes when the flow cavitation number is reduced, with corresponding increasing amounts of blade cavitation. The effect is somewhat similar to increasing blade thickness. Figure 3 , reproduced from van Manen (1972) illustrates the mean pressure variation measured along the wall of a water tunnel near an operating propeller as a function of cavitation number and thrust coefficient. The

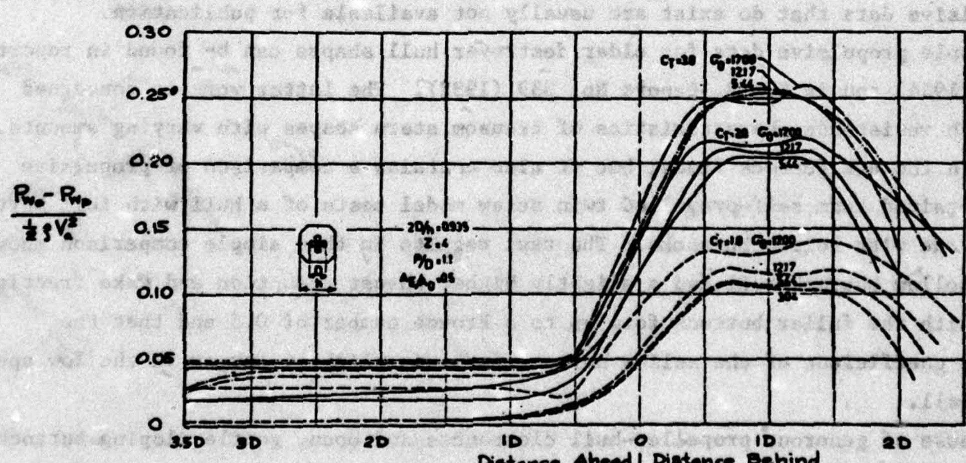

Figure 3 - Influence of Cavitation and Thrust Loading on Propeller-Induced Pressure Distributions Along Tunnel Wall (From van Manen (1972))

pressures P_{W_p} and P_{W_o} refer to the wall static pressures with and without the propeller, respectively. The effective pressure at infinity is evidently changed by the operation of the propeller in the tunnel, and the influence seems to grow with larger C_T which causes a greater slipstream contraction. For the lower values of C_T the effect of reduced cavitation is clearer than for the larger C_T. There is a reduction of the pressure peak near the propeller as σ_v is reduced, indicating the influence of partial cavitation. It is not diffucult to see that this can have important consequences on the thrust deduction of a planing hull at full scale cavitation numbers, since t is dependent on the horizontal component of the integrated pressure force over the hull surface.

A special class of planing hull propulsion interaction problems is encountered when propellers are operated within tunnels near the transom. In addition to the parasitic drag increase due to the tunnels themselves, there are interesting variations in the wake fractions for various tunnel depths and also due to propeller tip clearances. Propulsion characteristics for a series of partial-diameter tunnels have been studied by Harbaugh and Blount (1973), and for a 100 percent tunnel by Ellis and Alder (1977).

High Speed Displacement Hulls. Ship forms intended for operation at speeds at least as high as $V_K/\sqrt{L} = 1.5$ typically have transom sterns, very fine hull lines, and also display long, sloping, nearly flat boundaries aft near the propellers. Several series of such hull forms have been tested in towing basins to determine their resistance characteristics. An example is the Series 64, presented by Yeh (1965). A list of other published work on high speed hull forms is given by Dobay and Gregory (1974). Unfortunately, information on propulsive interaction factors for such ship forms is scarce. Since the typical naval application of these hulls would be for a destroyer, the propulsive data that do exist are usually not available for publication.

Example propulsive data for older destroyer hull shapes can be found in reports by Pitre (1934) and in E.M.B. Report No. 339 (1932). The latter work is concerned mainly with resistance characteristics of transom stern shapes with varying amounts of fullness in the aft buttock lines; but it also contains a comparison of propulsive factors obtained form self-propelled twin screw model tests of a hull with full buttock lines and one with hollow buttocks. The test results in this simple comparison showed that the hollow buttock hull had a slightly higher thrust deduction and wake fraction compared with the fuller buttock form up to a Froude number of 0.5 and that the propulsive coefficient of the hollow buttock form was slightly larger in the low speed range as well.

Because of generous propeller-hull clearances and open, gentle sloping buttock lines, the interaction factors typical of high speed displacement ships are never dramatically large. However, the wakes tend to be very non-symmetirc and despite good

clearances, this can mean troublesome propeller-induced vibration characteristics. Also, since the usual self-propulsion tests are Froude-scaled, the influences of cavitation number on the propulsive characteristics of useful high speed hull forms are largely unknown.

Meanwhile there exists published information on the effects of cavitation number on propulsive interaction factors determined from model experiments with single propellers operating behind conventional ship hull forms. In separate experimental programs using different facilities, dissimilar test techniques and different model sizes, Bavin and Miniovich (1963) and Prishchemikhin (1975) have shown that there are noticeable changes in the thrust deduction for increasing amounts of partial cavitation on the propeller blades. Although these results are not directly useful for any practical high speed ship design, they are remarkable in that both static pressure measurements on the hull and the inferred thrust deduction confirm the concept that as the cavitation number is decreased, the blade cavities grow and are responsible for a constriction of the flow through the propeller disk. The effect is similar to increasing blade thickness, in that the suction region forward of the propeller gradually becomes a positive pressure region as the blade cavities grow.

The experiments by Bavin and Miniovich (1963) were conducted in a towing basin using a 19 foot model fitted with a 0.656 foot diamter propeller having a pitch-to-diameter ratio of 1.4. Reduced cavitation number was simulated by forced air ventilation. Results indicate a definite decrease in the thrust deduction t for decreasing cavitation number and increasing thrust loading coefficient C_T. A systematic reduction of the propeller-induced suction peak in front of the propeller was observed in the measured static pressure data. At the same time, the wake fraction remained unchanged, within a band of scatter, but with no discernible trend with respect to reduced cavitation number. These results stand as the first of their kind, as far as is known. But they have been of little direct use because of the meager description of the geometry of the hull shape.

Experiments by Prishchemikhin (1975) were performed in a cavitation towing tank using a 14.8 foot long, block 0.69 model of the 'Victory' ship hull form fitted with a 0.59 foot diameter, pitch-to-diameter ratio 1.4 propeller. In this case, reducing the facility ambient pressure was used to achieve low cavitation numbers. Figure 4, reproduced from Prishchemikhin (1975), is a sketch of the after hull profile and propeller arrangement, and the location of the hull static pressure taps. Figure 5 shows the variation in the change of pressure acting on the hull at location number 2, as a function of cavitation number and advance coefficient. Of course the figure includes data well into the fully cavitating regime, but the trend from the non-cavitating curve (definite suction pressure) through the partial-cavitating cases illustrates the distinctive reduction of the suction pressure level changing to positive induced pressure as the cavitation number is reduced. The most dramatic shifts occur at low J values where the blade angles of attack are large. The effects

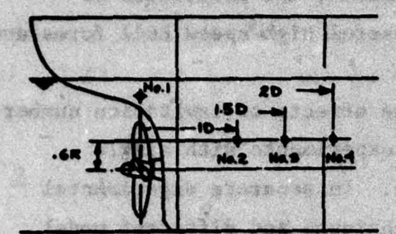

Figure 4 - Profile of Victory Ship Stern and Propeller, Showing Location of Pressure Transducers (From Prishchemikhin (1975))

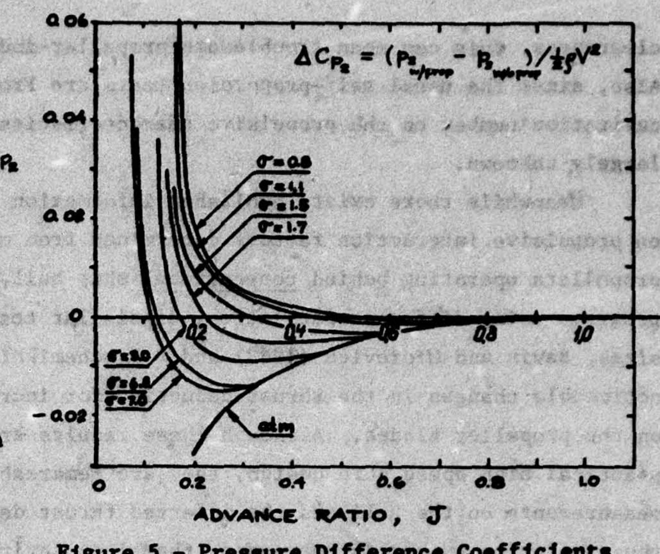

Figure 5 - Pressure Difference Coefficients on Ship Near Cavitating Propeller. Location No. 2 (From Prishchemikhin (1975))

of thrust loading and cavitation number on the net thrust deduction fraction t are shown in Figure 6, where zero or even slightly negative values of t were measured under extreme conditions of thrust loading.

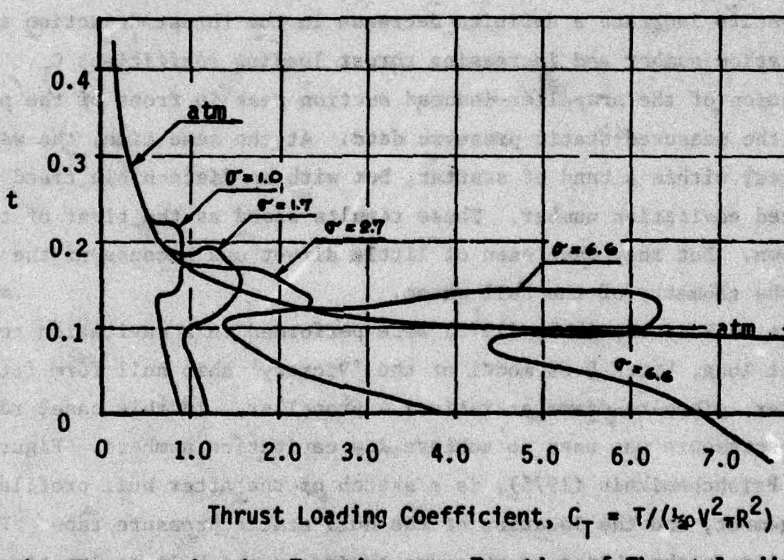

Figure 6 - Thrust Deduction Fraction as a Function of Thrust Loading and Cavitation Number for 'Victory' Ship Hull Driven by Cavitating Propeller (From Prishchemikhin (1975))

It should be noted that the geometries of the single screw conventional hull forms used by Bavin and Miniovich (1963) and by Prishchemikhin (1975) are condusive to showing effects of propeller cavitation on thrust deduction, because of the relatively close propeller-hull spacing and the amount of vertical-sloped hull boundary just

upstream of the propeller disk.

Theoretical work on predicting the pressure field induced on ship hulls by a partially cavitating propeller has tended to concentrate on the unsteady effects and the blade-rate pressure distributions. Recent advances have been made, for example, in applying lifting line theory to partially cavitating propellers by Noordzij (1976) and Noordzij and Officier (1977).

SWATH Ships

The usual propulsor-hull arrangement on a SWATH ship involves a pusher propeller mounted behind each of the two submerged cylindrical demi-hulls. The speed range typical of these vehicles, as presently conceived, is below 30 knots, so that the expected partial cavitation effects would be relatively insignificant. Propulsive interaction factors determined in Froude-scaled experiments in a towing basin are likely to be fairly accurate.

Example propulsion data for specific SWATH configurations are given by Lin and Day (1974) and by Yeh and Neal (1977). Typical experimental values of overall propulsive coefficients (PC) for several SWATH arrangements are between 0.70 and 0.75. Despite the apparent similarity between the SWATH demihull-plus-propeller and a submarine-propeller configuration, the high PC values of submarines are not realized with the SWATH because the propeller is not as thoroughly immersed in the hull wake as in the case of a submarine. Hence the favorable hull efficiency $\eta_H = (1 - t)/(1 - w)$ of a submarine has not been achieved with the SWATH arrangements considered thus far.

Measured three component wake data in the propeller plane of one hull of a tested pair of SWATH model hulls are presented by Kirkman, et al (1976).

Recent progress in understanding and scaling of propulsive interaction factors for axisymmetric bodies has been reported on by Huang, et al (1976) who also have included an extensive bibliography of the classical references on propulsive interaction for submersibles and conventional surface ships. These references are generally of little use for most high performance craft geometries.

Near Foil/Pod/Strut

Sub- or transcavitating propellers for use on hydrofoil craft are typically associated with the moderate speed range below 50 knots where subcavitating foils, pods, and struts are employed. The propulsive interaction factors for these arrangements are usually somewhat smaller than those on large hull-propeller combinations. The reason for this is that on hydrofoils the propeller-induced drag augmentation occurs on an element such as a pod or a local foil panal that contributes relatively little to the overall drag.

Nevertheless, the effects are measurable and some published work is available for

guidance.

Mavlyudov, et al (1973) have presented an extensive discussion of the subject of propeller-hydrofoil system interactions, including the calculation of induced velocity fields; location and strength of tip vortices; effect of propeller pressure field on nearby foils; influence of free surface waves on propeller thrust and torque; and an outline of the potential propulsive benefits of locating propellers in the vortex wakes just aft of the tips of a submerged hydrofoil, each with rotation opposing the sense of the tip vortex angular velocity field. Numerous references to technical literature of the USSR are cited in this book.

For the arrangement of a propeller located behind and possibly offset from a hydrofoil chord line, Beveridge (1962) has provided analytical estimates and experimental data for the mutual interaction effects. Both theory and experimental results are given for the thrust deduction. Wake fraction values are estimated from published NACA experiments and the resulting influence on fluctuating thrust are presented.

Sample measured wake data in the plane of the propeller disk behind nacelles combined with lifting foils and struts can be found in references by Moore (1964), Davis and English (1968), and Mavlyudov, et al (1973).

Propellers can also be used in the tractor mode (mounted at the forward end of a pod) for hydrofoil propulsion, as for example, with the forward propeller of the tandem arrangement used on the Patrol Craft Hydrofoil PC(H). In the course of developing propulsion data for the PC(H)-1 Mod 0 and Mod 1, many variations of sub-, trans-, and supercavitating propellers were considered. A summary evaluation of these combinations was outlined by Peck and Hecker (1971). Their cited references are also useful.

Unique propulsive interaction data has been reported on by Peck (1966) from water tunnel tests of three different model propellers operated ahead of a PC(H) nacelle-wing-strut model. Cavitation numbers varying between 4.0 and 0.45 were investigated. Two of the propellers tested could be referred as high-speed or transcavitating designs. Figure 7 reproduced from Peck (1966) shows the measured drag augmentation (thrust deduction) plotted versus advance ratio for the high expanded area ratio TMB designed propeller. The marked influence of cavitation number can be seen.

The propeller-wing interaction problems treated in classical aerodynamic works on interference such as the references by Koning (1935) and Ferrari (1957) typically deal with how the propeller race velocity field affects the lift performance of a wing located behind or in front of a propeller.

In recent years elaborate computer calculation methods using lifting surface methods have been applied to wing/jet interactions. Some examples are Levinsky, et al (1970) and Schollenburger (1973) and numerous references cited therein.

Other wake-related studies involve the velocity patterns and tip-vortex paths from the forward foil system in way of the after foil. Some example data for the PC(H) hydrofoil craft have been obtained by Layne (1969), Day (1970), and Power (1971). A

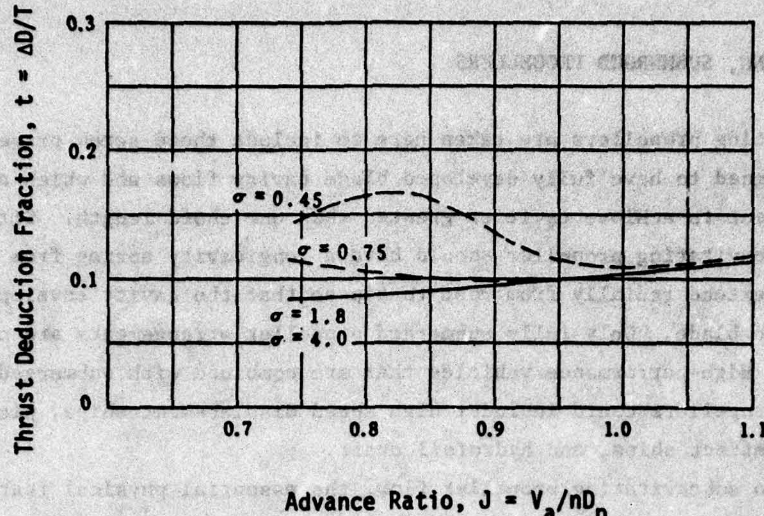

Figure 7 - Thrust Deduction Fraction of Propeller 3897 Operating in Tractor Mode on PC(H) Model Nacelle. V_a = Effective Advance Speed (From Peck (1966))

theoretical analysis for the wing-induced downwash behind a submerged hydrofoil has been given by Kaplan, Breslin, and Jacobs (1960).

Comments and Recommendations

- Experimental data should be generated for the pressure field, free of other wall effects, induced at a flat boundary located near a partially-cavitating propeller. Special attention should be paid to the spatial variation of the mean pressure field.
- Forced ventilation of a propeller is an established technique used to simulate cavitating flows and could be used in towing tank powering experiments representing certain types of partially-cavitating conditions. Systematic experiments with propellers in a range of vapor cavitation numbers could be performed, including wall pressure measurements, to test the validity and define the limits of this idea.
- A workable analytical prediction scheme for propulsion factors for propeller-driven planing hulls is needed. A much improved analysis of planing hull flow through the entire practical speed range is required to do this.
- There is a great lack of published data on propulsion factors applicable to combinations of high speed displacement hulls with well-chosen high performance propellers.
- Very large subcavitating hydrofoil systems being considered will probably focus attention on propulsive interaction problems, including free surface effects on propellers and lifting hydrofoils at lower Froude numbers than are typical for existing hydrofoil craft.

2. SUPERCAVITATING, SUBMERGED PROGELLERS

Supercavitating propellers are taken here to include those screw propellers specifically designed to have fully developed blade cavity flows and which are operated at speeds sufficient to achieve cavities greater than one chord length. Strictly speaking, a supercavitating propeller should have a long cavity spring from each blade leading edge and extend radially from root to tip so that the cavity envelopes the whole side of each blade. Only fully submerged propeller arrangements are considered in this section. High-performance vehicles that are combined with submerged supercavitating propellers could include: high speed displacement ships, planing craft, sidehull surface effect ships, and hydrofoil craft.

Analogous to subcavitating propeller flow, the essential physical feature of supercavitating propellers relating to interactions is the pressure field induced ahead or alongside the disk location. The presence of fully developed blade cavities whose size and shape can vary considerably with advance coefficient complicate the simple picture of induced pressure distribution that can be derived for a non-cavitating propeller. Measurements by Rozhdestvensky (1958) and analysis by Bavin (1965) and Nelson (1964) indicate that the presence of constant pressure cavities on the back side of supercavitating propellers blades limits the level of the induced suction pressure region ahead of the propeller disc. The net effect of the blade cavities is similar to increased blade thickness. Since there is a smaller area for the flow to pass through, and since the velocity is limited, roughly speaking, by the vapor cavitation number velocity $U_o\sqrt{(1+\sigma_v)}$, the approaching flow is retarded instead of accelerated through the propeller disk. There is a competition between the thrust loading effect (suction ahead) and the thickness effect (overpressure ahead).

Gorshkoff (1972) has outlined a history of some of the work on supercavitating propeller flow fields and the consequences on steady propulsive interactions, and has provided an interesting bibliography. Mavlyudov, et al (1973) have presented a survey of engineering calculations applicable mainly to hydrofoil craft using approximate methods for estimating performance of supercavitating propellers. The Lockheed Technology Design Manual (1974_a) presents a large collection of information on supercavitating propellers with a primary orientation toward SES applications.

Near Hulls

There are two general high-performance hull types that could reasonably be paired with submerged supercavitating propellers: high speed displacement ships and planing hulls. As far as is known, there are no published results on propulsion data for either combination.

The experimental studies mentioned in the previous section by Bavin and Miniovich

(1963) and by Prishchemikhin (1975) have provided example propulsion interaction data for conventional ship forms well into the supercavitating regime. The slight upward then eventual downward trend of thrust deduction with decreasing cavitation number has been noted, and is reiterated here in another plot reproduced from Prishchemikhin (1975) in Figure 8. The effect of decreasing advance coefficient on producing reduced

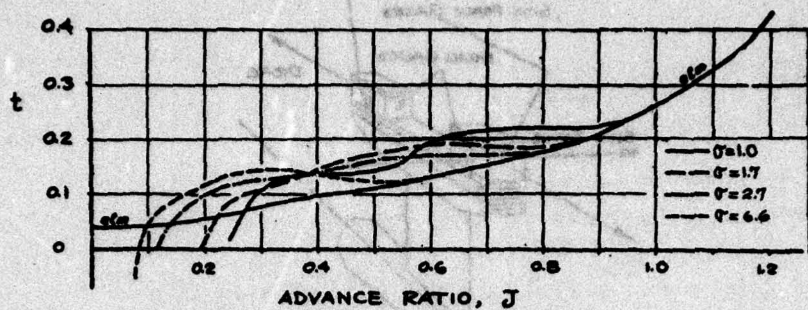

Figure 8 - Thrust Deduction Fraction as a Function of Advance Ratio and Cavitation Number for Cavitating Propeller Driving a 'Victory' Ship Hull (From Prishchemikhin (1975))

or even slightly negative thrust deduction is shown very clearly. This is expected because the low J range corresponds to large blade angles of attack and large cavities which should accentuate the flow- retarding qualities of a supercavitating screw. Unfortunately the geometries of the conventional hull forms used in these experiments are not close enough to high-performance forms to be of much use in that application. The same can be said for all the known published experimental work obtained in the Netherlands Vacutank or in the large water tunnel facilities in Sweden and Norway on the performance of tanker or merchant ship hulls operating with cavitating (partial) screw propellers.

It is speculated that because of the gentle buttock slopes of typical transom stern high-speed displacement hull forms forward of the propeller disk location, the dramatic effects on thrust deduction observed with a fully-cavitating propeller near a steep-ended Victory ship hull will not be realized.

Near Strut/Pod

Supercavitating propellers mounted on strut-pod arrangements have been considered as propulsor systems for large, high speed SESs. Such configurations could conceivably also be used on high speed displacement ships or for planing hull propulsion as well.

The propeller mounted on a strut-pod arrangement may be either a tractor or a pusher. Striking differences in their characteristics are due mainly to propulsive interactions.

Propulsion performance of <u>tractor</u> propellers mounted on parabolic-shaped pods have been studied experimentally, for example, by Hecker and Peck (1969) and by Scherer and Barr (1969). Tractor propellers have some advantage over pusher arrangements in that they operate in clear, open flow, and thus avoid unsteady forces due to

circumferential variations in blade loading in a wake, as well as the cavitation and erosion that also accompany the wake. They do have special problems such as induced drag on the pod-strut combination, side forces induced by the strong rotation of the propeller slipstream, and possible strut and pod erosion due to cavity collapse.

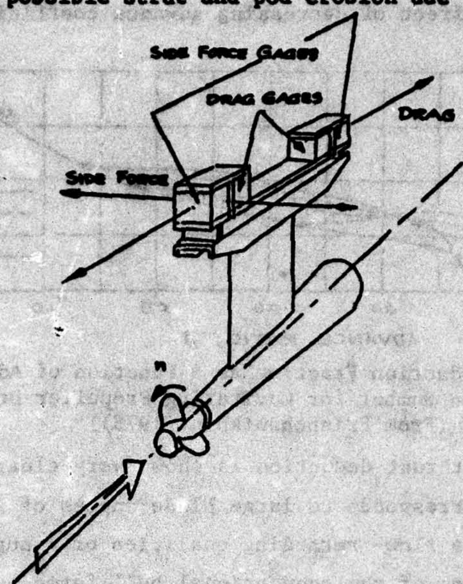

Figure 9a- Schematic of Tractor Propeller Model Mounted to Pod-Strut (Hecker and Peck (1969))

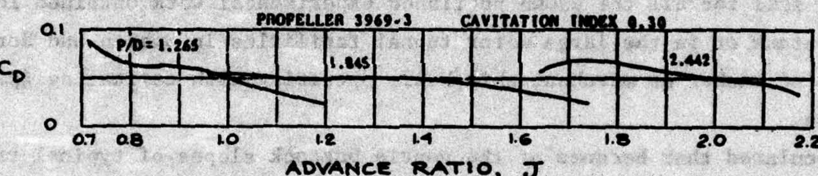

Figure 9b- Thrust-Induced Drag Coefficient Measured on Pod-Strut System (From Hecker and Peck (1969))

Figure 9a is a sketch of the model geometry tested by Hecker and Peck (1969) in a 36-inch water tunnel, using an existing 3-bladed, controllable-pitch, supercavitating propeller. Figure 9b shows example measured propeller-induced drag increment coefficients displayed versus advance coefficient, with contours of the three pitch-to-diameter ratios tested, at a centerline cavitation number of 0.3 (53.5 knots). Corresponding curves for the side force on the strut-pod-propeller combination are shown in Figure 10.

The supercavitating tractor propeller model tested by Scherer and Barr (1969) in a free surface water channel is shown schematically in Figure 11. The net drag, lift, and side force on the entire strut-pod-propeller combination were measured, so the open water propeller characteristics of the model propeller must be used to estimate the performance of the propeller in the 'ahead' condition. Figure 12 is a plot of measured drag and net thrust versus advance coefficient scaled to prototype size for simulated operation at 80 knots ($\sigma_v = 0.125$). A dramatic increase in induced pod-strut drag is

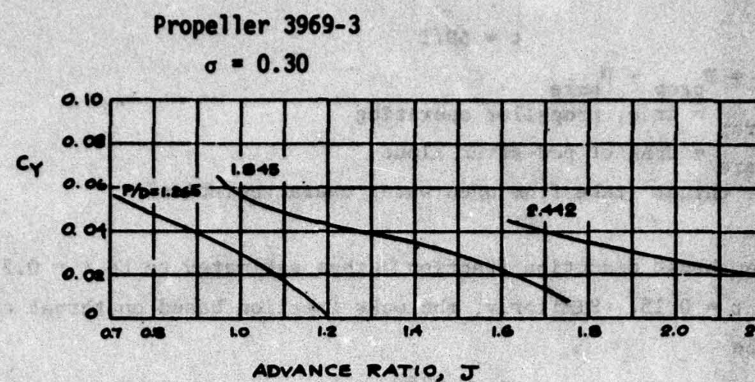

Figure 10 - Thrust-Induced Side Force Coefficients on Pod-Strut System of Figure 9a (From Hecker and Peck (1969))

seen in the low J range. This is thought to be caused mainly by the pressure distribution associated with the large blade cavities. If the bare pod drag is interpreted as appendage drag, then the thrust deduction fraction for this configuration is dependent on the <u>difference</u> in pod-strut drag due to the action of the propeller,

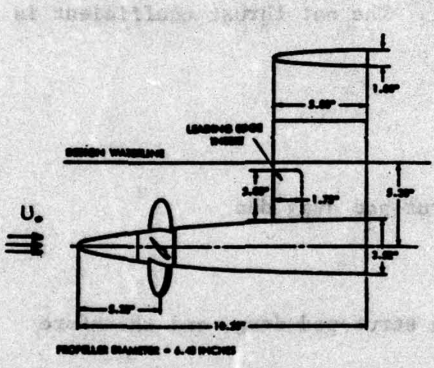

Figure 11 - Schematic of Tractor Propeller Model Mounted to Pod-Strut (From Scherer and Barr (1969))

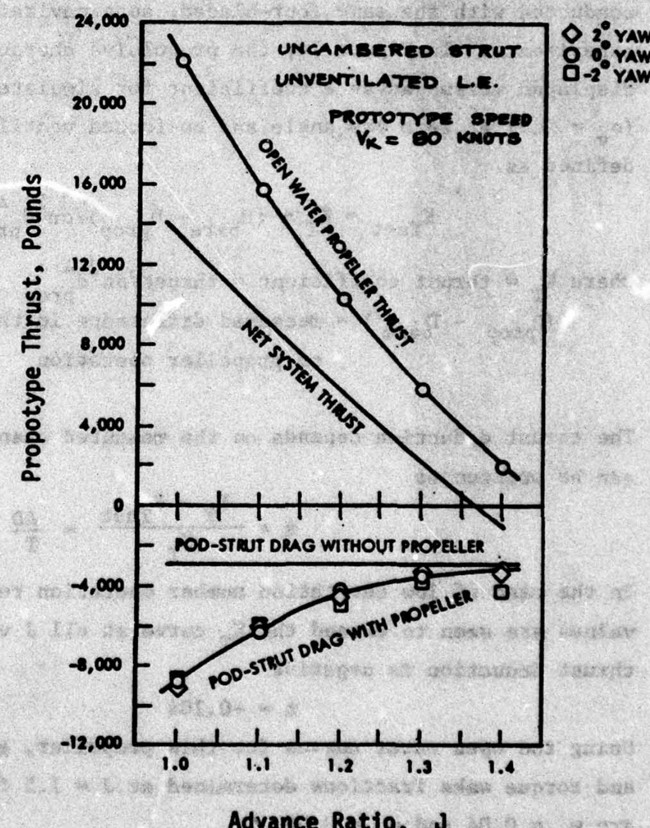

Figure 12 - Scaled Thrust and Drag versus Advance Ratio for Supercavitating Tractor Propeller of Figure 11 (From Scherer and Barr (1969))

$$t = \Delta D/T$$

where $\Delta D = D_{prop} - D_{bare}$

D_{prop} = drag, propeller operating

D_{bare} = drag of pod-strut alone

T = thrust (take from open water characteristics)

At J = 1.0, the thrust deduction fraction is thus estimated to be t = 0.27, and at J = 1.2, it is t = 0.15. Similarly, the wake fraction based on thrust can be estimated at J = 1.2 to be

$$w_T = -0.025.$$

Supercavitating pusher propeller arrangements of strut-pod-propeller have been tested by Barr (1969) and by Altmann (1969_a) using unstepped- and stepped-pod designs, respectively.

Example results are included here from the work of Altmann (1969_a) that illustrate negative thrust deduction. The configuration pictured in Figure 13 is a stepped-pod version of the smooth-pod arrangement tested by Barr (1969). Test were conducted with the same four-bladed, supercavitating propeller designed for Barr's experiments. In Figure 14, the propulsive characteristics of this arrangement are displayed versus advance coefficient for simulated 60 knot prototype operation ($\sigma_v = 0.2$) at zero yaw angle and no forced ventilation. The net thrust coefficient is defined as

$$K_{Tnet} = K_T + (D_{bare} - D_{prop})/\rho n^2 d^4_{prop}$$

where K_T = thrust coefficient = thrust$/\rho n^2 d^4_{prop}$

$(D_{prop} - D_{bare})$ = measured difference in the strut-pod drag due to propeller operation

The thrust deduction depends on the measured change in strut-pod drag, and therefore can be written as

$$t = \frac{K_T - K_{Tnet}}{K_T} = \frac{\Delta D}{T}$$

In the case of low cavitation number operation represented by Figure 14, the $K_{T_{net}}$ values are seen to exceed the K_T curve at all J values, and for example at J = 1.5, the thrust deduction is negative

$$t = -0.104$$

Using the open water curves for this propeller, as provided by Barr (1969), the thrust and torque wake fractions determined at J = 1.5 for the case represented by Figure 14 are $w_T = 0.04$ and $w_Q = 0.08$.

Considerably more supercavitating propeller propulsive data are available in Altmann's report, including the effects of yaw angle, forced air ventilation issuing from the base of the step, and comparisons with the smooth-pod results of Barr (1969).

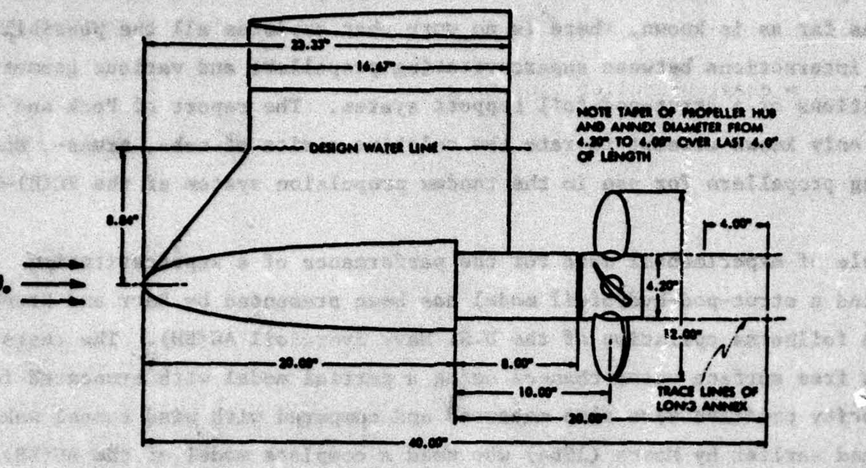

Figure 13 - Schematic of Pusher Propeller Mounted on Stepped Pod-Strut (From Altmann (1969_a))

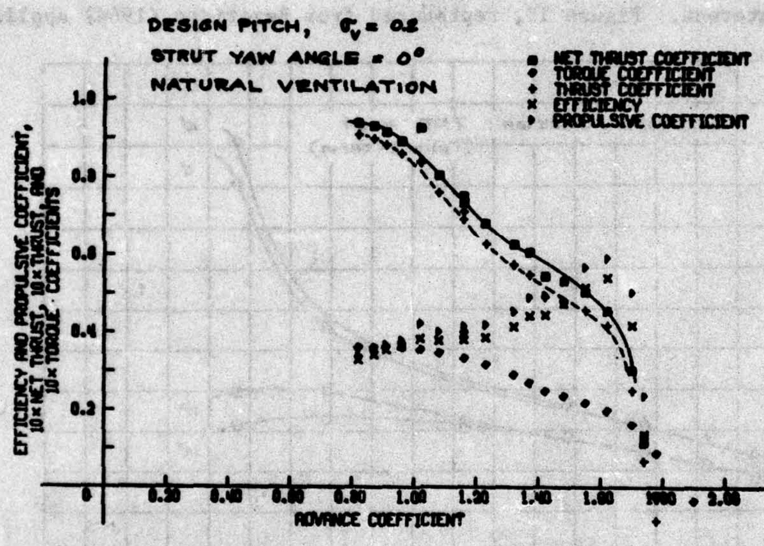

Figure 14 - Measured Supercavitating Pusher Propeller Performance versus Advance Ratio (From Altmann (1969_a))

The latter report itself contains a wealth of propulsive data pertinent to supercavitating propeller operation with the original unstepped-pod-strut configuration.

Near Strut/Pod/Foil

The presence of a hydrofoil attached to or located near the pod can alter somewhat the propulsive interactions of the strut-pod-propeller combination, if only due to changes on the wake pattern. Supercavitating hydrofoils and base vented struts

will undoubtedly exhibit different thrust deduction properties than fully wetted foils and struts. As far as is known, there is no work that explores all the possibilities of propulsive interactions between supercavitating propellers and various geometries and flow conditions of a strut-pod-foil support system. The report of Peck and Hecker (1971) is the only known attempt to rate the relative merits of sub-, trans-, and supercavitating propellers for use in the tandem propulsion system of the PC(H)-Mod 0 and Mod 1.

An example of experimental data for the performance of a supercavitating propeller behind a strut-pod-hydrofoil model has been presented by Barr and Stephens (1965) for the foilborne operation of the U.S. Navy Hydrofoil AG(EH). The tests were performed in a free surface water channel using a partial model with truncated foils. Some wake velocity profiles were also measured and compared with wind tunnel wake surveys obtained earlier by Moore (1964) who used a complete model of the AG(EH) hydrofoil strut-nacelle-wing arrangement.

For the interaction between a hydrofoil and fully cavitating propeller located a distance of 0.72 radius behind the foil trailing edge, the brief report by Beveridge (1964) is of some interest. Figure 15, reproduced from Beveridge (1964) applies to the

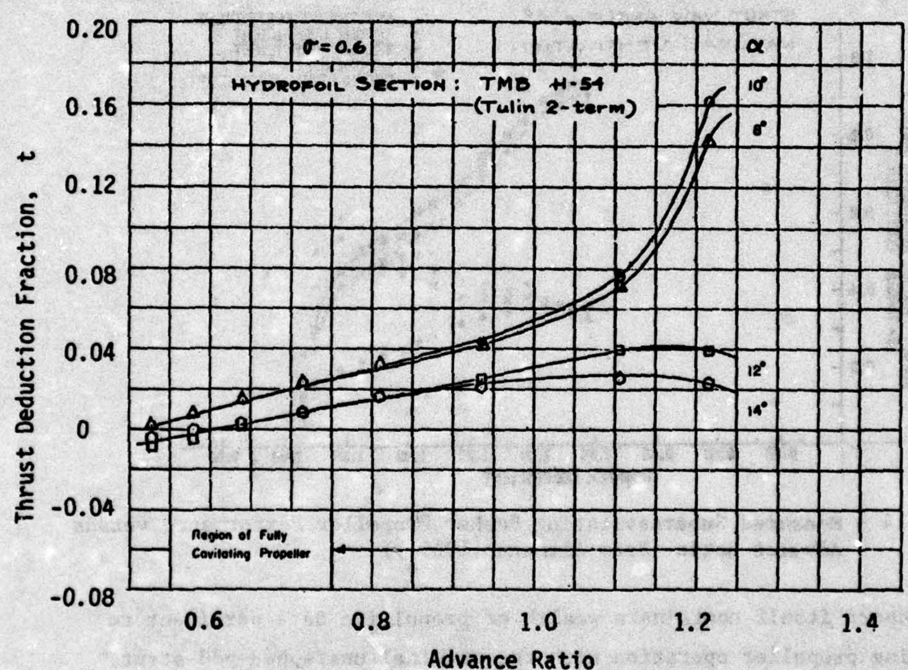

Figure 15 - Measured Thrust Deduction Fraction for a Hydrofoil Mounted in Front of a Fully Cavitating Propeller (From Beveridge (1964))

case of $\sigma_v = 0.6$, and shows the decrease of measured thrust deduction with reduced J at several values of foil angle of attack. Slightly negative values are observed for $J < 0.6$ and very large angles of attack. Beveridge also presented results of velocity field calculations ahead of and behind the propeller using Kerwin's (1964) propeller

lifting surface program.

Comments and Recommendations

- Propulsion interaction data are not available for fully cavitating propellers driving true high-performance displacement hull shapes. Should experiments with such arrangements ever be performed, careful documentation of the pressure field induced on the hull is vital to better understanding of the inferred interactions.
- Future propulsion studies on strut-pod-propeller and hydrofoil arrangements should explore the many possible combinations of both partial - or fully - cavitating foils, struts, pods and propellers and should entail a direct display of the propulsive interaction properties.
- There will unquestionably be severe propulsion problems for very high speed hydrofoil craft, such as a vehicle that could use the recently developed technology for high speed struts and foils (Shen and Wermter (1976)). Experiments and analysis on propulsive interactions must play an important role in achieving practical arrangements.

3. PARTIALLY-SUBMERGED, SUPERCAVITATING PROPELLERS

Partially-submerged supercavitating propellers are free screw propulsors (typically) whose blades are immersed over only a part of one revolution. Under ideal conditions, the blades operate self-ventilated, each blade providing the ventilation path through the trailing cavities open to the atmosphere.

General performance features of partially-submerged propellers are described, for example, by Hadler and Hecker (1968) and by Hecker (1973) using data obtained in a towing basin; and by Bohn and Altmann (1975) using data obtained in a free surface water channel. A wide ranging collection of information on supercavitating propellers, including partially-submerged propellers, has been provided by Lockheed (1974_a). Hecker and Altmann (1976) have presented an extensive review and bibliography on the subject, also encompassing partially-submerged propellers.

As regards the topic of interactions, this type of supercavitating propeller is discussed separately from the fully-submerged variety because of the special mixture of physical effects that characterize their operation. Problems stem from the fact that true blade self-ventilation (complete vented cavities on the suction side, fully wetted pressure side) occurs over only a narrow J-range, and that the model scaling becomes more complicated both at the high J and low J ends of the complete range. At high J-values, partial cavitation and ventilation are mixed, and the transition to full ventilation may be accompanied by great flow unsteadiness and vibration. See Kruppa (1972). At low J-values, thick blade cavities are under the influence of local

cavitation and are known to grow in adjustment to the flow retardation through the disk. Additionally, massive air entrainment out of the large cavities will alter the extent of ventilation, possibly limited by the cavity choking phenomenon. The necessary flow of air down into the ventilated cavity also dictates that the air pressure-to-cavity pressure be correctly modeled in experiments at low J values.

Other problems are associated with the distortion of the free surface near the propeller. Particularly at low J-values, the surface elevation can rise significantly ahead of the disk. In the lateral direction, the surface is drawn down near blade entry and pushed up near the exit on the opposite side.

These effects combine in such a way that there is no simple way to perform an open water test with a partially-submerged propeller. Merely the surface distortion that occurs near the propeller will change the submergence ratio as a function of thrust loading and speed. If a flat test boat or plate is placed in front of the disk, there will be an influence of the wake from the boundary layer. To date, what little propulsive interaction data exists has been obtained by measuring the propeller performance (in place) and the forces on the support structure separately.

Near Hulls

There are two known examples of propulsion experiments with partially-submerged propellers near hulls, and they both involve variations of narrow SES sidehulls. Altmann (1969_b) has presented results of tests with a 6-bladed semi-submerged propeller operated behind three similar SES sidehull condigurations, all fitted with a cylindrical fairing just upstream of the propeller. Independent measurements were made of the sidehull drag and the propeller forces. Cavitation scaling was employed. Figure 16, reproduced from Altmann (1969_b), shows curves of the changes in model drag versus advance coefficient that seem to display the expected negative thrust deduction effect. The dip in the measured ΔDRAG values was not anticipated. At J-values below the sudden decrease in ΔDRAG, there was reported a noticeable unsteadiness in the drag readings that was not matched by fluctuations in the propeller thrust or by obvious ventilation of a local region on the hull. Apparently there was sufficient uncertainty regarding these drag changes, that they were not used to generate net thrust coefficients from the measured thrust data. Phenomena like this should provoke further study.

The model propeller-sidehull configuration tested by Barr and Altmann (1970) became part of the basis for the propulsion system used on the Bell Company SES 100B. In order to satisfy the thrust requirements at low speed, a twin-ramp system pictured in Figure 17 was used to adjust the flow level entering the propeller disk. The same separate sidehull drag and propeller force measurement scheme employed by Altmann (1969_b) was used. In addition, static pressure data were taken at 15 points on each ramp, and these showed a noticeable overpressure effect building up at low J-values for

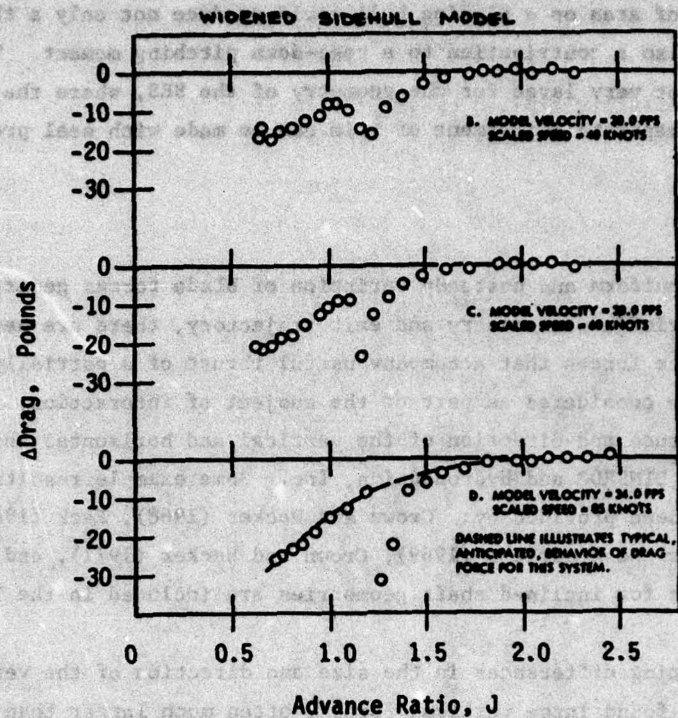

Figure 16 - Induced Drag on a Model SES Sidehull Due to Operation of Partially-Submerged Propeller (From Altmann (1969$_b$))

the cases displayed.

As far as is known, there are no data for drag increments or pressure measurements on a planing hull located near an operating partially-submerged propeller. It is anticipated that an overpressure ahead of a supercavitating propeller integrated

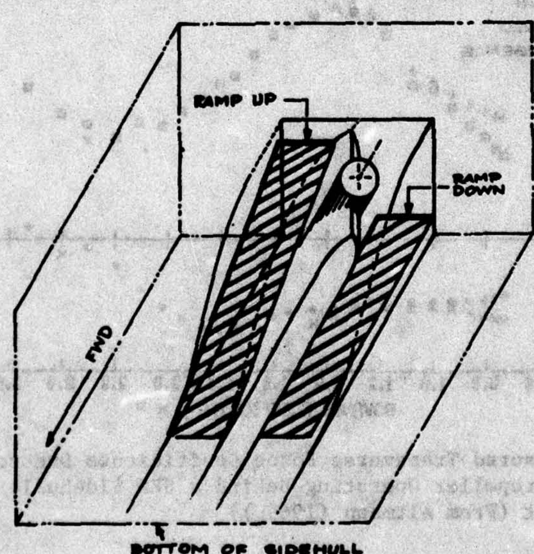

Figure 17 - Twin Ramp System for Partially-Submerged Propeller Mounted on a SES Sidehull. (From Hecker and Altmann (1976))

over the broad expanse of area on a planing hull could produce not only a thrust deduction effect, but also a contribution to a nose-down pitching moment. These effects are evidently not very large for the geometry of the SES, where the hulls are very narrow, and where separate adjustment of trim can be made with seal pressures.

Transverse Forces

Owing to the non-uniform and unsteady variation of blade forces generated as the blades perform their periodic water entry and exit trajectory, there are net vertical and horizontal transverse forces that accompany useful thrust of a partially-submerged propeller. These can be considered as part of the subject of interaction.

Data on the magnitude and direction of the vertical and horizontal forces have been obtained mainly at DTNSRDC and Hydronautics, Inc. Some example results on transverse forces have been provided by: Crown and Hecker (1968), Peck (1968), Hecker and Crown (1969), Hecker and Hendrican (1969), Crown and Hecker (1971), and Bohn and Altmann (1975). Results for inclined shaft geometries are included in the latter two reports.

There are interesting differences in the size and direction of the vertical force. Altmann (1969_a) found large vertical forces, often much larger than the thrust. Figure 18, for example, shows the vertical and horizontal force coefficients based on

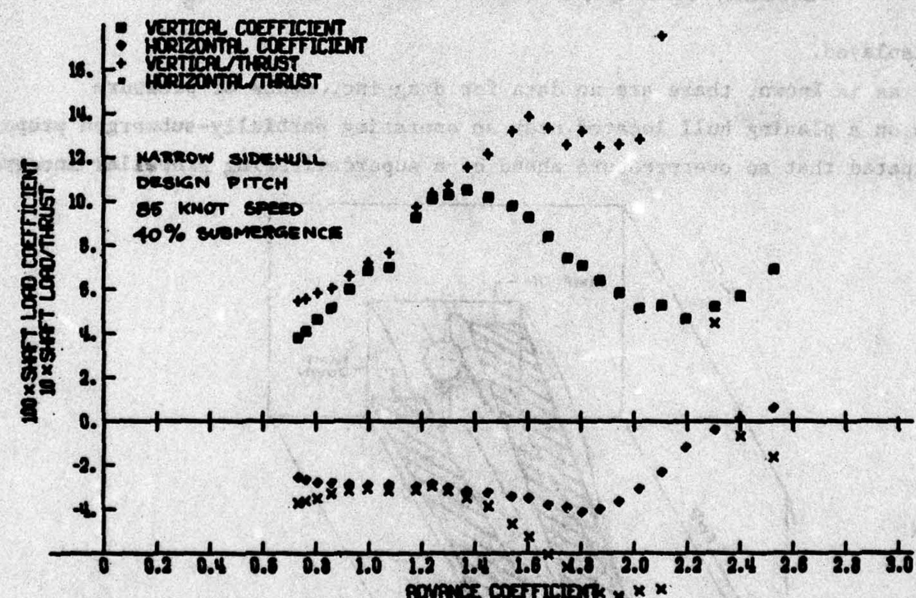

Figure 18 - Example Measured Transverse Force Coefficients Due to a Partially-Submerged Propeller Operating Behind a SES Sidehull. Water Channel Test (From Altmann (1969_b))

propeller diameter D, and rotational speed n

$$K_H = F_H/\rho n^2 D^2$$
$$K_V = F_V/\rho n^2 D^2$$

and their ratios with thrust plotted versus advance ratio. It should be noted that the sign of the horizontal force is opposite from the convention used presently. With the propeller-SES sidehull arrangement having twin ramps, Barr and Altmann (1970) found generally smaller magnitude vertical forces. Just how the differences in propeller geometries and/or in the sidehull geometries between these two experiments can account for these changes is not clear.

Different trends in the vertical forces, sometimes negative values, were observed by Hecker and Crown (1969). The effect of blade thickness was found by Crown and Hecker (1968) to cause a definite negative trend for K_V, as shown in Figure 19. Raked blades on propellers at an inclination angle seemed to reduce the magnitude of vertical force, as reported by Crown and Hecker (1971).

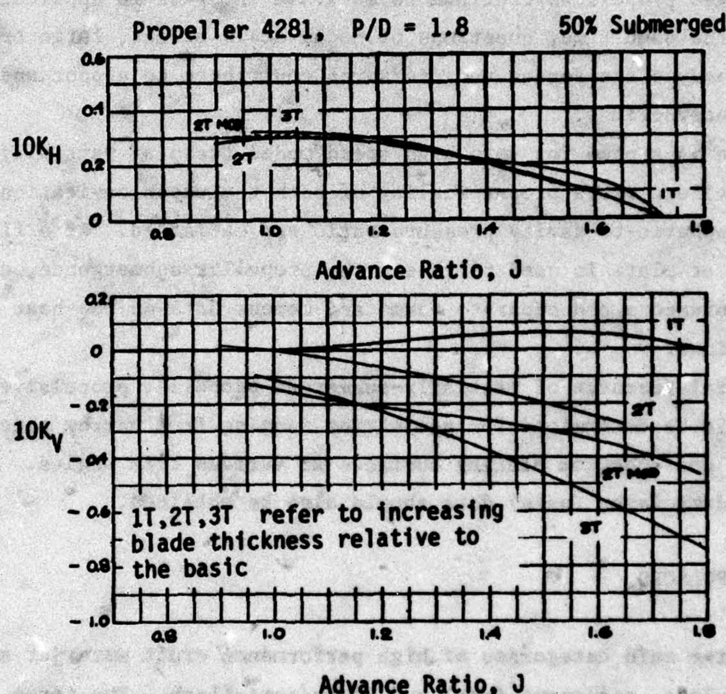

Figure 19 - Horizontal and Vertical Transverse Force Coefficients Produced by Propeller 4281 (Three Thickness). Towing Basin Test (From Crown and Hecker (1968))

Unsteady Transverse Forces

Highly unsteady blade forces and pressure distributions are distinctive features of partially-submerged propeller operation. Example experimental observations of the fluctuating force magnitudes and time histories have been reported on by Kopko (1969), Dobay (1971), and Altmann (1974). Information on the unsteady pressure histories and analysis can be found in the report by Altmann, Bohn, and Schaeffer (1975).

Tandem Arrangements

There has been a general feeling that tandem arrangements of supercavitating propellers would be poor performers because of adverse interactions between blade cavities. From a recent experimental study with closely spaced, offset, and slightly overlapping partially-submerged propellers performed by Roddy (1976), it appears that there is no dramatic destructive interference, and that net propulsion performance can be fairly well estimated by adding the results of separate (single) propulsion experiments.

Comments and Recommendations

The high apparent efficiencies and potentially low appendage drag of partially-submerged propellers continue to motivate interest in applications of these propulsors. At the same time, questions of model scale effect, large transverse forces, and unsteady blade forces and pressures contribute to a poor understanding of hull-propeller interactions.

- There is a need for very high speed model tests of partially submerged propellers where proper scaling of both the vapor cavitation number and atmospheric-to-cavity pressure ratio are satisfied. If a flat bottom test boat or plate is used to govern the propeller submergence, careful pressure measurements and separate force and moment data on the boat should be obtained.
- General features of partially-submerged propeller propulsive interactions should be determined for geometries ranging from narrow sidehulls to wide flat and V-bottom planing surfaces at various trim angles. Careful boundary layer (wake) data should also be obtained.

4. WATERJET PROPULSORS

There are two main categories of high performance craft waterjet systems, based on the type of inlet: pod-strut (ram) and flush/semi-flush. The first type seems well suited for hydrofoil craft applications, although pod-strut arrangements mounted on hulls have also been employed. The second type appears appropriate for planing boats and for sidehull air cushion craft. An interesting up-to-date review of the applications of waterjet propulsors as of 1976 has been given by Etter (1976).

Judging from the published material on waterjet design methodology, it appears that techniques of dealing with the propulsive interactions require a somewhat different approach than the classical naval architecture point of view. The idea of accounting for propulsor-hull efficiency and an isolated propulsor efficiency is not generally applicable. This is because the flow geometries of the waterjet systems are often so integrated with the hull or support structure that a separate characterization

of the system elements falls into a different form than the familiar thrust deduction, wake fraction, and relative rotative efficiency.

Two examples of efforts to organize the propulsion properties of generalized reaction-propulsors (including waterjets) for high speed craft along the traditional lines of interaction can be found in selected chapters in the works of Kulikov and Khramkin (1970) and Mavlyudov, et al (1973). When it comes down to specific waterjet systems, however, these authors have employed hydraulic performance parameters similar to those used in the literature of the U.S. and Europe.

Propulsive interaction in a waterjet system entails a bookkeeping problem of what penalties to assign to the performance of various elements. The connection between propulsor and vehicle is essential, and the bookkeeping must be able to account for ingested boundary layer flow (influence of the hull) on thrust and on the quality of flow presented to the pump. One successful scheme of describing what amounts to a hydraulic circuit for the waterjet system is that presented by Barr (1974) and Johnson (1974). The essential relationships are outlined by E. Miller in Appendix 8 of this ATTC volume.

The basic idea for sizing a waterjet arrangement for a given vehicle of known bare hull drag, is to match the vehicle drag with the net thrust (thrust available) produced by the waterjet in place and operating. Added drag due to the waterjet installation must be subtracted from the gross thrust capability. If the on-board weight within the ducting is counted as part of the bare hull vehicle weight, the net thrust of the installed waterjet is

$$T_{net} = \rho Q(V_j - V_m) - C_{D_1} \tfrac{1}{2}\rho U_o^2 A_1$$

where the notation of E. Miller, Appendix 8 applies.

With reference to the basic expressions for waterjet system performance outlined by Miller, only a brief reiteration is necessary here. For general waterjet systems the propulsive interactions are also embodied in the performance factors:

C_{D_1} = external drag coefficient of the inlet added to the bare hull plus any appendages associated with the installation $= D_1/(\tfrac{1}{2}\rho U_o^2 A_1)$

$K = k + 2g\Delta h/V_*^2$ = total loss coefficient

$k = 2gh_L/V_*^2$ = internal and diffusion head loss coefficient

V_m/U_o, V_*/U_o = momentum and energy velocity ratios of nonuniform flow passing through the inlet area, A_1

Energy recovery at the downstream end of the diffuser section is related to (1-K) with some adjustment for elevation differences.

The most important interaction effects between hull and waterjet performance are

dependent on the inlet external drag coefficient C_{D_i}, and the two flow quality parameters V_m/U_o and V_*/U_o. To a lesser extent the internal geometry and loss schedule as revealed in the energy recovery, (1-K), can also reflect influences exerted by the external flow.

Experiments to obtain these performance factors must be carefully chosen since it is usually possible to satisfy only one out of the three major scaling parameters involved: cavitation number, Reynolds, and Froude numbers. For high speed inlets or inlets that must accomodate large inlet velocity ratio excursions, the cavitation number is most important, although scaling the boundary layer thickness with Reynolds number should also be accounted for. For external interaction properties, the Froude number and the complex ventilation scaling take on added importance.

An important feature of waterjet systems that can exert an interaction effect is the weight of on-board water, which will cause an increase in the basic hull resistance over the empty craft resistance by the amount $W_w(D/L)_v$. Here W_w is the weight of water within the ducting system and $(D/L)_v$ is the hydrodynamic drag-to-lift ratio. The added weight can also alter the trim of the vehicle, introducing direct drag changes to a trim-sensitive craft.

Most of what is known about performance factors and how they scale is scattered throughout numerous reports, but detailed and well founded data exist for relatively few and specific flow geometries. Overall reviews of the literature, state-of-the-art design discussions, and bibliographies are to be found in references such as Brandau (1968), Barr and Stark (1973), Barr (1974), Callenen and Nelka (1974), and the Lockheed Technology Design Manual (1974_b).

Pod-Strut (Ram) Inlets

Examples of current design methods for pod-strut inlets have been presented by Sherman and Lincoln (1969), Levy and Meggitt (1971), and Developmental Sciences, Inc. (1973). The first two deal with details of analysis and design. For example, Sherman and Lincoln (1969) illustrate succinctly the characteristic trade-off between external inlet drag coefficient and the internal losses for several variations of ram inlet systems. Figures 20a,b reproduced from Sherman and Lincoln, show the schematic of a base-vented ram inlet (step at maximum thickness) designed for cavitation-free operation at 100 knots, and the corresponding calculated variation of the external drag coefficient C_{D_i} and internal loss factor $K_i = 2gh_L/U_o^2$, plotted versus inlet velocity ratio V_i/U_o. As far as is known, the performance predictions of Sherman and Lincoln have not been verified experimentally.

Barr (1974) has included a substantial portion of his review to hydrodynamic problems of pod-strut inlet combinations using hydraulic estimation techniques.

Experiments have been carried out at DTNSRDC on a variable inlet area, pod-strut inlet with a translating plug centerbody designed by DSI. Performance data with regard to overall drag, internal head loss, and cavitation inception boundaries were obtained

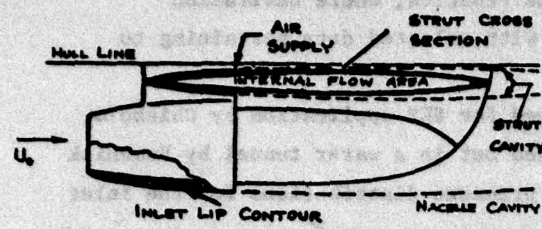

Figure 20a- Schematic of Base-Vented Pod Inlet System (Lincoln and Sherman (1969))

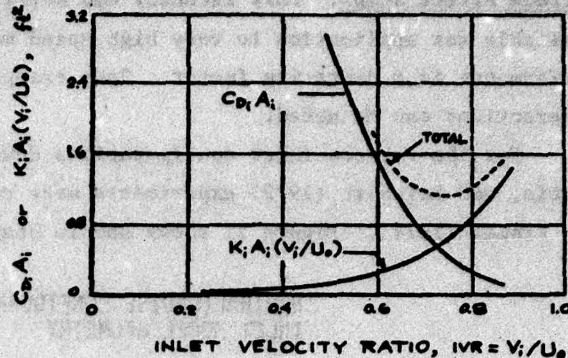

Figure 20b- Calculated External drag and Internal Loss Factors for Base Vented Pod Inlet System (From Lincoln and Sherman (1969))

and reported on in preliminary fashion by Sobolewsky (1977).

A collection of external drag coefficients and internal loss coefficients for various scoop shapes has been assembled by Hoerner (1965).

Schwind (1969) has presented results of wind tunnel experiments to determine pressure recovery characteristics of a scoop-like inlet operated at various submergences within a wall boundary layer, including a case with the inlet centered at the edge of the layer. The two unique features about the arrangement were the 45 degree back-angled scoop lip and the abrupt dump diffusion. Application of this inlet to a waterjet would require careful checks on the lip surfaces and scoop-wall juncture for cavitation problems.

Flush/Semi-Flush Inlets

Flush and semi-flush inlets can be regarded as being imbedded in the hull surface. Such inlets fit naturally into the geometry of low deadrise planing hulls. Their application to surface effect ships usually entails the use of a special fairing or bulge to provide a locally flat region in the otherwise thin, high deadrise sidehull.

Representative design methods have been presented by Johnson, et al (1972) (reviewed and updated by Krishnamoorthy (1977)), Chisholm, Kintis, and Reichert (1972), and Aerojet General Corp. (1972). The Lockheed Technology Design Manual (1974_b) provides an extensive design compendium with an orientation toward SES applications.

The classical work on submerged inlets by Mossman and Randall (1948) still serves as an excellent level of achievement for flush inlet performance, without regard to cavitation. It contains extensive data on the external drag and internal pressure recovery for inlets imbedded in a flat wall.

Surface Effect Ships. Only recently has sufficient data for flush inlets become available for application to very high speed marine vehicles, where cavitation performance is a dictating factor. Some examples with selected data pertaining to interactions can be noted.

For the various inlet configurations developed for SES application by Chisholm, Kintis, and Reichert (1972) experiments were carried out in a water tunnel by Humenick and Kramer (1974). Figure 21 shows sample static pressure distributions for the inlet

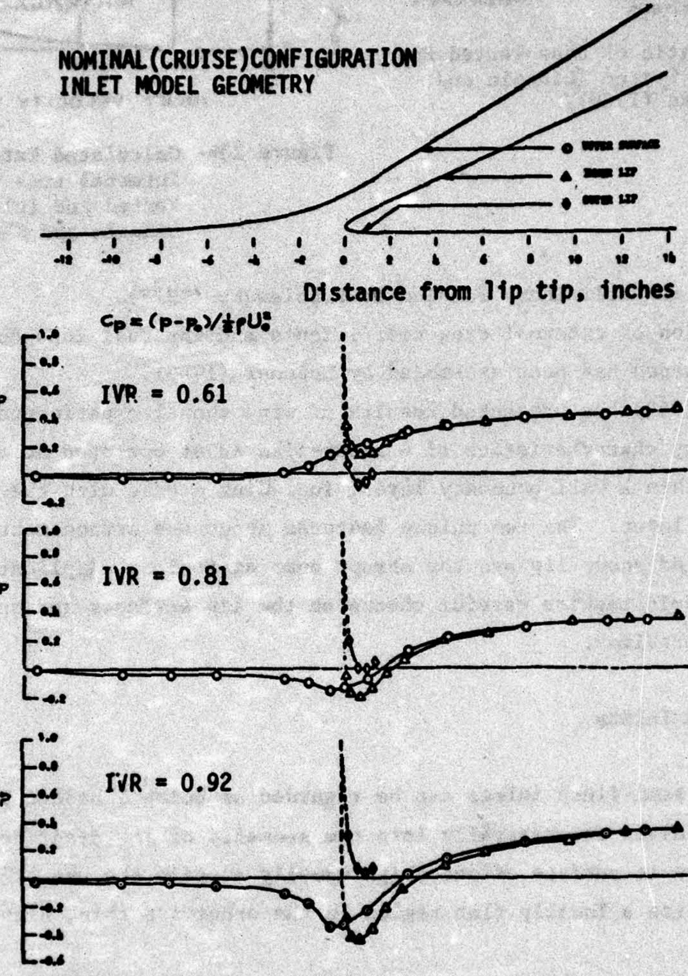

Figure 21 - Sample Pressure Distributions on a Model Flush Inlet
(From Humenick and Kramer (1974))

at cruise condition at three different inlet velocity ratios, IVR = $V_i/U_o = Q/A_iU_o$. It is interesting to note that as the IVR increases, there occurs a deepening suction valley on the upper surface (ramp), and that the effect extends forward of the lip as well. An opposite pattern of pressure occurs on the outside lip. The slight suction peak at low IVR gives way to mostly positive pressures at higher IVRs. One can easily imagine net interaction forces arising from the external pressure integration.

Data were also gathered by Humenick and Kramer (1974) for the duct velocity profiles at the diffuser outlet and head loss factors.

Extensive data has been obtained over several years at Hydronautics, Inc. on the characteristics of deformable ramp, variable area, flush/semi-flush waterjet inlet

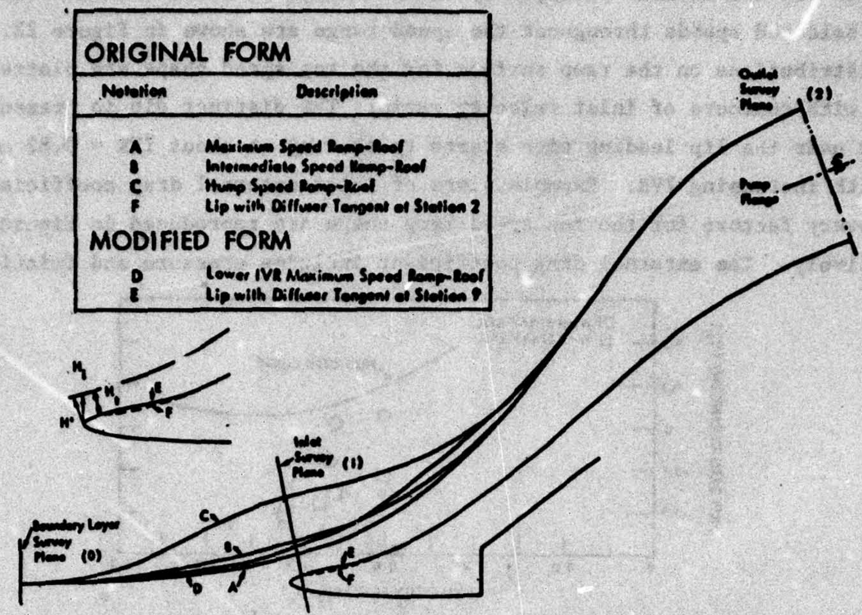

Figure 22 - Shapes of a Deformable-Ramp, Variable-Area Flush Inlet for SES Application (From Etter and Stark (1976))

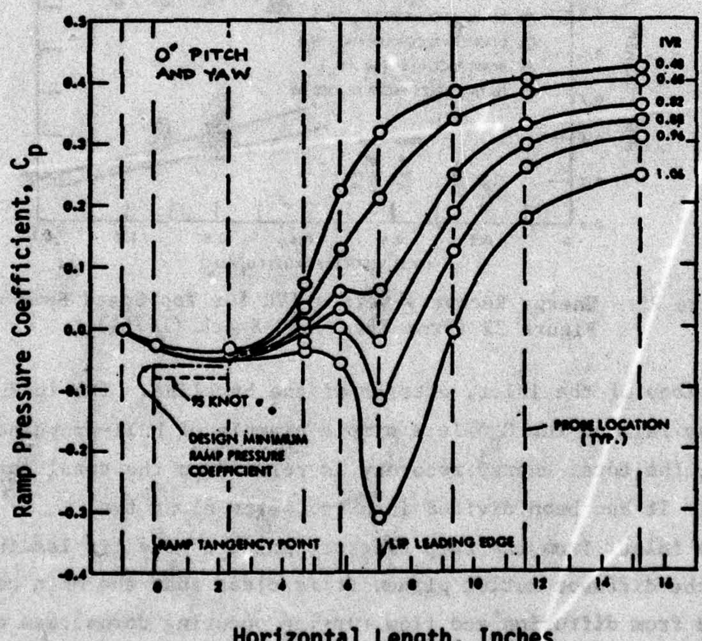

Figure 23 - Measured Effect of IVR Ramp Pressure Destributions for Top Speed Ramp (From Etter and Stark (1976))

configurations principally for installation in the sidehulls of high speed SESs. For example, Etter and Stark (1976) have presented inlet performance data from water channel tests for the backfit waterjet system installed on the SES 100A. Various ramp shapes for selected speeds throughout the speed range are shown in Figure 22. Static pressure distributions on the ramp surface for the top speed shape are plotted in Figure 23, with contours of inlet velocity ratio. The distinct dip in pressure coefficient near the lip leading edge starts to show up at about IVR = 0.82 and deepens steadily with increasing IVR. Example plots of inlet external drag coefficient and energy recovery factors for the top speed ramp shape are reproduced in Figures 24 and 25, respectively. The external drag coefficient includes pressure and friction drag on

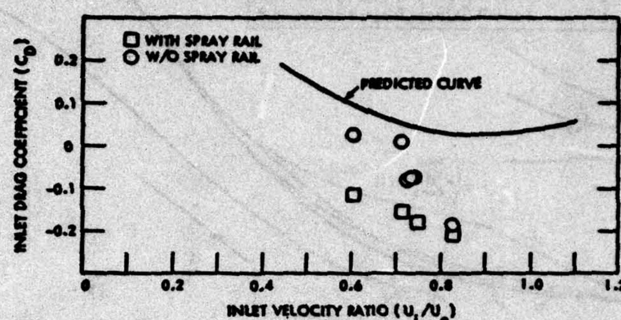

Figure 24 - Inlet External Drag Coefficient versus IVR for Modified Top Speed Ramp of Inlet in Figure 22 (From Etter and Stark (1976))

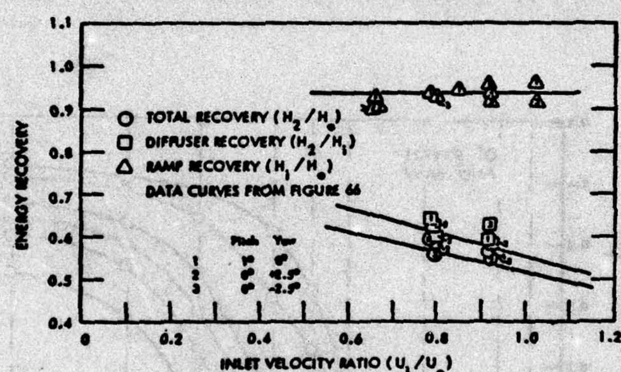

Figure 25 - Energy Recovery versus IVR for Top Speed Ramp of Inlet in Figure 22 (From Etter and Stark (1976))

the external portions of the inlet, outside of the baseline. The influence, in this case, of the spray rail on the C_{D_i} is a simple example of hull-propulsor interaction. As noted earlier, the total energy recovery is related to the total internal losses from all sources. It has been divided into two parts along the the length of the inlet: from the ramp tangency point to the lip leading edge, and from the lip to the diffuser outlet plane. It is clear that the main contribution to energy loss comes from diffusion and flow turning occuring downstream of the lip. Note that the effects of the small pitch and yaw changes on energy recovery appear to be small, but measureable.

Similar performance data to Reference 35 has been generated by Poquette, et al (1976) for a flush-mounted waterjet inlet-diffuser system designed for the large SES project.

A considerable amount of waterjet performance data has been collected from experiments with the SES testcraft XR-1B fitted with semi-flush inlets, and has been reported on by Burke, et al (1972). Included are ramp and lip pressure distributions, loss factors, boundary layer profiles, internal duct velocity and pressure contours.

The Rohr Industries Summary Report on waterjet inlets (1976) for the large SES is a major assemblage of data on the drag, internal loss, and cavitation limit performance for a semi-flush waterjet system employing a flexible ramp roof, variable-area geometry. Data for a droop lip arrangement is also included.

<u>Planing Hulls</u>. As regards performance characteristics of flush inlets for use in planing hull propulsion, the known experimental programs have been carried out on a completely different scale than for the SES applications. Considerably less detailed information is available on waterjet systems for planing craft, but the applications in the sport boat field are widespread (see Hart (1975)).

In general, the requirements are different than those for a SES application. The speed range is lower and therefore the design cavitation number is larger. Limits on geometry imposed by cavitation inception become less important than flow separation limits. Fixed area inlets are the rule rather than the exception. Also, the hull trim angle excursions expected during operation are very much larger than those allowed for SES hulls, and from the point of view of interactions may play a more noticeable role in the variation of energy recovery.

Alder (1976) has reported on a full scale experiment with a 31 foot, 12,600 pound planing boat. The tests concentrated on the internal velocity and static pressure profiles along two vertical paths in the duct just ahead of the pump impeller. Figure 26 illustrates a typical finding for the velocities and shows the marked tendency for upper surface separation at the higher craft speeds.

Purnell (1976) has examined possible benefits for planing boat propulsion using very wide flush inlets to ingest more boundary layer flow than is possible with narrower inlets. This could be a positive exploitation of a propulsion interaction effect. The complexities of the interaction are subtle. Although there are clear gains to be achieved by drawing in slower moving fluid for the thrust capability, the non-uniformities of the velocity field have a way of aggrevating internal losses farther downstream, especially when combined with flow diffusion.

Towing basin experiments have been performed with a model planing boat (DTNSRDC Model No. 5222) free to heave and trim, and fitted with two different aspect ratio flush inlets of width-to-height equal to 1.0 and 3.187. The design inlet velocity ratio was accurately modeled, but the nozzles were designed such that self-propulsion

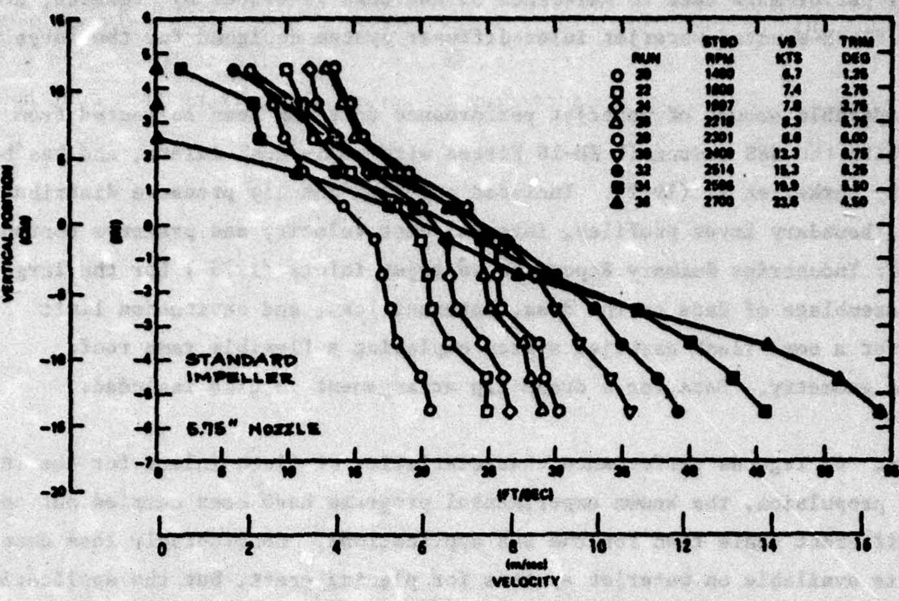

Figure 26 - Measured Velocity Distributions Across Duct in a Jacuzzi Waterjet Pump Installed in a Planing Boat (From Alder (1976))

thrust was not achieved. Some preliminary results were reported by Ellis (1976). Figure 27 reproduced from that reference shows example trim and horizontal force (model drag plus jet thrust) for three cases: bare hull, model with narrow inlet, model with

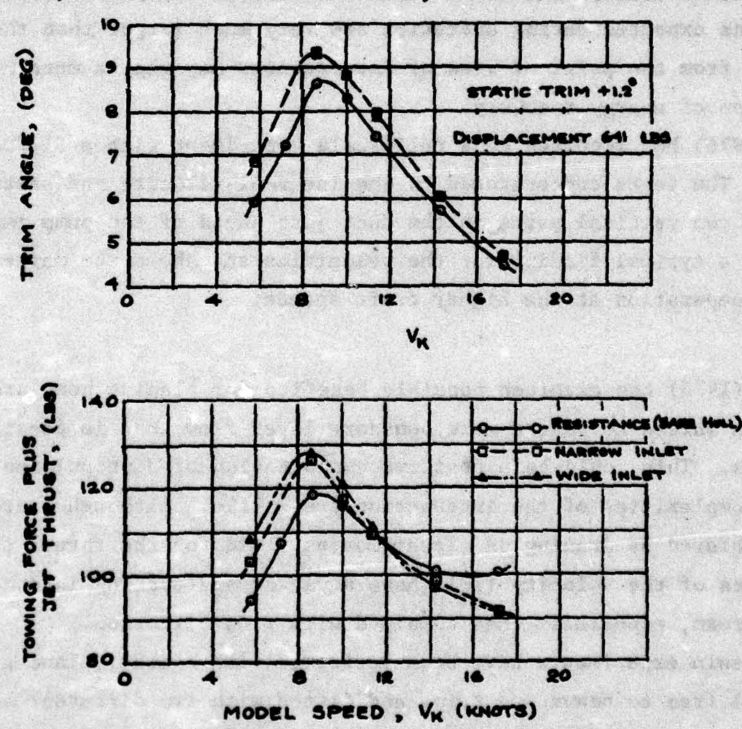

Figure 27 - Trim and Net Drag Performance of a Planing Boat Model versus Speed (From Ellis (1976))

wide inlet. The curves are for scaled flow rates that match the known prototype flow rates needed to achieve self-propulsion. It is seen that the trim is always greater for the waterjet-installed cases. The model evidently experienced a positive added drag at low speeds, and a negative added drag at speeds above 12 knots. Just how all the interaction effects fit together to give this result is not clear. Added on-board weight (not included in the static trim) acted to increase the trim over the bare hull values. Pressure distributions induced by the operating inlet also contribute to the trim changes. It was anticipated that the expected larger suction pressures on the ramp roof at higher IVRs (lower forward speed) would have acted to provide a negative added drag in the low speed range.

Interesting towing basin experiments to determine the external drag and internal head loss for flush inlet systems have been described by Grinpress and Mavlyudov (1968), who used an instrumental towing sled pictured in Figure 28. Tare drag values

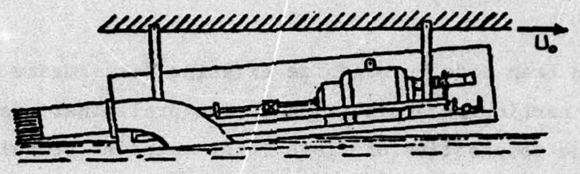

Figure 28 - Schematic of Towed Sled Arrangement for Testing Waterjet Propulsion Systems (From Grinpress and Mavlyudov (1968))

D_{tare} were obtained with the inlet closed off. The drag increment due to the operating waterjet was obtained at each forward speed and pump RPM using

$$\Delta D_i = T - (D_{meas} - D_{tare})$$

with the waterjet thrust computed using $T = \rho Q(V_j - U_o)$. For the planing boat flush inlet pictured in Figure 29a, tests were conducted with the flat bottom of the towing

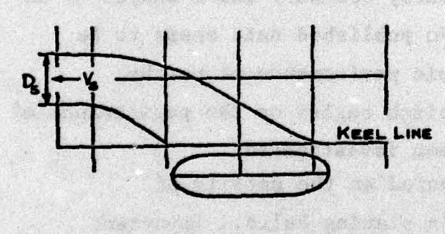

Figure 29a- Waterjet Inlet for a Planing Motorboat

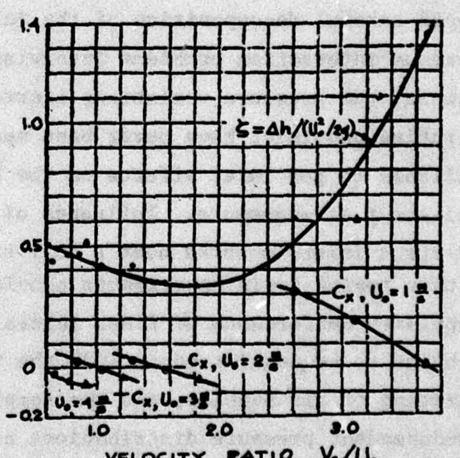

Figure 29b- Measured Coefficients of Internal Loss and Added Drag for the Waterjet Inlet of Figure 29a (From Grinpress and Mavlyudov (1968))

sled held fixed at 5 degrees, at speeds of U_o = 0, 1, 2, 3, and 4 meters/second. Coefficients of the total head loss Δh measured at the impeller plane and the inlet added drag ΔD_i are shown in Figure 29b, plotted versus V_s/U_o, where V_s = internal flow velocity at the impeller plane. Here the head loss coefficient and added drag coefficient are defined as

$$\zeta = \Delta h/(U_o^2/2g)$$
$$C_x = \Delta D_i/\tfrac{1}{2}\rho U_o^2(\pi D_s^2/4)$$

where D_s = diameter of pump impeller. The internal head loss coefficients display little speed dependence, and seem to collapse fairly well onto one curve. However, there seems to be a distinct Froude number effect on the inlet added drag coefficients. Unfortunately there is no information available on the width or wetted length of the towing sled.

<u>Other</u>. Some efforts have been made to organize existing performance data for the purpose of demonstrating particular applications. The preliminary design study of Manins (1970) explored the possibility of flush inlet waterjet propulsion of a destroyer.

A review paper by Kruppa, et al (1968) presented among other things some internal loss performance data obtained with a small scale planing scoop inlet.

Comments and Recommendations

- There is a need for more verification experiments and/or analysis on pod-strut inlet designs, covering both the fixed area and variable area types, with a view toward careful decomposition of the inlet external drag and internal losses.
- Numerous interaction problems involving pod-strut inlets need exploration. For example, the pressure variations exerted on a nearby boundary (hull shape) by an operating pod-inlet have never been measured. No published data seems to be available on pod inlet effects on the hydrodynamic performance of nearby foil-strut arrangements. Influence of yaw and pitch angles on the performance of pod-strut inlets mounted near a hull have not been investigated.
- Further towing basin experiments should be conducted on the details of propulsive performance of flush inlets mounted in planing hulls. Important problems to be considered include the effects of angle of attack (trim), ingestion of air bubbles, and the complex interactions created by the IVR-dependent pressure distributions acting near the operating inlet.
- An experiment on waterjet propulsion of a high speed displacement ship should be considered, with the jet discharge located underwater within the hull wake.

5. AIR PROPULSORS FOR AIR CUSHION CRAFT

This section is concerned with interaction aspects of air propulsor devices applied to high performance air cushion craft such as fully skirted air cushion vehicles (ACV) and wing-in-ground-effect (WIGE) craft. There are possibilities of employing air propulsors on other marine craft, such as on small planing boats or hydrofoils, but these are usually not regarded as practical alternatives for large vehicles because of the high thrust levels and large propulsor diameters required.

A variety of air propulsion schemes have been developed or suggested including: free screw propellers, shrouded screw propellers, ducted fans, air jets, gas turbine jets, and cushion bleeding. Mantle (1975) has provided perhaps the most comprehensive review of the technology, references, and outline of basic estimating formulas applied to air cushion craft propulsion.

For an ACV, the general propulsor-hull arrangement usually consists of a free or shrouded air screw operating alongside of, or near the end of, and sometimes behind a box-like body.

For many WIGE arrangements the air propulsors are positioned much as they would be on an airplane, usually on nacelles, with generous clearances away from wings and tails, and operating in a tractor mode. For the case of a power-augmented ram wing arrangement, the propeller slipstreams play a crucial role in providing augmented lift as well as sufficient propulsive thrust.

Propellers Near Bodies

Surprizingly little is available in the aeronautical literature specifically on the mutual interference between a propeller (either free or shrouded) and a nearby hull. It is fair to state that this subject has attracted very little attention simply because the effects are small by design and by arrangement in most airplane geometries.

Physically, interactions can arise from three main sources: (i) non-uniform flow due to the hull boundary layer and/or wake, (ii) asymmetrical thrust-induced flow through the propulsor disk due to the presence of a nearby boundary and (iii) non-uniform flow through the propeller disk caused by the displacement velocity field about the body. No information on the first item could be located, relevant to the geometries of ACVs.

Regarding item (ii), the results of experiments of Trebble (1968_a) are helpful. Wind tunnel tests of a 1.6-foot diameter, 4-bladed free propeller mounted on 4.3-inch diameter nacelle were performed with the propeller positioned next to a flat wall parallel to the rotation axis. The propeller could be placed near a flush-mounted circular intake having radiused lips. Figure 30, reproduced from Trebble (1968_a), shows the coefficients of power absorbed and thrust produced by the propeller, plotted versus advance ratio, at four different blade angle settings. Three cases are

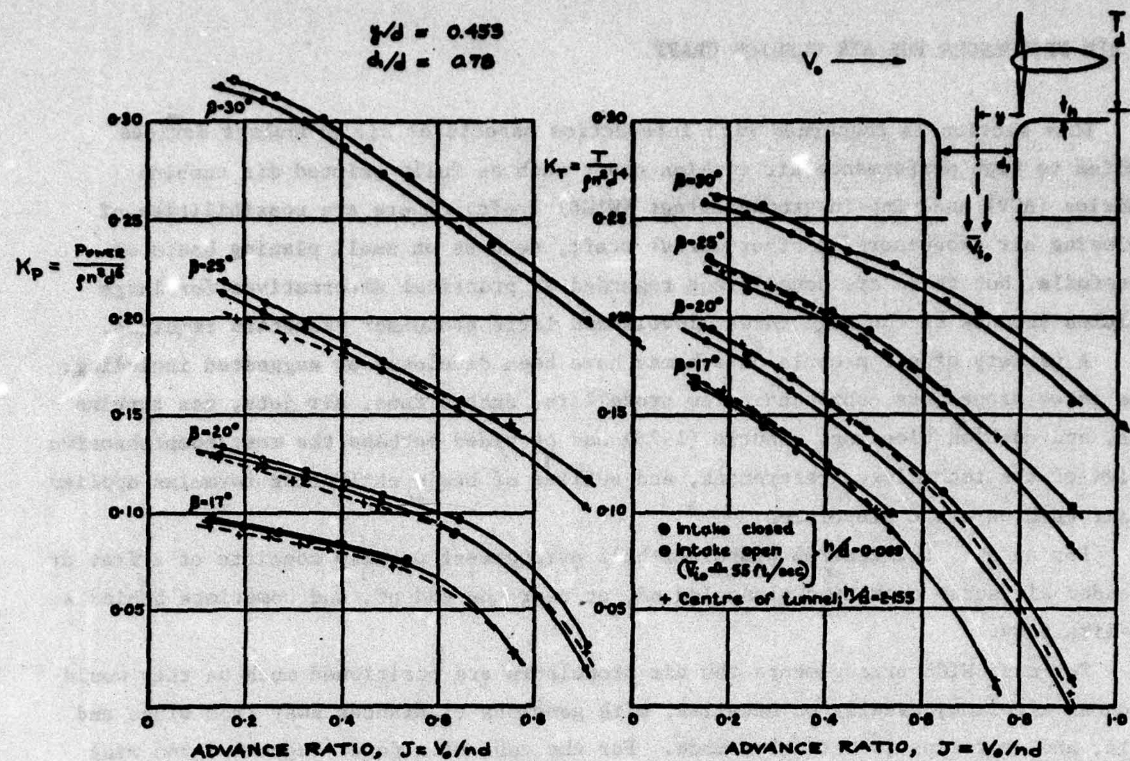

Figure 30 - Power and Thrust Performance of a Single Propeller Near a Flat Wall (From Trebble (1968_a))

displayed: one is essentially an open air result, with the inlet closed and the propeller mounted at the tunnel centerline well away from the wall (h/d = 2.155); and two cases are for small tip clearance, h/d = 0.089, with and without the intake open. It can be seen from the plots for the two cases of intake closed that the presence of the nearby wall causes a slight decrease in thrust and increase in power, exaggerated by low J-values. With the intake open and ingesting air, the thrust level is increased, and the power is increased further. It is interesting to note that this geometry is rather similar to the propulsor-intake arrangement of the British Hovercraft Corp. ACV, the BH 7. Mk 5, for example.

In connection with item (iii), potential flow calculations could be implemented to determine the body-induced velocities through a propeller disk location. As far as is known, no such calculations have been performed for ACV shapes. Some work exists on approximate computation of velocity fields induced by narrow fuselages, nacelles, etc. The slender body formulation developed for such a purpose by Yaggy (1951) was employed, for example, by Rogallo (1952).

A wind tunnel test of the free propeller-driven air cushion vehicle CC - 2 was reported on by Trebble (1968_b). The data includes bare hull drag versus speed (with and without air cushion) and the installed propeller thrust and power performance. Without open air propeller performance, this very interesting work unfortunately cannot be used to obtain detailed propulsive interactions.

Air Jets

An attractive (less expensive and quieter) alternative to propeller propulsion for an ACV is an air jet scheme where ambient air is drawn into a centrifugal fan and ducted to a nozzle directed downstream. The sketch in Figure 31 illustrates the

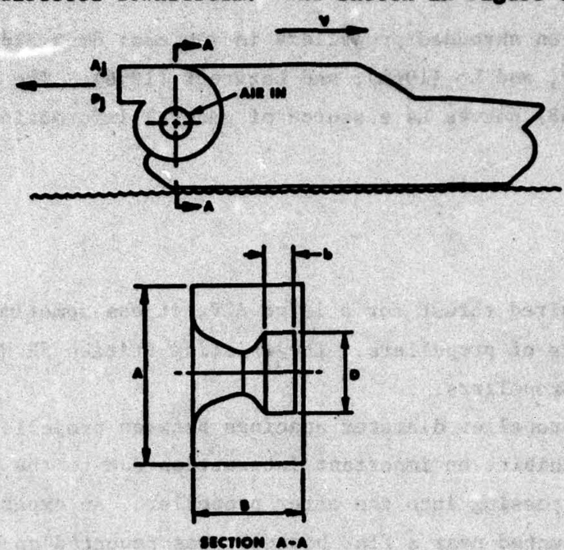

Figure 31 - Air Jet Propulsion for an ACV (From Mantle (1975))

arrangement. Mantle (1975) has presented simple estimating formulas for performance, but includes no detailed information on geometry-dependent interaction problems.

The resemblance between the air jet arrangement and waterjet flush inlets is sufficient to suppose that the same system of waterjet performance parameters described earlier could apply equally well. The difference is that less information is available for the geometries typical of the air jet systems.

The intake geometry, characterized by its added drag and internal loss is one major source of interaction problems. High ram recovery and good flow quality (minimum non-uniformity) are clearly desirable. Improvements in air jet intakes can be derived from advances being made with cushion air intakes such as are discussed by Wheeler (1976). Some detailed performance data are available in the aeronautical literature under the topic heading of fan-in-body aerodynamics. For example, ram recovery properties and lip pressure distributions for a circular intake hole imbedded in an airplane body have been studied experimentally by Aoyagi, Hickey, and de Savigny (1961). The effects of a wide range of ingested air flow rates, body angle of attack, and a lip-mounted turning vane are included. Some useful general data on flush or recessed normal intakes are given by Hoerner (1965).

Yawed Propellers (Isolated)

In a narrow sense the changes in the net thrust delivered by a propeller in yaw

are part of the subject of interaction. In the broadest sense, all the forces and moments arising from a non-aligned propulsor belong to the subject of interaction.

A considerable amount of information exists on isolated free and shrouded propellers in yaw. Example references on performance of yawed free propellers are: McLemore and Cannon (1954), Yaggy and Rogallo (1960), Crigler and Gilman (1952), and Wickens (1966).

Example references on shrouded propellers in yaw are: Grunwald and Goodson (1962), Greenberg, Ordway, and Lo (1965), and Lazareff (1968). The review paper by Weissinger and Maass (1968) serves as a source of general information and references on shrouded propellers.

Tandem Propellers

To deliver the required thrust for a large ACV, it has sometimes been necessary to use tandem arrangements of propellers. The existing British SR.N4 ACV, for example, has two pairs of tandem propellers.

Even with several propeller diameter spacings between propellers, the tandem airscrew configuration exhibits an important interaction due to the slipstream produced by the forward propeller passing into the after propeller. An experimental study of tandem free propellers mounted near a flat boundary was reported on by Trebble (1968_a). In addition to considering the influence of two different distances between the in-line propellers, the data includes the effect of air ingested through a circular, flush-mounted intake located at several distances upstream of the aft propeller. Typical results of this experiment are displayed in Figure 32, which shows the coefficients of power absorbed and thrust plotted versus advance ratio for the aft propeller spaced 3.475 diameters behind the forward propeller. Direct comparison between the curves for blade angle $\beta = 17$ degrees is possible from this plot, and indicates the large loss of thrust and power, especially at low J. Evidently the more forward position of the intake is better for reducing (slightly) the effect of the impinging slipstream.

Shank (1973) has analyzed the same basic tandem screw geometry (without the effects of the intake and the nearby wall) using actuator disk theory, following classic work on tandem propellers by Glauert (1935).

WIGEs and Augmented Ram Wing

Usual arrangements of propellers on WIGEs resemble airplane geometries. The expected propeller-wing interactions can be treated by methods outlined in the classic references on propeller interference. These include: Glauert (1935), Koning (1935), and the survey article by Ferrari (1957). Weinig's (1947) book on aerodynamics of propellers contains several sections on interference problems, such as finding the flow angularity caused by fuselage-like bodies.

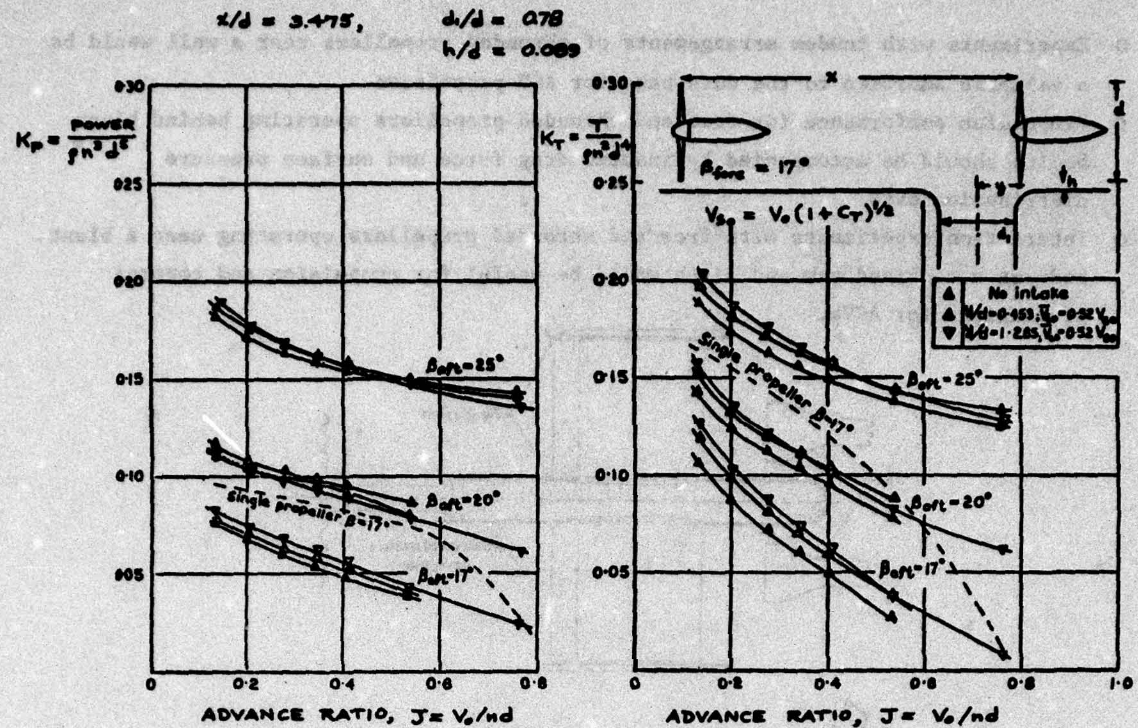

Figure 32 - Power and Thrust Performance of the Aft propeller of Tandem Pair Near a Flat Wall (From Trebble (1968_a))

The power-augmented ram wing, such as is pictured in Figure 33 is a type of ground-effect aircraft that features a propulsion system mounted forward of and exhausting under the wing. This arrangement is capable of generating augmented under-the-wing pressures that produce wing lift even at zero forward speed. A useful thrust is also produced. Experimental work with the jet-augmented WIGE model shown in the figure was reported on by Huffman and Jackson (1974) for operation only at zero forward speed. Figure 34 shows that there is a net axial thrust experienced by the wing when the jet streams are directed under the wing with total thrust C_μ = .0111. Here, C_μ is the total thrust coefficient of the nozzles based on wing planform area, C_A is the induced axial drag force coefficient, δ_j is the jet deflection angle with respect to the longitudinal axis, C_N is the normal force coefficient, and h/c and h_f/c are identified in the sketch of Figure 34.

Analyses by Gallington (1976) and Gallington and Chaplin (1976) have shown that the size of the incoming jet is very important to achieving high pressures under the wing, with the optimum arrangement being one where the jet exhaust height is about equal to the height of the wing from the ground plane. A summary of work on the wide jet power-augmented WIGE was given by Gallington, et al (1976).

- Experiments with tandem arrangements of shrouded propellers near a wall would be a valuable addition to the data base for ACV propulsion
- Propulsion performance for free and shrouded propellers operating behind blunt bodies should be accompanied by induced drag force and surface pressure distribution data
- Interaction experiments with free and shrouded propellers operating near a blunt body at a combined yaw and pitch would be useful for propulsion and control predictions for ACVs.

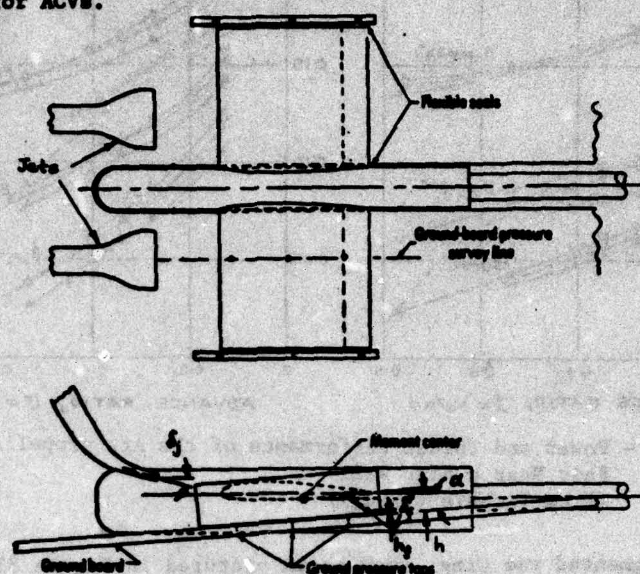

Figure 33 - Model of Power Augmented Ram Wing (From Huffman and Jackson (1974))

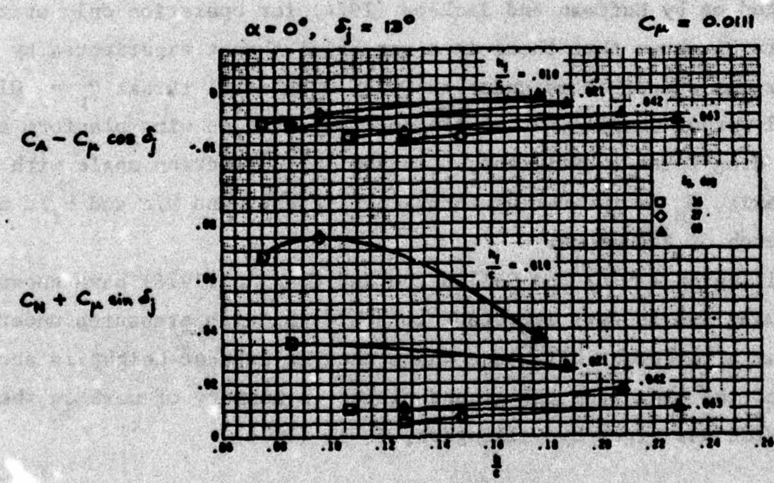

Figure 34 - Net Horizontal and Normal Force Performance of Powered Static Air-Cushion System (From Huffman and Jackson (1974))

REFERENCES*

1. (L) Aerojet-General Corporation, Surface Effect Ships Division, "Waterjet Inlet Analysis Program Final Report," Report AGC-T-338, Dec 1972.

2. (L) Alder, R.S., "Inlet Velocity Distribution of a Full Scale Flush Inlet Waterjet," DTNSRDC Department Report SPD-718-01, Aug 1976.

3. (L) Altmann, R., "Studies of Stepped-Pod Propulsion Units for Surface Effect Ships," Hydronautics, Inc. Report TR 816-2, Jun 1969a.

4. (L) Altmann, R., "Model Tests of a Semi-Submerged, Supercavitating, Controllable-Pitch Propeller Behind Three CAB Sidehull Configurations," Hydronautics, Inc. Report 946-1, Nov 1969b.

5. (L) Altmann, R., "Non-Steady Performance Measurements on Model Supercavitating Propellers for Surface Effect Ships," Hydronautics Inc. Report 7307-4, Dec 1974.

6. (L) Altmann, R., J. Bohn, and K. Schaefer, "Non-Steady Performance Features of Semi-Submerged Supercavitating Propellers," Hydronautics Inc. TR 7307-5, Aug 1975.

7. Aoyagi, K., D. Hickey, and R. deSavigny, "Aerodynamic Characteristics of a Large-Scale Model with a High Disk-Loading Lifting Fan Mounted in the Fuselage," NASA TN D-775, Oct 1961.

8. (L) Barr, R.A., "Design Studies for SES Supercavitating Propeller Systems, Vol. II Measured Performance," Hydronautics Inc. Report 816-1 (II), May 1969.

9. (L) Barr, R.A., "State-of-the-Art Technology and Performance Prediction Methods for Waterjet Propulsion Systems for High Speed Naval Ships," Hydronautics Inc. Report TR 7224-7, Jun 1974.

10. Barr, R.A. and L.K. Stephens, "Design and Measured Performance of Propellers for the Hydrofoil Craft AG(EH)," Hydronautics Inc. Report TR 502-1, Jun 1965.

11. (L) Barr, R. and R. Altmann, "Model Tests of Semi-Submerged Supercavitating Controllable-Pitch Propellers Behind a CAB Sidehull Configuration," Hydronautics Inc. Report TR 7028-1, Jul 1970.

12. Barr, R.A. and N.R. Stark, "Current State-of-the-Art of Waterjet Inlet Systems for High Performance Naval Ships," Hydronautics Inc. TR 7224-5, Dec 1973.

13. Bavin, V.F., "Theory of Interaction of an Ideal Cavitating Propeller with a Ship Hull," Collection of Articles on Ship Hydrodynamics, Shipbuilding Publ. House, Part I, USSR, 1965.

14. Barvin, V.F. and I.J. Miniovich, "Experimental Investigations of Interaction Between Hull and Cavitating Propeller," Proc. Tenth I.T.T.C. Vol. 2, Teddington, 1963.

15. Beveridge, J.L., "Thrust Deduction due to a Propeller Behind a Hydrofoil," DTMB Report 1603, Oct 1962.

* References denoted by (L) are known to be limited in distribution at the present time.

16. Beveridge, J.L., "Induced Velocity Field of a Fully Cavitating Propeller and Interaction Experiments with a Fully Cavitating Propeller Behind a Hydrofoil," NSRDC Report 1832, Apr 1964.

17. Blount, D.L., "Resistance and Propulsion Characteristics of a Round-Bottom Boat (Parent Form of TMB Series 63)," DTMB Report 2000, Mar 1965.

18. Blount, D.L., G.R. Stuntz, D.L. Gregory, and M.J. Frome, "Correlation of Full-Scale Trials and Model Tests for a Small Planing Boat," Trans. R.I.N.A., 1968.

19. (L) Bohn, J. and R. Altmann, "Analysis of Supercavitating Propeller Model Test Data," Hydronautics Inc. Report TR 7307-3, Apr 1975.

20. Brandau, J.H., "Performance of Waterjet Propusion Systems - A Review of the State-of-the-Art," J. Hydronautics, Vol. 2, No. 2, Apr 1968.

21. (L) Burke, F., N. Wener, P. Shipps, C. Horine, and A. Walker, " R&D Testcraft-SR-1B Semi Flush Inlets," Rohr Industries Report RHR-72-941, Oct 1972.

22. (L) Callanen, S. and J. Nelka, "Waterjet Propulsion, A Guidance for Preliminary Design and A Brief State-of-the-Art Review with an Extensive List of References," NSRDC Ship Performance Dept Techn Note 250, Jan 1974.

23. (L) Chisholm, M.A., D.H. Kintis, and G. Reichert, "Analysis Report Waterjet Inlet Hydrodynamics," Lockheed Missiles and Space Co. Report LMSC/D 313023, Dec 1972.

24. Crigler, J. and J. Gilman, "Calculation of Aerodynamic Forces on a Propeller in Pitch or Yaw," NACA TN 2585, Jan 1952.

25. (L) Crown, D.E. and R. Hecker, "The Effect of Blade Thickness on the Performance of a Supercavitating Partially-Submerged Propeller," NSRDC T&E Report 249-H-04, Nov 1968.

26. (L) Crown, D.E. and R. Hecker, "Inclined Shaft Performance of Two Partially Submerged Propellers Behind a Test Boat," NSRDC T&E Report 249-H-14, Oct 1971.

27. Davis, B.V. and J.W. English, "The Evolution of a Fully Cavitating Propeller for a High-Speed Hydrofoil Ship," Seventh ONR Symposium on Naval Hydrodynamics, Rome, 1968.

28. (L) Day, W.G., Jr., "Velocity Surveys of Several 1/8-Scale PCH Forward Hydrofoil Configurations," NSRDC Department T&E Report 326-H-02, Nov 1970.

29. (L) Developmental Sciences, Inc., "Theoretical Calculations of Pod Inlets for Surface Effect Ships," DSI Final Technical Report 7210-F, Contract No. N00024-72-C-0901 Jan 1973.

30. Dobay, G., "Time Dependent Blade-Load Measurements on a Screw-Propeller," Proc. 16th ATTC, Sao Paulo, Brazil, Aug 1971.

31. Dobay, G.F. and D.L. Gregory, "The State-of-the-Art of Powering Prediction of High Performance Marine Vehicles," Proc. 17th ATTC, California Institute of Technology Pasadena, CA, 1974.

32. Ellis, W.E. and A.D. Sobolewski, "Propulsion Experiment with a Planing Hull Having Two Flush Inlet Configurations," DTNSRDC Departmental Report, SPD-786-01, Nov 1977.

33. (L) Ellis, W.E. and R. Alder, "Propulsion Experiments with a Deep Tunnel Planing Hull," DTNSRDC Departmental Report SPD-717-01, Feb 1977.

34. Etter, R.J. "Waterjet Propulsion - An Overview," Marine Propulsion, Ocean Engineering Div. Vol. 2, Edited by J. Sladky, Jr., ASME, N.Y. 1976.

35. (L) Etter, R.J. and N.R. Stark, "Waterjet Inlet/Duct Development Phase I, SES 100A Hydrodynamic Design and Testing," Hydronautics Inc. Report 7244-3, Mar 1976.

36. Experimental Model Basin, "Test of Transom Sterns on Destroyers," E.M.B. Report No. 339, Nov 1932.

37. Ferrari, C., "Interaction Problems," Section C, Aerodynamic Components of Aircraft at High Speeds(Vol. VII of High Speed Aerodynamics and Jet Propulsion) Edited by Donovan and Lawrence, Princeton University Press, 1957.

38. Gallington, R., "Sudden Deceleration of a Free Jet at the Entrance of a Channel," DTNSRDC ASED Report 350, Jan 1976.

39. Gallington, R. and H. Chaplin, "Theory of Power Augmented Ram Lift at Zero Forward Speed," DTNSRDC ASED Report 365, Feb 1976.

40. Gallington, R.W., H.R. Chaplin, F.H. Krause, J.A. Miller, and J.C. Pemberton, "Recent Advances in Wing-in-Ground Effect Vehicle Technology," AIAA Paper 76-874, AIAA/SNAME Advanced Marine Vehicles Conf., Arlington, VA, Sep 1976.

41. Glauert, H., "Airplane Propellers," Division L, Vol IV of Aerodynamic Theory, edited by W.F. Durand, Dover Publ. Inc.,1963.

42. Gorshkoff, A.S., "Interaction Between a Cavitating Propeller and a Ship (State of Art)," Proc. Thirteenth ITTC, Vol. 1, Berlin/Hanburg, 1972.

43. Greenberg, M., D. Ordway, and C. Lo, "A Three-Dimensional Theory for the Ducted Propeller at Angle of Attack," THERM, Inc. TAR-TR 6509, Dec 1965.

44. (L) Gregory, D.L., "Correlation of Model Tests and Full-Scale Trials for a Twin-Screw LCVP, NSRDC Department T & E Report 199-H-02, Jan. 1970.

45. Grinpress, V.M. and M.S. Mavlyudov, "Experimental Determination of the Drag of Water Intakes of Waterjet Propulsive Systems," Sbornik Statey po Gidromekhanike i Dinamike Sudna, Shipb. Publ. House, 1968.

46. Grunwald, K.J. and K.W. Goodson, "Aerodynamic Loads on an Isolated Shrouded-Propeller Configuration for Angles of Attack from -10^{o} to 100^{o}," NASA TN D-995, Jan. 1962.

47. Hadler, J.B., "The Prediction of Power Performance on Planing Craft," Trans. S.N.A.M.E. Vol. 74, pp. 563 - 602, 1966.

48. Hadler, J.B. and R. Hecker, "Performance of Partially Submerged Propellers," Seventh ONR Symposium on Naval Hydrodynamics, Rome, Italy, 1968.

49. Hadler, J.B. and E.N. Hubble, "Prediction of Power Performance of The Series 62 Planning Hull Forms," Trans. S.N.A.M.E. Vol. 79, 1971.

50. Harbaugh, K.H. and D.L. Blount, "An Experimental Study of a High Performance Tunnel Hull Craft," Paper presented at Spring Meeting of S.N.A.M.E., April 1973.

51. Hart, D., "Jet Drives," Motorboat, Jan. 1975.

52. Hecker, R., "Experimental Performance of a Partially Submerged Propeller in

Inclined Flow" Paper presented at Spring S.N.A.M.E. Meeting, Lake Buena Vista, Florida, April, 1973.

53. (L) Hecker, R. and A. Hendrican, "Design Charts Based on Experimental Results of Partially - Submerged Propeller 4281," NSRDC T&E Report 249-H-09, Aug. 1969.

54. (L) Hecker, R. and D. Crown, "The Steady - State Performance of Two Skewed Partially Submerged Propellers," NSRDC T&E Report 249-H-08, June 1969.

55. (L) Hecker, R. and J.G. Peck, "Experimental Performance of a Base - Vented Right - Angled Drive System with Tractor Propeller," NSRDC Department T&E Report 314-H-01, May 1969.

56. Hecker, R. and R.J. Altmann, "High Performance Marine Propellers -- An Overview," Marine Propulsion Ocean Engine Div. Vol. 2, ASME Winter Annual Meeting, New York, 1976.

57. Hoerner, S.F., Fluid - Dynamic Drag, Published by the Author, 1965.

58. Hough, G.R. and D.E. Ordway, "The Generalized Actuator Disc," Developments in Theoretical and Applied Mechanics, Vol. II, Pergamon Press, 1965.

59. Hough, G.R. and D.E. Ordway, "Mean Flow Streamlines of a Finite - Bladed Propeller," J. Aircraft, Vol. 4, No. 6, pp. 561 - 562, 1967.

60. Huang, T., H. Wang, N. Santelli, and N. Groves, "Propeller/Stern/Boundary Layer Interaction on Axisymmetric Bodies: Theory and Experiment," DTNSRDC Report 76-0013, Dec. 1976.

61. Huffman, J. and C. Jackson,Jr., "Investigation of the Static Lift Capability of a Low - Aspect - Ratio Wing Operating in a Powered Ground - Effect Mode," NASA TM X-3031, July 1974.

62. (L) Humenick, W. and R.L. Kramer, "Waterjet Inlet Hydrodynamics Phase II Test Report," Lockheed Missiles and Space Co. Report LMSC/D356523, March 1974.

63. Johnson, V.E., Jr., "Waterjet Propulsion for High - Speed Hydrofoil Craft," J. Aircraft, Vol. 3, No. 2, 1966.

64. (L) Johson, V.E., R.J. Etter, P. van Dyke, G.M. Poquette, J.R. Hill, L.K. Stephns, and N.R. Stark, "Design and Performance of Diffusers, Fixed-Area Inlets, and Variable Area Inlets in Intergrated Inlet - Diffuser Subsystems," Hydrodynamics Inc. Report TR 7152-1, Aug. 1972.

65. Kaplan, P., J. Breslin, and W.R. Jacobs, "Evaluation of the Theory for Flow Pattern of a Hydrofoil of Finite Span," J. Ship Research, Vol. 3, No. 4, pp 13 - 29, March 1960.

66. Kerwin, J.E. and R. Leopold, "A Design Theory for Subcavitating Theory," Trans. S.N.A.M.E., Vol. 72, pp 294 - 335, 1964.

67. Kirkman, K.L., B.J. Young, J.W. Kloetzli, and P. Majumbar,"Model Tests and Engineering Studies of the SWATH VII Small Waterplane Area Twin-Hull Ship," Hydronautics, Inc Technical Report 7694-1," Nov 1976.

68. Koning, C., "Influence of the Propeller on Other Parts of the Airplane Structure," Division M, Vol. IV of Aerodynamic Theory, edited by W.F. Durand, Dover Publ., Inc., 1963.

69. (L) Kopko, W., "Fluctuating Forces Measured on the Partially Submerged 45° Skewed Model SES Propeller," NSRDC T&E Report 249-H-10, Oct 1969.

70. (L) Krishnamoorthy, V., "Flush or Semi-Flush Waterjet Inlet and Duct Design Manual," Hydronautics Inc. Report 7405-6, May 1977.

71. Kruppa, C., C. Brandt, and C. Oestergaard, "Waterjet Propulsion Systems for High Speed Vessels," Jahrbuch STG, Vol. 62, 1968.

72. Kruppa C., "Testing of Partially Submerged Propellers," Proc. Thirteenth I.T.T.C. Vol. 1, Berlin/Hamburg, Sept. 1972.

73. Kulikov, S.V. and M.F. Khramkin, Waterjet Propulsion Systems (Theory and Design), Shipbuilding Publishing House, Leningrad, 1970.

74. (L) Layne, D.E., "Velocity Survey of 1/8 - Scale PCH Forward Hydrofoil In Way of Aft Foil," NSRDC Department T&E Report 326-H-01, April 1969.

75. Lazareff, M., "Aerodynamics of Shrouded Propellers," Paper D of The Aerodynamics of V/STOL Aircraft, AGARDograph 126, May 1968.

76. Levinsky, E.S., H.V. Thommen, P.M. Yager, and C.H. Holland, "Lifting - Surface Theory for V/STOL Aircraft in Transition and Cruise," J. Aircraft, Vol 7 No. 1, 1970.

77. Levy, J. and D.J. Meggitt, "Study of Waterjet Propulsion for 400 - Ton Hydrofoil Ship," Aerojet Electrosystems Co. Report No. 4366, Oct 1971.

78. Lin, W.C. and W. Day, "The Still - Water Resistance and Propulsion Characteristics of Small - Waterplane - Area Twin - Hull (SWATH) Ships," AIAA/SNAME Advanced Marine Vehicles Conference, Paper No. 74 -325, San Diego, Calif., February 1974.

79. (L) Lockheed Missiles and Space Co., "Surface Effect Ships Propulsion Technology Design Manual, Vol. III, Supercavitating Propellers," May 1974_a

80. (L) Lockheed Missiles and Space Co., "Surface Effect Ships Propulsion Technology Design Manual, Vol IV, Waterjet Propulsion," May 1964_b

81. Manins, P.C., "A Study of Hydraulic Jet Propulsion in a Destroyer," Australian Dept. of Supply, Aeronautical Research Laboratories, Mechanical Engineering Note 316, July 1970.

82. Mantle, P.J., "A Technical Summary of Air Cushion Craft Development," DTNSRDC Report 4727, Oct. 1975.

83. Mavlyodov, M.A., A.A. Rusetskiy, Yu. M. Sadovnikov, and E.F. Fisher, Propulsion Units for High Speed Ships, Izdatel'stvo Sudostroyeniye, 1973, Translational by U.S. Joint Publications Research Service, JPRS 64897, June 1975.

84. McLemore, H. and M. Cannon, "Aerodynamic Investigation of a Four - Blade Propeller Operating Through an Angle-of-Attack Range from 0° to 180°," NACA TN 3228, June 1954.

85. Moore, W.L., "Wake Surveys Behind Hydrofoil-Strut-Nacelle Configurations - -- For Application to the AG(EH)," DTMB Report 1864, June 1964.

86. Mossman, E.A. and L.M. Randall, "An Experimental Investigation of the Design Variables for NACA RM No. A7130, Jan. 1948.

87. Nelson, D.M., "The Effect of Propeller Cavitation on Thrust Deduction," U.S. Naval Ordnance Test Station Report NAVWEPS Rep. 8549, Sept 1964/

88. Noorzij,L., "Pressure Field Induced by a Cavitating Propeller," Intern. Shipb. Progress, Vol. 23, No. 260, 1976.

89. Noordzij L. and M.J. Officier, "The Effect of Camber on the Pressure Field of a Supercavitating Propeller," Intern. Shipb. Progress, Vol. 24, No. 260 1976.

90. Peck, J.G., "Cavitation Tests of a Tractor Propeller Arrangement for the PC(H)," DTMB Report 2154, Jan. 1966.

91. (L) Peck, J.G., "Performance Characteristics and Horizontal Forces of a Supercavitating Propeller Designed for Partially - Submerged Operation," NSRDC T&E Report 249-H-02, Aug 1968.

92. (L) Peck, J.G. and R. Hecker, "Hydrofoil Craft Propeller System Evaluation," NSRDC Department T&E Report 264-H-10, April 1971.

93. Peck, J.G. and Moore, D.H., "Inclined Shaft Propeller Performance Characteristics," NSRDC Report 4127, April 1974.

94. Pitre, A.S., "Propulsion Problems of a Destroyer," U.S. Experimental Model Basin Report No. 390, Oct. 1934.

95. (L) Poquette, G.M., L.K. Stephens, K.M. Schaefer, and R.J. Etter, "Design and Test of a Parent Form Flush Inlet Waterjet Inlet/Duct System Suitable for a Surface Effect Ship," Hydronautics Inc. Report TR 7358-1, April 1976.

96. (L) Power, J.L., "Path of Tip Vortex from 1/8-Scale Model of PCH Forward Foil," NSRDC Department T&E Report 326-H-03, Aug. 1971.

97. Prishchemikhin, Y.N., "A Study of the Cavitating Propeller and Ship Hull Interaction in Cavitation Towing Tank," Proc. Fourteenth I.T.T.C., Vol. 3, Ottawa, Canada, 1975.

98. Purnell, J.G., "The Performance Gains of Using Wide, Flush Boundary Layer Inlets on Water-Jet Propelled Craft," DTNSRDC Report PAS 75-45, March 1976.

99. (L) Roddy, R.F., "Investigation of the Feasibility of Propelling Large Surface Effect Ships with Widely Spaced, Partially Submerged, Supercavitating Propellers," DTNSRDC Dept. Report SPD-249-15, Dec. 1976.

100. Rogallo, V.L., "Effects of Wing Sweep on the Upwash at the Propeller Planes of Multiengine Airplanes," NACA TN 2795, Sept. 1952.

101. (L) Rohr Industries, "Addendum to Waterjet Inlet Summary Report," Document No. DP3S00701A, July 1976.

102. Rozhdestvensky, O.V., "The Measurements of the Velocity Field in Front of a Cavitating Propeller," Proc. Of the Kryloff Shipbuilding Research Institute, Vol. 127, 1958.

103. Scherer, J.O. and R.A. Barr, "Model Studies of Tractor Propeller Propulsion System," Hydronautics, Inc. Report TR 816-3, Dec 1969.

104. Schollenberger, C.A., "A Three-Dimensional Wing/Jet Interaction Analysis Including Jet Distortion Influences," Paper presented at 6th Fluid and Plasma Dynamics Conference of AIAA, Palm Springs, Calif., July 1973.

105. Schwind, R.G., "A High-Efficiency Inlet Diffuser for Water Jet Propulsion. Generalization of Test Results and Optimization," AIAA Paper No. 69-824, 2nd Advanced Marine Vehicles and Propulsion Meeting, Seattle, Wash., May 1969.

106 Shank, S.R. Jr., "Performance Prediction of Tandem Air Propeller Arrangements for Large Surface Effect Vehicles," NSRDC Report 27-664, Dec. 1973.

107. Shen, Y.T. and R. Wermter, "Recent Studies of Struts and Foils for High Speed Hydrofoils," AIAA Paper No. 76-851, Sept. 1976,

108. Sherman, P.M. and F.W. Lincoln, "Ran Inlet Systems for Waterjet Systems," AIAA Paper No. 69-418, May 1969.

109. (L) Sobolewsky, A.D., "Hydrodynamic Performance of the Model of a Variable Area Waterjet Inlet Designed for a 200 Tow, 100 Knot Hydrofoil Ship," DTNSRDC Departmental Report SPD-735-01, Feb. 1977.

110. Trebble, W.J.G, "Investigation of the Mutual Interference of Propellers Mounted in Tandem," British R.A.E. Technical Report 68282, Dec. 1968_a

111. Trebble, W.J.G., "Low-Speed Wind-Tunnel Tests on a 1/6th Scale Model of an Air-Cushion-Vehicle (Britten-Norman Cushioncraft C.C.- 2), British A.R.C. C.P. No. 983, 1968_b

112. van Manen, J.D., "The Effect of Cavitation on the Interaction Between Propeller and Ship's Hull" Intern. Shipb. Progress, Vol. 19, No. 209, pp. 3-20, Jan 1972.

113. Weinig, F., "Aerodynamics of the Propeller, Springer, Berlin, 1940 (English Translation: Air Documents Division, Intelligence Dept, U.S. Air Material Command, Dayton Ohio, 1947.

114. Weissinger, J. and D. Maass, "Theory of the Ducted Propeller - A Review" Seventh ONR Symposium on Naval Hydrodynamics, Rome, Italy 1968.

115. Wheeler, R.L., "Recent United Kingdom Hovercraft Development," AIAA Paper No. 76-863, Presented at 3rd Advanced Marine Vehicle Conference, Arlington, Va, Sept 1976.

116. Wickens, R.H., "Aerodynamic Force and Moment Characteristics of a Four-Bladed Propeller Yawed Through 120 Degrees," Canadian National Research Council Aeron. Report LR-454, May 1966.

117. Yaggy, P., "A Method for Predicting the Upwash Angles Induced at the Propeller Plane of a Combination of Bodies with an Unswept Wing," NACA TN 2528, Oct 1951.

118. Yaggy, P.F. and V.L. Rogallo, "A Wind - Tunnel Investigation of Three Propellers Through an Angle-of-Attack Range From 0^o to 85^o, NASA TN D - 318, May 1960.

119. Yeh, H.Y.H., "Series 64 Resistance Experiments on High-Speed Displacement Forms," Marine Technology, Vol. 2, No. 3, July 1965.

120. Yeh, H.Y.H. and E. Neal, "Powering Characteristics of SWATH 6-A in Calm Water and Head Seas Represented by Model 5337-A and Using Propellers 4415-4416," DTNSRDC Department Report SPD-396-20, March, 1977.

WATERJET PROPULSOR THRUST MEASUREMENT USING A REACTION ELBOW

by

Robert E. Eilers and Larry S. Shrout
Boeing Marine Systems

ABSTRACT

An experimental study was conducted of the hydrodynamic characteristics of reaction thrust elbows used for determination of waterjet propulsor gross thrust. Apparatus was developed to accurately measure the error of a thrust elbow. The influence of tailpipe length, diameter, configuration and jet characteristics on reaction elbow thrust error was evaluated. Three reaction elbow configuration options were developed from which resulting thrust values were accurate within 1/2%.

INTRODUCTION

Propulsor thrust is an important parameter controlling advanced ship performance and it is desirable that thrust uncertainties be minimized. Significant thrust uncertainties have been associated with performance measurements on large installed propulsors, particularly waterjet propulsors with a close-coupled pump and nozzle. Test stand calibration problems usually are the source of installed ship thrust error. If these errors are compensated by applying large thrust margins for future designs, excess propulsion system cost may result. An accurate and reliable method to determine waterjet propulsion gross thrust in a test stand is needed to reduce uncertainty in propulsor thrust.

The reaction thrust elbow is a good candidate for waterjet thrust measurement on a test stand because of the simplicity of measurement and the directness of data transformation into thrust. In its simplest form, the jet exit flow is turned 90^{0} with respect to the nozzle jet exit axis. A typical reaction elbow test setup is shown in Figure 1. The gross thrust produced by the propulsor is calculated simply using the horizontal component of the momentum equation. (for example, Ref. 1):

$$\Sigma F_x = \int \rho_W V_x^2 dA$$

or

$$\left\{\begin{array}{l}\text{Sum of External}\\ \text{forces acting on}\\ \text{control volume}\\ \text{in x-direction}\end{array}\right\} = \left\{\begin{array}{l}\text{Net outflow of}\\ \text{momentum from}\\ \text{control volume}\\ \text{in x-direction}\end{array}\right\}$$

If the flexure system is aligned properly and the load cell axis is horizontal, then the only external horizontal force on the control volume is the load cell connection. Horizontal and vertical forces may be applied to the thrust elbow and the load cell calibrated to correct for small misalignment and slight errors due to deflection. The gross horizontal thrust produced is equal to the load cell reading corrected for misalignment and jet deflection. Details of the internal flow, such as cavitation and energy losses, are not required, since the reaction force analysis is developed from the fluid momentum change. The only requirement for a reaction elbow is that the average exit component of the fluid momentum be turned normal to the jet exit and that after turning, the component parallel to the nozzle flow, be negligibly small.

Errors associated with reaction elbows stem mainly from failure to achieve the desired exit flow alignment. Since the function of the tailpipe leg is to produce uniform parallel exit flow, the question arises as to how long the exit leg must be to ensure that this condition is met, (i.e. to ensure an adequate straightener length-diameter ratio). A small angular error in the jet exit angle, for example, produces a relatively large thrust error. (A one degree angle error gives about a two percent thrust error).

A series of tests were performed to identify the elbow geometry required to ensure accurate thrust values. The test results gave a direct measurement of thrust elbow error. A large number of configurations were tested to determine the thrust elbow geometry sensitivity over a wide range of total pressures (20 to 250 psig). Cavitation number and Froude number typical of full scale waterjets were simulated. The highest Reynolds number was, however, about an order of magnitude less than experienced full scale. The test was intended to simulate the elbow error encountered in testing full scale. The dominant features in simulating full scale effects were judged to be the inertial forces and the internal cavitation flow pattern. Viscous (Reynold's number), gravitational (Froude number) and surface tension (Weber number) force effects were expected to be secondary in determining the exit flow pattern. This assumption was evaluated experimentally be testing over a range of Froude, Reynolds, and Weber numbers.

EXPERIMENTAL APPROACH

Accurate determination of thrust error for the models tested was accomplished by directly measuring the nozzle thrust minus the elbow reaction force with the nozzle and reaction elbow physically connected together and mounted as a unit on a balance system. To determine the baseline thrust for each test configuration and nozzle total pressure, a preliminary nozzle thrust calibration was performed. A schematic diagram of the test setup is shown in Figure 2-a for the preliminary nozzle thrust calibration (T determination) and Figure 2-b for the basic error determination (T_c determination). Application of the horizontal component of the momentum equation to Figure 2-b gives a measurement of the difference between the horizontal component of the waterjet gross thrust and the elbow reaction force, which is a direct indication of the thrust elbow error.

$$\left\{\begin{matrix}\text{LOAD CELL} \\ \text{FORCE}\end{matrix}\right\} = \left\{\text{THRUST ELBOW ERROR}\right\} = \rho_W Q V_{exit} \sin(\theta_E)$$

Dividing by the nozzle thrust provides the percent thrust elbow error:

$$\%\ \text{Thrust Elbow Error} = \frac{\text{LOAD CELL READING (WITH ELBOW)}}{\text{LEAD CELL READING (NO ELBOW)}}\ (100)$$

Application of the momentum equation in the vertical direction shows the vertical reaction force felt by the elbow support is nearly the same magnitude as the horizontal reaction force, thus care must be exercised to ensure that the load cell support link and other support structures have the correct angular orientation.

The accuracy with which the thrust elbow error can be determined using the technique of Figure 2-b was evaluated by considering a thrust elbow installation with a measured thrust elbow error of 2 pounds, and a nozzle thrust equal to 200 pounds (from pretest calibration). If nozzle thrust is known within $\pm$ 4 pounds and the error (thrust-reaction) is $\pm$ 0.04 pounds so that

$$\frac{T_c}{T} \times 100 = \frac{2\text{ lbs} \pm 0.04\text{ lbs}}{200\text{ lbs} \pm 4\text{ lbs}} \times 100 = 1 \pm 0.04,$$

an uncertainty of 0.04 percent. A more conventional method, where the thrust and reaction force are measured separately with the same instrumentation accuracy, gives:

$$\frac{T_c}{T} \times 100 = \frac{\text{THRUST - REACTION FORCE}}{\text{THRUST}} \times 100$$

$$= \frac{(200 \pm 4) - (198 \pm 4)}{(200 \pm 4)} \times 100$$

$$= 1 \pm 4,$$

an uncertainty of 4 percent. The thrust elbow error determination method of Figure 4-2-b is approximately 100 times more accurate than separately measuring reaction and thrust forces, and was therefore used in this study.

EXPERIMENTAL TEST DESCRIPTION

The basic thrust stand setup, including flexures, load cell connection, stagnation chamber and support structure was used previously for waterjet thrust augmentation studies and is described in detail in Reference 2. The water supply available from the pumping supply system had the capability of pumping 250 GPM at 300 psig to the test stand apparatus with the existing supply lines. Hydrodynamic error of each thrust configuration was obtained by measurement of the nozzle thrust minus the elbow reaction force, using a sensitive horizontal load cell. (0 to 25 lbs). The total pressure in the stagnation chamber was measured by two independent means: a 0 to 300 psig dial gauge and a 0 to 300 psig transducer. During portions of the test, a high frequency response transducer and recorder were added to determine total pressure variations under several operating conditions. The water flow rate was measured by a 0 to 250 gpm rotating type flow meter (Potter meter) installed in the upstream line. The nozzle used in the basic test series was modeled after the JETFOIL propulsor pump/nozzle geometry with a center pintle. A recorder with paper tape printout was used to record digital data for each flow condition over about a 30 second period after the flow had stabilized.

Three basic thrust elbow configurations were tested with variations made on each of the three basic configurations. The configurations tested were:

a) a simple 90^o elbow

b) A 90^o elbow with a straightener section, and

c) a 90^o double flow elbow

The test was conducted in two phases. The first test phase consisted of obtaining thrust error data for the three basic configurations with varying elbow tailpipe length and nozzle total pressure. The tailpipe length was varied for each configuration by cutting off the tailpipe leg. The second phase consisted of determining the sensitivity of the three configurations to variations in the waterjet characteristics. Five variations in the jet character were introduced, and thrust elbow error sensitivity to these variations was measured for each of three configurations over a range of jet total pressure from 20 to 250 psig. The five variations tested were:

a) jet swirl

b) jet offset

c) total pressure fluctuations

d) jet velocity profile, and

e) jet alignment

EXPERIMENTAL RESULTS

A summary of typical experimental results is shown in Figure 3 in the form of thrust elbow error ($\frac{Tc}{T}$) versus the tailpipe length/diameter ratio. The symbols indicate average values of the error data for 5 to 10 data points taken over a range from 20 to 250 psig nozzle total pressure. The reaction force error for each of the cases shown is dependent upon the average elbow exit flow angle. Positive errors indicate under-turning of the flow, while negative errors indicate overturning (back towards nozzle). Figure 4 shows results typical of those obtained during the portion of the test investigating the sensitivity of the results to jet characteristics. Based on these and other data, a specific choice of length and diameter was made for each of the three thrust elbow configurations for which the average thrust elbow reaction force error was less than 1/2%. (Reference 3). These three configuration choices are given in Figure 5.

CONCLUSIONS

Based on the investigation and results, it was concluded that a reaction thrust elbow system can provide a reliable method of determining waterjet propulsor gross thrust. The error associated with elbow exit flow misalignment with the elbow internal surface is less than one-half percent for the three configuration options developed. The most significant parameters identified were the elbow tailpipe angle in the plane of turning and the tailpipe straightener length/diameter ratio. The test results also indicated that the reaction force is independent of moderate variations in inlet jet characteristics (swirl, offset, total pressure fluctuations, jet angle, and jet velocity profile). Significant potential error (1-2%) was found to be associated with temperature stabilization effects and forces normal to the horizontal reaction force. Special procedures and corrections were used to minimize resulting error for the laboratory test setup. These considerations may also be necessary for full scale thrust measurements.

REFERENCES

1) Dynamics and Thermodynamics of Compressible Flow, A. Shapiro, Ronald Press, 1953

2) "Waterjet Thrust Augmentation by Gas Injection," R. E. Eilers, Boeing Document D321-51505, January 1976

3) "General Specifications for a Waterjet Thrust Elbow," R. E. Eilers, Boeing Document D324-12002-1, August 1976

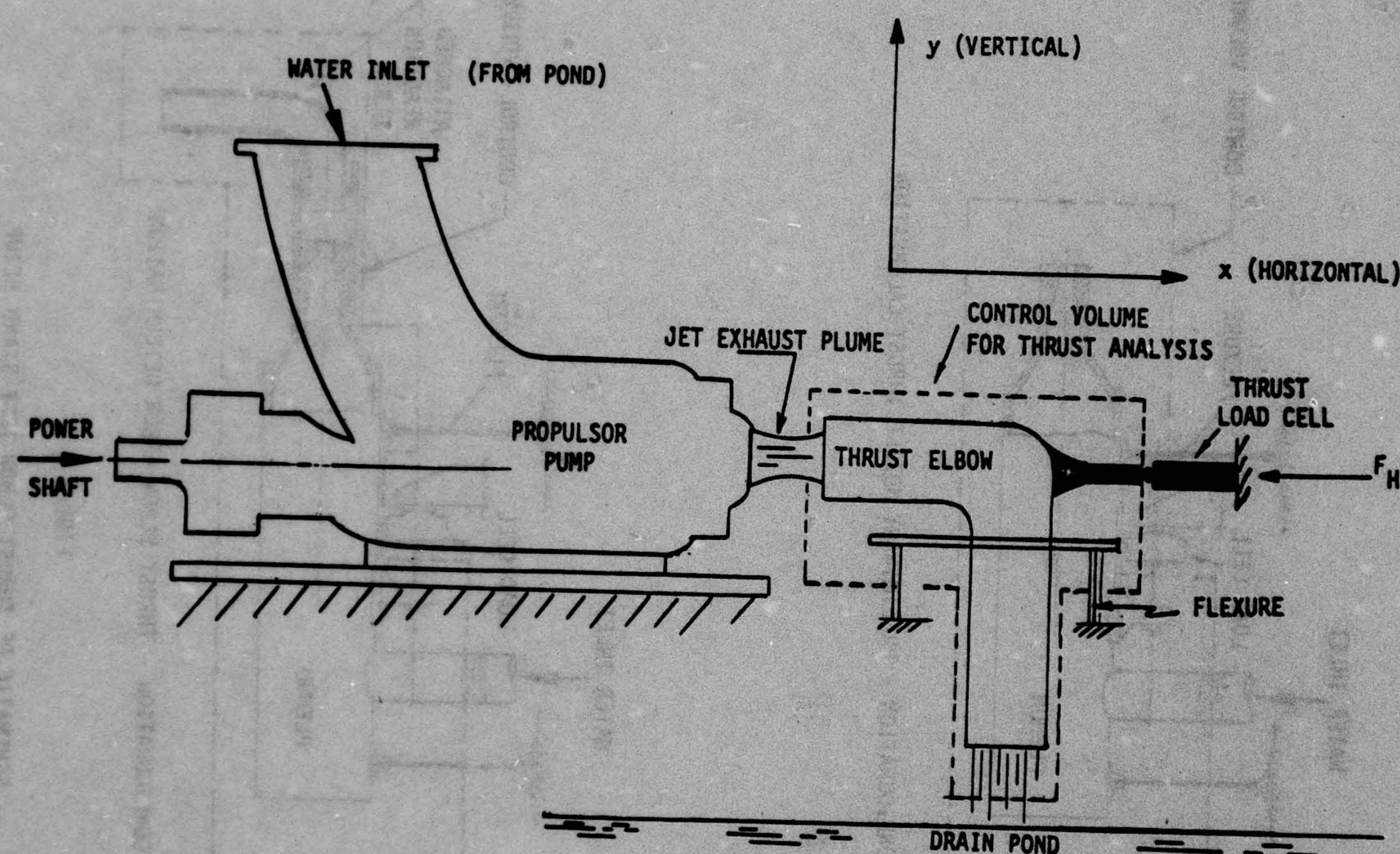

FIGURE 1 SCHEMATIC OF TYPICAL THRUST ELBOW TEST SETUP FOR FULL-SCALE WATERJET THRUST MEASUREMENT

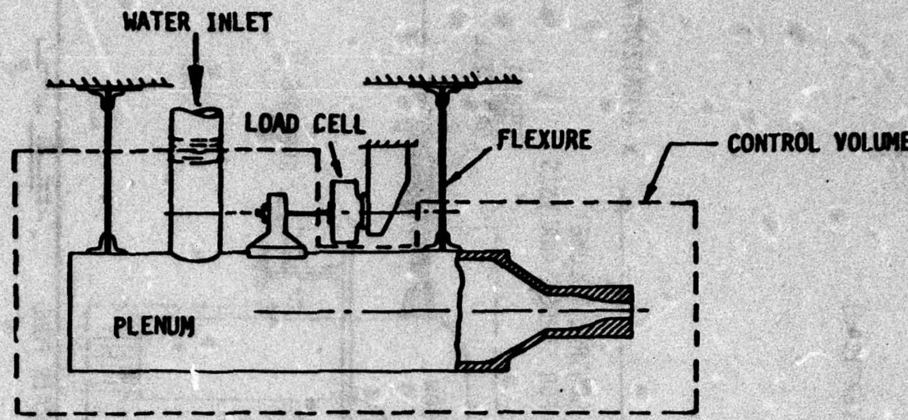

a) TEST CONFIGURATION - PRELIMINARY NOZZLE THRUST CALIBRATION

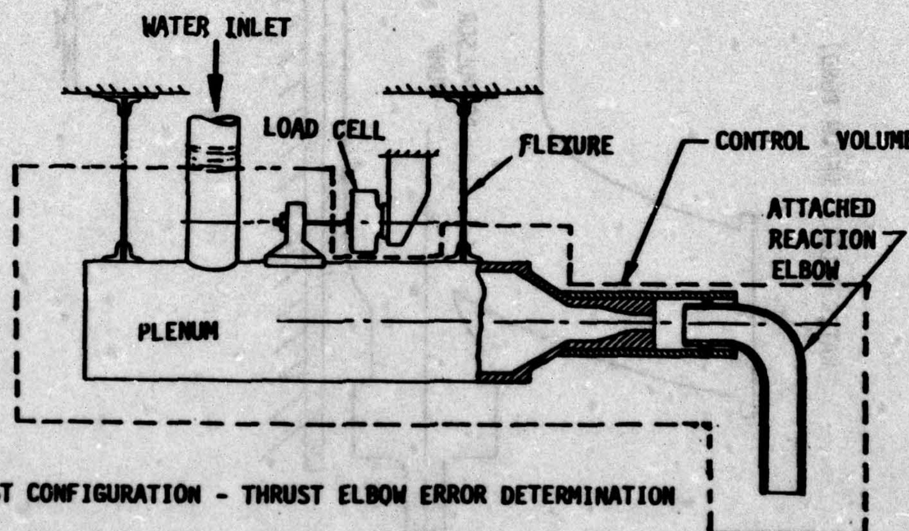

b) TEST CONFIGURATION - THRUST ELBOW ERROR DETERMINATION

FIGURE 2

SCHEMATIC OF THRUST ELBOW TEST STAND SETUP

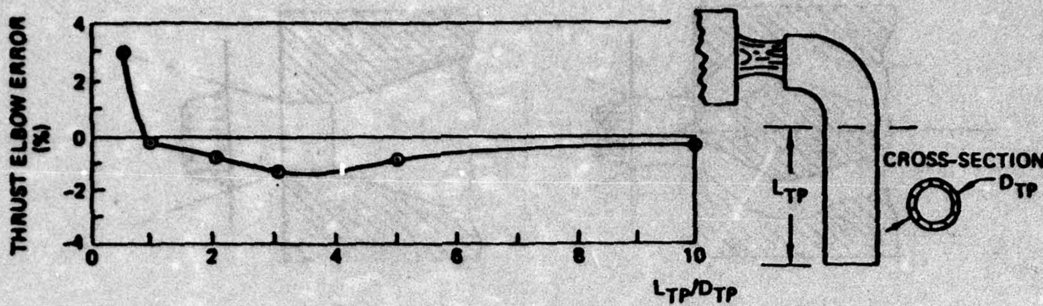

SIMPLE 90° ELBOW WITH LONG VERTICAL TAILPIPE

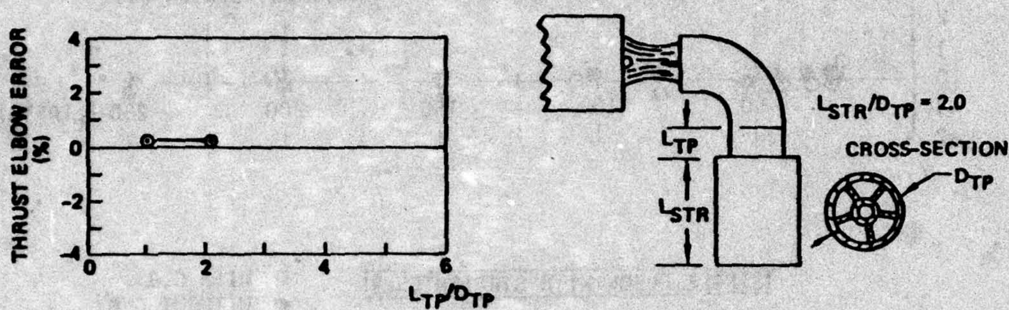

SIMPLE 90° ELBOW WITH SHORT VERTICAL TAILPIPE
AND STRAIGHTENER SECTION

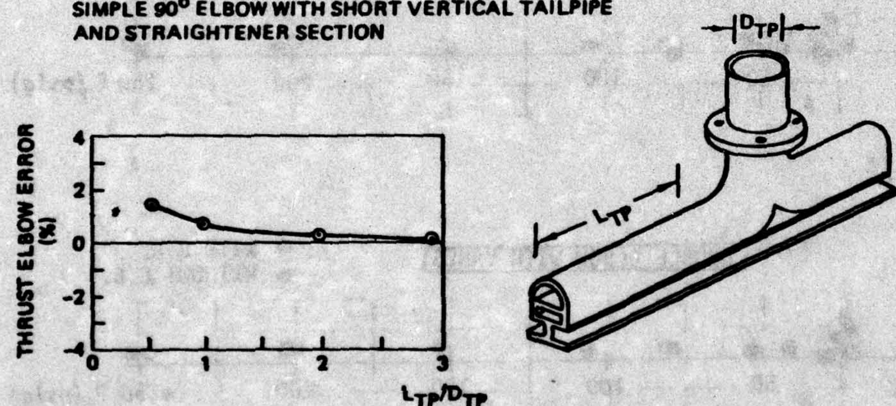

SPLIT FLOW ELBOW WITH HORIZONTAL TAILPIPE AND
STRAIGHTENER VANES

FIGURE 3 SUMMARY OF WATERJET THRUST MEASUREMENT ERROR RESULTS

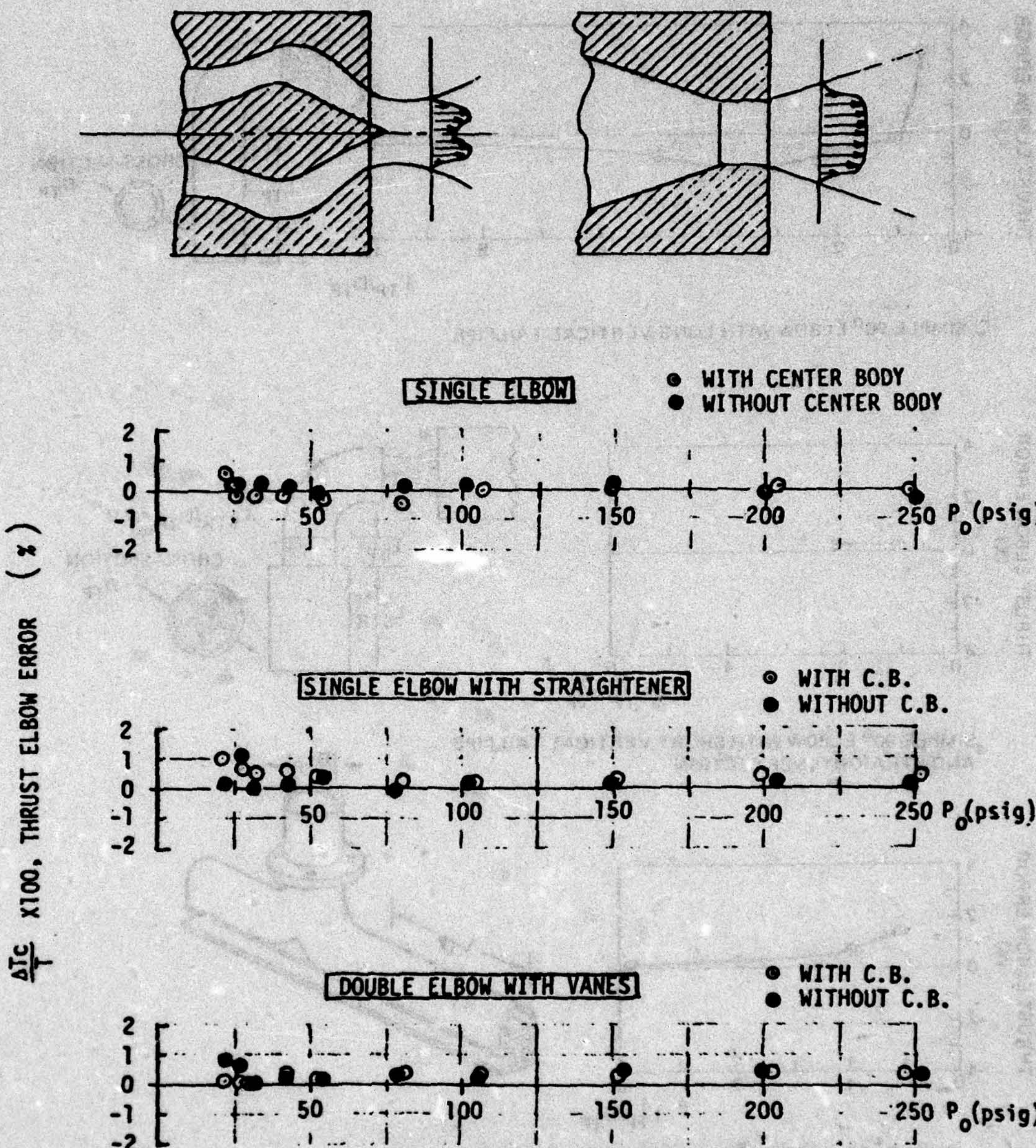

FIGURE 4 EFFECT OF JET VELOCITY PROFILE

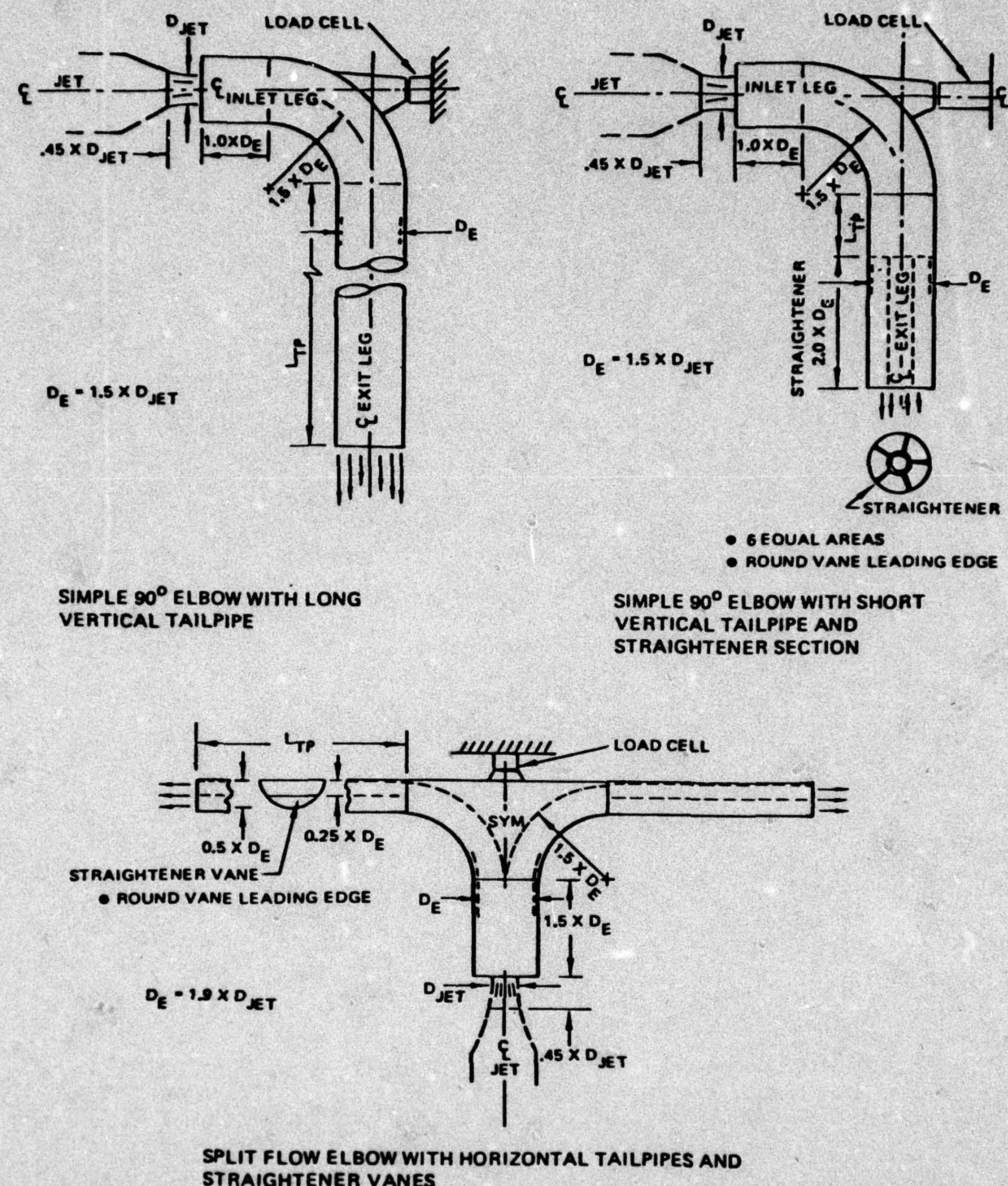

FIGURE 5 THRUST ELBOW CONFIGURATION OPTIONS DEVELOPED FROM EXPERIMENTAL DATA

EXPERIMENTAL DETERMINATION OF PERIODIC PROPELLER BLADE LOADS IN A TOWING TANK

by

Robert J. Boswell

Stuart D. Jessup

David W. Taylor Naval Ship Research and Development Center

ABSTRACT

The periodic loads were measured on a single blade of a model propeller operating in various circumferentially nonuniform flow fields in a towing tank. These flow fields were generated by a single-screw transom-stern hull, upstream wire-grid screens, and propeller shaft inclination.

These experiments demonstrate the value of towing tank experiments for determining the effect of various parameters on periodic propeller blade loads. The results indicate that existing analytical techniques are reasonably adequate for predicting periodic blade loads in axial wakes near design advance coefficient; however, existing analytical techniques substantially underpredict periodic blade loads in tangential wakes.

INTRODUCTION

It is well known that the blades of a propeller operating in a circumferentially nonuniform wake pattern experience periodic loading. It is necessary to have an accurate method for calculating these periodic loads, in order to design propellers so that they possess adequate strength, including consideration of fatigue stresses. This is especially critical for high-power controllable-pitch propellers, since for these propellers the blade loads are transmitted through a complex and space-limited pitch changing mechanism.

Existing experimental data and analytical prediction techniques have been summarized recently by Boswell, et al[1,2]; therefore, no such summary will be presented here.

In order to obtain data by which to validate analytical prediction procedures, an experimental program was undertaken to measure the six components of loading (Figure 1) on a model propeller operating in wakes generated by a single-screw transom-stern hull, upstream wire-grid screens, and propeller shaft inclination. The experimental results were correlated with predictions based on unsteady lifting surface theory as developed by Tsakonas, et al[3], and with the quasi-steady method of McCarthy[4]. The results behind the model hull were also correlated with strains measured on the corresponding full-scale propeller at sea.

EXPERIMENTAL TECHNIQUE

All experiments were conducted on Carriage I of the David Taylor Model Basin. For all experiments the propeller was driven from downstream. For the measurements behind the model hull the propeller was located in its proper position relative to the model hull but was isolated from the model (Figure 2).

The downstream drive system was necessary in order to obtain the required characteristics of the system for measuring unsteady loading, i.e., isolation from extraneous vibration, no natural frequencies near the frequencies of the measured quantities, good sensitivity and very small interactions.

The sensing elements consisted of strain-gaged flexures located in the propeller hub. The flexures were statically and dynamically calibrated before and after the experiments.

During the experiment, data were collected, stored, and analyzed on-line using a digital computer. Data were also stored on magnetic tape for later more detailed analyses.

The dynamometry system, calibration procedures, and analysis procedures have been described in detail by Boswell, et al[1,2]; therefore, these details are omitted here.

MEASUREMENTS BEHIND MODEL HULL

Wake surveys were conducted with and without the downstream body (dynamometer boat) to determine the influence of this body on the distribution of the flow in the propeller plane. These surveys (Figure 3 shows a typical radius) indicate that the downstream body has only a small effect on the circumferential variation of the flow; therefore, the downstream body should have only a small effect on the periodic blade loading. This was confirmed by comparative calculations in the two wake patterns (i.e., with and without the downstream body) using the procedures of Tsakonas, et al[3] and McCarthy[4].

These wake surveys also indicated that for this hull the circumferential variation of the tangential component of velocity is much larger than the circumferential variation of the axial component of velocity.

The periodic blade load measurements were made on the model propeller shown in Figure 4. This propeller has the following geometric characteristics: diameter = 0.23 meters; number of blades = 5; expanded area ratio = 0.83; pitch ratio at 0.7 radius = 1.06. For the experiments behind the model hull, the propeller operated at an advance coefficient of 0.8.

Figure 5 presents the variation of all measured loading components (except for radial force which was small) with blade angular position. These data indicate that for all loading components the extreme values occur near the angular positions

AD-A062 506 NAVAL ACADEMY ANNAPOLIS MD F/G 5/11

PROCEEDINGS OF THE GENERAL MEETING (18TH) OF THE AMERICAN TOWIN--ETC(U)

1977 B JOHNSON, B NEHRLING

UNCLASSIFIED NL

4 OF 4

AD
A062506

END

DATE
FILMED

3 -- 79

DDC

for which the blades are horizontal*, and the variation is predominately a once per revolution variation. This suggests that the tangential component of the wake is the primary driving force (see Figure 3).

Figure 6 presents correlation between the model results and full scale results for bending moment about the blade nose-tail line at the 40-percent radius. For the full-scale data this bending moment was deduced from strains measured on the surface of the blade at the 40-percent radius. For the model data this bending moment component was calculated from the measured force and moment components as shown in Figure 1. Figure 6 shows that the model data and full scale data give approximately the same peak to peak variation.

Figure 7 presents correlation between the model results and theoretical calculations for bending moment about the nose-tail line at the 40-percent radius. The theoretical calculations were made using the method of Tsakonas, et al[3] which is based on unsteady lifting surface theory; and using the method of McCarthy[4] which is a quasi-steady technique utilizing the open-water characteristics of the propeller.

This comparison indicates that the experimental periodic blade loads are considerably higher than the calculated values. This result is in agreement with other experimental results for which the tangential wake is the primary driving force[5,6,7,**]; however, reasonably good agreement between theory and experiment has been obtained often in the past for cases in which the primary driving force is the axial wake[8,9].

Upon evaluation of these results it was hypothesized that the poor agreement for periodic blade loads in tangential wake patterns was due to either, (1) failure of the theories to properly represent the flow field, or (2) interaction between the propeller and nearby solid boundaries. Additional blade loading experiments in idealized flows were conducted to check these hypotheses, as described in the following section.

MEASUREMENTS IN IDEALIZED WAKE PATTERNS

Figure 8 shows the arrangement for experiments in idealized flows. The wake screen was designed to produce a dominantly once per revolution variation in axial flow which would produce approximately the same angle-of-attack variation of the blades as would a 10-degree propeller shaft inclination in uniform flow. Figure 9 shows one typical radius of the measured wake behind the screen.

*Throughout this report the blade angular position, such as in Figure 5, is measured from the upward vertical position, positive clockwise looking upstream, whereas the angular position in the wake, such as in Figure 3, is measured from the upward vertical position, positive counterclockwise looking upstream.
**Results obtained at DTNSRDC behind a twin screw transom stern configuration will be reported in the near future. These unreported results agree with the results presented here.

Measurements were made on the propeller shown in Figure 4 over a range of advance coefficients and a range of propeller to plate clearances behind the wake screen at zero shaft inclination, and without the wake screen at 10-degrees shaft inclination.

The results showed that for operation in either axial or tangential wakes the periodic blade loads did not change with tip clearance over the range 0.2 diameter to 2.0 diameter. It is clear, therefore, that interaction between the propeller and a nearby boundary is not the cause of the discrepancy between theory and experiment in tangential wakes.

Figures 10 and 11 show some typical results* behind the wake screen at zero shaft inclination, and at 10-degrees shaft inclination in uniform flow, respectively. The results in the axial wake indicate satisfactory agreement between the experimental results and the analytical calculations[3,4] for advance coefficients near design, but at low advance coefficients the theories underpredict the periodic loading. By contrast, for operation in the tangential wake the analytical procedures dramatically underpredict the unsteady loading at all advance coefficients, although the discrepancy with experiment is greater at the low advance coefficients. At all advance coefficients the theory is substantially closer to experimental results in the axial wake than it is in the tangential wake. Except at higher than design advance coefficients (low propeller time-average loading), the quasi-steady procedure of McCarthy[4] is in better agreement with the experimental results than is the unsteady procedure of Tsakonas, et al[3]. This is not surprising since for the cases under consideration in this paper the dominant periodic loading is at a low reduced frequency and the dominant first harmonic of the wake is in phase radially.

Based on these results, it appears that the available analytical procedures are not properly considering all of the important characteristics of the flow field for operation in inclined flow. All available procedures assume that the propeller slipstream follows the propeller axis rather than the free stream velocity which is at an angle to the propeller axis in inclined flow. It is speculated that this failure to consider the true direction of the slipstream is the major factor in the analytical underprediction of the periodic blade loads in inclined flow.

CONCLUSIONS

The towing tank is a valuable tool for determining the effect of various parameters on unsteady blade loading. The towing tank experiments in idealized wake patterns were critical to determining the importance of the various parameters on the discrepancy between theory and experiment.

*The experimental results shown have not yet been corrected for interaction between the various components; however, these interactions are small and will not affect the trends or conclusions drawn form these data.

Existing theories substantially underpredict unsteady blade loads in tangential wakes.

Existing theories are reasonably adequate for predicting unsteady blade loads in axial wakes near design advance coefficient.

For a given wake pattern the unsteady blade loads are not significantly influenced by the blade tip clearance.

REFERENCES

1. Boswell, R.J., et al, "Experimental Determination of Mean and Unsteady Loads on a Model CP Propeller Blade for Various Simulated Modes of Ship Operation," Transactions of the Eleventh ONR Symposium on Naval Hydrodynamics, Government Printing Office (1976).

2. Boswell, R.J., et al, "Experimental Unsteady and Mean Loads on a CP Propeller Blade on a Model of the FF1088 for Simulated Modes of Operation," David W. Taylor Naval Ship Research and Development Center Report 76-0125 (October 1976).

3. Tsakonas, S., et al, "An Exact Linear Lifting Surface Theory for Marine Propeller in a Nonuniform Flow Field," Journal of Ship Research, Vol. 17, No. 4, pp 196-207, (December 1974).

4. McCarthy, J.H., "On the Calculation of Thrust and Torque Fluctuations of Propellers in Nonuniform Wake Flow," David Taylor Model Basin Report 1533 (October 1961).

5. Albrecht, K. and Suhrbier, K.R., "Investigation of the Fluctuating Blade Forces of a Cavitating Propeller in Oblique Flow," International Shipbuilding Progress, Vol. 22, No. 248, p 132-147, (April 1975).

6. Bednarzik, R., "Untersuchung uber die Belastungs-schwankungen am Einzelflugel schrag angestromter Propeller," Schiffbauforschung, Vol. 8, No. 1/2, p 57-80, (1969).

7. Gutsche, F., "The Study of Ships' Propellers in Oblique Flow," Defence Research Information Centre Translation No. 4306, Copyright Controller: Her Majesties Stationary Office, London, England (October 1975); English Translation of "Untersuchung von Schiffsschrauben in schrager Anstromung," Schiffbauforschung, Vol. 3, No. 3/4, pp 97-102 (1964).

8. Boswell, R.J. and Miller, M.L., "Unsteady Propeller Loading-Measurement, Correlation with Theory, and Parametric Study," Naval Ship Research and Development Center Report 2625 (October 1968).

9. Schwanecke, H., "Comparative Calculations on Unsteady Propeller Blade Forces," Proceedings of the Fourteenth International Towing Tank Conference, Vol. 3, pp 357-397, (1975).

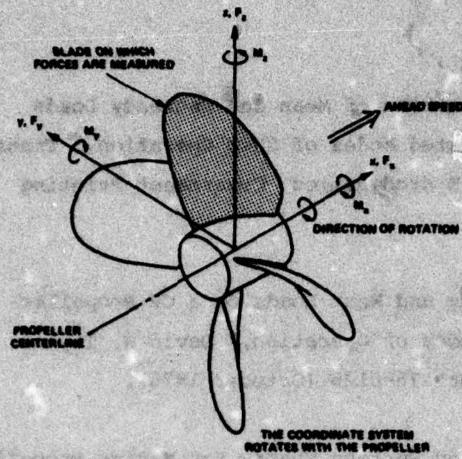

Figure 1 - Components of Blade Loading

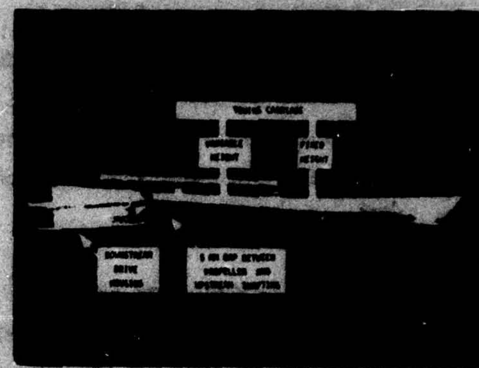

Figure 2 - Arrangement for Experiments Behind Model Hull

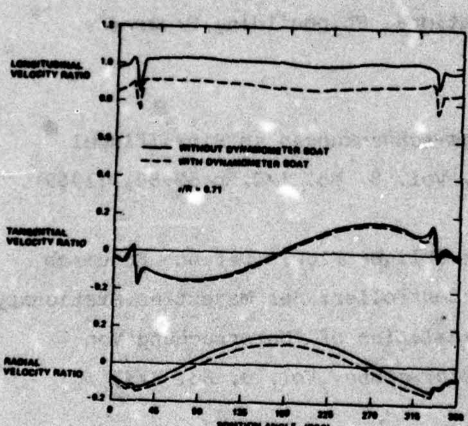

Figure 3 - Wakes Behind Model Hull

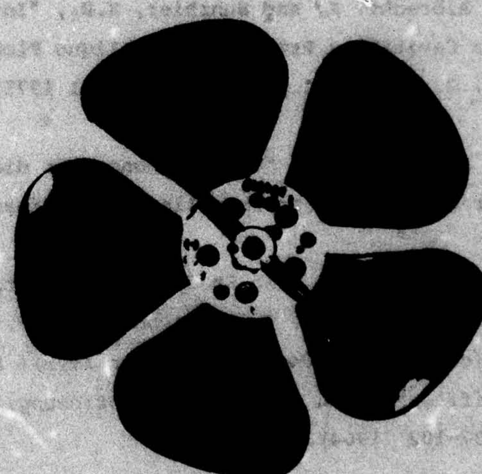

Figure 4 - Model Propeller

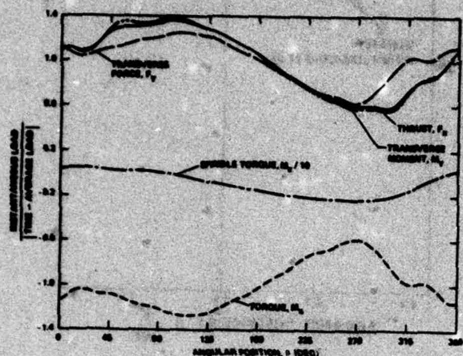

Figure 5 - Periodic Loads Behind Hull; Model Data

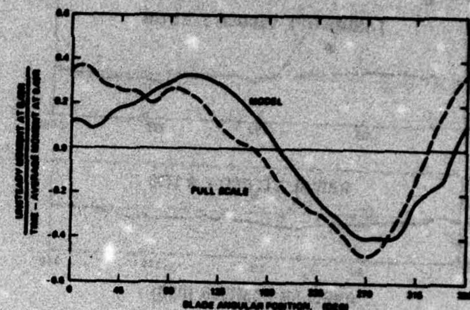

Figure 6 - Periodic Loads Behind Hull; Comparison of Model and Full-Scale Data

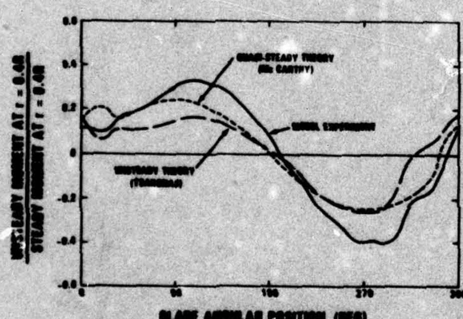

Figure 7 - Periodic Loads Behind Hull; Comparison of Model Experiment and Theory

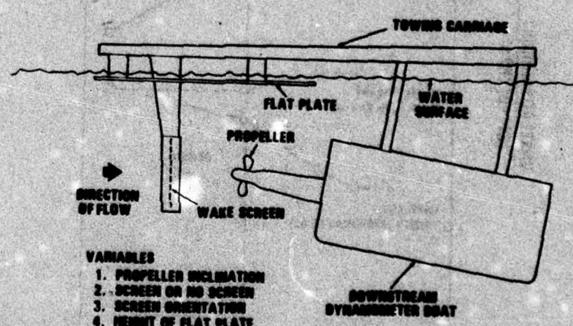

Figure 8 - Arrangement for Idealized Flow Experiments

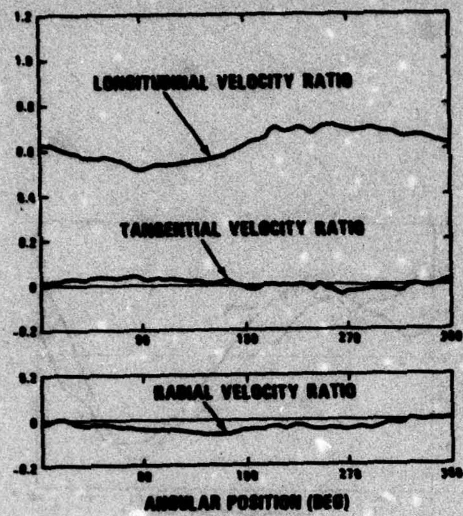

Figure 9 - Wake Generated by Screen

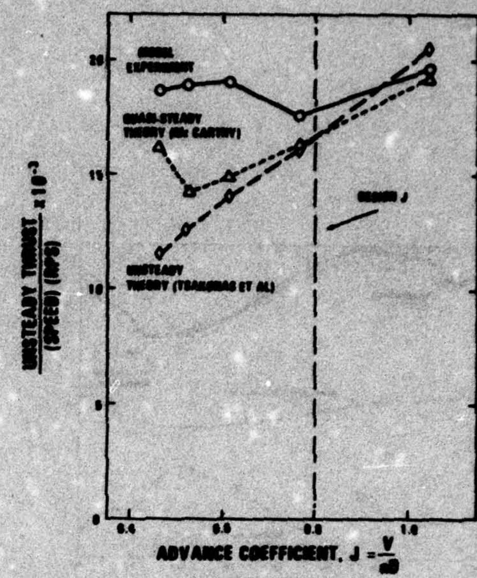

Figure 10 - Periodic Loads in Axial Wake Generated by Screens

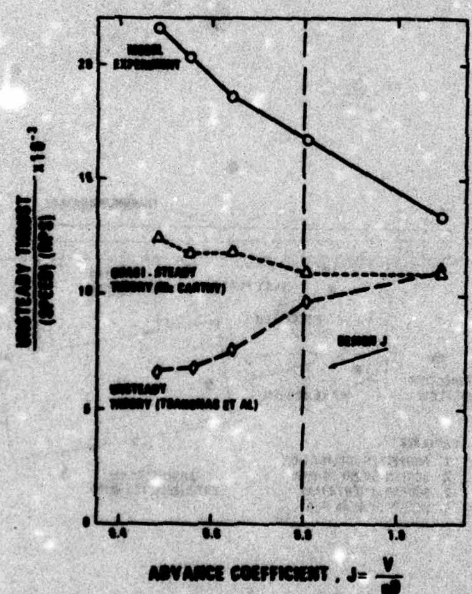

Figure 11 - Periodic Loads in Tangential Wake Generated by Shaft Inclination

EXPERIMENTAL DETERMINATION OF THE WAKE OF A HIGH BLOCK SHIP

by

Carl A. Scragg

ABSTRACT

This paper reports the progress of an experimental investigation of the wake distribution of a full form ship. Using three component hot-wire anemometers, the flow field in the wake region of a double model of the 200,000 DWT tanker Ryuko-Maru is being experimentally determined in the wind tunnel at David W. Taylor Naval Ship R&D Center. Results of an initial series of experiments are presented and compared with measurements obtained from towing tank experiments of a seven meter model of the same hull by Namimatsu and Muraoka.

Introduction

Ideally, the naval architect should have, as an input to the propeller design process, a complete knowledge of the flow field in which the propeller will be operating. Unfortunately, such information has proved to be rather elusive, particularly for full-form ships.

The quantity which is most easily measured is what we refer to as the model scale nominal wake, i.e. the flow field at the propeller plane of a towed model without propellers. But since the propellers of most ships operate, at least partially, within the boundary layer of the hull, and since there exist very great differences between the Reynolds numbers of the ship and its model, one must expect that the nominal wake of the ship might be quite different from the measurements made behind the model. However, the effects of scale upon the nominal wake represent but one half of the problem since we have not yet addressed the hull/propeller interaction.

The quantity which is needed as an input to the propeller design process is not the nominal wake, but rather the effective wake, which can be defined as the flow field behind the self-propelled ship minus the propeller induced velocities. Of course, if there were no hull/propeller interactions, then the effective wake would be equal to the nominal wake, and our problem would be greatly simplified. Unfortunately, the alteration of the boundary layer which is caused by the action of the propeller is

sometimes just as important as the change in the boundary layer due to scale effects.

This project has, as a long-range objective, the development of an engineering tool which would enable the naval architect to predict the effective wake of the ship from measurements of the nominal wake of the model. Considerable progress has been made in the attempt to treat this problem analytically for some hull forms, particularly bodies of revolution (see Huang and Cox[1]). These methods rely upon the assumption that the hull/propeller interaction can be treated as an inviscid flow problem and that the effects of a change in scale can be treated by boundary layer theory. However, such an approach runs into immediate and severe complications when one attempts to find the effective wake of a full-form ship. Such a ship can experience a flow separation, commonly referred to as the bilge vortex, which can be severe enough to dominate the flow field in the wake region. In the presence of a strong bilge vortex, the flow field will clearly violate the boundary layer assumptions and the use of existing three-dimensional boundary layer calculation methods becomes untenable. Since it would appear that we are still a number of years away from being able to treat such a hull-form analytically we have decided to persue a more empirical approach.

Our initial efforts are being directed towards the experimental determination of the flow field in the wake region of a full-form ship. Measurements are being conducted both with and without propellers at four different stations near the propeller plane. Such a complete set of data should be valuable not only in the development of empirical techniques but also in the evaluation of three-dimensional turbulent boundary layer prediction schemes.

Experiments

The hull which was selected for our experiments is that of the 200,000 DWT tanker "Ryuko-Maru". This hull has already been examined quite extensively by Namimatsu and Muraoka.[2] These authors have published wake surveys of the full-scale ship, its 30 m. model, and its 7 m. model. All of our experiments are being conducted in the wind tunnel with a 3 m. double model. Once completed, our experiments, together with the previous studies, will include fully-propelled wake surveys at four Reynolds numbers and bare hull wake surveys at two different Reynolds numbers (including a duplication at one Reynolds number which will be used as comparison of the different experimental techniques).

The use of a double model or mirror image model, requires the assumption that the presence, or lack, of a free surface does not significantly affect the flow field in the region near the propeller. While we recognize that this may be a rather bold assumption, given that the on-set of separation is strongly dependent upon the pressure gradients, it is felt that, since such a ship operates at a very low Froude number, the errors introduced by the zero Froude number approximation will be justified by the

gains in experimental accuracy and simplicity which can be realized in the wind tunnel.

We have constructed a 3 m. (1/100 scale) mirror image model (see Figures 1 and 2), and have conducted the initial series of experiments in the anechoic flow facility at DTNSRDC. The original intent was to use three-dimensional hot-wire anemometers to map the flow field for the case where the propellers were not operating, and to use both the hot-wire anemometers and the laser doppler velocimeter (LDV) to map the flow field when the propellers were operating. The LDV was to be used to measure the flow at points immediately in front of the propeller, since the probe body of a standard hot-wire would interfere with the propeller in such a region. Unfortunately, we experienced severe problems with the LDV, caused by reflection of the laser beams off the body surface. This made accurate 3-D measurements impossible and it was decided, therefore, to construct special 3-D hot-wire probes with an "L shaped" body, which could be placed in front of an operating propeller. As of now, we have not returned to the wind tunnel to complete the measurements and our experimental results are missing the important points immediately in front of the propeller.

The measurements include three upstream stations (.25, .9, 1.9 propeller diameters forward of the propeller) and one downstream station (.5 propeller diameter aft of the propeller). All three components of the velocity were measured both with and without the propeller operating.

Results

Figures (3) and (4) show the results obtained at the station immediately in front of the propeller disk when there were no propellers operating. The flow clearly indicates the presence of the bilge vortex and accompanying cross flow, but it should be noted that this particular wake is considerably simpler than some of the wakes found by other researchers studying similar full form ships. For the case where the propellers were operating, the measurements only include points outside of the propeller disk. For the longitudinal velocity component, everything of interest occurs within the propeller disk, but the in-plane component is presented here since it suggests a phenomenon which was not observed by Namimatsu and Muraoka when they studied the same hull. Note that in Figure (5), the in-plane component is altered markedly just outside the propeller disk. This seems to suggest a substantial acceleration of the bilge vortex caused by propeller suction. This phenomenon has been observed by Hoekstra[3] in his recent study on hull propeller interaction. We should be able to clarify this point after we complete the next series of tests.

Figure (6) is reproduced from Namimatsu and Muraoka[2] and presents the results of their measurements on the 7 m. towed model. It can be seen that the longitudinal component of the velocity agrees quite well with our measurements and so does the magnitude of the in-plane velocity. However, the direction of the in-plane velocity

differs by as much as 45 degrees in some locations. The reasons for this remain unclear and we hope to elucidate the situation when we return for future experiments.

References

1. Huang, T. T. and Cox, Bruce D., Interaction of Afterbody Boundary Layer and Propeller. Symposium on Hydrodynamics of Ship and Offshore Propulsion Systems, Oslo, March 1977.

2. Namimatsu, M. and Muraoka, K., Wake Distribution Measurements on Actual Tanker and its Large Scale Model. 14th International Towing Tank Conference, Ottawa, 1975.

3. Hoekstra, M., An Investigation into the Effect of Propeller Hull Interaction on the Structure of the Wake Field. Symposium on Hydrodynamics of Ship and Offshore Propulsion Systems, Oslo, 1977.

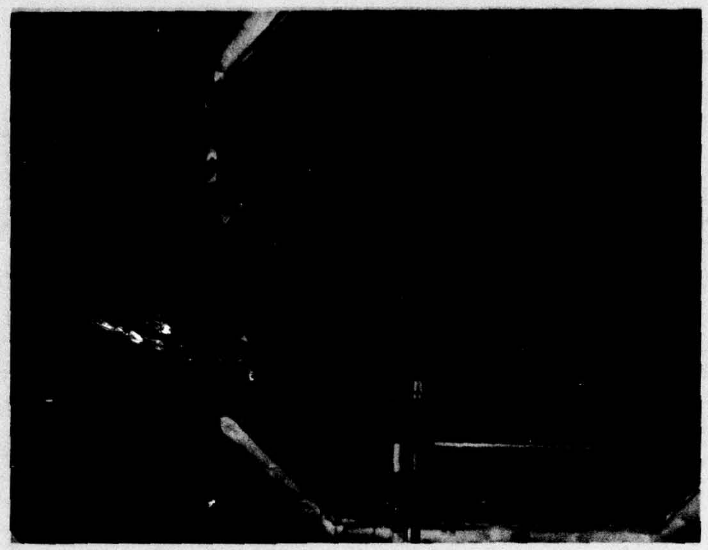

Figure 1: Double model mounted in wind tunnel. View is looking downstream

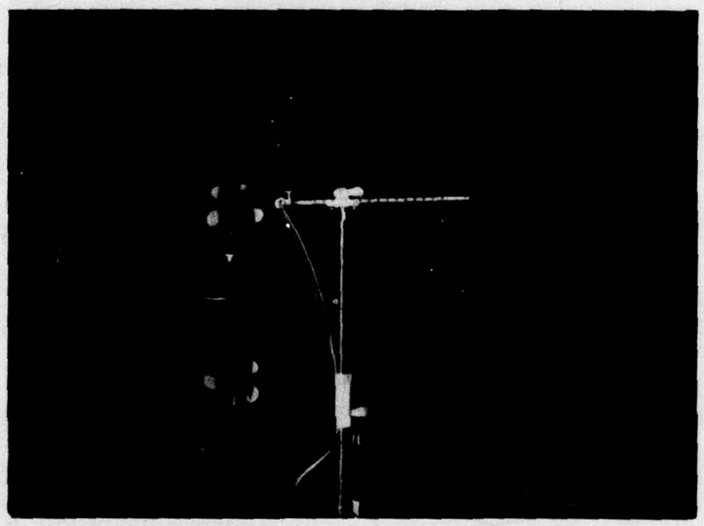

Figure 2: Stern view of double model showing propellers and support for hot-wire probes

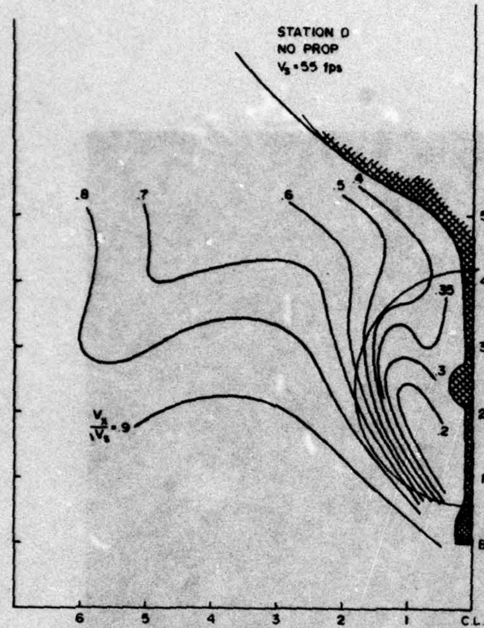

Figure 3: Axial velocity component measured with no propellers operating. Measuring station is one fourth of the propeller diameter forward of the propeller station.

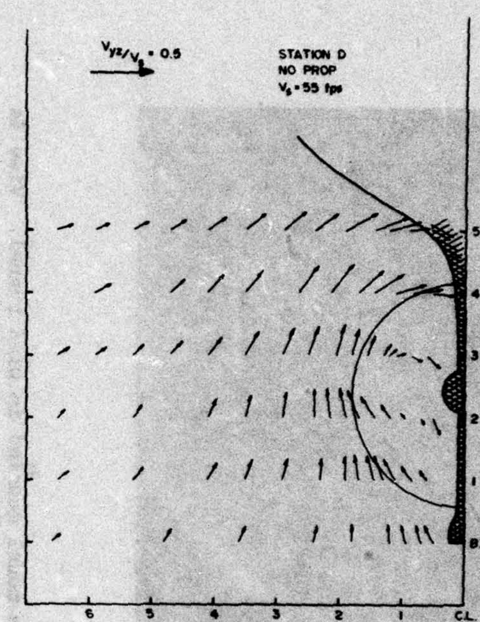

Figure 4: In-plane component of the velocity measured with no propellers operating.

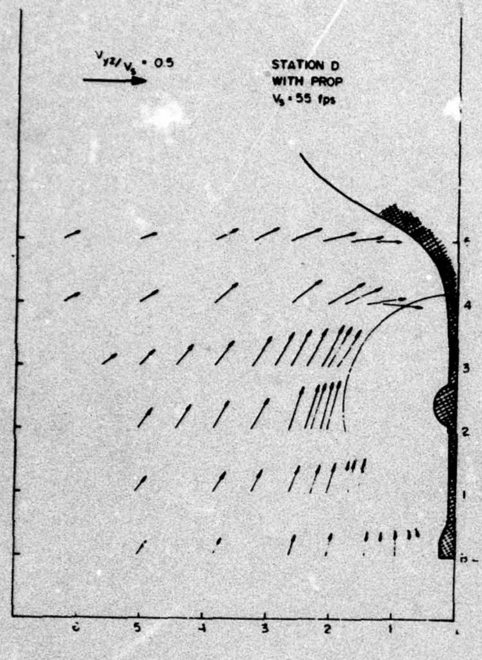

Figure 5: In-plane component of the velocity measured with propellers operating

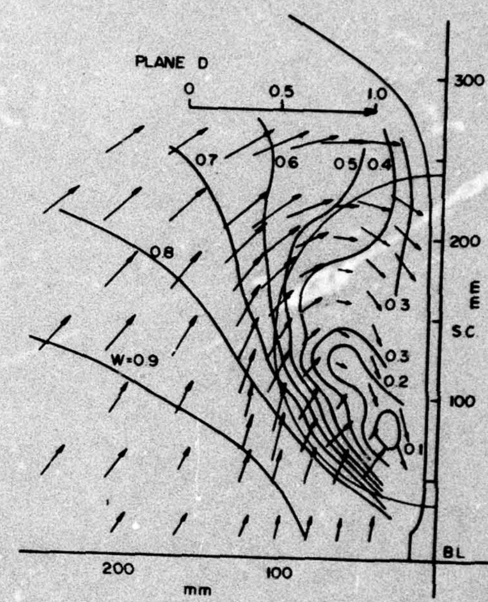

Figure 6: Results obtained by Namimatsu and Muraoka[2] for 7 m model of the same hull.

DISCUSSION OF WRITTEN CONTRIBUTIONS TO THE PROPULSION COMMITTEE REPORT

Edited by W. G. Day, Jr., of DTNSRDC

PERFORMANCE OF DUCTED PROPELLERS FITTED TO SURFACE CRAFT, Gearhardt and Henderson

Written Discussion:

M. B. Wilson, David W. Taylor Naval Ship R&D Center

This discussion concerns the statement in the paragraph following Equation (5) of Appendix 6 to the effect that "diffusing ducts will not produce any performance gains in overall performance as compared to nondiffusing ducts." There may be a semantics problem of identifying what is meant by 'performance gains,' but in the most straight-forward sense of a comparison, the statement is not true. Rather it is incomplete, lacking certain crucial qualification. It should be noted that at relatively low speeds, for a given rotor and duct diameter and length, a diffusing duct can most certainly be shaped to deliver more thrust-per-unit power than a nondiffusing duct. The speed range and power loading are essential parameters in determining the sign and magnitude of performance augmentation, however.

The proofs of performance benefits of duct diffusion exist both theoretically (ideal flow analysis) and experimentally. The reason for improved performance can be understood in terms of the higher thrust induced on the ring wing (duct) due to higher camber ––– as was pointed out by J.O. Scherer ––– or in terms of a one-dimensional momentum analysis as outlined below.

Ideal ducted propeller performance limits, including the effects of duct diffusion, have been worked out for example, by M. Lazareff (1968) in Reference 6.1. Figure 6.A illustrates the flow geometries associated with nondiffusing and diffusing ducts, and shows the effect of diffusion in expanding the final exit stream flow out to area S_4 with average velocity V_4, compared with the rotor area S_1, velocity V_1, of the nondiffused duct. The thrust is

$$T = \dot{m} (V_4 - V_o)$$

and the ideal power needed, ignoring the shipstream rotation, is

$$P = \tfrac{1}{2} \dot{m} V_4^2 - \tfrac{1}{2} \dot{m} V_o^2$$

where the mass flow rate through the device is

$$\dot{m} = \rho V_1 S_1 = \rho V_4 S_4$$

The diffusion ratio is denoted by

$$\sigma = S_4/S_1$$

and as indicated in the sketch, σ may be different than the duct geometrical ratio S_{exit}/S_1. The ideal thrust efficiency is therefore

$$\eta = \frac{TV_o}{P} = \frac{2}{1 + \frac{V_4}{V_o}} = \frac{2}{1 + \frac{1}{\sigma}\frac{V_1}{V_o}}$$

which shows that for ducted propellers having the same through-disk velocity ratio V_1/V_o, the effect of diffusion ($\sigma > 1$) is to increase efficiency.

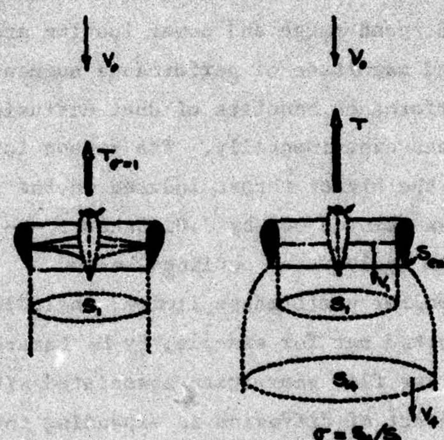

Figure 6.A - Flow Geometries and Notation for Nondiffusing and Diffusing Ducted Propeller

In addition to these inviscid relations, Lazareff (1968) has also included a realistic estimate of the total viscous drag on the duct. Figure 6.B, reproduced from Lazareff (1968) is an example comparison of the predicted performance of a free propeller, a ducted propeller with $\sigma = 1$, and a ducted propeller with $\sigma = 1.4$ shown with thrust-to-power ratio plotted versus forward speed, for a power loading of $P/S_1 = 200\ kW/m^2 = 24.92\ hp/ft^2$. This shows that the benefits of diffusion in

improving the thrust delivered for a given power are greatest at low speeds (approaching the bollard condition $V_o = 0$). For the case $V_o = 0$, the ideal power required becomes

$$P = \frac{T^{3/2}}{2(\rho\sigma S_1)^{1/2}}$$

which indicates the distinct performance improvement afforded by diffusion at the bollard condition.

Lazareff (1967) has also provided example experimental evidence of performance increase on a propeller duct with diffusion in Reference 6.2. Figure 6.C is a sketch taken from Lazareff (1967) of a model propeller-hub-duct arrangement having 45 degree duct diffusion aft of the blade tips. Blowing slot boundary-layer-control was used to suppress separation on the duct inner surface and on the aft end of the hub. Based on tests in air at the bollard condition, Lazareff (1967) has reported the achievement of a static merit coefficient of $M_1' = 1.17$. Here the M_1' is defined as

$$M_1' = \frac{T^{3/2}}{2P(\rho S_1)^{1/2}}$$

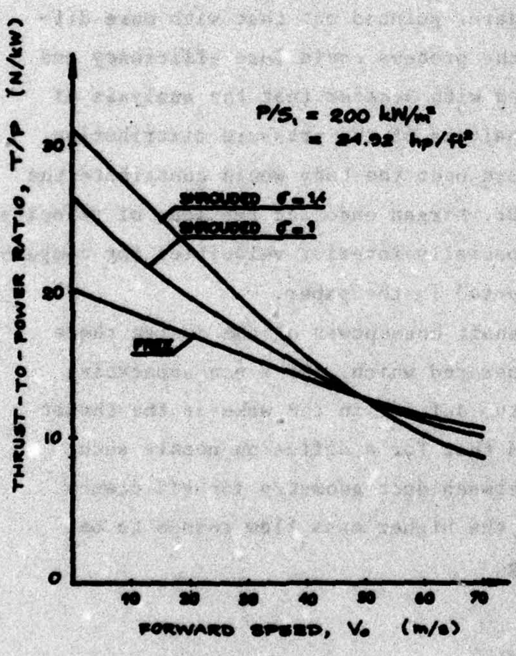

Figure 6.B - Comparison of Thrust-to-Power Ratio with Free Propeller and the Effect of Diffusion (From Lazareff (1968))

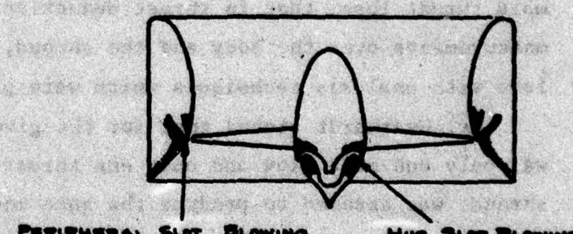

Figure 6.C - Sketch of Model Ducted Propeller with Diffusion, Tested by Lazareff (1967) in Air

For an ideal ducted propeller without diffusion $M_1' = 1$, and for an ideal free propeller $M_1' = \sqrt{0.5}$; so that the model experimental value of $M_1' = 1.17$ is impressively high. Unfortunately, experiments with forward speed were not reported, so the cross-over points for vanishing performance-augment due to diffusion (as in Figure 6.B) are not available as a function of speed and power loading for Lazareff's model.

REFERENCES

6.1 Lazareff, M., "Aerodynamics of Shrouded Propellers," Paper D of the Aerodynamics of V/STOL Aircraft, AGARD ograph 126, May 1968.

6.2 Lazareff, M., "Controle de Diffusion aval sur Helice Carenee," AGARD Conference Proceddings No. 22, September 1967.

Oral Discussion:

Otto Scherer of Hydronautics, Inc. stated that the inviscid analysis performed by Mr. Gearhardt shows that diffusion in the nozzle did not seem to make any difference in the thrust analysis. However, Mr. Scherer pointed out that with more diffusion and a greater mass flow in the nozzle the process could lose efficiency and therefore thrust. Dr. Morgan of DTNSRDC agreed with Scherer that the analysis of the diffusing duct did not allow a complete analysis of the pressure distribution over the body as well as the duct. The pressure over the body would contribute the main thrust loss, that is thrust deduction. Dr. Morgan endorsed the idea of velocity measurements over the body and the shroud, especially interior velocities for comparison with analysis techniques which were presented in the paper.

Mr. Gearhardt stated that for the given shaft horsepower of the design there was only one mass flow and only one thrust generated which, for a non-separating shroud, was assumed to produce the same momentum deficit in the wake as the thrust deduction analysis. Mr. Gearhardt also stated that for a diffusion nozzle such as had been discussed there was a trade-off between duct geometry for efficiency, and mass flow for loading on the blades since the higher mass flow tended to be less efficient but produced less blade loading.

WATERJET PROPULSION SYSTEM PERFORMANCE ANALYSIS, Miller

Oral Discussion:

Mr. Jack Brandau agreed with Mr. Miller's presentation of the waterjet performance analysis and pointed out that one of the problems associated with these systems is the claim of high pump efficiencies which leads designers to expect system efficiencies of the same high value. Mr. Brandau noted that the experimental techniques and analysis procedures are not well known to designers and significant losses occur unless careful attention is paid to those component analyses described by Mr. Miller. Mr. Scherer added that as an aid to those working in waterjet system design, the I.T.T.C. is preparing a nomenclature list and an analysis summary of thrust and drag of waterjet systems which is intended to make component evaluation more uniform.

Mr. Miller agreed that design evaluation is minimal in these cases since a complete evaluation is somewhat expensive and requires strong justification.

A SURVEY OF PROPULSOR-VEHICLE INTERACTION ON HIGH PERFORMANCE MARINE CRAFT, Wilson

Oral Discussion:

Mr. Dan Savitsky of the Davidson Laboratory asked if tunnel propellers were not included in the paper. Mr. Wilson noted that there was a contribution in the paper drawn from two references in the bibliography. Dr. Breslin added that calculation of relative rotative efficiencies in shear flows such as might be expected in a tunnel were being performed at Davidson Lab. The optimum performance was then being compared to that of a similar propeller in uniform flow. Mr. Crago of the British Hovercraft Corporation commented on the airscrew propulsion analysis. In systems in which one prime mover provides both fan and propulsion power, losses on the propeller efficiency due to low inflow velocities can sometimes be made up by increases in fan efficiency with the total craft system efficiency not being reduced a great deal.

WATERJET PROPULSOR THRUST MEASUREMENT USING A REACTION ELBOW, Eilers and Shrout

Oral Discussion:

Dr. Blaine Parkin of the Applied Research Laboratory, Penn State, asked about Figure 2-b of the paper which shows the water inlet penetrating one of the control

surfaces. Dr. Parkin asked what precautions were required to keep this inlet flow from invalidating the thrust-error measurements which were the objective of the model experiments.

Mr. Eilers reviewed the process by which the inlet flow interactions were reduced or eliminated. The best method found was the use of a long solid pipe (approximately 10 feet in length). Pressure tares and vertical interactions were taken throughout the assembly of the system. Mr. Shrout added that the biggest problem was the vertical force interaction with the thrust flexures and that this interaction had to be taken out of the final data as a tare.